Leibniz-Institut für Kristallzüchtung

im Forschungsverbund Berlin e.V.

Annual Report

2013

Leibniz-Institut für Kristallzüchtung
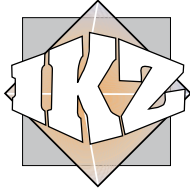Acting Director: Prof. Dr. Günther Tränkle
Max-Born-Straße 2
12489 Berlin

Phone   +49 (0)30 6392 3001
Fax   +49 (0)30 6392 3003
Email   cryst@ikz-berlin.de
Online   www.ikz-berlin.de

Annual Report 2013

Leibniz-Institut für Kristallzüchtung
im Forschungsverbund Berlin e.V.

Annual Report 2013

Dear readers, dear colleagues,

For the Leibniz Institute for Crystal Growth (IKZ), the year 2013 has been characterized by the change in management. After ten years as director of the institute, Prof. Roberto Fornari was appointed professor at the University of Parma as of October 1, 2013.

During this last decade, the institute has become *the* European Center for Crystal Growth. In 2013, it once more succeeded to consolidate this reputation. Due to its unique competencies, the institute is internationally recognized for its research and development activities in the field of crystalline materials and corresponding production technologies. The materials presently under development are of fundamental importance for innovations in areas like power- and microelectronics, photovoltaics, and optical technologies. Thus, the institute contributes significantly to application areas relevant to the society, namely environment, mobility, communication, and information.

Certain semiconductors, dielectrics, and wide bandgap materials with highest perfection and purity are only available at IKZ. One example is semiconducting oxides as basis for transparent oxide electronics. Research activities comprise the whole value chain, from growth of substrate crystals and their preparation up to the deposition of functional layers with tailored properties.

A technological challenge, but also one of the institute's core competencies is the growth of semiconductor single crystals meeting highest demands regarding purity and crystalline perfection. IKZ's high expertise in this area is particularly indispensable in an ongoing project addressing the growth of isotopically pure silicon crystals, which aims at no less than newly defining the kilogram as unit for mass with even higher accuracy.

The development of new crystalline materials is of fundamental importance for technological innovation. This includes, among others, high-performance UV light emitting diodes for medical applications, water treatment, and production technology. To this end, the institute is developing a growth technology suitable for in-

Liebe Leserinnen und Leser, liebe Kolleginnen und Kollegen,

2013 war für das Leibniz-Institut für Kristallzüchtung (IKZ) durch den Wechsel in der Institutsleitung gekennzeichnet. Prof. Roberto Fornari, der das Institut in den vergangenen zehn Jahren geleitet hatte, war zum 1. Oktober dem Ruf auf eine Professur an die Universität in Parma gefolgt.

In dieser vergangenen Dekade hat sich das Institut zu *dem* europäischen Zentrum für Kristallzüchtung entwickelt. Es konnte in 2013 sein Renommee weiter festigen. Dank seiner seine einzigartigen Kompetenzen bei der Erforschung und Entwicklung von kristallinen Materialien und von Technologien für deren Produktion ist das Institut international anerkannt. Die am Institut erforschten Materialien sind Grundlage für Innovationen, etwa in der Leistungs- und Mikroelektronik, der Photovoltaik und den optischen Technologien. Damit leisten die Ergebnisse des IKZ einen bedeutenden Beitrag zu Entwicklungen in gesellschaftsrelevanten Anwendungsfeldern wie Umwelt, Mobilität, Kommunikation und Information.

Bestimmte Halbleiter, Dielektrika und Materialien mit großer Bandlücke sind in höchster Perfektion und Reinheit ausschließlich am IKZ verfügbar. Ein Beispiel sind halbleitende Oxide, die die Grundlage für eine transparente Oxidelektronik bilden. Die Forschungsarbeiten am Institut umfassen die gesamte Wertschöpfungskette von der Züchtung von Substraten über die Präparation von Wafern bis hin zu der Abscheidung von funktionellen Schichten mit maßgeschneiderten Eigenschaften.

Die Herstellung von klassischen Halbleiter-Einkristallen höchster Perfektion und Reinheit ist eine technologische Herausforderung und Kernkompetenz des Instituts. Die umfassende Expertise in diesem Bereich spielt insbesondere im laufenden Projekt zur Züchtung isotopenreiner Silizium-Einkristalle eine entscheidende Rolle, mit dem das Kilogramm als Maßstab für das Gewicht neu und präziser als bisher definiert werden kann.

Die Entwicklung neuer kristalliner Materialien ist von grundlegender Bedeutung für technologische Innovationen. Zu diesen zählen unter anderem leistungsfähige UV-Leuchtdioden für Anwendungen in den Bereichen Medizin, Wasserbehandlung und Produktionstechnik. Hierfür entwickelt das IKZ eine Züchtungstechnologie für die industrielle Herstellung von einkristallinem Aluminiumnitrid höchster Qualität und mit definierten optischen und elektronischen Eigenschaften. Dazu hat sich das IKZ in 2013 mit acht weiteren Forschungseinrichtungen und 14 Industrieunternehmen zum Konsortium „Advanced UV for Life" zusammengeschlossen, das sich im Wettbewerb „Zwanzig20 – Partnerschaft für Innovation" des Bundesministeriums für Bildung und Forschung durchgesetzt hat.

Neben der Erforschung neuer Materialien werden Prozesse und Technologien für die Züchtung etablier-

dustrial production of single crystalline aluminum nitride with highest quality along with defined optical and electronic properties. This issue is addressed in the frame of the "Advanced UV for Life" consortium, comprising eight further research institutions and 14 industrial partners – this proposal has succeeded in the competition" Zwanzig20 – Partnerschaft für Innovation" announced by the Federal Ministry of Education and Research.

In addition to the research on new materials, processes and technologies suitable for the growth of established materials are developed, mostly in cooperation with or by order of industrial partners. The application of magnetic fields to crystal growth as developed by IKZ, for example, leads to enhanced crystalline quality as well as higher yields. This technology is applied to the growth of classical materials like silicon for photovoltaics and gallium arsenide for microwave and high-frequency technology.

In any case, IKZ's successful research activities will be pursued seamlessly. To fill the managing position quickly, a joint appointment procedure with the Humboldt-Universität Berlin has already been initiated – the new director is expected to take up his or her duties in 2015. Until then, the colleagues at IKZ will continue their excellent work and I, as the acting director, will actively support them. The same holds for our long-term partners in research and industry whom I like to express my appreciation for the good and inspiring cooperation. I would also like to thank our funding authorities for sustainably supporting the institute's issues.

I wish you an inspiring reading.

Yours sincerely,

Günther Tränke

ter Materialien entwickelt, meist in gemeinsamen Forschungsprojekten mit oder im direkten Auftrag für die Industrie. So lassen sich bei der am Institut entwickelten Technologie zur Züchtung von Kristallen im Wandermagnetfeld die Kristallqualität verbessern und die Ausbeute erhöhen. Diese Technologie kommt bei bereits etablierten Materialien wie Silizium für die Photovoltaik oder Galliumarsenid für die Mikrowellen- und Hochfrequenztechnologie zum Einsatz.

Die erfolgreichen Forschungsaktivitäten des IKZ werden nahtlos weitergeführt werden. Um die Leitungsposition des Instituts rasch wieder zu besetzen, wurde mit der Humboldt-Universität bereits ein gemeinsames Berufungsverfahren eingeleitet; die Neubesetzung mit einer Direktorin oder einem Direktor ist für 2015 geplant. Bis dahin werden die Kolleginnen und Kollegen am IKZ ihre exzellenten Forschungsarbeiten fortführen. Als kommissarischer Direktor werde ich sie dabei aktiv unterstützen. Dies gilt auch für die langjährigen Partner in Forschung und Industrie, denen ich hiermit herzlich für die sehr gute Zusammenarbeit danke. Wir danken auch unseren Zuwendungsgebern in Bund und Land für ihre Förderung der Belange des Instituts.

Eine anregende Lektüre wünscht Ihnen, Ihr

Günther Tränkle

Content

Leibniz-Institut für Kristallzüchtung
im Forschungsverbund Berlin e.V.

FOUNDED 1992
PART of Forschungsverbund Berlin e.V.
MEMBER of the Leibniz Association (WGL)

STAFF	**105**
Scientists	59 (external funding: 36)
Ph.D. students	13
Technicians	46 (external funding: 11)
Trainees	4

BUDGET 2013:	**10.7 Mio €**
Basic funding	8.6 Mio €
Third-party funding	2.1 Mio €

Foto: Lothar M. Peter

The Leibniz Institute for Crystal Growth is a governmental research and service institute, which is theoretically and experimentally investigating the scientific-technical fundamentals of crystal growth, processing and physico-chemical characterisation of crystalline solids. This ranges from explorative fundamental research to pre-industrial development. The materials presently in development are of fundamental importance in micro- , opto- and power electronics, in photovoltaics, in opto- and laser technology, in acousto-electronics and sensor technology as well as for fundamental research.

The research activities of the institute include bulk single crystals as well as crystalline layers and nanostructures, but also the development of comprehensive crystal growth technologies, which are suitable for different materials.

The research and service tasks of the institute include:

- Development of technologies for growth, processing and characterization of bulk crystals and of crystalline structures with dimensions in the micro- and nanometer range and of comprehensive growth technologies
- Supply of crystals with non-standard specifications for research and development purposes
- Modelling and investigation of crystal growth processes
- Experimental and theoretical investigations of the influence of process parameters on crystal growth processes and crystal quality
- Development of technologies for the chemo-mechanical processing of crystalline samples and scientific investigation of related processes
- Physico-chemical characterisation of crystalline solids and development of suitable methods; investigation of the correlation between physical properties and related physical processes
- Development and construction of components for growth, processing and characterization of crystals

Das *Leibniz-Institut für Kristallzüchtung* (IKZ) ist eine staatliche Forschungs- und Service-Einrichtung, die sich experimentell und theoretisch mit den wissenschaftlich-technischen Grundlagen des Wachstums, der Züchtung, der Bearbeitung und der physikalisch-chemischen Charakterisierung von kristallinen Festkörpern beschäftigt. Dies reicht von der Grundlagenforschung bis hin zum Vorfeld industrieller Entwicklung. Die zurzeit entwickelten Materialien finden vorwiegend Verwendung in der Mikro-, Opto- und Leistungselektronik, der Photovoltaik, in Optik und Lasertechnik, in der Sensorik und Akustoelektronik.

Das Forschungsgebiet des IKZ umfasst Volumenkristalle, kristalline Schichten und Nanostrukturen sowie die Entwicklung von materialübergreifenden Kristallzüchtungstechnologien.

Arbeitsschwerpunkte des Institutes sind:

- Entwicklung von Züchtungs-, Bearbeitungs- und Charakterisierungsverfahren für Massivkristalle sowie kristalline Gebilde mit Abmessungen im Mikro- und Nanometerbereich sowie von materialübergreifenden Kristallzüchtungstechnologien
- Bereitstellung von Kristallen mit speziellen Spezifikationen für Forschungs- und Entwicklungszwecke
- Modellierung und Erforschung der Kristallwachstums- und Kristallzüchtungsprozesse
- Experimentelle und theoretische Untersuchungen zum Einfluss von Prozessparametern auf Kristallzüchtungsvorgänge und Kristallqualität
- Erarbeitung von Verfahren zur Kristallbearbeitung und Erforschung der dabei ablaufenden Vorgänge
- Physikalisch-chemische Charakterisierung kristalliner Festkörper und damit verbunden die Entwicklung geeigneter Methoden; Untersuchung von Materialeigenschaften und den zugrundeliegenden Vorgängen
- Entwicklung und Bau von Anlagenkomponenten für die Züchtung, Bearbeitung und Charakterisierung von Kristallen

Crystals are grown from the melt, from solutions and from the vapour phase and new techniques are developed and improved for the preparation of crystalline layers.

With the combination of bulk crystal growth and layer deposition, the institute possesses ideal conditions to produce customized substrate/layer-combinations.

Materials presently in development:

- Wide band gap semiconductors (crystalline AlN and GaN) for high temperature, power- and optoelectronics
- Oxide and fluoride crystals for acousto-electronics, laser-, opto- and sensor technology
- Si-crystals for power electronics and photovoltaics
- Si/Ge-crystals for radiation detectors and diffraction gratings
- Si layers an amorphous substrates for photovoltaics
- Crystalline layers with dimensions in the micro- and nanometer range (semiconducting or ferroelectric oxide layers, SiGe-microstructures and Si-nanowhisker)
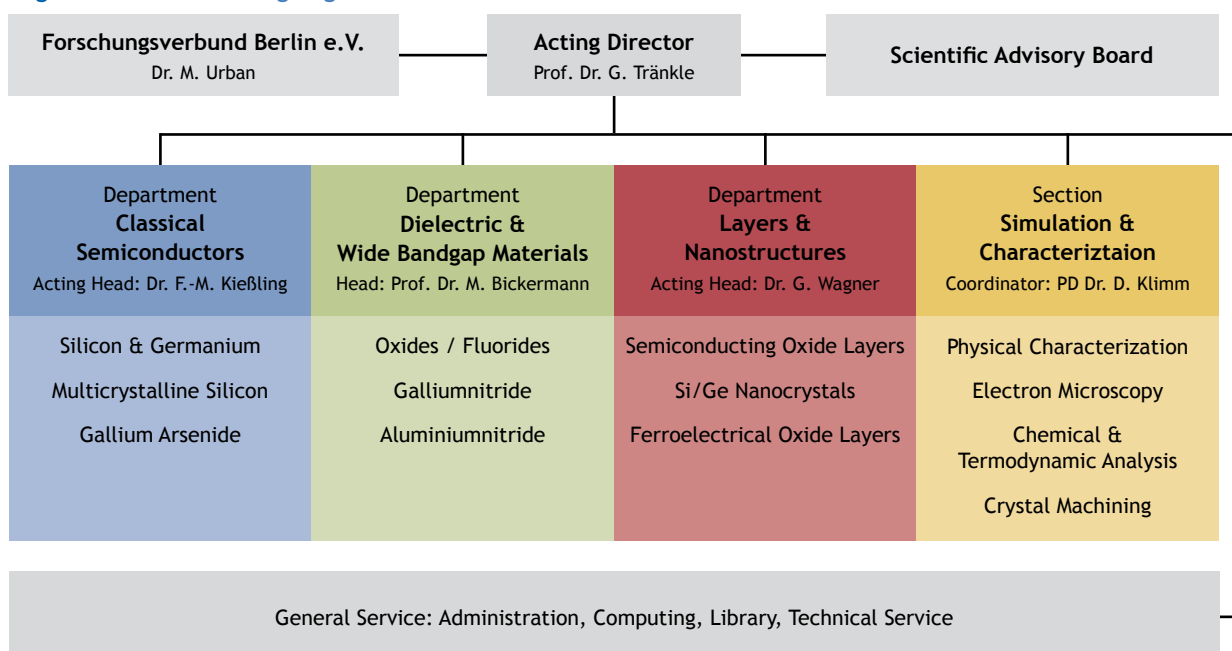
Als Züchtungsverfahren werden Methoden der Züchtung aus der Schmelze, aus der Lösung, aus der Gasphase und davon abgeleitete Verfahren zur Herstellung kristalliner Schichten verwendet.

Durch die mögliche Synergie zwischen Volumenkristallzüchtung und der Abscheidung von Schichten verfügt das Institut über ideale Voraussetzung zur Herstellung von Substrat/Schicht-Kombinationen mit maßgeschneiderten Eigenschaften.

Materialien:

- Halbleiter mit großem Bandabstand (AlN- und GaN-Kristalle) für Hochtemperatur-, Leistungs- und Optoelektronik
- Oxidische und fluoridische Kristalle für Lasertechnik, Optik, Sensorik und Akustoelektronik
- Silizium-Kristalle für Leistungselektronik und Photovoltaik
- Silizium/Germanium Kristalle für Strahlungsdetektoren und Beugungsgitter
- Silizium Schichten auf amorphen Unterlagen für die Photovoltaik
- Kristalline Schichten mit Dimensionen im Mikro- und Nanometerbereich (epitaktische halbleitende oder ferroelektrische oxidische Schichten, SiGe-Mikrostrukturen und Si-Nanowhisker)

Organisation Chart / Organigramm

Forschungsverbund Berlin e.V. Dr. M. Urban	Acting Director Prof. Dr. G. Tränkle	Scientific Advisory Board

Department **Classical Semiconductors** Acting Head: Dr. F.-M. Kießling	Department **Dielectric & Wide Bandgap Materials** Head: Prof. Dr. M. Bickermann	Department **Layers & Nanostructures** Acting Head: Dr. G. Wagner	Section **Simulation & Characteriztaion** Coordinator: PD Dr. D. Klimm
Silicon & Germanium	Oxides / Fluorides	Semiconducting Oxide Layers	Physical Characterization
Multicrystalline Silicon	Galliumnitride	Si/Ge Nanocrystals	Electron Microscopy
Gallium Arsenide	Aluminiumnitride	Ferroelectrical Oxide Layers	Chemical & Termodynamic Analysis
			Crystal Machining

General Service: Administration, Computing, Library, Technical Service

Scientific Advisory Board 2013 / Wissenschaftlicher Beirat 2013

- **Dr. Stefan Eichler (Chairman)**
  Freiberger Compound Materials GmbH, Freiberg

- Dr. Lothar Ackermann
  Forschungsinstitut für mineralische und metallische Werkstoffe, Edelsteine/Edelmetalle – FEE GmbH, Idar-Oberstein

- Dr. Hubert Aulich
  SC Sustainable Concepts GmbH, Erfurt

- Prof. Dr. Silke Christiansen
  Helmholtz-Zentrum Berlin für Materialien und Energie HZB, Berlin

- Prof. Dr. Knut Deppert
  Department of Solid State Physics, Lund University, Sweden

- Prof. Dr. Fritz Henneberger
  Department of Physics, Humboldt-Universität zu Berlin

- apl. Prof. Dr. -Ing. Michael Heuken
  Faculty of Electrical Engineering and Information Technology, RWTH Aachen University & Vice President of Research and Development AIXTRON AG, Aachen

- Prof. Dr. Michael Kneissl
  Institute of Solid State Physics, Technische Universität Berlin

- Prof. Dr. Jürgen Reif
  Institute of Physics and Chemistry, Brandenburgische Technische Universität BTU Cottbus

- Dr. Ulrich Steegmüller
  Head of Research and Technology OSRAM Opto Semiconductors GmbH, Regensburg

- Prof. Dr. Eicke Weber
  Fraunhofer Institute for Solar-Energy-Systems ISE, Freiburg

Representative of the State of Berlin
- Dr. Katharina Spiegel, Marie Trappiel
  Senatsverwaltung für Wirtschaft, Technologie und Forschung, SenWTF Berlin

Representative of the Federal Republic
- Dr. Klaus Heller
  Bundesministerium für Bildung und Forschung, BMBF Bonn / Berlin

Guests
- Dr. Manuela Urban
  Forschungsverbund Berlin e.V.

- Prof. Dr. Martha Ch. Lux-Steiner
  Helmholtz-Zentrum für Materialien und Energie HZB, Berlin

Report of the IKZ Summer School 2013

Bericht über die IKZ-Sommerschule 2013

Professor Dr. Jörg Weber of the Technical University Dresden was engaged as the lecturer for this year's IKZ Summer School which was held in the period October 7-9, 2013 at the IKZ. The topic of this Summer School was "(Point) Defects in Crystals". Prof. Jörg Weber holds the chair for semiconductor physics at the TU Dresden since 1999, after being an assistant of Prof. Queisser at the Max-Planck-Institute for Solid State Research in Stuttgart. He is engaged in the study of impurities and defects in various semiconductors. His present area of specialization is the study of hydrogen in various hosts and its importance in device technology. Since 2013, Prof. Jörg Weber is director of the Institute of Applied Physics of the TU Dresden. He was Coeditor of several special issues of "Applied Physics" and chaired several meetings and workshops. Since 1984, he organizes the yearly workshop on "Point Defects in Semiconductors" in Dresden.

It is well known that many properties crucial for the application of a material are based on defects – selective doping with impurity atoms brought into the crystal as point defects may serve as one prominent example. Other defects manifest themselves as a local disturbance of the lattice, e.g. vacancies, interstitials, and defect complexes. Since defects directly influence the electrical and optical properties, their understanding and, eventually, control is essential for many semiconductor applications. It becomes obvious, why this topic is of high importance for material scientists and crystal growers. Therefore, the summer school met a high interest in the scientific community and we were pleased to welcome 15 external guests, some of them travelling to Berlin just to attend the course.

A defect always interacts with the host lattice, and there is no suitable "microscope" to observe the resulting structure of the defect directly. The simultaneous presence of a variety of different defects and defect configurations significantly impedes any unambiguous assignment. As a consequence, a number of defects are still unidentified even in the most investigated materials such as silicon. That means that many of the properties observed could not yet be assigned to a distinct structure or contamination, and thus not be selectively regulated and controlled.

Für die 7. IKZ-Sommerschule, die im Zeitraum 7.-9. Oktober 2013 stattfand, konnte Prof. Dr. Jörg Weber von der Technischen Universität Dresden als Vortragender zu dem Thema „(Punkt-)Defekte in Kristallen" gewonnen werden. Prof. Jörg Weber ist seit 1999 Lehrstuhlinhaber für Halbleiterphysik an der TU Dresden, davor war er langjähriger Mitarbeiter von Prof. Queisser am Max-Planck-Institut für Festkörperforschung in Stuttgart. Er untersucht Verunreinigungen und Defekte in verschiedenen Halbleitern. Aktuell erforscht er Wasserstoff in verschiedenen Materialumgebungen und dessen Relevanz in der Bauelementtechnologie. Prof. Jörg Weber ist seit 2013 Direktor des Instituts für Angewandte Physik der TU Dresden. Er war Co-Editor mehrerer Sonderausgaben von "Applied Physics" und organisiert seit 1984 die "Punktdefekttreffen" in Dresden.

Viele Halbleiteranwendungen beruhen auf der kontrollierten Einstellung von Defekten und damit verbunden der elektrischen und optischen Eigenschaften. So lassen Sich bestimmte Materialeigenschaften erst gezielt über (Punkt-)Defekte generieren, beispielsweise über die Dotierung – als das gezielte Einbringen von Fremdatomen in den Kristall. Aber auch Verunreinigungen beeinflussen die Materialeigenschaften, und weitere Defekte entstehen als lokale Störung des Kristallgitters, z.B. Leerstellen, Zwischengitteratome und Defektkomplexe. Entsprechend spielt das Thema Defekte für die Materialentwicklung und in der Kristallzüchtung eine große Rolle. Die Teilnahme von 15 externen, teils extra angereisten Gästen an dem Kurs spricht ebenfalls für das Interesse der Community an dieser Fragestellung.

Ein Defekt tritt immer in Wechselwirkung mit dem umgebenden Kristallgitter auf, und es gibt keine direkte Methode, mit der man die resultierende Struktur des Defekts sichtbar machen kann. Die gleichzeitige Anwesenheit oder Möglichkeit einer Vielzahl von Defekten und Defektkonfigurationen behindert eine eindeutige Zuordnung erheblich. So sind auch in den am besten untersuchten Materialien wie z.B. Silizium viele Defekte bislang nicht identifiziert worden. Das heißt, viele beobachtete Eigenschaften können noch immer nicht einer Struktur oder dem Einbau von Fremdatomen zugeordnet und damit auch gezielt eingestellt und kontrolliert werden.

Jörg Weber is an acknowledged expert on this topic, whose priority is not on the phenomenological view of defect generation during crystal growth, but on the semiconductor physics emphasizing identification and quantification of defects. During the five lessons of this summer school, we went into the details of how defects operate in a semiconductor and how to determine their structure and density. Only the combination of different characterization methods allows establishing the chemical-physical structure of a defect and hence to understand its effect. In the following lessons, Jörg Weber presented shallow and deep level defects, transition metals, and hydrogen in semiconductors. At this point we would like to thank him again cordially for his profound and demanding physical approach to this topic and the resulting high gain in knowledge for his listeners.

Jörg Weber ist ein Experte auf dem Gebiet der (Punkt-)Defekte, denen er sich nicht vorrangig im Sinne einer phänomenologischen Betrachtung der Defektgeneration während des Kristallwachstums widmet, sondern aus der Warte der Halbleiterphysik, die den Fokus auf die Defektidentifikation und -quantifizierung legt. In den fünf Doppelstunden der Sommerschule wurde ausführlich darauf eingegangen, welche Wirkung Defekte im Halbleiter haben und wie man ihre Struktur und Konzentration bestimmen kann. Nur durch die Kombination unterschiedlicher Charakterisierungsmethoden ist es schließlich möglich, die chemisch-physikalische Struktur eines Defekts nachzuweisen und damit auch seine Wirkung zu verstehen. In den folgenden Doppelstunden stellte Jörg Weber flache und tiefe Störstellen, Übergangsmetalle und Wasserstoff in Halbleitern vor. Für seine anspruchsvolle und tiefgehende physikalische Betrachtungsweise der Thematik und den dadurch hohen Erkenntnisgewinn für die Zuhörenden danken wir dem Vortragenden an dieser Stelle noch einmal herzlich.

Awarded

Ausgezeichnet

In 2013, B. Sc. Franziska Schütte has been awarded by The Association of German Engineers VDI Berlin-Brandenburg for her bachelor's degree. She performed her thesis in IKZ group "Si/Ge-Nanocrystals". Franziska Schütte graduated at Brandenburgisch-Technische Hochschule BTU Cottbus-Senftenberg, Physics Department.

Frau B. Sc. Franziska Schütte wurde 2013 für ihren Bachelor-Abschluss im Fachbereich Physik der Brandenburgisch-Technischen Hochschule BTU Cottbus-Senftenberg mit dem Absolventenpreis des Vereins Deutscher Ingenieure VDI Berlin-Brandenburg ausgezeichnet. Frau Schütte fertigte ihre Bachelor-Arbeit in der Gruppe „Si/Ge-Nanokristalle" am IKZ an.

Dr. Jan Schmidtbauer received his Ph.D. degree at Brandenburgisch-Technischen Hochschule Cottbus-Senftenberg with honors. He prepared his thesis on „MBE Growth and Characterization of Germanium Nanowires" at IKZ group "Si/Ge-Nanocrystals", where he currently continues his research.

Herr Dr. Jan Schmidtbauer hat seine Promotion zu dem Thema „MBE Growth and Characterization of Germanium Nanowires" in 2013 an der Brandenburgisch-Technischen Hochschule Cottbus-Senftenberg mit Auszeichnung abgeschlossen. Herr Dr. Schmidtbauer führte seine Arbeiten in der Gruppe „Si/Ge-Nanokristalle" durch, in der er das Forschungsthema derzeit weiter bearbeitet.

Professional education at IKZ

Ausbildung am IKZ

The institute engages in education, not only by supervising and supporting graduating students during their theses, but also by training for different professions. Currently, four apprentices are working at IKZ and are preparing to become office executive, cutting machine operator, IT system technician and as electronics technician for administration and maintenance.

In 2013, our first apprentice as office executive, Wiebke Fruwert, completed her training successfully.

Neben der Betreuung von wissenschaftlichen Graduierungsarbeiten bildet das Institut auch in Lehrberufen aus. Derzeit bereiten sich vier Auszubildende am Institut auf die Berufsbilder Zerspanungsmechaniker, Bürokauffrau, Informatiker Systemtechnik und Elektroniker für Betriebstechnik vor.

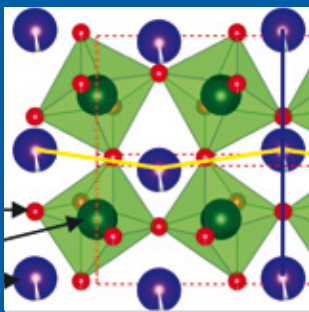In 2013 konnte Frau Wiebke Fruwert ihre Ausbildung zur Bürokauffrau am Institut mit Erfolg abschließen.

Highlights

Bulk growth and epitaxy of ß-Ga$_2$O$_3$ for transparent electronics application

Arrangement of ferroelectric domains in strained NaNbO$_3$ thin films

Bulk growth and epitaxy of ß-Ga$_2$O$_3$ for transparent electronics application

**Kristallzüchtung und Epitaxie von ß-Ga$_2$O$_3$ für die transparente Oxid-Elektronik**

Transparent electronics is currently one of the hot topics for a wide range of device applications. The key components are wide bandgap semiconductors, where oxides with different compositions play an important role. The compound semiconductor system based on the so-called sesquioxides gallium oxide (Ga$_2$O$_3$) and indium oxide (In$_2$O$_3$) has an enormous potential to pioneer new transparent semiconductor device technologies. Among them, the ß phase of gallium oxide (ß-Ga$_2$O$_3$) is particularly interesting because of its extended transparency up to the deep ultraviolet wavelength range as the result of its wide bandgap of 4.8 eV. The application of ultraviolet light is increasing in the fields of lithography, surface modification, anion generation, sterilization, and curing, thus enhancing the importance of materials compatible with deep UV optics. Therefore, ß-Ga$_2$O$_3$ is a new attractive semiconductor material for ultraviolet (UV) optoelectronic devices such as solar blind photo detectors [1,2].

Another very important application is the next generation of power devices such as inverters for photovoltaics and automotive. The wide bandgap of ß-Ga$_2$O$_3$ can provide a very high breakdown voltage (8 MV/cm), which allows to minimize switching losses in high power and high voltage electronics. Furthermore, ß-Ga$_2$O$_3$ may become an attractive substrate for the fabrication

Der Einsatz transparenter Elektronik in elektronischen Geräten ist derzeit ein vielbeachtetes Thema. Die Schlüsselkomponenten dazu sind Halbleiter mit großer Bandlücke, in diesem Fall konzentriert sich die Forschung vor allem auf Oxid-Halbleiter. Das Potential, neuartige Bauelemente und Technologien mit transparenten Halbleitern aufzubauen, wird dabei vor allem in Halbleitersystemen gesehen, die auf sogenannten Sesquioxiden wie z.B. Gallium- (Ga$_2$O$_3$) oder Indiumoxid (In$_2$O$_3$) basieren. Das Interesse konzentriert sich dabei hauptsächlich auf die ß-Phase des Galliumoxids (ß-Ga$_2$O$_3$), da diese aufgrund der großen Bandlücke von 4,8 eV bis in den tiefen Ultaviolett (UV)-Wellenlängenbereich hinein lichtdurchlässig (transparent) ist. Die Anwendung von UV-Licht zur Lithographie, Oberflächenbehandlung, Desinfektion/Sterilisation, Generation von Ionen und zur Polymerisation von Kunststoffen (z.B. Lackhärtung) wird heutzutage immer wichtiger, und deshalb nimmt auch die Bedeutung von UV-kompatiblen Materialien ständig zu. Somit ist ß-Ga$_2$O$_3$ ein attraktives Halbleitermaterial für die Anwendung in der UV-Optoelektronik, wie zum Beispiel für „sonnenblinde" Photodetektoren [1,2].

Eine weitere bedeutende Anwendungsmöglichkeit besteht in der Leistungselektronik der nächsten Generation, z.B. Inverter für die Photovoltaik oder für die Elektromobilität. Aufgrund der großen Bandlücke von ß-Ga$_2$O$_3$ werden Bauelemente mit sehr hoher Durchbruchspannung (8 MV/cm) und somit noch geringeren Schaltverlusten in der Hochleistungs- und Hochspannungelektronik möglich. ß-Ga$_2$O$_3$ könnte zudem ein attraktives Substratmaterial für die Herstellung effizienter, vertikal strukturierter Leuchtdioden (LEDs) werden, so sind GaN-basierte blaue LEDs [3] denkbar, die ß-Ga$_2$O$_3$-Substrate und/oder -Epitaxieschichten verwenden. Transistoren basierend auf ß-Ga$_2$O$_3$ könnten die Qualität heutiger Flachbildschirme verbessern, indem sie für eine klarere und hellere Hintergrundbeleuchtung sorgen. Auch viele weitere elektronische Geräte haben durchsichtige Bereiche, die mit neuen Schaltkreisen und Funktionen ausgestattet werden könnten. Transparente Elektronik kann in Fensterglas oder in Windschutzscheiben eingebaut werden und damit neue Funktionalitäten erzeugen oder Informationen sichtbar darstellen. All

1 cm
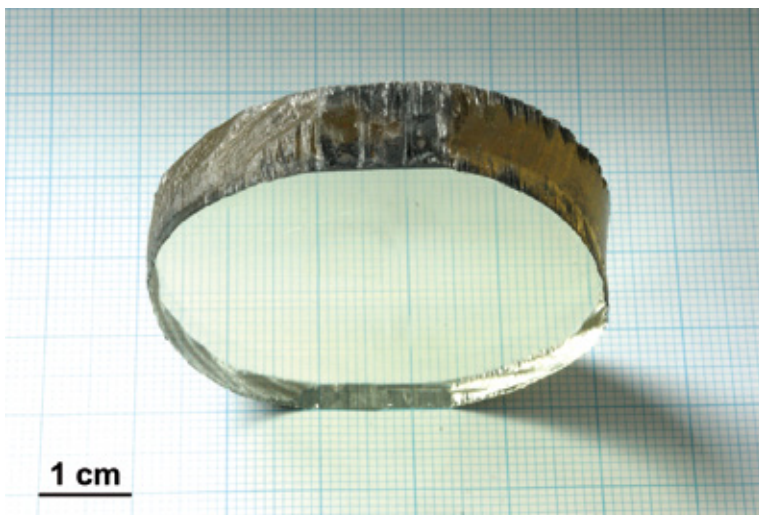
of efficient high-brightness vertically structured light emitting diodes (LEDs), e.g. GaN-based blue LEDs [3] using ß-Ga$_2$O$_3$ epitaxial layers and substrates. ß-Ga$_2$O$_3$ based transparent transistors might improve the quality of flat panel displays, making the displays more clear and bright. Many electronic devices such as flat panel displays have transparent areas which could accommodate new circuits or functions. Transparent electronic devices built into window glass or the windshield of a vehicle allowing a range of new functions or the transmission of visual information, will benefit from the superior performance of this single-crystalline semiconducting material.

From the technological point of view, ß-Ga$_2$O$_3$ single crystal substrates can be fabricated from bulk crystals grown from the melt e.g. by the optical floating zone (OFZ), the edge-defined film-fed growth (EFG), and the Czochralski (CZ) methods [4-6]. The OFZ technique has proved very useful for laboratory-scale studies, but its application is limited to crystals of 1 inch in diameter due to the optical heating. To increase the single crystal diameter to 2 inch, which is considered the minimum diameter required for industrial scale production, the EFG technique provides an alternative. This method utilizes an inductively heated iridium crucible containing molten Ga$_2$O$_3$ and a die located on the top of the crucible with well defined slits. The melt is transported to the top of the die by capillary forces where a crystal seed is contacted and pulled upwards. Temperature gradients above the die allow for crystallization of the melt on the crystal seed to form single crystal ribbons. The reported dimensions for the crystal ribbons were 3 mm, 50 mm, and 70 mm for the thickness, width, and length, respectively. The crystalline perfection of these ß-Ga$_2$O$_3$ crystals is acceptable and their capability for the development of power device has been demonstrated.

Nevertheless, a large crystal volume and high crystal quality is required for mass production. These conditions are typically satisfied in a better way by the Czochralski method, if a crystal can be grown by that technique. As an example, this method is used to fabricate large silicon crystals of 300–450 mm in diameter and 2 meters in length. At the Leibniz-Institute for Crystal Growth (IKZ) we developed a Czochralski based technology for growing bulk ß-Ga$_2$O$_3$ single crystals with reasonably low cost and energy consumption. This method provides crystals of high quality and purity, and can be scaled up to large diameters (probably up to 3 inch) that exceed the accessible range of other techniques.

In this technology, the Ga$_2$O$_3$ starting material is molten in an inductively heated iridium crucible at around 1820°C under a growth atmosphere containing CO$_2$. Due to the temperature-dependent CO$_2$/CO equilibrium, this atmosphere is dynamic and self adjusting in respect to the oxygen partial pressure in the system. That way, crystals can be grown in an oxidizing atmos-

diese Anwendungen können von der überlegenen Performance profitieren, die dieses einkristalline Halbleitermaterial bietet.

Einkristalline ß-Ga$_2$O$_3$ Substrate können durch Schmelzzüchtung hergestellt werden z.B. mittels optischem Zonenschmelzen (Optical Floating Zone OFZ), mittels der Edge-Defined Film-Fed Growth (EFG) Methoder oder mittels dem Czochralski-Verfahren [4-6]. Das optische Zonenschmelzen hat sich in Laborstudien bewährt, aber aufgrund der optischen Heizung ist die Anwendung auf die Herstellung von Kristallen mit maximal 1 Zoll Durchmesser beschränkt. Für die Herstellung von Kristallen mit 2 Zoll Durchmesser (als relevanter Mindestdurchmesser für die industrielle Produktion) kommt die EFG-Züchtung in Betracht. Bei dieser Methode wird ein induktiv geheizter Tiegel aus Iridium verwendet, auf dessen Oberfläche ein Formgeber mit einer definierten Anordnung von Schlitzen angebracht ist. Aufgrund der Kapillarkräfte wandert die Schmelze durch die Schlitze und wird oberhalb des Formgebers an den Keim kontaktiert. Durch Herausziehen des Keims entstehen durch den Kristallisationsprozess in einem geeigneten Temperaturfeld Keims bandförmige Einkristalle. Die flachen Kristalle werden bis zu 3 mm dick, bei einer Oberfläche von bis zu 50 mm x 70 mm. Die strukturelle Qualität der so hergestellten Einkristalle ist akzeptabel und die Herstellung von Leistungsbauelementen auf diesen Kristallen konnte erfolgreich demonstriert werden.

Für eine Massenfertigung wird ein großes Kristallvolumen bei hoher Kristallqualität benötigt. Diese Bedingungen werden generell besser mit dem Czochralski-Verfahren erreicht, sofern diese Züchtungsmethode anwendbar ist. Großtechnisch lassen sich beispielsweise 2 Meter lange Siliziumkristalle mit Durchmessern von 30–45 cm mit diesem Verfahren herstellen. Am Leibniz-Institut für Kristallzüchtung (IKZ) wurde ein Czochralski-Verfahren entwickelt zur kostengünstigen und energieeffizienten Herstellung von ß-Ga$_2$O$_3$-Volumenkristalle. Die auf diese Weise hergestellten Kristalle besitzen eine gute strukturelle Qualität und hohe Reinheit, und das Verfahren bietet im Gegensatz zu anderen Methoden auch die Möglichkeit für die Züchtung größerer Kristalle (ggf. bis zu 75 mm Durchmesser).

In diesem Verfahren wird Ga$_2$O$_3$ als Rohmaterial in einem induktiv geheizten Iridiumtiegel in einer CO$_2$-haltigen Atmosphäre bei etwa 1820°C aufgeschmolzen. Durch das temperaturabhängige CO$_2$/CO-Gleichgewicht passt sich die Züchtungsatmosphäre dynamisch dem Sauerstoffpartialdruck im System an. Dadurch wächst der Kristall in einer oxidierenden Atmosphäre, während gleichzeitig die Iridiumteile, die bei niedrigeren Temperaturen schnell oxidieren, nicht angegriffen werden. Dennoch hat der (begrenzt einstellbare) Sauerstoffpartialdruck im Züchtungsraum Auswirkungen auf die Zersetzung und damit auch auf die Zusammensetzung des wachsenden ß-Ga$_2$O$_3$-Einkristalls. Diese wiederum beeinflusst die elektrischen und optischen Eigenschaf-

1 cm

phere while the iridium components, which easily oxidize at low and moderate temperatures, are not attacked. Still, the oxygen partial pressure in the growth chamber (provided by any means) affects the decomposition rate of ß-Ga$_2$O$_3$ and thus its stoichiometry, which in turn influences the electrical and optical properties of the obtained crystals and thus also the crystal coloration. Other factors that influence growth behavior and properties of the crystals are the initial stoichiometry of the starting material, temperature gradients in the crystal growth furnace, convection and evaporation of the melt surface, the growth atmosphere, intentional doping (or unintentional impurities) and operating parameters. As a consequence, optimization of growth conditions is a quite complex task [7]. Regarding the controllability of electrical properties, it was found that Mg doping leads to insulating behavior, while n-type behavior can be modified in a wide spectrum by growth condition, doping with Sn and/or by proper annealing [7, 8].

Today, we are able to grow ß-Ga$_2$O$_3$ crystals of 20–22 mm in diameter and 50–80 mm in length reproducibly and our research focuses on single crystal diameter enlargement. Recently, we achieved the growth of a crystal with 2 inch in diameter [7], but upscaling the process still suffers from various growth issues and requires further optimization. The high structural quality of the ß-Ga$_2$O$_3$ single crystals obtained by the Czochralski technology developed at the IKZ is characterized by typical values of the rocking curve full width at half maximum (FWHM) measured on the (100) plane of around 50-100 arcsec and an etch pit density (EPD) at the level not exceeding 5000 cm^{-2}. Both values are comparable of even better than the ones of crystals obtained by the EFG method.

ß-Ga$_2$O$_3$ has a monoclinic crystal structure, i.e., the properties depend on the crystal orientation. As a consequence, ß-Ga$_2$O$_3$ exhibits two cleavage planes parallel to {100} and {001}. This means that growing the crystals by the Czochralski method along [100] and [001] axis is rather not possible, due to easy cleavage and blistering of the seed. Therefore the growth is conducted along the [010] direction which is parallel to both cleavage planes. Note that due to the differences in growth technology resulting in "flat" crystals, available orientations

ten des Kristalls und damit auch dessen Färbung. Die Kristallzüchtung wird zudem auch durch die Stöchiometrie des Rohmaterials, die Temperaturverteilung im Züchtungsraum, die Konvektion und Abdampfrate der Schmelzoberfläche, die Zusammensetzung der Atmosphäre, gezielte Dotierung (bzw. Einfluss von Verunreinigungen) und den Prozessparametern beeinflusst. Als Folge davon ist die Optimierung der Wachstumsbedingungen komplex [7]. Die elektrischen Eigenschaften sind dagegen gut kontrollierbar: Eine Dotierung mit Magnesium führt zu semi-isolierendem Verhalten, die n-Leitfähigkeit kann dagegen in einem breiten Ladungsträgerkonzentrationsbereich durch die Wachstumsbedingungen, eine Dotierung mit Zinn und/oder gezielte Temperung eingestellt werden [7,8].

Zurzeit werden am IKZ ß-Ga$_2$O$_3$-Einkristalle mit 20–22 mm Durchmesser und 50–80 mm Länge reproduzierbar hergestellt. Im Fokus der Entwicklung steht die Durchmesseraufweitung. Kürzlich ist es uns gelungen, einen Kristall mit 2 Zoll Durchmesser herzustellen [7], aber der Prozess der Durchmesseraufweitung ist noch mit einigen Züchtungsproblemen verbunden und erfordert weitere Optimierung. Typische Halbwertsbreiten der Rockingkurve gemessen auf der (100)-Fläche von 50–100 arcsec sowie Versetzungsdichten unterhalb von 5000 cm^{-2} zeigen, dass die mit dem am IKZ entwickelten Czochralski-Verfahren gezüchteten Kristalle eine hohe strukturelle Qualität aufweisen. Beide Werte sind vergleichbar oder besser als die Werte, die an mittels EFG-Verfahren hergestellten Kristallen gemessen wurden.

ß-Ga$_2$O$_3$ besitzt eine monokline Kristallstruktur, d.h. die Eigenschaften sind von der Kristallorientierung abhängig. Als Folge davon besitzt ß-Ga$_2$O$_3$ zwei Spaltebenen parallel zu den {100}- und {001}-Flächen. Dadurch ist die Züchtung von Kristallen mit dem Czochralski-Verfahren entlang der [100]- and [001]-Richtungen nicht oder zumindest nur schwer möglich, da der Keim leicht abplatzt. Die Züchtung erfolgt deshalb in [010]-Richtung parallel zu den Spaltebenen. Aufgrund der unterschiedlichen Züchtungstechnologie führt die EFG-Züchtung dagegen ausschließlich zu flachen Kristallen und ß-Ga$_2$O$_3$-Substraten mit {100} oder {-210}-Oberflächen.

Am IKZ besteht die einzigartig günstige Möglichkeit, die Züchtung von Einkristallen mit hoher kristalliner Perfektion, die Präparation von einkristallinen Substraten und die Abscheidung von epitaktischen Schichten mit kontrollierten elektrischen Eigenschaften miteinander zu kombinieren. Darüber hinaus verfügt das IKZ über eine große Vielfalt von analytischen Methoden und Verfahren zur Bestimmung der strukturellen und elektrischen Eigenschaften dieser neuen Klasse von Halbleitern.

Erst vor einigen Jahren wurde die homoepitaktische Abscheidung dünner ß-Ga$_2$O$_3$-Schichten auf Ga$_2$O$_3$-Substraten durch Molekularstrahl-Epitaxie (MBE) beschrieben [9-11]. Die auf dieser Basis hergestellten Schottky-Dioden und Feldeffekttransitoren demons-

of ß-Ga$_2$O$_3$ wafers grown by EFG are currently restricted to {100} or {-210} surfaces.

At the IKZ, we have the unique possibility to combine growth of high quality bulk ß-Ga$_2$O$_3$ single crystals with subsequent homoepitaxial deposition of ß-Ga$_2$O$_3$ layers with controlled electrical properties. Additionally, the IKZ hosts a wide spectrum of analytical methods to study the structural and electrical properties of this new class of semiconductors.

In recent years, homoepitaxy of ß-Ga$_2$O$_3$ thin films by molecular beam epitaxy (MBE) [9–11] clearly demonstrated the feasibility of Schottky barrier diodes and field-effect transistors (FETs) fabrication on ß-Ga$_2$O$_3$ substrates. In contrast, metal organic vapour phase epitaxy (MOVPE), which is more suitable for large scale production, was reported only on foreign substrates such as sapphire. So far, ß-Ga$_2$O$_3$ homoepitaxy by MOVPE is performed only at the IKZ. After starting the deposition of ß-Ga$_2$O$_3$ on c-oriented sapphire substrates in 2012, the first successful homoepitaxial deposition of ß-Ga$_2$O$_3$ on homemade substrates was achieved in 2013 [12]. Furthermore, adding indium provides the possibility to adjust the band gap of the layers.

The epitaxial growth is performed in a commercial vertical low-pressure MOVPE system with pure argon (Ar) as carrier gas. Trimethylgallium (TMGa) and water vapour (H$_2$O) are used as precursors for Ga and O, respectively. The structural properties of the ß-Ga$_2$O$_3$ layers are analysed in close cooperation with the Physical Characterization and Electron Microscopy groups at the IKZ by means of high resolution X-ray diffraction and transmission electron microscopy. In addition, spectroscopic ellipsometry, atomic force microscopy, and scanning electron microscopy investigations are used to determine the layer thickness and composition and to reveal the surface morphology of the epitaxial layers. When using water vapour as oxidant, we succeeded to grow coherent monocrystalline layers. The presence of hydrogen in the reactor showed a positive effect on the kinetic conditions of the substrate surface, supporting the growth of smooth layers. However, the crystalline quality of the layers was disturbed by the presence of stacking faults and disorder, leading to enlargement of the lattice parameter in [110].

trierten beeindruckend die Eignung und das große Potential dieser Halbleiterverbindung. Im Gegensatz dazu konnten bislang mittels der Metallorganischen Gasphasenepitaxie (MOVPE) – ein bei der Produktion mikroelektronischer Bauelemente etabliertes Verfahren – ß-Ga$_2$O$_3$-Schichten nur auf artfremden Substraten, wie zum Beispiel auf Saphir, abgeschieden werden. Bisher wird die Homoepitaxie von Ga$_2$O$_3$ mit dem MOVPE Verfahren nur am IKZ durchgeführt. Beginnend mit der Abscheidung und Untersuchung von Ga$_2$O$_3$-Schichten auf Saphir in 2012, gelang in 2013 erstmals die Herstellung homoepitaktischer Schichten auf im IKZ gezüchteten Ga$_2$O$_3$-Kristallen bzw. Substraten [12]. Die Zugabe von Indium ermöglicht es dabei zusätzlich, auch die Bandlücke der Schichten gezielt zu variieren.

Für das homoepitaktische Wachstum wird ein kommerzielles vertikales MOVPE System verwendet. Die Schichten werden bei niedrigem Druck und unter Einsatz von Argon als Trägergas abgeschieden. Trimethylgallium (TMGa) und ultrareiner Wasserdampf (H$_2$O) werden als Ausgangsmaterialien für Gallium und Sauerstoff verwendet. Die strukturellen Eigenschaften der Ga$_2$O$_3$-Schichten werden in enger Kooperation mit den IKZ-Gruppen „Physikalische Charakterisierung" und „Elektronenmikroskopie" durch hochaufgelöste Röntgenbeugung und Transmissionselektronenmikroskope ermittelt. Darüber hinaus werden die Schichten mit spektroskopischer Ellipsometrie, Atom-Kraft-Mikroskopie (AFM) und Raster-Elektronen-Mikroskopie (SEM) charakterisiert um Informationen über die Schichtdicke, die Zusammensetzung und die Oberflächenmorphologie zu erhalten. Durch die Verwendung von ultrareinem Wasserdampf als Sauerstoffquelle konnten wir erfolgreich geschlossene, einkristalline Schichten abscheiden. Die Anwesenheit von Wasserstoff während der Schichtabscheidung hat dabei einen positiven Effekt auf die kinetischen Bedingungen an der Substratoberfläche. Dadurch wird das Wachstum einer glatten, geschlossenen Epitaxieschicht wesentlich unterstützt. Die Analyse der kristallinen Perfektion der Schichten ergab Stapelfehler und Zwillingskorngrenzen als wesentliche Defekte, die Ursache für eine verstärkte vertikale Fehlordnung darstellen. Diese Fehlordnung äußert sich in einer Vergrößerung der Gitterkonstante in [100].

By injecting a sufficiently high amount of indium (In) precursors into the reactor, a significant reduction of the defect density was detected. The concentration of structural defects like stacking faults and twins decreased dramatically. The main defects in the grown (Ga$_{1-x}$In$_x$)$_2$O$_3$ layers were found to be growth striations corresponding to surface terraces which are formed as a result of step flow growth and step-bunching. These results can be explained by the tendency of indium to float on the growing ß-Ga$_2$O$_3$ surface without significant alloying, which modifies the growth mode by changing surface energy and surface kinetics such as the diffusion of Ga and O adatoms. In this way, the indium has an effective surfactant effect.

In order to adjust its energy gap, ß-Ga$_2$O$_3$ can be alloyed with In$_2$O$_3$ which is characterized by an optical bandgap of 3.75 eV. The growth of (Ga$_{1-x}$In$_x$)$_2$O$_3$ epitaxial layers is performed on sapphire (0001) substrates by using H$_2$O as oxygen source and trimethylgallium (TMGa) as well as trimethylindium (TMIn) as metal precursors. In the gas phase, TMIn directly reacts with H$_2$O and the resulting compounds either desorb too fast from the layers to be incorporated or are directly expelled through the exhaust system. As a consequence, the reactor base pressure was increased to values between 50 and 200 mbar in order to minimize the desorption process. In this pressure range, the In incorporation is proportional to the amount of TMIn introduced into the reactor. But since the growth rate decreases with increasing pressure as well as increasing TMIn flux, a compromise must be achieved in order to grow layers with a definite amount of In with a reasonable growth rate. Under the above-mentioned experimental conditions, the solubility limit of In in (Ga$_{1-x}$In$_x$)$_2$O$_3$ is found to be roughly at ~10% in atomic percent, corresponding to a partial In composition of x = 0.25. The mixed (Ga$_{1-x}$In$_x$)$_2$O$_3$ phase is evidenced by a shift towards smaller angles of the 2θ position of x-ray diffraction peaks in respect to the bulk ß-Ga$_2$O$_3$ values. Since the shift increases with In content, this phenomenon can be correlated to the increase of the lattice parameter of ß-Ga$_2$O$_3$ due to the substitution of Ga^{3+} (r_{ion}=0.62 Å) with In^{3+} (r_{ion}=0.81 Å). At In contents exceeding the solubility limit, phase separation occurs due to the different crystallographic systems of monoclinic ß-Ga$_2$O$_3$ and cubic In$_2$O$_3$.

Summarizing, the IKZ research teams are actively pursuing their study of ß-Ga$_2$O$_3$, In$_2$O$_3$ (not shown here) and (Ga$_{1-x}$In$_x$)$_2$O$_3$ compounds as bulk crystals and epitaxial layers that could have a function as a key material for a new class of transparent electronic devices. Research activities focus on enlargement of diameter to technological relevance in bulk crystal growth as well as on the deposition of high quality layers with precisely defined electronic properties. These activities are supported the institute's characterization groups. This synergy provides excellent research opportunities and will accelerate the development of new applications in oxide electronics.

Durch die Zugabe einer geringen Menge von Indium in den Reaktor während der Schichtabscheidung wurde eine erhebliche Abnahme der Defektdichte in den Schichten beobachtet. Die Konzentration von Stapelfehlern und Zwillingen verringerte sich stark. Als Hauptdefekte in den abgeschiedenen (Ga$_{1-x}$In$_x$)$_2$O$_3$ Schichten sind Wachstums-Striations zu beobachten. Diese sind auf Terrassen auf der Substratoberfläche, in Folge einer leichten Abweichung von der [100] Orientierung, zurückzuführen. Durch das Angebot an Terrassenstufen auf der Wachstumsfläche wird ein Stufenfluss-Modus möglich, welcher bei unterschiedlichen Stufenfluß-Geschwindigkeiten zu einem „Step-bunching„-Prozess führt. Diese beobachteten Effekte bei der Schichtabscheidung werden durch eine Anreicherung von Indium an der Wachstumsfront interpretiert, das sich in äußerst geringer Konzentration in die wachsende Schicht einbaut. Durch die Anreicherung von Indium vor der Wachstumsfront wird die Oberflächenenergie und die Oberflächenkinetik, wie zum Beispiel die Oberflächendiffusion von Ga- und Sauerstoffatomen, beeinflusst. Die Anwesenheit von In vor der Wachstumsfront hat einen oberflächenaktiven Effekt, der zu einem Übergang von einem zwei- bzw. dreidimensionalen Keimwachstum zu einem Stufenfluss-Wachstum beiträgt.

Um den Bandabstand zu verändern, wurde während der Abscheidung von Ga$_2$O$_3$ -Schichten In$_2$O$_3$ hinzu legiert, das eine optische Bandlücke von 3,75 eV besitzt. Die Abscheidung von (Ga$_{1-x}$In$_x$)$_2$O$_3$ Epitaxieschichten wurde zuerst auf Saphir (0001)-Substraten realisiert. Als Sauersoff, In- und Ga-Quellen wurden Wasserdampf, Trimethylindium (TMIn) und Trimethylgallium verwendet.

In der Gasphase reagiert bevorzug TMIn mit Wasserdampf. Wegen des höheren Dampfdruckes desorbieren die entstehenden In-Komponenten jedoch sehr schnell von der Wachstumsfläche oder werden direkt aus dem Reaktor abgeführt. Um diesem Effekt entgegenzuwirken wurde der Reaktordruck bei der Schichtabscheidung auf Werte zwischen 50 mbar und 200 mbar erhöht. Dadurch wurde die Desorption der In-Komponenten reduziert. In diesem Druckbereich ist der In-Einbau in den Schichten proportional zum TMIn-Fluss in den Reaktor. Gleichzeitig wurde eine Abnahme der Wachstumsgeschwindigkeit mit ansteigenden Reaktordruck und zunehmendem TMIn-Fluss beobachtet. Zur Abscheidung von (Ga$_{1-x}$In$_x$)$_2$O$_3$ Epitaxieschichten wurden Abscheideparameter ermittelt, die einen Kompromiss zwischen der eingebauten In-Konzentration und einer praktikablen Wachstumsgeschwindigkeit darstellen. Bei geeigneter Wahl der Abscheidebedingungen wurde eine maximale In Löslichkeit in (Ga$_{1-x}$In$_x$)$_2$O$_3$ Epitaxieschichten von 10 at% erreicht, was einen Molenbruch von x=0,25 entspricht. Die Existenz einer homogenen Mischphase von (Ga$_{1-x}$In$_x$)$_2$O$_3$ wurde durch eine Verschiebung der typischen Röntgenbeugungsreflexe der Schichten hin zu kleineren 2θ–Beugungswinkeln verglichen mit denen des Ga$_2$O$_3$-Einkristalls nachgewiesen. Da die Peak-Verschiebung mit steigenden

References

[1] Y. Kokubun, K. Miura, F. Endo, S. Nakagomi, Appl. Phys. Lett. 90, 031912 (2007)

[2] T. Oshima, T. Okuno, N. Arai, N. Suzuki, S. Ohira, and S. Fujita, Appl. Phys. Express 1, 011202 (2008)

[3] K. Shimamura, E. G. Víllora, K. Domen, K. Yui, K. Aoki, and N. Ichinose, Jpn. J. Appl. Phys. 44, L7 (2005)

[4] Z.Galazka, R. Uecker, K. Irmscher, M. Albrecht, D. Klimm, M. Pietsch, M. Brutzam, R. Bertram, S. Ganschow, R. Fornari, Cryst. Res. Technol. **45,** 1229 (2010)

[5] E. G. Víllora, K. Shimamura, Y. Yoshikawa, K. Aoki, and N. Ichinose, J. Crystal Growth 270, 420 (2004)

[6] H. Aida, K. Nishiguchi, H. Takeda, N. Aota, K. Sunakawa, and Y. Yaguchi, Jpn. J. Appl. Phys. 47, 8506 (2008)

[7] Z. Galazka, K. Irmscher, R. Uecker, R. Bertram, M. Pietsch, A. Kwasniewski, M. Naumann, T. Schulz, R. Schewski, D. Klimm, M. Bickermann, J Crystal Growth (2014) manuscript in press, DOI: 10.1016/jcrysgro.2014.07.021

[8] K. Irmscher, Z. Galazka, M. Pietsch, R. Uecker, R. Fornari, J. Appl. Phys. 110, 063720 (2011)

[9] T. Oshima, S. Fujita, Phys. Stat. Sol. C 5, 3113 (2008)

[10] M. Higashiwaki, K. Sasaki, A. Kuramata, T. Masui, S. Yamakoshi, App. Phys. Lett. 100, 013504 (2012)

[11] M. Tsai, O. Bierwagen, M.E. White, J.S. Speck, J. Vac. Technol.A, 28, 354 (2010)

[12] G. Wagner, M. Baldini, D. Gogova, M. Schmidbauer, R. Schewski, M. Albrecht, Z. Galazka, D. Klimm, R. Fornari, Phys. Status Solidi A 211, 27 (2014)

In-Gehalt in den Schichten zunimmt, kann dieser Effekt mit einer Vergrößerung der Gitterparameter und damit durch den Einbau von Indium in Ga$_2$O$_3$ durch die Substitution von Ga^{3+} (r$_{ion}$=0,62 Å) mit In^{3+}(r$_{ion}$=0,81 Å) erklärt werden. Wenn die In-Konzentration die Löslichkeitsgrenze von 10 at% überschreitet, findet eine Phasenseparation in ß-Ga$_2$O$_3$ und In$_2$O$_3$ statt, verursacht durch die unterschiedlichen kristallographischen Systeme von monoklinem Ga$_2$O$_3$ und kubischem In$_2$O$_3$.

Als Resümee der zuvor gemachten Erläuterungen lässt sich zusammenfassen, dass sich ß-Ga$_2$O$_3$, In$_2$O$_3$ und ternäre (Ga$_{1-x}$In$_x$)$_2$O$_3$ Verbindungen als mögliche Schlüsselmaterialien für eine neue Klasse von transparenten Halbleiterbauelementen darstellen. Die Forschungen im IKZ in diesem Umfeld konzentrieren sich auf die Entwicklung von Technologien zur Züchtung von oxydischen Einkristallen in technologisch relevanten Größen und auf die Abscheidung defektarmer Schichten mit definierten elektronischen Eigenschaften. Beide Aktivitäten werden durch die im IKZ vorhandenen analytischen Methoden begleitet und qualifiziert. Die dabei erzeugten Synergieeffekte schaffen die Voraussetzung für eine Forschung auf höchstem Niveau und werden zur Beschleunigung der technologischen Entwicklung auf dem Gebiet der Oxidelektronik beitragen.

Arrangement of ferroelectric domains in strained NaNbO$_3$ thin films

Ausrichtung von ferroelektrischen Domänen in dünnen NaNbO$_3$ Schichten

Introduction

In epitaxial ferroelectric thin films, the inherent coupling between lattice strain and electrical polarization allows the engineering of the functional properties of the films by adequate choice of the substrate ("strain engineering"). It is now established that incorporation of lattice strain is a favorable strategy for tuning the characteristics of ferroelectric films, for example shift the Curie temperature, enhancement of the remnant polarization, transition from the para- to the ferroelectric state [1]. A further effect can be the generation of ferroelectric domains, which can provide an effective way to accommodate lattice strain. However, their size and symmetry as well as the nature of the domain walls have large impact on ferro- and piezoelectric properties of the films. Consequently, understanding and controlling of domains are essential for further application in nanometer sized electronic devices. Hence in recent years the interest in domain and domain walls properties have became one focus of fundamental research.

In ferroelectric epitaxial films formation of domains is the result of the balance between elastic energy, domain wall energy and electrostatic energy [2,3,4]. Beside the elemental composition and structural/compositional ordering epitaxial strain is used as a degree of freedom to tune domain configuration. Symmetry of the domain pattern, crystallographic orientation, size of the individual domains, and structure of the domain walls are strongly influenced by the incorporated lattice strain induced by the substrate.

Theoretical and experimental efforts have been undertaken to achieve a more detailed understanding of domain formation depending on lattice strain [4,5]. Most results refer to biaxial symmetric ('isotropic') strain in tetragonal films deposited on a cubic substrate. However, they do not consider the general case of biaxial non-symmetric ('anisotropic') in-plane strain which is often the case for orthorhombic perovskite materials systems, like for example the alkaline niobates [6,7]. The most interesting predictions of such stability diagrams for epitaxial perovskite ferroelectrics tend to be those for tensile in-plane strain [8,9], as compressive

Einleitung

Die inhärente Kopplung zwischen Gitterverspannung und elektrischer Polarisation in dünnen epitaktischen, ferroelektrischen Schichten erlaubt die gezielte Manipulation der funktionalen Eigenschaften der Schichten („Strain engineering"). Dies kann durch eine geeignete Wahl des Substrates erreicht werden. Der Einbau einer Gitterverspannung ist heutzutage eine anerkannte Methode, um die charakteristischen Eigenschaften von ferroelektrischen Schichten einzustellen. Dazu gehören z.B. die Verschiebung der Curie Temperatur, die Erhöhung der remanenten Polarisation oder der Übergang vom para- zum ferroelektrischen Zustand [1]. Ein weiterer möglicher Effekt ist die Bildung von ferroelektrischen Domänen, die dazu beitragen können Gitterverspannungen abzubauen. Jedoch haben Größe und Symmetrie der Domänen sowie die Natur der Domänenwände einen großen Einfluss auf die ferro- und piezoelektrischen Eigenschaften der Schichten. Infolgedessen sind Verständnis und Kontrolle der Domänen wesentlich für weitere Anwendungen in elektronischen Bauelementen mit funktionalen Einheiten im Nanometerbereich. In den letzten Jahren ist daher das Interesse an Domänen und Domänenwänden in den Fokus der Grundlagenforschung gerückt.

In ferroelektrischen, epitaktischen Schichten ist die Bildung von Domänen das Ergebnis der Ausgleichs zwischen elastischer Energie, Domänenwandenergie und elektrostatischer Energie [2,3,4]. Neben der chemischen Zusammensetzung der Schichten und ihrer strukturellen/kompositionellen Ordnung wird die eingebaute epitaktische Verspannung als zusätzlicher Freiheitsgrad eingesetzt um die Domänenkonfiguration in den Schichten einzustellen. Symmetrie der Domänenmuster, kristallographische Orientierung, Größe der individuellen Domänen und Struktur der Domänenwände sind stark beeinflusst durch die eingebaute Gitterverspannung, welche durch das Substrat induziert wird.

Theoretische und experimentelle Untersuchungen führten zu einem detaillierteren Verständnis der Domänenbildung abhängig von der Gitterverspannung [4,5]. Die meisten Veröffentlichungen beziehen sich auf eine biaxiale, symmetrische (´isotrope´) Verspannung in

strains mainly induce an enhancement of out-of-plane polarization. However, since lattice parameters of most available perovskite substrates are often smaller than those of the film material, experimental verification critically depends on the availability of adequate substrates. Hence domain structures with purely in-plane polarization have not been much investigated. But such structures are potentially useful, for example, in optical devices where in-plane domains, with vertical domain walls, could be manipulated optically, or in ultra-thin films, where avoiding of depolarization field effects is necessary.

NaNbO₃ based materials have attracted scientific interest due to their complexity of phase transitions and excellent dielectric properties. While the formation of domain structures in NaNbO₃ single bulk crystals is known for a long time, little is known for epitaxial thin films; in particular, the evolution of domain structure with increasing film thickness and the impact of plastic strain relaxation on the domain formation have not been studied yet in detail. In films under tensile lattice strain increase of the Curie temperature and large polarization in-plane components are expected making them potentially interesting for instant for surface acoustic wave devices.

Deposition of well-ordered films and systematic investigation of the strain effect in NaNbO3 films have only been successful by a close, fruitful cooperation of several groups at IKZ. Use of two different deposition methods permitted the growth of stoichiometric films and the investigation of the influence of non-stoichiometry and vacancy on structural properties and domain formation. Based on the unique availability of a variety of oxide single crystals at IKZ the (anisotropic) strain state of the epitaxial films can be tailored in a wide range facilitating film growth under varying compressive or tensile stresses. High resolution x-ray diffraction, including grazing incidence measurements at DESY and BESSY, and high resolution transmission electron microscopy have provided detailed structural properties of the films.

Effect of tensile in-plane lattice strain

Tensile lattice strain was incorporated in stoichiometric NaNbO₃ thin films by the epitaxial growth on oxide substrates with larger in-plane lattice parameters by means of metalorganic chemical vapor deposition (MOCVD) and pulsed laser deposition (PLD). Variation of the in-plane lattice strain was achieved by the use of a sequence of rare-earth scandates (ReScO₃ with Re = Dy, Tb, Gd, see Table I). We have figured out that the magnitude of the tensile in-plane lattice mismatch significantly modify structural and ferroelectric properties of the observed domains and provoke differences in strain relaxation process as a function of film thickness.

der Schichtebene in tetragonalen Schichten, die auf kubischen Substraten abgeschieden werden. Jedoch wird hier nicht der allgemeinere Fall der biaxialen, asymmetrischen (´anisotropen´) Verspannung betrachtet, welcher aber für orthorhombische Perowskit-Materialsysteme, wie z.B. bei den Alkali-Niobaten [6,7], anzunehmen ist. Die interessantesten Vorhersagen aus diesen Stabilitätsdiagrammen für epitaktische, ferroelektrische Perowskite betreffen die Schichten, die unter tensiler in-plane Verspannung aufgewachsen sind [8,9]; kompressive Verspannungen induzieren im wesentlichen eine Erhöhung der vertikalen Polarisation. Allerdings, da die Gitterparameter der meisten verfügbaren Perowskitsubstrate oftmals kleiner sind als die der Schichtmaterialien, hängt die experimentelle Verifikation in kritischer Weise von der Verfügbarkeit geeigneter Substrate ab. Daher wurden bisher Domänenstrukturen mit einer Polarisation, die ausschließlich in der Filmebene liegt, kaum untersucht. Solche Strukturen sind potentiell von praktischem Nutzen, z.B. in optischen Devices, wo Domänen mit Polarisationsvektoren in der Filmebene und vertikalen Domänenwänden optisch manipuliert werden können oder in ultradünnen Schichten, in denen die Vermeidung von Depolarisationsfeldeffekte notwendig ist.

Aufgrund seiner komplexen Phasenübergänge und exzellenten dielektrischen Eigenschaften besteht ein wissenschaftliches Interesse an NaNbO₃-basierten Materialien. Während die Bildung der Domänenstrukturen in NaNbO₃ Einkristallen schon seit längerem gut untersucht ist, ist für epitaktische Schichten nur wenig darüber bekannt. Insbesondere wurden die Entwicklung der Domänenstruktur mit zunehmender Schichtdicke und der Einfluss der plastischen Gitterrelaxation auf die Domänenbildung bisher nicht im Detail untersucht. Für Schichten, die unter Zugspannung stehen, wird ein Anstieg der Curie Temperatur und eine große horizontale Komponente der Polarisation erwartet, was sie potentiell interessant macht beispielweise für akustische Oberflächenwellenbauteile.

Die Abscheidung von gut geordneten Schichten und die systematische Untersuchung des Verspannungseffektes in NaNbO₃ Schichten wurde durch eine enge, fruchtbare Kooperation von mehreren IKZ-Gruppen ermöglicht. Der Einsatz von zwei verschiedenen Abscheidemethoden erlaubte das Wachstum von stöchiometrischen Schichten und die Untersuchung des Einflusses von Nicht-Stöchiometrie und Fehlstellen auf die strukturellen Eigenschaften und die Domänenbildung. Basierend auf der einzigartigen Verfügbarkeit verschiedener Oxidkristalle im IKZ zur Verwendung als Substrat konnte zielgerichtet ein (anisotroper) Verspannungszustand in den epitaktischen Schichten eingebaut werden. Der Verspannungszustand wurde in einem weiten Bereich variiert, was das Schichtwachstum unter unterschiedlicher tensiler und kompressiver Verzerrung ermöglichte. Hochauflösende Röntgenbeugung, einschließlich

Table I: Lattice parameters of the (110) surface unit cell of the ReScO$_3$ substrates and lattice mismatch to NaNbO$_3$.

substrate	surface unit cell (Å) in [1-10]$_o$ / [001]$_o$	lattice mismatch in [1-10]$_o$ / [001]$_o$
DyScO$_3$(110)	3.947 / 3.952	-0.81 % / -0.94 %
TbScO$_3$(110)	3.960 / 3.959	-1.14 % / -1.12 %
GdScO$_3$(110)	3.970 / 3.966	-1.40 % / -1.29 %

NaNbO$_3$ films with a thickness of 10 nm were grown fully strained on TbScO$_3$(110). While vertical piezoresponse force microscopy (VPFM) measurements resulted in featureless images with very weak piezoresponse, the lateral piezoresponse force microscopy (LPFM) signal is strong and shows a very well ordered domain pattern with domain walls exclusively arranged parallel to the [001]$_{TSO}$ direction (Fig. 1a). From LPFM measurements we conclude that 90° domains, whose polarization vectors are arranged in the film plane and rotated by 90° for adjacent domains, have evolved. These domains are typically described as a$_1$/a$_2$/a$_1$/a$_2$. Figure 1(d) shows the alignment of the polarization vectors in the domains. The observed 1D domain arrangement cannot be attributed to the orthorhombic structure of the TbScO$_3$ substrate, since unit cell of the TbScO$_3$(110) surface is almost quadratic (see Table I). However, despite the nearly squared in-plane lattice, the symmetry of this surface is not fourfold, but twofold according to the positions of the Tb and O atoms showing a zig-zag pattern along [001]$_{TSO}$, while they are lined up in straight rows

Messungen unter streifendem Einfall bei DESY und BESSY, und hochauflösende Transmissionselektronenmikroskopie lieferten detaillierte strukturelle Eigenschaften der Schichten.

Effekt der tensilen in-plane Verspannung

In stöchiometrischen NaNbO$_3$ Schichten wurde eine tensile Gitterverspannung durch das epitaktische Wachstum von Schichten auf Oxidsubstraten mit größeren Gitterparametern eingebaut. Die Abscheidungen wurde mit Hilfe der metallorganischen Gasphasendeposition (MOCVD) und der gepulsten Laserdeposition (PLD) durchgeführt. Die Variation der Gitterverspannung in der Filmebene wurde erreicht durch die Verwendung einer Sequenz von Seltenerd-Scandaten (ReScO$_3$ mit Re = Dy, Tb, Gd, siehe Tabelle I) erreicht. Wir haben herausgefunden, dass die Größenordnung der tensilen Gitterfehlanpassung signifikant die strukturellen und ferroelektrischen Eigenschaften der Domänen modifiziert und Unterschiede im Strainrelaxationsprozess abhängig von der Schichtdicke hervorruft.

Tabelle I: Gitterparameter der (110) Oberflächenzelle der ReScO$_3$ Substrate und Gitterfehlanpassung zu NaNbO$_3$.

Substrat	Oberflächeneinheitszelle (Å) in [1-10]$_{sub}$ / [001]$_{sub}$	Gitterfehlanpassung in [1-10]$_{sub}$ / [001]$_{sub}$
DyScO$_3$(110)	3.947 / 3.952	-0.81 % / -0.94 %
TbScO$_3$(110)	3.960 / 3.959	-1.14 % / -1.12 %
GdScO$_3$(110)	3.970 / 3.966	-1.40 % / -1.29 %

NaNbO$_3$ Schichten mit einer Schichtdicke von 10 nm wurden voll verspannt auf einem TbScO$_3$(110) Substrat aufgewachsen. Während vertikale Piezoresponse Force Mikroskopie (VPFM) Messungen strukturlose Bilder mit sehr schwachen Piezoresponse ergaben, war das laterale Piezoresponse Force Mikroskopie (LPFM)-Signal sehr stark und zeigte ein sehr gut geordnetes Domänenmuster mit Domänenwänden, die ausschließlich parallel zur [001]$_{TSO}$ Richtung angeordnet sind (Abb. 1a). Aus den LPFM Messungen schließen wir, dass sich 90° Domänen, deren Polarisationsvektoren in der Schichtebene angeordnet und gegenüber benachbarten Domänen um 90° gedreht sind, entwickelt haben. Diese Art von Domänen wird üblicherweise mit a$_1$/a$_2$/a$_1$/a$_2$ Domänen beschrieben. Abbildung 1(d) zeigt die Ausrichtung der Polarisationsvektoren in den Domänen. Die beobachteten 1D Domänenanordnung kann nicht auf die orthorhombische Struktur des TbScO$_3$ Substrates zurückgeführt werden, da die Einheitszelle der TbScO$_3$(110) Oberfläche nahezu quadratisch ist (siehe Tabelle I). Allerdings ist, trotz des annähernd quadratischen Oberflächengitters, die Symmetrie der TbScO$_3$ Oberfläche nicht vierfach, sondern nur zweifach bezüglich der Positionen der Tb und O Atome. Diese verlaufen
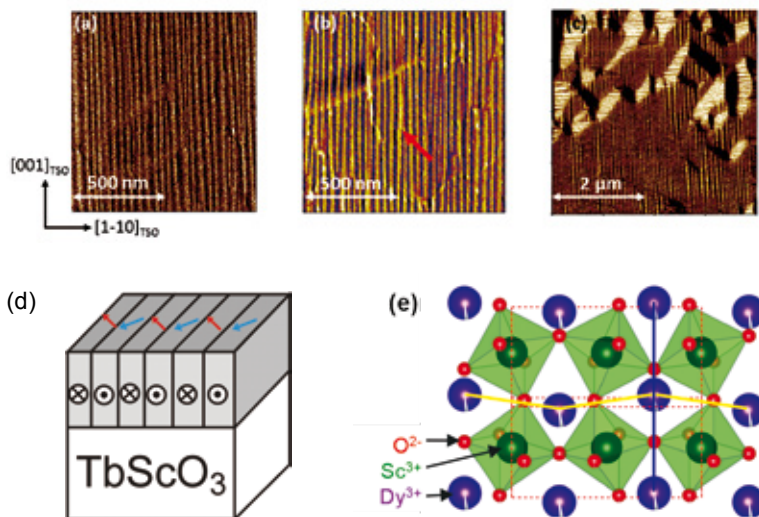

Fig. 1: LPFM of (a) 11 nm, (b) 21 nm and (c) 66 nm thick NaNbO$_3$ films on TbScO$_3$, (d) arrangement of the polarization vectors in fully strained films, and (e) schematic presentation of the TbScO$_3$(110) surface.
Abb. 1: LPFM von (a) 11 nm, (b) 21 nm und (c) 66 nm dicken NaNbO$_3$ Schichten auf TbScO3, (d) Anordnung des Polarisationsvektor in voll verspannten Schichten, und (e) schematische Darstellung der TbScO$_3$(110) Oberfläche.

along [110]$_{TSO}$ (Fig. 1e). This could lead to an additional anisotropy caused by chemical bonding, which may be associated with a distinct anisotropy in the NaNbO₃ domain wall energies. Since with increasing film thickness the film lattice decreasingly "feels" the asymmetry of the substrate's bulk lattice, it should have a decreasing impact on domain formation. Therefore, it is very instructive to investigate the domain pattern at higher film thicknesses. X-ray diffraction pattern have indicated that increasing the film thickness to ~21 nm onset of plastic strain relaxation has been detected for films on TbScO₃. Additionally, we have observed that the 1D anisotropy of the domain pattern gets more and more disturbed (see arrow in Fig. 1b), and the LPFM images of the 66 nm film reveals additional stripe domains perpendicular to the initial domain orientation (Fig. 1c).

Grazing incidence x-ray diffraction (GIXD) patterns were recorded to evaluate in-plane lattice strains. The intensity distribution (angular scan) in the vicinity of the 008 TbScO₃ in-plane reciprocal lattice point of the 11 nm film is given in Fig. 2(a). Besides, the sharp crystal truncation rod at $q_{1\text{-}10} = 0$, which is caused by the smooth sample surface and film/substrate interface, two broad in-plane satellite peaks (P1 and P2) can be observed along $q_{1\text{-}10}$, i.e. perpendicular to the 1D stripe domains. Contrastingly, corresponding satellite peaks do not show up in the vicinity of the 4-40 TbScO₃ in-plane reciprocal lattice point, where the in-plane scattering vector is collinear to the 1D stripe domains. This suggests that the satellite peaks in Fig. 2(a) are caused by 90° domains in the NaNbO₃ film observed in LPFM. The peak splitting is provoked by an in-plane monoclinic distortion of the unit cell leading to an in-plane tilting β* of the lattice planes with respect to the [1 10]$_{TSO}$ direction, as it is schematically shown in Fig. 2(b). The two variants of the domains are created by a 90° in-plane rotation of the NaNbO₃ orthorhombic unit cell. The monoclinic lattices of the two variants are coherently composed at the domain walls.

From the full widths at half maximum of the satellites peaks the domain size D perpendicular to the [001]$_{TSO}$ direction was calculated and the results are plotted in Fig. 3 (left ordinate axis) for film thicknesses between 7 nm and 66 nm. From the angular spacing between the two satellite peaks P1 and P2 the in-plane monoclinic distortion angle β* was determined for all samples under investigation (Fig. 3, right ordinate axis). For film thicknesses larger than about 20 nm, where plastic relaxation starts, we observe a constant value for β* close to the bulk value of 0.67° (see dashed line in Fig. 3). However, β* drastically decreases when the film thickness is reduced.

Evolution of the trend of β* at small film thicknesses indicates that lattice relaxation in NaNbO₃ films on TbScO₃ starts at very thin films (below 7 nm) and is tentatively explained by a two-step relaxation process: Below 21 nm film thickness the in-plane unit cell
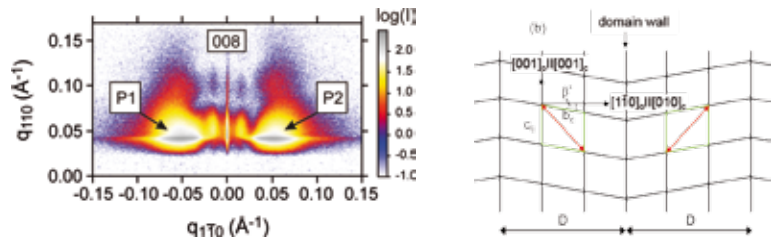

Fig. 2: (a) GIXD intensity distribution of a 11 nm NaNbO₃ film in the vicinity of the 008 TbScO₃ reciprocal lattice point. P1 and P2 mark two satellite peaks arising from adjacent NaNbO₃ domains. (b) Schematic view of the in-plane monoclinic domain structure. The green rhombus represents the unit cell of the NaNbO₃ films with monoclinic distortion angle β*. Adjacent domains (lateral size D) differing by a 90° in-plane rotation of the polarization vector (red arrows) are shown.

Abb. 2: (a) GIXD Intensitätsverteilung von einer 11 nm dicken NaNbO3 Schicht in der Nähe des 008 TbScO₃ reziproken Gitterpunktes. P1 und P2 bezeichnen zwei Satellitenpeaks die von benachbarten NaNbO₃ Domänen verursacht werden. (b) Schematische Ansicht der monoklinen Domänenstruktur. Der grüne Rhombus stellt die Einheitszelle der NaNbO₃ Schicht mit monoklinem Verzerrungswinkel β in der Schichtebene dar. Es sind zwei benachbarte Domänen (laterale Größe D), die sich durch eine Rotation des Polarisationsvektors (rote Pfeile) in der Schichtebene unterscheiden, gezeigt.*

in [001]$_{TSO}$ auf einer Zickzack-Linie, während sie in einer geraden Linie entlang der [1-10]$_{TSO}$ Richtung aufgereiht sind (Abb. 1e). Dies könnte zu einer zusätzlichen Anisotropie in den chemischen Bindungen führen, was wiederum mit einer gewissen Anisotropie in den Domänenwandenergien verbunden ist. Da mit zunehmender Schichtdicke das Schichtgitter immer weniger die Asymmetrie des Substratgitters „spürt", sollte dieses eine abnehmende Auswirkung auf die Domänenbildung haben. Deshalb ist es sehr aufschlussreich die Domänenmuster bei höheren Schichtdicken zu untersuchen. Röntgenbeugungsdaten haben gezeigt, dass für Schichten auf TbScO₃ bei der einer Zunahme der Schichtdicke auf ~21 nm plastische Gitterrelaxation einsetzt. Außerdem haben wir festgestellt, dass mit zunehmender Schichtdicke die 1D Anisotropie der Domänenanordnung mehr und mehr gestört wird (siehe Pfeil in Abb. 1b), und in LPFM Bilder einer 66 nm dicken Schicht können zusätzlich Streifendomänen senkrecht zur ursprünglichen Domänenorientierung beobachtet werden (Abb. 1c).

Röntgenmessungen unter streifendem Einfall (GIXD) wurden aufgenommen um die in-plane Gitterverspannungen zu bestimmen. Die Intensitätsverteilung (Winkelscans) in der Nähe des 008 TbScO₃ in-plane reziproken Gitterpunktes der 11 nm Schicht ist dargestellt in Abb. 2(a). Neben dem scharfen Crystal Truncation Rod bei $q_{1\text{-}10} = 0$, welcher durch die glatte Probenoberfläche und Schicht/Substrat-Interface verursacht wird, können zwei breite Satellitenpeaks (P1 und P2) entlang $q_{1\text{-}10}$, d.h. senkrecht zu den 1D Streifendomänen, beobachtet werden. Dahingegen tauchen entsprechende Satellitenpeaks nicht in der Nähe des 4-40 TbScO₃ reziproken Gitterpunktes auf, wenn der Beugungsvektor kollinear zu den 1D Streifendomänen verläuft. Das
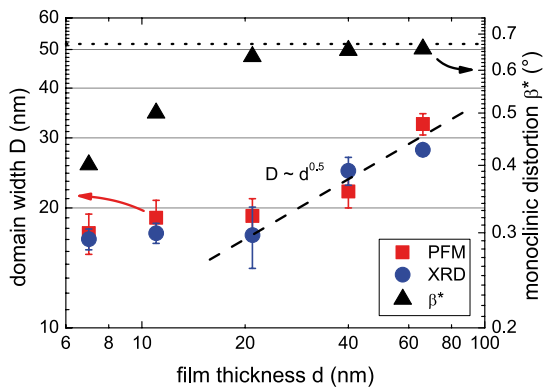
Fig. 3: Lateral domain width D, measured by PFM and GIXD, and monoclinic distortion ß* together with the corresponding NaNbO$_3$ bulk value (dotted line) as a function of film thickness d. The dashed line describes the square-root dependence of the domain size on film thickness theoretically predicted by Pertsev et al. [4].

Abb. 3: Laterale Domänengröße D, gemessen mit PFM und GIXD, sowie monokline Verzerrung ß* zusammen mit dem entsprechendem Volumenwert für NaNbO$_3$ (gepunktete Linie) als Funktion der Schichtdicke d. Die gestrichelte Linie beschreibt die Wurzelabhängigkeit der Domänengröße von der Schichtdicke wie sie von Pertsev et al. [4] theoretisch vorhergesagt wurde.

dimensions of NaNbO$_3$ are still adapted to the TbScO$_3$ substrate, but the unit cell exhibits a slight monoclinic in-plane distortion, which is nonzero but still below the bulk value, providing an elastic strain accommodation. At about 21 nm the NaNbO$_3$ bulk value of ß* = 0.67° is reached, and the thin film further relaxes by misfit dislocations changing the in-plane lattice parameter of the monoclinic NaNbO$_3$ unit cell. With ongoing plastic relaxation the (small) anisotropy induced by the TbScO$_3$

deutet daraufhin, dass die Satellitenpeaks in Abb. 2(a) durch die 90° Domänen, die in den LPFM Messungen an der NaNbO$_3$ Schichten beobachtet wurden, verursacht sind. Das Peaksplitting wird hervorgerufen durch eine monokline Verzerrung der Einheitszelle in der Schichtebene, was zu einer Verkippung ß* der Gitterebenen bezüglich der [1-10]$_{TSO}$ Richtung führt, wie es schematisch in Abb. 2(b) gezeigt wird. Die beiden Domänenvarianten entstehen durch eine ~90° Drehung der Einheitszelle von NaNbO$_3$ in der Schichtebene. Die monoklinen Gitter der beiden Varianten sind kohärent an den Domänenwänden zusammengesetzt.

Aus der Halbwertbreite der Satellitenpeaks wurde die Domänengröße senkrecht zur [001]$_{TSO}$ Richtung berechnet; die Ergebnisse für Schichtdicken zwischen 7 nm und 66 nm sind in Abb. 3 (linke Ordinate) dargestellt. Aus dem Winkelabstand der beiden Satellitenpeaks P1 und P2 wurde für alle untersuchten Proben der monokline Verzerrungswinkel ß* bestimmt (Abb. 3, rechte Ordinate). Für Schichtdicken größer als etwa 20 nm, d.h. mit Beginn der plastischen Gitterrelaxation, beobachten wir einen konstanten Wert für ß*, der dicht am Volumenwert von 0.67° von NaNbO$_3$ liegt (siehe gestrichelte Linie in Abb. 3). Allerdings nimmt ß* deutlich ab, wenn die Schichtdicke reduziert wird.

Der Verlauf von ß* bei geringen Schichtdicken deutet darauf hin, dass die Gitterrelaxation in NaNbO$_3$ Schichten auf TbScO$_3$ bei sehr geringen Schichtdicken (unter 7 nm) beginnt und wird durch folgenden zweistufigen Relaxationsprozess erklärt: Unterhalb einer Schichtdicke von 21 nm sind in der Filmebene die Dimensionen der Einheitszellen von NaNbO$_3$ denen der Oberflächeneinheitszelle des TbScO$_3$ Substrates noch angepasst. Dabei weist die NaNbO$_3$ Einheitszelle eine monokline Verzerrung in der Filmebene auf, die zwar ungleich Null ist aber noch unterhalb des Volumenwertes liegt. Dadurch kann ein elastischer Verspannungsabbau in den Gitterzellen realisiert werden. Bei etwa 21 nm wird Volumenwert für NaNbO$_3$ von ß* = 0.67° erreicht, und die dünne Schicht relaxiert weiter durch den Einbau von Misfit-Versetzungen, wo-
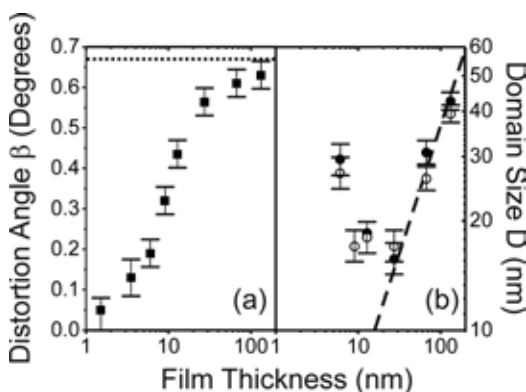
Fig. 4: (a) Monoclinic distortion angle ß* and (b) lateral domain size D deduced by PFM (o) and GIXD (•) as a function of film thickness. In (c) and (d) the orientation of the polarization vector for fully strained and partially relaxed films, respectively, is depicted.

Abb. 4: (a) Monokliner Verzerrungswinkel ß* und (b) laterale Domänengröße D abgeleitet von PFM (o) und GIXD (•) Messungen als Funktion der Schichtdicke. In (c) und (d) ist die Orientierung des Polarisationsvektors für voll verspannte und teilweise relaxierte Schichten anschaulich dargestellt.
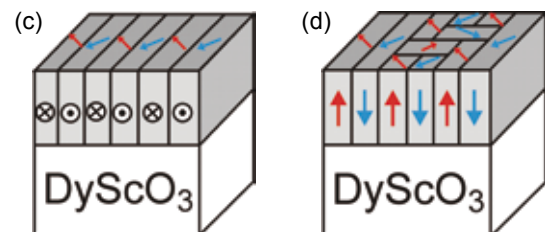
substrate is released leading to the creation of NaNbO$_3$ domains running also in [1-10]$_{TSO}$ direction and thus to the formation of a 2D domain pattern. These results were published in Ref. [10].

Variation of tensile lattice strain by the use of different substrates

By changing the substrate material the lattice mismatch between the thin film and the substrate can be intentionally tuned thus providing film growth under varying tensile stresses. Reduced tensile lattice strain (see Table I) for NaNbO$_3$ films on DyScO$_3$ leads to a slightly larger film thickness (~27 nm) were partial lattice relaxation was observed. Coherently strained films show a regular stripe domain pattern over several µm aligned along [001]$_{DSO}$ of the type a$_1$/a$_2$/a$_1$/a$_2$ with exclusive in-plane polarization, like for the fully strained films on TbScO$_3$ (Fig. 1a). For thicker films plastic strain relaxation is again accompanied by a transformation of the 1D stripe domain pattern into a 2D domain pattern. But in contrast to NaNbO$_3$/TbScO$_3$ additionally an out-of-plane component of the electric polarization has arisen (Fig. 4c), which is attributed to the lower tensile strain state here. For a thickness series from 1.5 nm to 130 nm we evaluated domain size D and monoclinic distortion angle ß* (Fig. 4a). In comparison to TbScO$_3$ the monoclinic distortion has not reached the bulk value of 0.67°, rather not till significantly larger film thickness (≥ 130 nm). That means while for films on TbScO$_3$ monoclinic distortion and plastic strain relaxation occur successively, for NaNbO$_3$ on DyScO$_3$ these mechanisms seem to occur simultaneously. Fig. 4(b) again shows that the domain width is adjusted by the film thickness. Here actually we have observed a minimum of D, when the domain size becomes comparable to the film thickness (~10 – 20 nm), where the electrostatic interaction with the opposite surface dominates.

We have also addressed the issue of matching an in-plane monoclinically distorted unit cell of NaNbO$_3$ on a squared unit cell of the substrate in the first growth stages. For this purpose films with a thickness of ~4 ML (~1.5 nm) have been deposited. For such a thin film no clear satellite peaks P1 and P2 like in Fig. 2(a) can be recorded implying the formation of an nearly rectangular in-plane unit cell of the film with a vanishing in-plane monoclinic distortion (ß* ≤ 0.05°) in the first monolayers. This is in accordance with PFM images, where no ferroelectric domain pattern can be observed. These results were published in Ref. [11].

Increased tensile lattice strain was achieved by the use of GdScO$_3$(110) as substrate (Table I). Even for 10 nm thick films the film lattice is partially relaxed resulting in a 2D domain pattern (Fig. 5a). With increasing film thickness incorporated tensile lattice strain is further reduce by the incorporation of defects. Hence ad-

durch es zu einer Änderung des Gitterparameters der monoklinen Einheitszelle von NaNbO$_3$ in der Filmebene kommt. Mit fortlaufender plastischer Gitterrelaxation wird auch die (geringe) substratinduzierte Anisotropie abgebaut, was zur Entstehung von NaNbO$_3$ Domänen führt, die auch in [1-10]$_{TSO}$ Richtung verlaufen und somit in der Bildung eines 2D Domänenmustern resultiert. Diese Ergebnisse wurden in Ref. [10] publiziert.

Variation der tensilen Gitterverspannung durch die Verwendung von verschiedenen Substraten

Die gezielte Einstellung der Gitterfehlanpassung zwischen Film- und Substratmaterial durch die Änderung des Substrats eröffnet die Möglichkeit, das Schichtwachstum unter unterschiedlicher tensiler Verzerrung zu untersuchen. Reduzierte Zugverspannung (siehe Tabelle I) für NaNbO$_3$ Schichten auf DyScO$_3$ führte zu einer leicht größeren Schichtdicke (~ 27 nm), bei der partielle Gitterrelaxation beobachtet wurde. Kohärent verspannt Schichten zeigen ein reguläres Streifenmuster des Typs a$_1$/a$_2$/a$_1$/a$_2$ über viele µm, das entlang der [001]$_{DSO}$ angeordnet ist und ausschließlich eine horizontale Polarisationskomponente aufweist, ähnlich wie die vollverspannten Schichten auf TbScO$_3$ (Abb. 1a). Bei dickeren Schichten ist die plastische Strainrelaxation wiederum begleitet von dem Übergang von einem 1D zu einem 2D Streifenmuster. Jedoch tritt hier im Gegensatz zu NaNbO$_3$/TbScO$_3$ zusätzlich eine vertikale Komponente der elektrischen Polarisation auf (Abb. 4c), was auf die geringere Zugspannung in den Schichten zurückgeführt wird. Für eine Schichtdickenserie von 1.5 nm bis 130 nm haben wir jeweils die Domänengröße D und den monoklinen Verzerrungswinkel ß* (Abb. 4a) ausgewertet. Im Vergleich zu TbScO$_3$ hat die monokline Verzerrung – selbst bei deutlich größeren Schichtdicken (≥ 130 nm) – noch nicht den Volumenwert von 0.67° erreicht, Das bedeutet, dass während für Schichten auf TbScO$_3$ die monokline Verzerrung der Einheitszelle und die plastische Strainrelaxation nacheinander ablaufen, für NaNbO$_3$

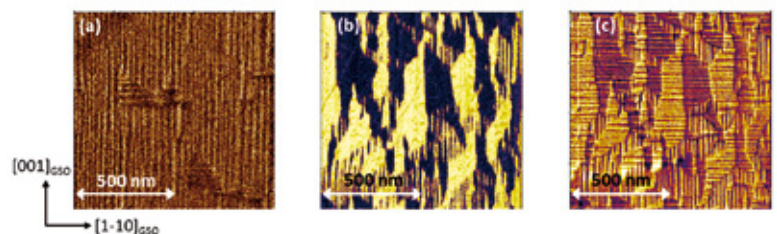*Fig. 5: (a) LPFM image of a 10 nm thick NaNbO$_3$ film on GdScO$_3$. (b) VPFM and LPFM images of a 30 nm thick NaNbO$_3$ film on GdScO$_3$.*

Abb. 5: (a) LPFM Aufnahme einer 10 nm dicken NaNbO$_3$ Schicht auf GdScO$_3$. (b) VPFM und LPFM Aufnahmen einer 30 nm dicken NaNbO$_3$ Schicht auf GdScO$_3$.

ditionally a strong out-of-plane component of the electric polarization evolves (Fig. 5b) similar to the partially relaxed films on DyScO$_3$ (Fig. 4c), but at significantly smaller film thickness.

In summary, we state that by the suitable choice of substrate material we can selectively adjust ferroelectric film properties and domain evolution, so that they match the technical requirements. Further improvement is expected by incuding potassium in the layers. Eventually, their applicability or electronic devices will be examined.

References

[1] D.G. Schlom et al., Annu. Rev. Mater. Res. **37,** 589 (2007).

[2] A. L. Roitburd, Phys. Status Solidi A **37,** 329 (1976)

[3] G. Catalan et al., Rev. Mod. Phys. **84,** 119 (2012)

[4] J.S. Speck et al., J. Appl. Phys. **76** (1994), 466; J.S. Speck et al., J. Appl. Phys. **78** (1995), 1696; J.S. Speck et al., J. Appl. Phys. **76** (1994), 477

[5] N.A. Pertsev et al., J. Appl. Phys. 78 (1995), 6170

[6] J. Schwarzkopf et al., J. Appl. Cryst. **45** (2012), 1015

[7] J. Schwarzkopf et al., J. Appl. Phys. **115** (2014), 204105

[8] O. Diéguez et al., Phys. Rev. B **72** (2005), 144101

[9] N.A. Pertsev et al. Phys. Rev. Lett. **80** (1998), 1988

[10] A. Duk et al, Appl. Phys. Lett. **102** (2013), 091903

[11] M. Schmidbauer et al, phys. stat. sol. **8** (2014), 522

auf DyScO$_3$ diese Mechanismen anscheinend gleichzeitig stattfinden. Abb. 4(b) zeigt, dass auch für NaNbO$_3$/DyScO$_3$ die Domänengröße D durch die Schichtdicke eingestellt werden kann. Hier haben wir tatsächlich auch ein Minimum in D beobachtet, wo die Domänengröße vergleichbar mit der Schichtdicke wird (~10 – 20 nm), wenn die elektrostatische Wechselwirkung mit der der gegenüberliegenden Oberfläche dominant wird.

Wir haben uns ebenfalls mit der Frage befasst, wie eine in der Schichtebene monoklin verzerrte Einheitszelle von NaNbO$_3$ auf eine quadratische Einheitszelle des Substrates im Anfangsstadium des Wachstums passt. Hierfür wurden Schichten mit einer Schichtdicke von ~4 Monolagen (~1.5 nm) abgeschieden. Für solch eine dünne Schicht konnten keine klar sichtbaren Satellitenpeaks P1 und P2 wie in Abb. 2(a) aufgenommen werden. Das impliziert die Bildung einer nahezu rechtwinkeligen Gitterzelle der Schicht in der Filmebene mit verschwindend kleiner monoklinen Verzerrung (ß* ≤ 0.05˚) in den ersten Monolagen. Dies ist in Übereinstimmung mit PFM Messungen, bei denen kein ferroelektrisches Domänenmuster beobachtet werden konnte. Diese Ergebnisse wurden in Ref. [10] veröffentlicht.

Erhöhte Zugspannung im Schichtgitter wurde durch die Verwendung von GdScO$_3$(110) als Substrat (Tabelle I) erreicht. Selbst für 10 nm dicke Schichten ist das Schichtgitter partiell relaxiert, was in ein 2D Domänenmuster resultiert (Abb. 5a). Mit zunehmender Schichtdicke wird die eingebaute tensile Gitterverspannung durch den Einbau von Defekten weiter reduziert. Demzufolge entwickelt sich eine signifikante vertikale Komponente der elektrischen Polarisation (Abb. 5b) ähnlich wie bei den teilweise relaxierten Schichten auf DyScO$_3$. (Abb. 4c), jedoch geschieht dies hier schon bei deutlich geringeren Schichtdicken.

Zusammenfassend lässt sich feststellen, dass wir die ferroelektrischen Domänen in den von uns untersuchten Schichten durch eine geeignete Wahl des Substratmaterials kontrollieren können. Damit lassen sich die ferroelektrischen Eigenschaften der Schichten gezielt einstellen. Weitere Verbesserungen werden durch die Zugabe von Kalium in den Schichten erwartet. Diese Schichten sollen in Zukunft auch im Hinblick auf ihre potentielle Anwendung in elektronischen Devices überprüft werden.

Silicon & Germanium

Multicrystalline Silicon
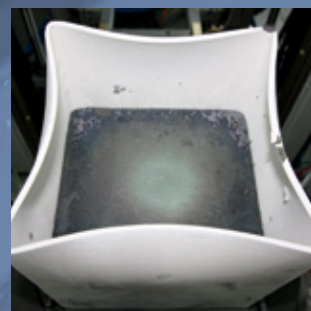
Gallium Arsenide

Classical Semiconductors

Die Abteilung „Klassische Halbleiter" weitete ihre Forschungsarbeiten und F&E Aktivitäten aus, obwohl vor allem die Themengruppen Multikristallines Silizium (mc-Si) und einkristallines Silizium & Germanium (Si&Ge) unter den Folgen der andauernden Krise der deutschen bzw. Europäischen Solarindustrie zu leiden hatten. Insbesondere die Gruppe mc-Si erweiterte ihre Arbeiten auf dem Gebiet der gerichteten Erstarrung von Si und übernahm die Ausrüstung der Roth & Rau AG. Diese beinhaltete eine G2-Erstarrungsanlage (75 kg) und eine Beschichtungslinie für Tiegel. In der Si&Ge-Themengruppe wurde eine neue Czochralski Ziehanlage für die Züchtung von hochreinen Ge-Kristallen unter Reinstwasserstoffatmosphäre in Betrieb genommen. Obwohl die Mittelbeschaffung zunehmend schwieriger wird, konnten fast 2/3 des wissenschaftlichen und technischen Personals der Abteilung über Drittmittel finanziert werden. Die Finanzierung gelang u.a. auf der Basis verschiedener industrieller bilateraler Forschungsaufgaben.

Wir sehen uns in der Verantwortung, Forschung und Entwicklung auf dem Gebiet der Massivkristallzüchtung weiter voranzutreiben, auch damit Europa und Deutschland mit hochentwickelten Technologien und Produkten weiter im Wettbewerb bestehen können. Hierzu sehen wir die Erforschung und die Anwendung magnetischer Wanderfelder (TMFs) bei der Kristallisation von mc-Siliziumblöcken und GaAs-Einkristallen als einen wesentlichen Beitrag an. Das am IKZ entwickelte Magnet-Heizer-Konzept KRISTMAG© bietet hierfür einzigartige Erfolgsaussichten zur Kontrolle der Schmelzenbewegung und der Wärmeflüsse. Optimierte Wachstumsbedingungen erlauben Verbesserung der Ausbeute und Qualität von GaAs-Kristallen und die Herstellung von Siliziumblöcken mit reduzierten Defektkonzentrationen. Trotz der genannten widrigen äußeren Bedingungen konnten die bilateralen Projekte mit deutschen und norwegischen Materialproduzenten in der Gruppe mc-Si fortgesetzt werden. Im Rahmen des BMU-Projektes „SolarWinS" wurden mehrere mc-Si Blöcke in Abhängigkeit von variierenden Wachstumsparametern in Kieselglastiegeln gerichtet erstarrt. Im Rahmen eines BMWi-Projektes wurden Prozessentwicklungen unter Anwendung von magnetischen Wanderfeldern zur gerichteten Erstarrung in der G2-Anlage begonnen.

Unter der Federführung der Physikalische-Technischen Bundesanstalt wurde das internationale Projekt „Kilogramm-2" in der Si&Ge-Gruppe begonnen, welches auf die Arbeiten des „Avogadro"-Projektes (zur Definition des Kilogramms-Maßstabs) aufbaut. Forschungsaktivitäten wurden zur Entwicklung des FZ-Verfahrens mit dem Ziel durchgeführt, den Durchmesser der Kristalle zu vergrößern. Grundlegende Untersuchungen befassten sich mit der Vermeidung von HF-Überschlägen durch den Einsatz einer isolierenden Separator Scheibe, das die Züchtung großer Kristalle auch bei Normaldruck gestattet und so die gefährlichen thermoelastischen Spannungen im wachsenden Kristall mindert. Der GaAs-Themengruppe gelang die Züchtung versetzungsarmer Kristalle nach dem VGF Verfahren im KRISTMAG©TMF. Dabei konnten mehrere Kristalle simultan in einem Rezipienten gezüchtet werden.

Despite the still ongoing crisis of the German and European Si-based photovoltaic industry in 2013 the department „Classical Semiconductors" has expanded its research tasks and started new R&D activities. Especially the groups "Multicrystalline Silicon" expanded its activities in the field of directional solidification of silicon and took over the equipment of the Roth & Rau AG including a G2-sized (75 kg) furnace and a coating line for solar crucibles. The group single crystalline "Silicon & Germanium" installed a new Czochralski puller for the growth of ultrapure Ge-crystals in hydrogen atmosphere. Even though the project funding becomes more and more difficult, nearly 2/3 of the scientists and technicians of the department „Classical Semiconductors" are still third-part funded also based on several bilateral R&D activities with industrial partners.

We feel that we have a responsibility to advance research and development and to provide sophisticated technologies to keep Europe and Germany competitive in crystal growth of bulk material. We believe that the research on and the application of travelling magnetic fields (TMF) for the crystallization of mc-Si and GaAs as a significant contribution to reach this objective. The IKZ concept of KRISTMAG© using combined heater magnet module is an excellent prerequisite for success. Here, the control of thermal and flow-optimized growth conditions allows to obtain improved yield and quality of GaAs crystals and to prepare silicon ingots with reduced defect concentrations. Despite of the adverse conditions mentioned above, in the mc-Si group bilateral projects have been continued with partners from German and Norwegian industry. Within the BMU project "SolarWinS" several mc-Si ingots have been directionally solidified in fused silica crucibles in dependence on varying growth parameters. In the G2-furnace equipped with heater magnet modules the development of directional solidification processes has started in the frame of a BMWi project.

The group single crystalline "Silicon & Germanium" started the international project "Kilogram-2" under the leadership of the German National Metrology Institute (Physikalisch-Technische Bundesanstalt). This project is based on the work of the project "Avogadro" (for a new definition of the kilogram). Research activities on the enlargement of FZ crystal diameter continued and fundamental studies have been done. Investigations have been continued to avoid high frequency flashover by using an isolating separator disk, thus allowing the growth of large crystals under normal pressure by reducing thermo-elastic stress in the growing crystal.

GaAs crystals with low dislocation density have been grown in the group GaAs by using the VGF method in KRIST-MAG© TMFs. Several crystals have been grown simultaneously in the same recipient.

Silicon & Germanium

Head: Dr. Nikolay Abrosimov

Team: M. Czupalla, J. Fischer, B. Hallmann-Seifert, L. Lehmann, Dr. R. Menzel, Dr. W. Miller, Dr. M. Neubert, K. Reinhold, M. Renner, Dr. H. Riemann, Dr. H. Rost, T. Turschner, N. Werner, Dr. M. Wünscher

Übersicht

Der Schwerpunkt der Themengruppe Silizium & Germanium bleibt, wie Jahre zuvor, sowohl die kundenspezifische Züchtung von Silizium Kristallen nach dem Floating Zone (FZ) Verfahren als auch die Züchtung von Germanium, Silizium und Silizium-Germanium Kristallen nach der Czochralski (CZ) Methode. Im Rahmen von Projekten und Kooperationen mit der Industrie, Forschungsinstituten und Universitäten werden Züchtungs- und Dotierungsmethoden entwickelt, die die Verbesserung der Kristallqualität und die Herstellung von einmaligen Kristallen ermöglichen.

Ein wichtiges Ereignis für die Gruppe in 2013 war der Beginn des Projektes „Kilogramm-2" – eines internationalen Projektes unter der Leitung und Finanzierung der Physikalisch-Technischen Bundesanstalt (PTB). Das Projekt ist eine indirekte Fortsetzung des Projektes „Avogadro" („New definition of kilogram mass"). Dessen Ergebnisse sind international anerkannt und führten zur Verbesserung der Definition der Avogadro-Konstante, auf Basis der Zählung der Atome in einem isotopenangereicherten Silizium Kristall, wobei die Messunsicherheit um etwa eine Größenordnung verringert werden konnte [1,2]. Die Aufgabe des IKZ ist die Züchtung zweier perfekter FZ Kristalle mit 100 mm Durchmesser aus angereichertem Silizium-28. Um bei Bedarf die Form des Kristalls besser zu kontrollieren, wurde eine zuvor am IKZ entwickelte automatische Regelung des Kristalldurchmessers installiert und erprobt. Die gezüchteten Kristalle dienen als Ausgangsmaterial für die Herstellung der Si-Kugeln, deren Vermessung zu der noch exakteren Bestimmung der Avogadro-Konstante beitragen soll.

Ein zweites großes Ereignis war die Installation und Inbetriebnahme der neuen CZ-Anlage für die Züchtung hochreiner Ge-Kristalle unter Wasserstoffatmosphäre (Projekt „GERDA"). Durch die verbesserten Züchtungsbedingungen sollen hochreine Ge-Kristalle (Verunreinigungen von wenigen 10^{10} Atome pro cm^3) mit einer definierten Versetzungsdichte gezüchtet werden. Die ersten Ergebnisse der Ge-Züchtung, noch in Ar-Atmosphäre, zeigen einen im Vergleich zur alten Anlage geringeren Pegel an Hintergrundverunreinigungen. Um die Wachstumsbedingungen zu optimieren, wurden erste Berechnungen der thermomechanischen Spannungen in den Kristallen durchgeführt.

Im Teilprojekt FZSil zur Reduzierung der Kosten des FZ-Züchtungsprozesses von Silizium wurde in 2013 weiter mit teilweise geänderten Aufgaben geforscht. Eine davon war die numerische Simulation der Abscheidung von Polysiliziumstäben im Siemensreaktor. Die Serviceleistungen wurden sowohl im Rahmen von Kooperationsverträgen, wie z.B. mit der Firma REC SOLAR GRADE SILICON LLC in Moses Lake / USA, als auch als Einzelaufträge von Firmen, Forschungsinstituten und Universitäten in großem Umfang weitergeführt. Die Weiterentwicklung des FZ-Prozesses konzentrierte sich auf die Anwendung einer Gasführung zur Kontrolle der Gastemperatur in Nähe des Induktors, was zur Stabilisierung der Züchtung von Kristallen mit großem Durchmesser (bis 200 mm Durchmesser) dient.

Die Dissertation „Analyse und Regelung der tiegelfreien Floating Zone (FZ) Kristallzüchtung von Silizium" von Dr. Nico Werner wurde vollendet und erfolgreich an der Technischen Universität Berlin verteidigt [3].

Overview

The activity of Silicon & Germanium group is focused as years before both on the growth of user-specific Si crystals by Floating Zone (FZ) technique and on the growth of silicon, germanium and silicon-germanium crystals by the Czochralski (CZ) method. In the frame of several projects and cooperation with industry and academia the group develops new growth and doping techniques for enhanced crystalline quality, which allow also the production of crystals with unique specifications.

One of the important events in Si/Ge group in 2013 has been the beginning of the international project "Kilogram-2" under the leadership of Physikalisch-Technischen Bundesanstalt (PTB) – German National Metrology Institute. This project is an indirect continuation of project "Avogadro" ("New definition of kilogram mass") which results were internationally accepted [1,2] and allowed the new definition of Avogadro constant by counting the atoms in an isotopically enriched silicon crystal with about one order better relative measurement uncertainty than

before. The task of IKZ is the growth of two perfect crystals, 100 mm in diameter, from enriched silicon-28 by FZ technique. For better control of the crystal shape if required, an automatic diameter control system, developed in IKZ, has been installed and proved. The crystals to be grown will be used for preparation of Si spheres whose measurement should give the possibility for further improvement of Avogadro constant definition.

Another important event has been the installation and implementing of the new CZ furnace for the growth of high pure Ge crystals in hydrogen atmosphere (project "GERDA"). Because of the impoved growth conditions, it will be possible to grow highly pure Ge crystals with about 10^{10} cm^{-3} impurity concentrations and well defined dislocation densities. First growth experiments in the new furnace under Ar atmosphere showed already reduced background impurity concentrations. For crystal growth optimisation and for control of thermomechanical stress global computer simulations have been carried out.

Apart from that, project FZSil focussing on cost reduction of the FZ growth process for silicon has been continued with modified tasks, including computer simulations of silicon deposition in the Siemens reactor. Si crystal growth as service was performed to a great extent both in frame of contracts with e.g. USA Company REC SOLAR GRADE SILICON LLC in Moses Lake / USA and on request of companies, research institutes and universities. Development work for the FZ process has been focused on the use of quartz plate placed under inductor to control gas flux near the Si melt zone to allow process stabilization during the growth of large crystals (up to 200 mm in diameter).

The PhD thesis of Niko Werner on analysis and control of the crucible-free floating zone (FZ) crystal growth of silicon [3] was completed and successfully defended at Technische Universität Berlin.

Results

Since in recent years the demand of the semiconductor industry for Si single crystals with diameter larger than 200 mm has increased, in 2013 a main focus of the group Silicon & Germanium was to investigate means to overcome known barriers for the growth of FZ Si crystals with large diameter. A major drawback is the risk of arc discharge at the high frequency (HF) inductor, as more electric power and, hence, higher voltage is required in such a process. Using higher pressure, adding nitrogen to the gas atmosphere or using lower frequency of the inductor current can reduce the risk of arcing but there are several limitations for these measures and further research is required to stabilize the process.

With respect to this, our activity was focused on the role of the temperature of the filling gas atmosphere containing mainly Ar and a small amount of N_2 (<1%). To evaluate the impact of the gas temperature on the risk of arcing, bachelor student Sandra Haufe conducted separate experiments at IKZ. With the help of a model set-up that provided similar conditions and gas composition as used during FZ growth, it could be confirmed that the breakdown voltage is significantly lower at higher gas temperature [3]. Hence, lowering the gas temperature near the gap of the HF inductor can be another way to prevent arcing.

To determine the thermal conditions in the gas atmosphere, our existing numerical model of the FZ process has been extended by a gas flow model, which is based on the assumption of laminar and steady state fluid flow. The results (see Fig. 1) show that the gas near the crystal surface is heated up, accelerated in vertical direction forming a thin hydrodynamic boundary layer and reaches temperatures near the melting point of silicon in the vicinity of the inductor. Conclusion was that the risk of arcing can be lowered if hot gas from below the inductor is hindered from entering the inductor gap.

Based on these findings, a method of guided gas flow has been developed and examined in growth experiments. Below the HF inductor, a quartz plate was mounted (see Fig. 2), which is transmissive to the major part of the radiation emitted from the melt surface and remains cold. During growth the gas pressure or the nitrogen content was lowered in-situ to a level where arc discharge is observed using the standard configuration without quartz plate. In both cases the breakdown voltage of the gas was higher compared to the benchmark experiments. This indicates a lower gas temperature in the inductor gap if the quartz plate is applied. Hence, the method of guided gas flow is an effective mean to stabilize the process for FZ Si crystals with larger diameter, where higher voltage is needed. The results as accepted paper will be published in Physica Status Solidi.

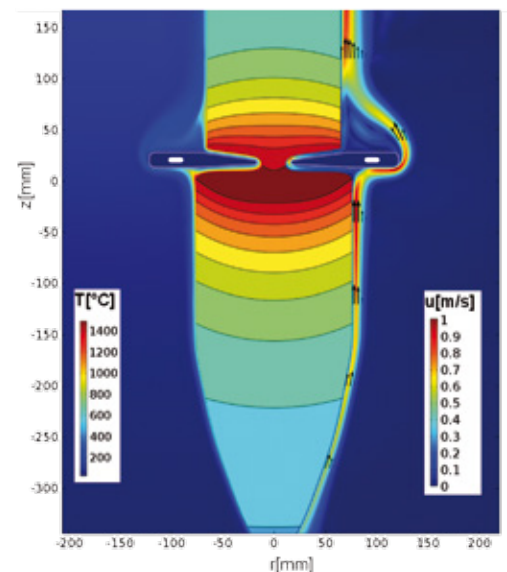
Fig. 1: Calculated temperature and velocity field in the gas atmosphere during a 6 inch FZ process.
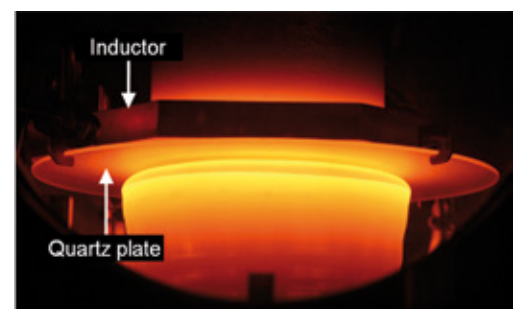

Fig. 2: FZ experiment using a quartz plate below the inductor to reduce the risk of arcing (5 inch process).

Polysilicon rods of high quality as the feed material for the FZ process are one of the main factors in the costs for FZ Si crystals. This is one reason why FZ Si has never established for solar cells, although high efficiencies up to 25 % have been demonstrated with this material. As a part of the FZ-Sil project, computer simulations aiming on optimization of the deposition process for polysilicon rods to increase the yield and lower the costs have been carried out at IKZ in cooperation with the polysilicon producer Silicon Products Bitterfeld GmbH and STR Group.

The rods produced by CVD in a Siemens reactor must be free of cracks and voids to be suitable for the FZ process. In particular too high residual stress in the rods must be avoided, as it can cause fracture during mechanical treatment for the FZ process or even during the cool-down in the reactor. During the CVD the U shaped rods are electrically heated by DC current, which inherently leads to radial temperature differences. This is the origin for the stress in the rods.

The amount of residual stress in the rods is determined by the whole thermal history of the CVD process and the subsequent cool-down phase in the reactor. In order to investigate the impact of different process conditions, temperature and stress evolution during cool-down has been numerically modelled at IKZ. The temperature distribution due to electric heating and convective cooling by the $HSiCl_3$ gas atmosphere was calculated by STR Group and results were used as initial conditions for the stress simulations at IKZ. Here, a transient-elastoplastic model within the software package COMSOL Multiphysics was applied.
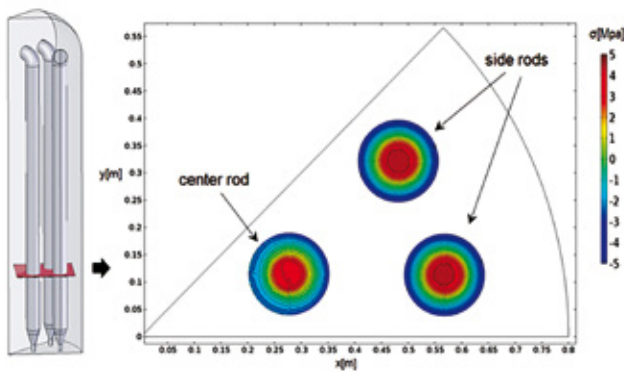

Fig. 3: Calculated residual stress in polysilicon rods (cross section of a 45° sector of a Siemens reactor).

Fig. 4: Test-shape of Si crystal for project "Kilogram-2" grown using the model-based diameter control system developed in IKZ.

Fig. 3 shows the calculated stress distribution in a cross section of a 45° sector of the reactor. Positive values (red) indicate tensile stress, whereas negative values (blue) show the region under compressive stress. It can be seen that the tensile stress maximum in the center rod is lower than in the side rods. The reason is a more homogeneous temperature distribution, as it is heated by the surrounding side rods. The influence of deposition temperature, different purging gases and rod diameter on the maximum stress in the rods have been examined.

Automatic diameter control is very important for crystal growth with respect to yield, quality, and reproducibility. Since there are no available diameter control systems for FZ Si crystal growth we developed such a system in Silicon & Germanium group. This work was done by Nico Werner in the frame of his PhD thesis [3] using model-based automation adapted for the FZ crystal growth equipment used in IKZ. A model-based controller gives a widely flexible handling of different growth parameters, different inductor types and different crystal diameters. A model-based state estimation technique, including an extended Kalman filter, and a model predictive controller were implemented to regulate the process without using additional controller components such as PID controller. The diameter control system developed and installed on two FZ furnaces was successfully proved for the growth of dislocation-free crystals with different diameters and even more it was used for test growth of FZ Si-crystal with changing diameter (Fig. 4). Such crystal shaping is intended for the ^{28}Si crystal in the project "Kilogram 2", since it allows the manufacturing of two silicon spheres using less of the monoisotopic and therefore extremely expensive raw material.

References

[1] Bureau International de Poids et Mesures http://www.bipm.org/en/scientific/mass/avogadro

[2] B. Andreas, Y. Azuma, G. Bartl, P. Becker, H. Bettin, M. Borys, I. Busch, M. Gray, P. Fuchs, K. Fujii2, H. Fujimoto, E. Kessler, M. Krumrey, U. Kuetgens, N. Kuramoto, G. Mana, P. Manson, E. Massa, S. Mizushima, A. Nicolaus, A. Picard, A. Pramann, O. Rienitz, D. Schiel, S. Valkiers, and A. Waseda, Phys. Rev. Lett. **106** (2011), 030801

[3] Werner, N., Analysis and control of the crucible-free Floating Zone (FZ) crystal growth of silicon, Dissertation, TU Berlin, 2014

[4] Haufe, S.; Untersuchung der Durchschlagfestigkeit von Schutzgasen in der FZ Silizium Kristallzüchtung in Abhängigkeit von der Temperatur; Bachelor Thesis; HU Berlin;2013

Multi-crystalline Silicon

Head: Dr. Frank M. Kießling
Team: D. Linke, Dr. T. Ervik

Überblick

In der Photovoltaik (PV) wird die Entwicklung neuer Technologien durch den immensen Preisdruck auf die Module getrieben. Die Entwicklungen zielen auf eine Steigerung der Ausbeute und Effizienz in der gesamten Wertschöpfungskette hin. Der PV-Markt wird dabei weiterhin durch die siliziumbasierte Solarzellenproduktion dominiert und es gilt, hohe Zelleffizienz bei geringen Kosten zu erreichen. Das Standardverfahren für die großtechnische Herstellung von multikristallinen (mc) Blöcken für Si-Solarzellen ist die gerichtete Erstarrung einer Siliziumschmelze. Geringere Herstellungskosten von mc-Si-Wafern sind trotz der geringeren Effizienz der Module im Vergleich zu einkristallinen Silizium-Wafern immer noch attraktiv. Während neue Zellkonzepte einen Entwicklungsschwerpunkt darstellen, wurden erhebliche Anstrengungen unternommen, um das gerichtet erstarrte mc-Si Material mit seinen vielfältigen, den Zellwirkungsgrad verringernden Defekten, zu verbessern. Ausbeute und Effizienz können bereits durch die Wahl der richtigen Züchtungsanlagen und Technologie erhöht werden. Dabei ist es wichtig, die Komplexität aller Verunreinigungsquellen und ihre Auswirkungen auf die Materialqualität zu verstehen. Von großem Interesses sind C-, O- und N-haltige zweite Phasen und Metallverunreinigungen aus verschiedenen Quellen. Diese Defekte haben weitreichende Auswirkungen auf das elektrische und mechanische Verhalten des Si-Materials. Während des Gesamtprozesses wird die Schmelze mit C, O und N und Übergangsmetallen wie Fe verunreinigt. Hauptsächlich durch Verunreinigungen verursachte Defekte und Versetzungsbündelungen wirken rekombinationsaktiv und führen zu deutlichen Effizienzverlusten der Solarzellen. Die Lebensdauer der Minoritätsträger kann als Indikator für die Qualität des Siliziummaterials betrachtet werden. Hochwertige Materialien mit hoher Lebensdauer der Minoritätsträger und Minoritätsträgerdiffusionslängen bieten das Potenzial, hohe Wirkungsgrade zu erreichen.

In den letzten Jahren wurden große Anstrengungen unternommen, um den Prozess des gerichteten Erstarrens in Bezug auf das Ofendesign, das Prozessgasmanagement, das Rühren der Schmelze und die thermischen Bedingungen vor, während und nach der Kristallisation zu optimieren. In Betracht gezogen wurden dabei die Nutzung von Keimplatten, Verunreinigungsreduzierung der Schmelze, günstige Keimbildungsbedingungen, kontrolliertes Korngrößenwachstum und die Verringerung anderer, die Lebensdauer begrenzenden rekombinationsaktiven Defekte, wie z.B. Versetzungsbündelungen. All diese Maßnahmen sind der Tatsache zu schulden, dass die Qualität des Kristalls wesentlich die Nachfolgeprozesse in der Wertschöpfungskette bestimmt.

Eine Möglichkeit, um den Schmelzenfluss, die Morphologie, die Form und die Temperaturstabilität der Wachstumsgrenzfläche zu steuern, ist die Verwendung nichtstationärer Magnetfelder. Eine technische Lösung bietet die Anwendung von Wandermagnetfeldern (TMFs), welche z.B. durch KRIST*MAG*® Heizer-Magnet-Module (HMM) erzeugt werden können, die vorzugsweise sowohl als Seiten- als auch Bodenheizer angeordnet sind. Diese Heizelemente erzeugen neben der üblichen Wärme für den Aufschmelz- und Kristallisationsprozess gleichzeitig magnetische Felder. Jedes Heizelement kann entweder nur mit Gleichstrom (DC), nur mit Wechselstrom (AC) oder in einem Mischbetrieb mit jedem beliebigen AC/DC-Verhältnis betrieben werden. Die entsprechenden Lorentzkräfte (F_L) können in ihrer Stärke und Richtung durch Änderung der AC-Amplitude ($F_L \alpha I_0^2$), der Frequenz ($F_L \alpha f$) und der Phasenverschiebung ($\Delta\varphi$) variiert werden. Diese Kräfte sind ausreichend, um die Schmelzenkonvektion gezielt zu steuern, was bereits in mehreren Publikationen beschrieben wurde [z.B. 1, 2].

Die Gruppe multikristallines Silizium hat ihre Forschungsaufgaben erweitert und neue F&E-Aktivitäten begonnen. Trotz der immer noch schwierigen Situation in der Europäischen Photovoltaikindustrie erweiterte das IKZ seine Aktivitäten auf dem Gebiet der gerichteten Erstarrung von Silizium unter dem Einfluss von Wandermagnetfeldern. Seit dem Frühjahr 2013 stehen der Gruppe mc-Silizium zusätzlich zu einer G1-Anlage (15 kg) eine weitere Anlage der Größe G2 (75 kg) und eine Beschichtungsstrecke für Solartiegel zur Verfügung. Die mit HMMs ausgerüsteten Vertical Gradient Freeze (VGF) Öfen sind Prototypen und bieten einzigartige Möglichkeiten, die Wachstumsbedingungen zu beeinflussen. Im Jahr 2013 wurde eine Kooperation mit der Roth & Rau AG und ein neues Projekt mit der Solarworld Innovations GmbH gestartet, während Erstarrungsversuche und Charakterisierungen für Industriepartner und das deutsche Forschungsnetzwerk "SolarWinS" fortgesetzt wurden.

Overview

The immense economic price pressure on photovoltaic (PV) modules drives the development of new technologies towards increased yields and efficiencies in the whole value chain. Silicon-based solar cell production dominates the PV market and the key issue is cell efficiency at low costs. Directional solidification (DS) is the standard process for large-scale production of multi-crystalline (mc) ingots for Si-based solar cells. Lower manufacturing cost of mc-Si wafers is very attractive despite the device efficiency of directionally solidified material being lower compared to single crystalline Si-wafers. While the development of new cell concepts is one issue, considerable efforts have been made to improve the less favourable crystalline structure of mc-Si with its various defects deteriorating the cell efficiency. Yield and efficiency can be increased already by choosing the proper growth equipment and technology. It is very important to understand the complexity of all impurity sources and their impact on the material quality. C-, O- and N-related second phase particles and metal contaminations from different sources are a major concern in mc-Si material with far-reaching impacts on its electrical and mechanical behaviour. During the growth the melt gets contaminated with C, O and N and transition metals like Fe. Mainly impurity-based defects and dislocation clusters are known to act as recombination active defects resulting in efficiency losses of solar cells. The lifetime of the minority carriers can act as an indicator for the quality of the as-grown silicon material. High quality materials provide the potential to reach high efficiencies, due to large minority carrier diffusion lengths and lifetime.

Big efforts have been made in the last years to optimize the directional solidification process in terms of furnace design, process gas management, melt stirring and thermal conditions before, during and after the solidification. In order to improve the crystal quality seeds were used, the contamination of the melt was reduced, favorable nucleation conditions were looked for, grain growth was controlled and the number of other lifetime-limiting recombination active defects, such as e.g. dislocation bundles were reduced. All these efforts have been taken due to the fact that the ingot quality determines significantly the post-processes in the value chain.

A possibility to control the melt flow, morphology, shape and temperature stability of the growth interface is the use of non stationary magnetic fields. One technological solution is the application of travelling magnetic fields (TMF) generated e.g. by KRIST*MAG*® heater magnet modules (HMMs), which are preferably arranged both as side and bottom heaters. These heaters are suitable to produce magnetic fields while maintaining the common function as a heat source during the solidification process. Each heater can operate eitherwith direct current (DC), with alternating current (AC) or in a mixed mode with any AC/DC ratio. The corresponding Lorentz forces (F_L) can be varied in strength and direction by setting AC amplitude ($F_L \alpha I_0^2$), frequency ($F_L \alpha f$) and phase shift ($\Delta \varphi$). These forces are qualified to control the melt convection in a way already well described in several publications [e.g. 1, 2].

The group multi-crystalline silicon has expanded its research tasks and started new R&D activities. Despite the still difficult situation in the European solar photovoltaic industry the IKZ expanded its activities in the field of directional solidification of silicon using processes under the influence of travelling magnetic fields. Since spring 2013 the group mc-silicon has at its disposal additionally to the G1-sized (15 kg) furnace a G2-sized (75 kg) furnace and a coating line for solar crucibles. The Vertical Gradient Freeze (VGF)-type furnaces equipped with HMMs are prototypes and offer unique possibilities to influence the growth conditions. In 2013 a co-operation with Roth & Rau AG and a new project with SolarWorld Innovations GmbH were started while growth and characterization activities have been continued with industrial partners and for the German research network "SolarWinS".

Results

First of all it has to be mentioned that travelling magnetic fields have been applied and adapted during all our experiments. The TMF fields have been chosen in order to meet the demands of the respective projects. The potential of our prototype growth furnaces have already been described in general [1, 2].

The German research network "SolarWinS" [3, 4] tries to answer the question of the fundamental potential limitation of directionally solidified mc-Si material. Investigations in the project are focused on fundamental interactions between silicon and its environment during crystallization, taking into account the influence of crucible purity, coating and working gas. In order to provide high-purity crucibles for silicon growth a Si_3N_4 coating process had to be adapted to the smooth surface of fused silica crucibles using our own technology on the IKZ coating line. It turned out that the high-purity, thin-walled fused silica crucibles were not suitable for the standard solidification process since the crucible side walls soften and deform. Since the softening temperature of fused silica is below the melting point of silicon, this results already during the melting of the Si feedstock in deformation of the crucible. It is easy to see (Fig.1) that this deformation of the crucible leads to undesirable flow patterns and velocities of the working gas on the melt surface. To be able to perform a comparative study of standard process parameters an overall process of direc-

tional solidification had to be developed using fused silica crucibles, but preventing crucible deformation. This process development included simultaneously parameter studies on gas supply and gas flow rates.

In the reporting period, the group mc-Si investigated the growth of multi-crystalline Si-ingots of different material qualities under ultra-clean conditions. From the start of the project it was known that there was no possibility to convert the hot-zone, made dominantly from carbon, to a carbon-free hot-zone. However, a significant reduction of the carbon impurity concentration could be achieved by advantageous flow conditions of the gas system, by variations of pressure, gas flow rates and geometric adjustments. It is known that among other reactions SiO evaporates from the melt during the process and reacts with the glowing graphite internals to CO. At the melt surface, CO decomposes to oxygen and carbon, leading to SiC formation when exceeding the solubility limit in the silicon melt. During the progress of the growth front, i.e. the directional solidification of silicon beginning from the crucible

Fig.1: Deformed fused silica crucible after a standard directional solidification process. The Si_3N_4 coating adhesion strength on the extremely smooth fused silica crucible surface is sufficient.

bottom, SiC can be captured and will be detected as a second phase in the solidified ingot. Information about the carbon content in the material can only be obtained through prepared samples but a realtime correlation would be extremely helpful. In general, the content of substitutional carbon is measured in the as-grown Si ingot by FTIR. To know the influence of the process conditions including the associated gas management on the carbon content, we have been looking for a realtime analytical method. Assuming that the amount of CO in the growth chamber correlates to the detected carbon concentration in the as-grown material, smaller CO concentrations should also lead to reduced carbon concentrations in the solidified ingot. Hence, the CO-concentration was measured ex-situ in dependence on the process and its related temperature regime.

In order to optimize the directional solidification process one has to understand the CO formation during the process. Figure 2 depicts a correlation of the CO-concentration. Depending on the melting procedure of the Si-feedstock the maximum of the produced CO-concentration shifts in respect to the process time. The CO concentrations can easily be correlated to the process temperatures while the gas stream and the pressure have been kept constant. After finding a suitable solidification process the gas flow rate has been changed. Figure 3 shows that the ex-situ detected CO-concentrations decrease with higher gas flow rates. FTIR measurements of C_s and O_i show that the concentrations can be reduced by one order of magnitude under optimized growth conditions and using TMFs. The course on the block height corresponds to the expected increase with increasing height for carbon and oxygen decrease.

Other activities of the group, especially bilateral projects with industry, are subject to restrictions and cannot be reported here. Further research activities will focus on the reduction of defects.

At this point I would like to thank especially Dr. Christiane Frank-Rotsch for continuous experimental support, Dr. Natascha Dropka for simulations and both for fruitful discussions.

Fig.2: CO-concentration in dependence on the process time: GM_02 corresponds to a fast melting process; GM_03 equals slow melting and GM_04 an optimized melting and growth process.
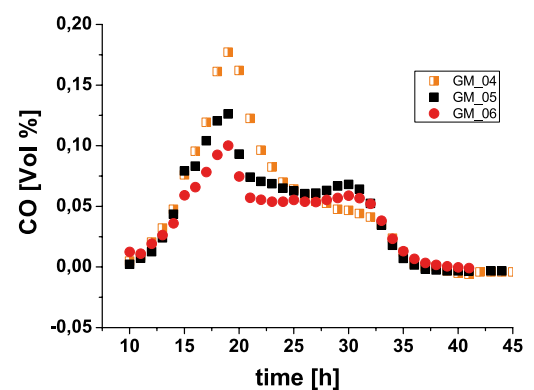
Fig.3: CO-concentration in dependence on the process time. The gas flow rate has been changed from run to run: GM_04 : GM_05 : GM_06 = 1 : 2 : 3.

References

[1]   F.-M. Kiessling, F. Büllesfeld, N. Dropka, Ch. Frank-Rotsch, M. Müller, P. Rudolph, J. Cryst. Growth 360 (2012) 81.

[2]   Ch. Kudla, A.T. Blumenau, F. Büllesfeld, N. Dropka, Ch. Frank-Rotsch, F. Kiessling, O. Klein, P. Lange, W. Miller, U. Rehse, U. Sahr, M. Schellhorn, G. Weidemann, M. Ziem, G. Bethin, R. Fornari, M. Müller, J. Sprekels, V. Trautmann, P. Rudolph, J. Cryst. Growth 365 (2013) 54.

[3]   W. Kwapil, A. Zuschlag, I. Reis, I. Schwirtlich, S. Meyer, R. Zierer, R. Krain, Frank M. Kießling, M.Schumann, C. Schmid and St. Riepe, in Proceedings of the 27th European Photovoltaic Solar Energy Conference, Frankfurt, 24Sep 2012 (WIP Renewable Energies, Munich, 2012) 627.

[4]   P. Karzel, M. Ackermann, L. Gröner, C. Reimann, M. Zschorsch, S. Meyer, F. Kießling, S. Riepe, and G. Hahn, J. Appl. Phys. 114 (2013) 244902.
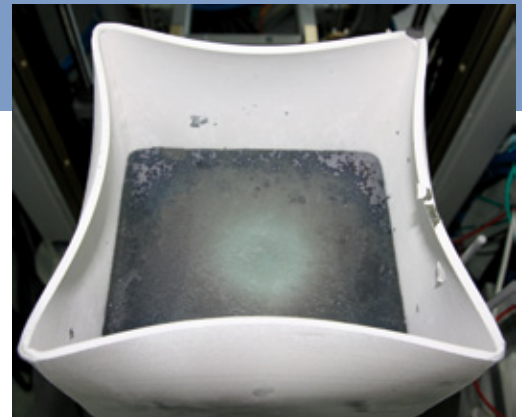
Gallium Arsenide

Head: Dr. Ch. Frank-Rotsch
Team: Dr. N. Dropka, A. Glacki, O. Root

Überblick

Der gezielte Einsatz von Magnetfeldern besitzt in der Kristallzüchtung ein großes Potential, da sich die Möglichkeit zur Verbesserung der Kristallqualität bei gleichzeitiger Verringerung von Herstellungskosten bietet. Die am IKZ entwickelte Technologie [1,2] ist für unterschiedliche Materialien erprobt worden, darunter die Halbleiter Galliumarsenid und Germanium. Galliumarsenid wird kommerziell in der WLAN-Kommunikation sowie in der Mikrowellen- und Hochfrequenz-Technologie eingesetzt. Aufgrund des ansteigenden Marktes für Smartphones ist entsprechend auch der GaAs-Bauelementemarkt weiterhin im Wachstum begriffen.

Die Forschungsaktivitäten des Themas „Galliumarsenid" konzentrierten sich im Berichtszeitraum weiter auf die Steigerung der Effizienz des VGF-GaAs-Züchtungsprozesses. Zur Lösung dieser technologischen und wissenschaftlichen Herausforderung wurden unterschiedliche Strategien verfolgt, wie die simultane Kristallisation in mehreren Tiegeln oder die Erhöhung der Kristallisationsgeschwindigkeit. Zur Steigerung der Prozesseffizienz ist eine definierte Kontrolle der Strömung in der Schmelze von entscheidender Bedeutung. Die gezielte Beeinflussung der Strömung durch Wandermagnetfelder wurde bereits erfolgreich am IKZ eingesetzt. Gegenwärtig sind zwei VGF-Anlagen mit KRIST*MAG*® Heizer-Magnet-Modulen (HMM) zur simultanen Erzeugung von Wärme und Wandermagnetfeld (TMF) ausgerüstet. Eine dieser Anlagen wurde dabei mit einer neuen Generation des HMMs ausgerüstet, welche die simultane Kristallisation von bis zu vier VGF-GaAs-Kristallen mit einem Durchmesser von 4 Zoll in einer Mehrtiegelanordnung ermöglicht. Die Konstruktion und die Prozessentwicklung wurden kontinuierlich durch 2D- und 3D-Simulationsrechnungen unterstützt, dabei kamen die kommerziellen Programme ANSYS CFX und Crys*MAS* zum Einsatz. Es ist anzumerken, dass das erlangte Know-how auch Potential für die Züchtung von anderen kristallinen Materialien liefert.

Im September 2013 wurden Untersuchungen zum Lösungsverhalten von festen GaAs unter definierten Bedingungen (z.B. Korngröße, Temperatur, Licht, Lösungsmittel) begonnen. Diese Untersuchungen werden im Rahmen des BMBF-Verbundprojektes „TEMPO" mit 13 weiteren Partnern aus Industrie und Forschung durchgeführt. Dieses Projekt zielt auf die toxikologische Bewertung von Halbleitermaterialien, darunter Galliumarsenid, zur Bereitstellung von belastbaren Erkenntnissen zur Risikowertung für den kompletten Produktionskreislauf von der Herstellung bis zur Entsorgung/Recycling der Materialien. Ausgangspunkt dieser Untersuchungen ist die aus den REACH- und CLP-Bestimmungen der EU entstandene Notwendigkeit, die noch vorhandenen Wissensdefizite zu den Eigenschaften und dem Lösungsverhalten dieser bedeutenden Halbeleitermaterialien systematisch zu ermitteln.

Overview

Crystal growth applying magnetic fields has the potential to enhance crystal quality while simultaneously reducing production costs. The technology developed at IKZ [1,2] has been applied to the growth of different crystalline materials, among them semiconductors like gallium arsenide or germanium. Gallium arsenide is commonly used i.a. for wireless communica-tion, in microwave or high frequency technology. And due to the increasing market for smart phones, the GaAs device market is predicted to grow still further.

The research activities of the Gallium Arsenide group were focused on the further improvement of the efficiency of VGF crystallization process. To meet this technological and scientific challenge, different strategies were applied, e.g. a simultaneous crystallization in multiple crucibles (numbering up approach), an increase of crystal growth velocity etc.. For process enhancement, an exact and permanent control of the melt flow is of a crucial importance. One possibility is to use travelling magnetic fields, which have been already successfully applied at IKZ. Currently two our VGF furnaces are equipped with a KRIST*MAG*® heater magnet module (HMM) for a simultaneous generation of heat and traveling magnetic field (TMF). Thereby one of the furnaces is provided with a new generation of HMM, that enables a simultaneous crystallization of four 4 inch VGF-GaAs crystals in four crucibles. Design of equipment and a process development was continuously supported by 2D/3D numerical modeling using commercial

software ANSYS CFX and CrysMAS. It is noteworthy that gained know-how by simulations can be extended to various materials and applications.

Furthermore, study of the solubility of solid GaAs as a function of specified parameter (e.g. grain size, temperature, light, solvent) started in September 2013. These research activities are carried out in a BMBF founded frame work "TEMPO" with 13 other partners from industry and research institutes. The project aims at the toxicological evaluation of semiconductor materials, amongst them gallium arsenide, to provide valuation methods for a risk assessment including the complete life cycle from production to disposal. These investigations have been triggered by the REACH and CLP regulations of the EU.

Results

During the reporting period, the growth of VGF-GaAs crystals in the KRIST*MAG*®-HMM under the influence of TMF was continued. Thereby, the main goal of the experiments was to control the solid/liquid interface bending using Lorentz forces in both: a single-crucible HMM as well as in the new developed multi-crucible HMM (Fig.1a).

The later design of multi-crucible HMM was particularly developed to increase the yield of the crystal growth process. Ideas and technologies for crystal growth in our multi-crucible setups are described in our patent application [3] in more detail. The challenge in the development of a multi-crucible HMM is to achieve a nearly symmetric distribution of temperature and Lorentz force density in each crucible. If this goal is reached, equal seeding and interface posi-tions in each crucible as well as a symmetric interface shape and therewith symmetric stress distributions in all crystals will be obtained. Other multi-crucible furnace designs described in litera-ture do not fulfill these requirements. On contrary, our simulation results indicated that our novel multi-crucible HMM design (see Fig. 1a), may pro-vide nearly equal temperature and magnetic flux density distribution in all crucibles (Fig. 1b). In the first crystal growth experiments performed in the multi-crucible set-up, two crystals were grown simultaneously, while the remaining two crucibles were filled with graphite dummies. Fig. 1c shows an image of these first two grown crystals. Both of them were single crystalline and were seeded nearly at the same axial position. The induced TMF markers were also nearly at the same axial position, indicating that the interface shape in the crystal was approximately symmetric. The investigations in the multi-crucible setup are in progress. For example, to stabilize the seed-ing, an increased axial temperature gradient will be beneficial.Therefore, the process optimization is continued.

Based on the KRIST*MAG*® concept we also studied scale-up of VGF crystallization process in magnetic fields as well as the TMF change with the progress of crystallization. During the reporting period, we adjusted the magnetic parameters of TMF and succeeded to grow Si-doped GaAs single crystals with a weight of up to 9 kg (Fig. 2) and the concave interface bending in the range from 1- 8 %. This represents a significant increase of the crystal loading (from 7 kg) since the last reporting period with improved interface morphology.

To investigate the separate influence of the TMF on the deflection of the solid/liquid interface, the magnetic field was switched on and off five times during one experiment. In comparison to the growth without TMF, the obtained results showed the reduced interface bending with TMF. The average reduction of interface deflection lied in the range of 30%. More details about the grown GaAs VGF crystals are given in [4].

Another promising approach to improve the magnetic control during crystal growth is application of pulsed TMF and development of a corresponding process. Simulation results showed the feasibility of pulsed TMF technology for a reduc-tion of still existing asymmetric distributions of magnetic field and temperature if disturbances originated from an asymmetric HMM design. Fig. 3 shows the predicted influence of pulsed TMF on the simulated temperature distribution in a GaAs melt. In case of a pulsed TMF (Fig. 3 left), more constant axial gradient with reduced inhomogeneity is assumed, compared to the case of "unmodified" TMF (Fig. 3 right), especially in the marked melt region.
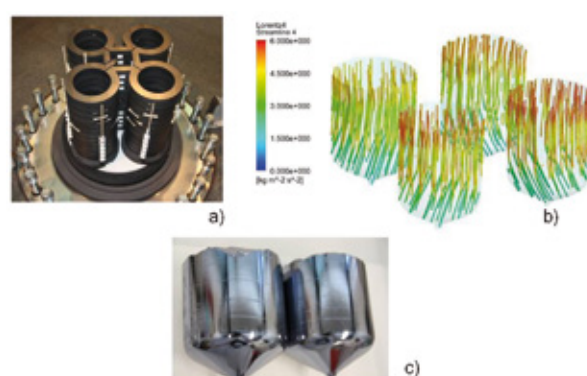

Fig. 1: a) 4-crucible heater-magnet module; b) simulated 3D distri-bution of Lorentz force density distri-bution in a 4-crucible setup; c) images of first two 4 inch GaAs single crystals simultaneously grown in a multi-crucible setup
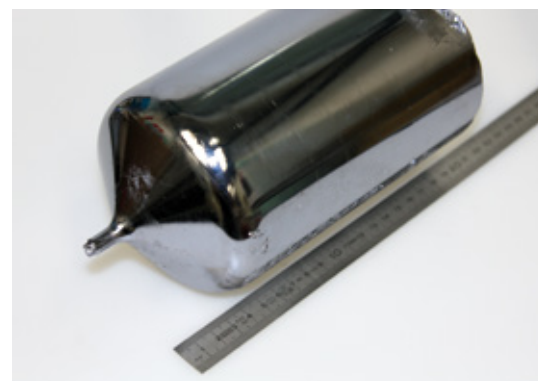

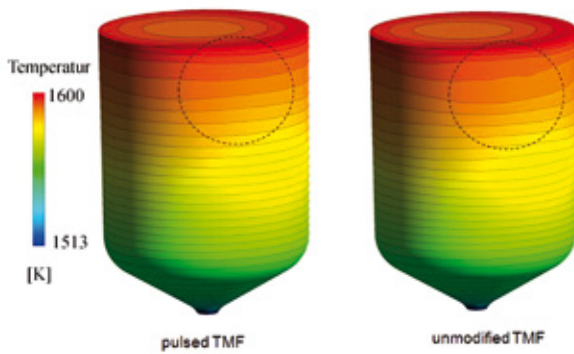*Fig. 2: 4 inch VGF-GaAs single crystal, m = 9 kg, <100>-ori-ented, grown in KRISTMAG®- HMM.*

Fig. 3: Simulated 3D temperature distribution in a GaAs melt using HMM with pulse TMF (left) and unmodified TMF (right).

Fig. 4: Temporal profiles of Lorentz force density of downward directed TMF after modulation of AC amplitude, using various modulation frequencies, modulation amplitudes and time average Lorentz force densities.

For a success of pulsed TMF technology, a selection and optimization of pulsing parameters of TMF are crucial. Figure 4 illustrates the influence of the modulation frequency, modulation strength and modulation amplitude on the Lorentz forces density (FL) in the GaAs melt. First results of the influence of pulsed TMF on the VGF-GaAs growth are given in [5] in more detail.

In summary, pulsed TMF offers a considerable potential for the further improvement of VGF-GaAs single crystal growth process. Therefore, the activities in this field will be intensified in the future.

The research results of GaAs group attracted broad international attention, which is evident in a number of invited talks on international conferences.

References

[1]   Ch. Frank-Rotsch, O. Klein, R.-P. Lange, B. Nacke, P. Rudolph, patent description DE 10 2007 028 548 B4

[2]   F. Büllesfeld, N. Dropka, W. Miller, U. Rehse, P. Rudolph, U. Sahr, patent description DE 10 2008 059 521 B4

[3]   N. Dropka, Ch. Frank-Rotsch, M. Ziem, P. Lange, patent description DE 10 2012 204 313 B3

[4]   Ch. Frank-Rotsch, N. Dropka, A. Glacki, U. Juda, Journal of crystal growth in press: http://dx.doi.org/10.1016/j.jcrysgro.2013.12.063

[5]   N. Dropka, Ch. Frank-Rotsch, Journal of Crystal Growth 386 (2014)146-153

Oxides/Fluorides

Gallium Nitride

Aluminium Nitride

Dielectric and Wide Bandgap Materials

Head of department: Prof. Dr. Matthias Bickermann

Die Abteilung „Dielektrika und Wide-Bandgap-Materialien" beschäftigt sich mit der Züchtung von Volumeneinkristallen und besteht aus den Themengruppen „Aluminiumnitrid (AlN)", „Galliumnitrid (GaN)" und „Oxide/Fluoride". Die Kristalle finden als Substrate Verwendung für neuartige Halbleiter- und multiferroische Anwendungen sowie als Laser- und nicht-linear optische Materialien und piezoelektrische Sensoren. In der Abteilung arbeiten 8 Wissenschaftler, 3 Post-Doktoranden, 5 Doktoranden und 8 Ingenieure/Techniker (Stand Januar 2014). Darüber hinaus wurden im Berichtszeitraum mehrere Bachelor- und Masterarbeiten betreut.

Basierend auf der etablierten Züchtung von Einkristallen mit Perowskit-Struktur wie z.B. Seltenerd-Scandaten (RE-ScO$_3$), -aluminaten, -gallaten und -tantalaten (z.B. LSAT) wurde in der Themengruppe Oxide/Fluoride ein Projekt zur Herstellung von Strontiumtitanat (SrTiO$_3$) mittels des Czochralski-Verfahrens gestartet. Ziel ist die Herstellung von Substraten für Multiferroika und topologische Isolatoren mit hoher struktureller Perfektion. Zudem wird die viel beachtete, einzigartige Entwicklung von Volumenkristallen neuer halbleitender Oxide wie z.B. β-Ga$_2$O$_3$, In$_2$O$_3$ und SnO$_2$ fortgesetzt. Neben der intensiven Zusammenarbeit mit den Gruppen der Abteilung „Schichten und Nanostrukturen" wird mit Wissenschaftlern aus der Humboldt-Universität, dem Paul-Drude-Institut und anderen an der Bestimmung der Materialeigenschaften und der potentiellen Anwendungsgebiete gearbeitet, um neue Funktionalitäten für die Leistungselektronik und die Spintronik zu erschließen.

Die Themengruppe AlN ist Teil des bundesweiten Konsortiums "Advanced UV for life", das erfolgreich im Förderwettbewerb „20zwanzig" des BMBF teilgenommen hat. In den kommenden Jahren werden AlN-Substrate dazu beitragen, die UV-Optoelektronik in medizinischen sowie umwelt- und produktionstechnischen Anwendungen zu etablieren. Hauptthema bei der AlN-Kristallzüchtung durch physikalischen Gasphasentransport ist die Vergrößerung des einkristallinen Durchmessers unter Beibehaltung der nahezu perfekten strukturellen Qualität der Keimkristalle. Andererseits wird ein tieferes Verständnis von Dotierproblemen und der Verunreinigungsproblematik erarbeitet. Schließlich wurden in der Themengruppe GaN neue Projekte begonnen, um das GaN-Wachstum mit kontrollierter Kohlenstoffdotierung mittels Pseudo-HVPE zu untersuchen, und um Nitride mit Hilfe der Synthese-Lösungszüchtung herzustellen, wobei ein induktiv gekoppeltes Plasma den aktivierten Stickstoff bereitstellt.

The department „Dielectric and Wide Bandgap Materials" is concerned with the growth of bulk single crystals and organized in the topical groups "Aluminium nitride (AlN)", "Gallium nitride (GaN)", and "Oxides/Fluorides". The crystals are used as substrates for novel semiconductors and multiferroic applications as well as for lasers, non-linear optical materials, and piezoelectric sensors. As of January 2014, 8 senior scientists, 3 post-doctoral scientists, 5 PhD students, and 7 technicians/engineers work in the department. Additionally, several bachelor and master theses were supervised.

Based on the well-established growth of crystals with perovskite structure such as rare-earth scandates (REScO$_3$), aluminates, gallates, and tantalates such as LSAT (La,Sr)(Al,Ta)O$_3$, the Oxide/Fluoride topical group launched a project on strontium titanate (SrTiO$_3$) bulk growth by the Czochralski method. The goal is to prepare substrates for multiferroics and topological insulators with high structural quality. Furthermore, the most remarkable, unrivalled work on novel transparent semiconducting oxides (TSO) such as β-Ga$_2$O$_3$, In$_2$O$_3$, and SnO$_2$ is continued. Apart from the strong cooperation with the in-house thin film growth activities, the oxide group is collaborating with researchers from the Humboldt University, the Paul Drude Institute, and others to evaluate the material properties as well as potential applications to enable new functionalities in power electronics and spintronics.

The AlN topical group is part of a national consortium "Advanced UV for life" that succeeded in the funding competition of the BMBF "20zwanzig" initiative. In the years to come, AlN substrates will help to establish UV optoelectronics for medical, environmental, and production applications. The main task in AlN bulk growth by physical vapour transport is to increase the single-crystalline diameter while perpetuating the nearly perfect structural quality of the seed crystals. But we also work on a deeper understanding of doping issues and impurity contamination. Last but not least, new projects in the GaN topical group have been launched to investigate growth of GaN with controlled carbon doping by the pseudo-halide vapour phase epitaxy, and to prepare nitrides by synthesis solute diffusion, using inductively coupled plasma for providing active nitrogen.

Oxides/Fluorides

Head: Dr. R. Uecker
Team: M. Bernhagen, M. Brützam, Dr. Z. Galazka, S. Ganschow, Dr. C. Guguschev, J. Philippen, M. Rabe, I. Schulze-Jonack, Dr. D. Schulz, A. Tauchert, E. Thiede

Überblick

Diese Gruppe befasst sich mit der Forschung zur Züchtung von oxidischen und fluoridischen Einkristallen. Die Kristalle werden mit Durchmessern bis zu 50 mm und Längen von 150 mm gezüchtet. Die Kristallzüchtung erfolgt überwiegend aus der Schmelze nach der Czochralski-Methode, der am höchsten entwickelten Methode zur Züchtung von qualitativ hochwertigen Volumenkristallen, aber auch nach Bridgman, Kyropoulos, Levitation-Assisted Self-Seeding Crystal Growth Method (eigenes Patent[1]), Physical Vapor Transport, Top Seeded Solution Growth und aus der Schmelzlösung. Das bearbeitete Kristallspektrum resultiert aus Anforderungen externer und interner Forschungspartner, von Industrieunternehmen und der eigenen Grundlagenforschung. Zwei weitere Methoden werden für die Züchtung von Kristallfasern mit Durchmessern bis zu 2 mm eingesetzt, die Laser Heated Pedestal Growth und Micro-Pulling Down Methode. Gegenwärtige Anwendungsschwerpunkte der hier gezüchteten Kristalle sind die Oxidelektronik, Optoelektronik, die Sensorik und Substrate für Perowskitschichten.

Auf dem Gebiet der Züchtung von transparenten halbleitenden Oxidkristallen hat sich das IKZ innerhalb der vergangenen fünf Jahre eine führende Stellung in der Welt erarbeitet. Diese Materialien finden potentielle Anwendungsmöglichkeiten in verschiedenen Gebieten wie der Hochleistungselektronik, in der transparenten Elektronik, für LEDs und Gassensoren, z.B. für die Abgaskontrolle. Die erstmalige Züchtung von In_2O_3- und SnO_2-Volumenkristallen[2,3,4] ermöglicht künftig die Homoepitaxie dieser Materialien. Daneben ist die Forschung auf dem Gebiet neuer hochtemperaturstabiler piezoelektrischer Kristalle Gegenstand einer langfristigen Industriekooperation mit der Kistler Instrumente AG, Winterthur/CH.

Besonders vielfältige und zukunftsträchtige Anwendungen ermöglichen Kristalle mit kubischer bzw. pseudokubischer Perowskitstruktur. Werden derartige Kristalle als dünne Schichten abgeschieden, kann man ihre Eigenschaften durch die gezielte Verspannung modifizieren („Strain Engineering"). Dieses Strain Engineering dünner Schichten beruht auf einer Gitterverspannung (bis in den Prozentbereich), die durch Epitaxie auf einem kristallinen Substrat mit leicht abweichender Gitterstruktur induziert wird. Es existiert eine Vielzahl von kommerziell verfügbaren Substratkristallen mit Perowskitstruktur. Oberhalb einer Gitterkonstante von 3,9 Å gab es jedoch bisher nur die Gruppe der Seltenerdscandate. Die Züchtung dieser Kristalle wurde am IKZ im Rahmen einer Forschungskooperation mit der Cornell University/USA entwickelt. Ein stufenloses Strain Engineering wird durch die Züchtung von Mischkristallen aus benachbarten Vertretern dieser Materialgruppe ermöglicht[5]. Während das IKZ nach wie vor der einzige Züchter dieser Kristalle weltweit ist, gelangen an der Cornell University spektakuläre Erfolge auf dem Gebiet des strain engineerings von darauf abgeschiedenen Epitaxieschichten[6]. Aber auch die Seltenerdscandate decken nur den Bereich bis 4,02 Å ab. Neue Materialien benötigen Perowskitsubstrate mit noch größeren Gitterkonstanten[7]. Einer der seltenen Kandidaten ist das $LaLuO_3$ (pseudokubische Gitterkonstante = 4,174 Å), das der Cornell University im Berichtszeitraum zur Verfügung gestellt werden konnte.

Eines der klassischen und immer noch wichtigsten Perowskitsubstrate ist das Strontium-titanat. Dieses Material erfordert spezielle Züchtungsbedingungen, die bisher ausschließlich mit Methoden realisiert werden konnten, in deren Ergebnis Kristalle relativ geringer Perfektion standen. Strontiumtitanat ist bisher das einzige Substratmaterial, mit dem ein oxidisches 2D-Elektronengas realisiert werden konnte, das wiederum die Herstellung neuer und miniaturisierten elektronischer Bauteile wie HEM-Transistoren, d.h. Transistoren mit hoher Elektronenbeweglichkeit, ermöglicht. Seine erfolgreiche Anwendung erfordert eine besonders hohe Kristallperfektion. Um sie zu erreichen, wurde im IKZ im Rahmen eines SAW-Projektes begonnen, eine Züchtungstechnologie für Kristalle hoher Qualität zu entwickeln.

Herr Dr. Jan Philippen schloss in 2013 seine Promotion mit dem Thema "Fiber crystal growth of cerium doped calcium scandate, strontium yttrium oxide and tristronstrium silicate", erfolgreich an der Technischen Universität Berlin ab.

Overview

This group is dealing with research in the growth of bulk oxide and fluoride single crystals. These crystals are grown with diameters up to 50 mm and lengths up to 150 mm. The main growth technique is the Czochralski method, although other ones are also utilized, such as the Bridgman, Kyropoulos, Levitation-Assisted Self-Seeding Crystal Growth Method (own patent[1]), Physical Vapor Transport, Top Seeded Solution Growth and flux. Based on a high technical level and degree of process automation the Czochralski method is the most developed method for growing high-quality bulk single crystals from the melt. A wide spectrum of oxide compounds have been grown and investigated as a result of requirements of external and internal research partners, of industrial companies and, of own basic research. Two further methods are used for the growth of single crystalline fibers with diameters up to 2 mm, including the Laser Heated Pedestal Growth and Micro-Pulling Down Method. Current application fields of our crystals are oxide electronics, optoelectronics, sensors and, substrates for perovskite thin films.

During the last five years IKZ achieved a worldwide leading position in the field of crystal growth of transparent semiconducting oxide crystals (TSOs) with a wide spectrum of potential applications, including high power electronics, transparent electronics, light emitting diodes and environmental control (gas sensor). The first-time growth of In_2O_3 and SnO_2 bulk crystals[2,3,4] will allow the homoepitaxy of these materials. Beside this long term collaboration in the field of new high temperature stable piezoelectric crystals connects this group with Kistler Instrumente AG, Winterthur/CH.

Fig. 1: Relation between free electron concentration and growth conditions: substrate tem-perature and $p(SnO)$ / $p(O_2)$ ratio.

Crystals with cubic or pseudo cubic perovskite structure enable numerous versatile and seminal applications. Deposited as thin films their physical properties can additionally be modified by strain engineering. Strain engineering of thin films is based on a lattice dilatation or compression (up to percent area) which forms by deposition on a substrate with slightly differing lattice structure. IKZ research activities can also be found in the report of the group Ferroelectric Oxide Layers, which is also supplied with substrates from our group. There is a plurality of commercially available substrate crystals with perovskite structure. However, the only employable candidates with a (pseudo) cubic lattice constant above 3.9 Å are the rare earth (RE) scandates. The growth process of these crystals was developed as a part of research collaboration with the Cornell University, Ithaka/USA. A stepless strain engineering is enabled by the growth of solid solutions of adjacent RE scandates[5]. While IKZ is still the only grower of these crystals worldwide, the Cornell University reached spectacular successes in the field of strain engineering of epitaxial layers deposited thereon[6]. But the RE scandates cover only the lattice parameter range until 4.02 Å. New advanced materials need perovskite substrates with even larger lattice constants[7]. One of such rare perovskite is $LaLuO_3$ with a pseudo cubic lattice constant of 4.174 Å which has been provided to the Cornell University in 2013.

Fig. 2: Bulk SnO_2 single crystal of 1 inch diameter grown on an R-plane sapphire substrate (a) and one-side epi-ready SnO_2 wafers (b).

One of the classic and still important perovskite substrates is strontium titanate. The growth of this material requires special conditions and advanced research, which so far could only be realized with methods producing low quality crystals. Nevertheless, strontium titanate is the only substrate crystal which allowed the realization of an oxide based two-dimensional electron gas hitherto, which in turn may allow new and smaller electronic components like high-electron-mobility transistors. Its successful application presupposes particularly high crystal perfection. The development of a growth technology for high quality strontium titanate crystals will be pursued in the frame of a project funded in the frame of the Leibniz Competition.

Finally, we are pleased to report that Dr. Jan Philippen graduated successfully at Technische Universität Berlin with his thesis "Fiber crystal growth of cerium doped calcium scandate, strontium yttrium oxide, and tristrontium silicate".
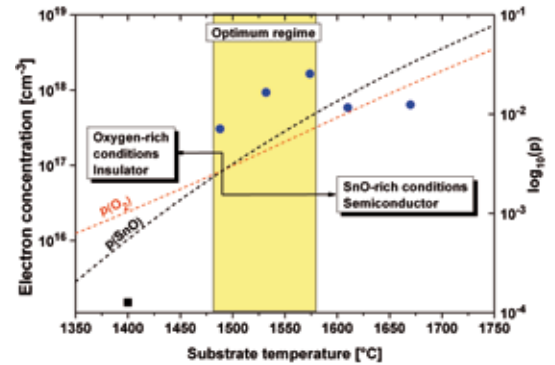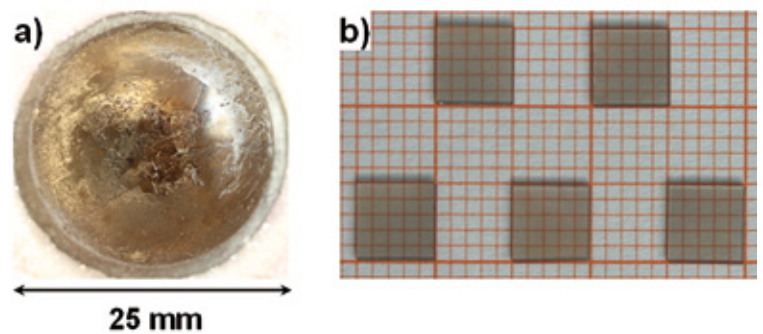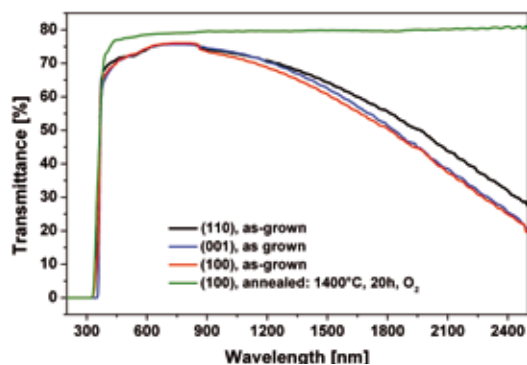
Fig. 3: Transmittance spectra of as-grown bulk SnO$_2$ single crystals. Sample thickness was 0.5 mm.

Results

The research on SnO$_2$ has been one of the main topics of the group during the report period. The most important results of this work have already been published[4,8]. SnO$_2$ is a transparent semiconducting oxide (TSO) with a wide bandgap of 3.5-3.8 eV. However, it is the most unstable compound at high temperatures as compared with other TSOs and growing SnO$_2$ from the melt by current, state-of-the-art growth techniques has not been reported yet. So far SnO$_2$ single crystals were grown from the gas phase and flux only. The crystals grown from the flux were needles of about 1 mm^2 in cross-section and were highly contaminated with flux elements. Growing SnO$_2$ by the chemical vapour transport (CVT) resulted in crystal size of about 2 mm^2 only. Much better results have been obtained by the physical vapour transport (PVT) with a maximum cross-section of the needle-shaped crystals up to 7x7 mm.

We performed a number of experiments in order to melt SnO$_2$ with oxygen partial pressures ranging from 0.05 to 140 bar and temperatures up to 2100°C, but no melting was observed. Our experiments clearly evidence that the melting point of nearly-stoichiometric SnO$_2$ (if exists) well exceeds 2100°C. The impossibility of melting and easy decomposition and evaporation of SnO$_2$ led us to the conclusion that the PVT method is possibly the most appropriate technique for obtaining truly bulk SnO$_2$ single crystals. The PVT growth occurs through decomposition of SnO$_2$ into SnO (g) + ½ O$_2$ (g) at high temperatures and subsequent oxidation of SnO(g) back into SnO$_2$(s) at lower temperatures in the presence of oxygen. For the PVT method we applied an iridium crucible containing the SnO$_2$ starting material, which was covered by a ring-shaped seed holder acting as a nest for a circular sapphire or rutile crystal seed (or substrate). The crucible was placed inside a thermal insulation and was heated up inductively. The source of the oxygen was CO$_2$, which provided a variable oxygen concentration vs. temperature. Fig. 1 shows the relation between the oxygen partial pressure from CO$_2$ and SnO partial pressure resulted from the decomposition of SnO$_2$ vs. temperature. When the crystals were grown at oxygen-rich conditions, the crystals were orange or pink-orange and electrical insulators. At approximately the same oxygen and SnO partial pressures the crystals were brownish, while at SnO-rich conditions – dark violet to almost black (for high SnO partial pressure). In both latter cases the crystals were semiconductors. The brownish crystals were turned to pink or colourless by annealing in the presence of oxygen at temperatures at least 800°C for at least several hours. For these specific growth conditions the best results were obtained for a substrate temperature between about 1480-1580°C and a source temperature higher by 100-130 K, when using CO$_2$ growth atmosphere at atmospheric pressure. The optimum growth rate was 0.5-0.6 g/h.

In this way large SnO$_2$ single crystals were obtained, 25 mm in diameter and 10-15 mm thick, from which substrates for epitaxy could be fabricated (Fig. 2). The FWHM of the rocking curve of the (200) peak was around 35 arcsec.

Fig. 3 illustrates the transmittance spectra of as-grown SnO$_2$ single crystals of different surface orientations. The spectra show a very steep absorption edge at 330-355 nm depending on orientation and good transparency in the visible spectrum. The absorption in the near infrared (NIR) spectrum (> 800 nm) is caused by the presence of free electrons at a density of about 1018 cm^{-3}. SnO$_2$ shows full transparency in the visible and NIR spectra when in insulating state, obtained after annealing in oxygen (> 800°C, at least several hours).
Table 1 summarizes the electrical properties of as-grown SnO$_2$ crystals at room temperature depending on the partial pressure ratio of SnO and O$_2$.

When the crystals were grown under p(O$_2$)>p(SnO) they were electrical insulators, otherwise the crystals were n-type semiconductors with a free electron concentration of 3×10^{17}– 2×10^{18} cm^{-3} and an electron mobility approaching 200 cm^{2}V^{-1}s^{-1}.

A second main topic of the group consisted in crystal growth and characterization of strontium titanate (SrTiO$_3$). SrTiO$_3$ is one of the most commonly used substrate crystals for the epitaxy of perovskite thin films. However, advanced applications are limited by the low quality of the currently commercially available crystals. As a part of a project funded by the Leibniz Association, our objectives are to provide high quality SrTiO$_3$ single crystals in a near-cylindrical shape grown from stoichiometric and non-stoichiometric melts and to investigate their properties in dependence on growth conditions. At the current stage we are working with different growth techniques and continuously improve quality and yield of this substrate material. Substrates made from such high quality crystals are especially attractive for the realization of oxide based two dimensional electron gases (2-DEG). So far such

Table 1: Electrical properties at room temperature of as-grown bulk SnO$_2$ single crystals.

p(SnO)/p(O$_2$)	Carrier conc. [cm^{-3}]	Carrier mobility [cm^{2}V^{-1}s^{-2}]	Resistivity [Ω cm]	Conduction type
≥ 1	3×10^{17}–2×10^{18}	125-202	0.03-0.11	n-type semiconductor
< 1	–	–	typical for insulators	

2-DEGs have been found only at the interface between one single substrate – SrTiO$_3$ – and the following oxide films: LaTiO$_3$[9], LaAlO$_3$[10], LaVO$_3$[11], LaGaO$_3$[12], GdTiO$_3$[13], and KTaO$_3$[14]. It also has been found in SrTiO$_3$/SrTi$_{0.8}$Nb$_{0.2}$O$_3$ superlattices[15].

In general, the method of choice for growing and producing high-quality bulk single crystals is the Czochralski method. However, so far this method was not successfully applied for the growth of SrTiO$_3$ single crystals.

In the report period we started growing SrTiO$_3$ crystals by the top-seeded solution growth method from self-flux, i.e., from non-stoichiometric melts[16]. Their etch pit density was in the order of 1-2x10^4/cm^2. To the best of our knowledge, near-cylindrical shaped SrTiO$_3$ crystals of several cm length and diameters of up to 15 mm were grown for the first time by this method ([8] and Fig. 4a). However, we are proud to present here the worldwide first top seeded solution grown SrTiO$_3$ crystal with a diameter larger than 1 inch. A crack-free <100> oriented and polished crystal section is shown in Fig. 4b. The {110} and {100} crystal facets can be seen at the rim of the slab. Because self-flux growth of large diameter SrTiO$_3$ crystals holds the risk of forming a disturbed core region the process still needs further optimization.

Exploring the reasons which hinder a successful use of the Czochralski method for SrTiO$_3$, we first investigated the heat transport during crystal growth. For that purpose we measured the high temperature optical absorptions. Because of the high melting point of SrTiO$_3$ (2350 K), the heat transport is dominated by radiation. If the crystal is effectively opaque at high temperatures, the dissipation of latent heat is hindered which can cause interface instabilities leading to a spiral formation. In self-flux solution growth, the liquidus temperature is lowered and the heat transport through the crystal increases. Thereby the risk of interface instabilities decreases.

To understand the temperature dependent optical absorption of SrTiO$_3$, UV/VIS and IR spectra of Verneuil (from external resources) and Czochralski grown samples were measured from 4 to ~1703 K. Some spectra are given in Fig. 5 as an example. The shift of the optical absorption edge is clearly visible. From the measured transmissions the absorption coefficients were calculated. SrTiO$_3$ has an indirect band gap, so around the absorption edge the absorption coefficient, α, is proportional to: $\alpha \propto (E_{photon} \pm E_{photon} - E_{gap})^2$

This means $\sqrt{\alpha}$ is linear when E_{photon} is approximately E_{gap} and if this is extrapolated to $\sqrt{\alpha}=0$, the band gap energy is found (see Fig. 6). These energies can be extrapolated to the melting point. They give an insight into the fundamental photon absorption, the intrinsic free carrier density and through that the free carrier absorption. These will be discussed in an upcoming publication and allow for an estimate of the high temperature heat transport which is important for further optimization of the crystal growth process. The Czochralski method is also under an intensive research and some results are shown in Fig. 1c-d. We succeeded in growing spiral-free crystals up to 2 inch diameter (Fig. 4c) and up to 15 mm length (Fig. 4d). In contrast to self-flux growth, core regions were not observed here.

In addition to the activities described above, several research institutes were provided with different oxide and fluoride crystals: TU Bergakademie Freiberg: Tantalites; HMI Berlin: BiVO$_4$; FEE Idar-Oberstein: Tb$_2$Ti$_2$O$_7$; Humboldt Universität Berlin: In$_2$O$_3$, Ga$_2$O$_3$; Universität Magdeburg: SnO$_2$, In$_2$O$_3$; Max-Planck-Institut für Physik des Lichts Erlangen: Ga$_2$O$_3$; Helmholz Zentrum Rossendorf: Ga$_2$O$_3$; Universität Hamburg: In$_2$O$_3$; ISAS Berlin: Ga$_2$O$_3$; TU Berlin: In$_2$O$_3$; PDI Berlin: In$_2$O$_3$, Ga$_2$O$_3$; Universität Münster: Mg$_2$SiO$_4$; KTH Stockholm/S: BaMgF$_4$; Cornell University Ithaka/USA: SAGT, Sm$_2$Ti$_2$O$_7$, LaLuO$_3$, Cr:GSGG, SnO$_2$; University of Notre Dame/USA: Ga$_2$O$_3$; Alabama University/USA: SnO$_2$; NIMS Tsukaba/Japan: SnO$_2$; Korea Aerospace University/South Korea: Ga$_2$O$_3$; University of Canberra/AUS: Cr:Al$_2$O$_3$.

Fig. 4: SrTiO$_3$ crystals (tausonite) grown from non-stoichiometric melt (a,b) by the Top Seeded Solution Growth and from stoichiometric melt (c,d) by the Czochralski method.
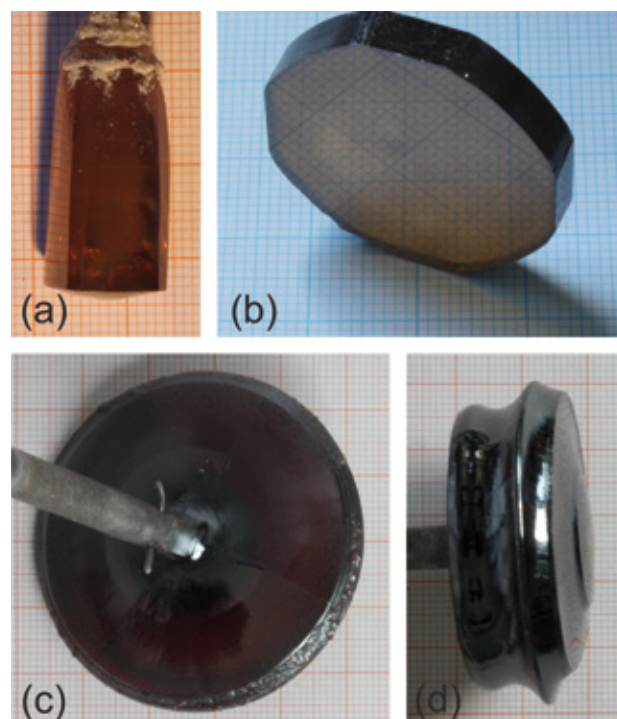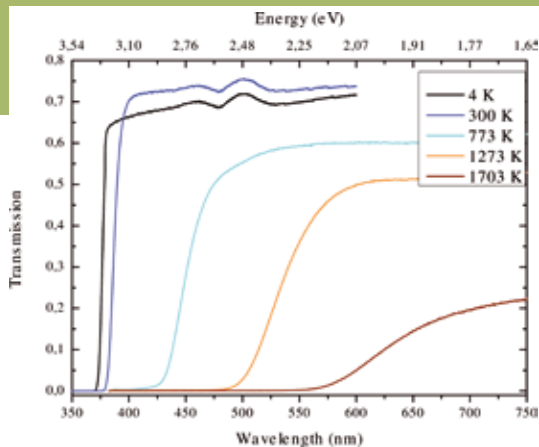
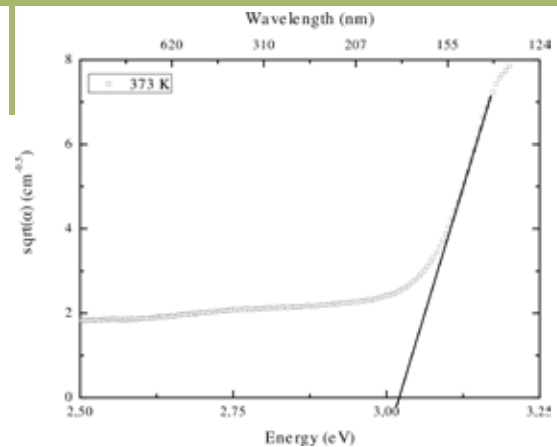Fig. 5: Spectra of SrTiO$_3$ (Verneuil grown) measured at different temperatures.

Fig. 6: Determination of the band gap. The linear part of the curve is extrapolated to $\sqrt{\alpha}$=0 to find the energy.

References

[1] Z. Galazka, R. Uecker, R. Fornari, PCT/EP2012/057447

[2] Z. Galazka, R. Uecker, K. Irmscher, D. Schulz, D. Klimm, M. Albrecht, M. Pietsch, S. Ganschow, A. Kwasniewski, R. Fornari, J. Crystal Growth 362 (2013) 349

[3] Z. Galazka, R. Uecker, R. Fornari; J. Cryst. Growth 388 (2014) 61

[4] Z. Galazka, R. Uecker, D. Klimm, K. Irmscher, M. Pietsch, R. Schewski, M. Albrecht, A. Kwasniewski, S. Ganschow, D. Schulz, C. Guguschev, R. Bertram, M. Bickermann, R. Fornari, physica status solidi (a) 211 (2014) 66

[5] R. Uecker, D. Klimm, R. Bertram, M. Bernhagen, I. Schulze-Jonack, M. Brützam, A. Kwasniewski, Th. M. Gesing, D.G. Schlom, Acta Physica Polonica A 124 (2013) 295

[6] C.H. Lee, N.D. Orloff, T. Birol, Y. Zhu, V. Goian, E. Rocas, R. Haislmaier, E. Vlahos, J.A. Mundy, L.F. Kourkoutis, Y. Nie, M.D. Biegalski, J. Zhang, M. Bernhagen, N.A. Benedek, Y. Kim, J.D. Btock, R. Uecker, X.X. Xi, V. Gopalan, D. Nuzhnyy, S. Kamba, D.A. Muller, I. Takeuchi, J.C. Booth, C.J. Fennie, D.G. Schlom, Nature 502 (2013) 532

[7] D. G. Schlom, L. Q. Chen, C. J. Fennie, V. Gopalan, D. A. Muller, X. Pan, R. Ramesh, R. Uecker, MRS Bulletin 39 (2014) 118

[8] Z. Galazka; Handbook of Crystal Growth, Second Edition, Ed. by T. Nishinaga, P. Rudolph, T. Kuech, Chapter 04-2, Vol. IIa, Elsevier, 2014, in print.

[9] A. Ohtomo, D. Muller, J. Grazul, H. Hwang, Nature, 419 (2002) 378

[10] A. Ohtomo, H.Y. Hwang, Nature, 427 (2004) 423

[11] Y. Hotta, T. Susaki, H.Y. Hwang, Physical Review Letters, 99 (2007) 236805.

[12] P. Perna, D. Maccariello, M. Radovic, U.S. di Uccio, I. Pallecchi, M. Codda, D. Marre, C. Cantoni, J. Gazquez, M. Varela, S.J. Pennycook, F.M. Granozio, Applied Physics Letters, 97 (2010) 152111

[13] P. Moetakef, T.A. Cain, D.G. Ouellette, J.Y. Zhang, D.O. Klenov, A. Janotti, C.G. Van de Walle, S. Rajan, S.J. Allen, S. Stemmer, Applied Physics Letters, 99 (2011) 232116

[14] A. Kalabukhov, R. Gunnarsson, T. Claeson, T. Winkler, arXiv, 0704.1050 (2007).

[15] H.Y. Hwang, A. Ohtomo, N. Nakagawa, D.A. Muller, J.L. Grazul, Physica E: Low-dimensional Systems and Nanostructures, 22 (2004) 712

[16] C. Guguschev, D. Klimm, F. Langhans, Z. Galazka, D. Kok, U. Juda, R. Uecker, CrystEngComm, 16 (2014) 1735

Gallium Nitride

Head: apl. Prof. Dr. D. Siche
Team: Dr. D. Gogova, Dr. S. Golka, K. Kachel, R. Nitschke, R. Zwierz

Überblick

Galliumnitrid (GaN) ist ein Basismaterial für die Optoelektronik und die hochfrequente Leistungselektronik. Das Fehlen kostengünstiger Massivkristalle führt zur Suche nach Züchtungsmethoden, die eine Alternative zur mehr oder weniger etablierten haliden Gasphasenepitaxie (HVPE) auf Saphir oder den Lösungszüchtungsmethoden, wie Natriumflux- oder Ammonothermalzüchtung darstellen können. Letztere sind noch weit von der industriellen Massenproduktion entfernt, haben aber das bessere Potenzial, die Anforderungen an eine kostengünstige Substratproduktion zu erfüllen.

Massive GaN – Kristalle für Homo-Epitaxiesubstrate sind eine wesentliche Voraussetzung, um in den gewachsenen Schichten die Versetzungsdichte und die thermischen Spannungen um Größenordnungen zu senken und damit die Leistungsfähigkeit der Bauelemente signifikant zu verbessern. Scheinbar führt die Züchtung aus der Gasphase auf diesem Gebiet zu keinem realen Durchbruch. Frei stehende HVPE – Substrate sind nur eine vorübergehende Lösung. Sie sind defektreich, zeigen eine geringe Effizienz der Umwandlung der Quellmaterialien und bleiben daher teuer. Trotzdem bleibt das Wachstum aus dem Ga-Dampf für die Schichtabscheidung sehr wünschenswert. Im Jahr 2013 haben wir die Experimente zur Nutzung von Mikrowellen-Plasma aktivierten Stickstoff und Ga – Dampf bei der Züchtung von GaN – Schichten mit einer Doktorarbeit abgeschlossen [1]. Außerdem wurde ein neuer, kleiner Reaktor für die gesteuerte pseudo-halide Gasphasenepitaxie (PHVPE), bei der CN⁻ - Ionen als chemisches Transportmittel wirken, in Betrieb genommen. In diesem Zusammenhang wurde das Projekt QuartzGaN zum Studium der kontrollierten C-Dotierung bei der Reaktion von GaCN mit Ammoniak zu GaN in Zusammenarbeit mit dem Institut für Festkörperphysik der Technischen Universität Berlin, Prof. A. Hofmann, von der DFG genehmigt. In einem etwas kleineren Projekt, im Rahmen des Zentralen Innovationsprogrammes Mittelstand (ZIM) des BMWi, begannen wir mit der Lösungszüchtung in einer Metallschmelze, die mit induktiv gekoppelten Plasma (ICP) aktiviertem Stickstoff übersättigt wird. Die erforderliche Reaktortechnologie wird in Zusammenarbeit mit zwei kleinen Firmen, Plasmetrex GmbH, Berlin und DTF Technology GmbH, Dresden, entwickelt.

Overview

Gallium nitride (GaN) is a basic semiconductor for opto- and high frequency power electronics. The lack of cost effective bulk crystals drives the search for growth methods, alternative to the more or less established Halide Vapour Phase Epitaxy (HVPE) on sapphire or to solution growth methods like sodium flux growth or ammonothermal growth. The latter ones are far from industrial mass production, but have a better potential to fulfill requirements for cost efficient substrate production.

Bulk GaN crystals for homo-epitaxial substrates are essential to reduce dislocation density and thermal stresses in grown layers by orders of magnitude, thus enhancing the performance of devices significantly. It seems that vapour phase growth will not yield in a real breakthrough in this field. Free standing substrates from HVPE are a temporary solution only. They are defect rich, show low source material conversion and therefore stay expensive. Nevertheless, the growth from Ga vapour stays highly promising for layer deposition. In 2013 we finished the experiments utilizing microwave plasma-activated nitrogen and Ga vapour to grow GaN layers in the frame of a PhD thesis [1]. A small new reactor for the controlled Pseudo-Halide Vapor Phase Epitaxy (PHVPE), where the CN⁻ ion acts as chemical Ga transport agent, was put into operation. In this context the DFG project QuartzGaN was approved recently, intending to study controlled C doping at the reaction of GaCN with ammonia to GaN in collaboration with the Institute of Solid State Physics at the Technical University Berlin, Prof. A. Hofmann. In a somewhat smaller project, in the frame of the Central Innovation Program for Small and Medium-sized Businesses (ZIM), we started solution growth in a metal melt, oversaturated with nitrogen produced via Inductively Coupled Plasma (ICP) activated N_2. The required reactor technology is developed in cooperation with two small companies, Plasmetrex GmbH, Berlin and DTF Technology GmbH, Dresden.
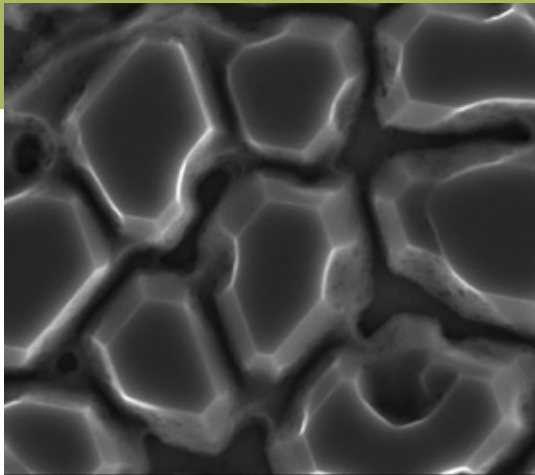
Fig. 1: GaN crystallites grown on GaN/Al2O3 template (SEM images) [1].

Results

1) GaN growth from Ga PVT and microwave plasma activated nitrogen

The microwave-plasma based experiments were performed in cooperation with the Leibniz Institute for Plasma Science and Technology INP in Greifswald even after funding by the Joint Initiative for Research and Innovation of the Leibniz Association had ended. The same holds for the Institute of Applied Physics (IAP) in Nizhni Novgorod, Russia, the fruitful discussions and the scientific support went well beyond the project..

In spite of some obstacles with the cavity tuning, described in the last annual report, a series of growth experiments has been conducted in the inductively heated stainless steel reactor. The microwave (MW) nitrogen plasma source [2], made of molybdenum (Mo) and implemented in the growth region, has been operated at moderate pressure (200 – 800 mbar). **Fig. 1** shows a GaN single crystalline layer grown on GaN/Al$_2$O$_3$ template by means of MW plasma enhanced vapour phase epitaxy (MWVPE). The much too low temperature of the seed T_{seed} = 900 °C prevented the complete coalescence of the layer, which consists of GaN islands, typically of 5 µm in diameter. EDX maps confirmed that these crystallites are composed of Ga and N. Additionally, some carbon impurities were revealed in the layers. Even though plasma is enclosed by the Mo cavity and cannot come into contact with graphite parts, some graphite particles or carbon dust might be transported by the carrier gas into the growth region. The C doping level has been measured by secondary ion mass spectrometry (SIMS) and compared with the results obtained for samples grown by pseudo-halide vapour phase epitaxy (PHVPE) [3] and Na-flux [4]. Incorporation of C into GaN layer increases exponentially with the growth temperature T_{growth}. However, the GaN layer grown at 930 °C by means of MWVPE revealed higher C content (3×10^{19} cm^{-3}) [1], than in GaN PHVPE samples grown at 1070 °C (1×10^{19} cm^{-3}) [3] (Fig. 2). This peculiarity may be explained in terms of local overheating of the seed surface by sub-atmospheric MW plasma, which would not be revealed by pyrometer temperature measurements on the seed backside.
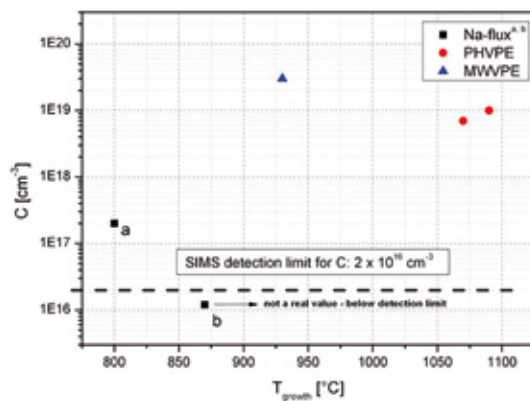
The optical emission spectroscopy (OES) was utilized for qualitative in-situ plasma characterization. At growth temperature no neutral and ionized molecules, N_2^* and N_2^+, and atomic nitrogen N could be detected, yet the bands of cyanide ions (CN) were unambiguously identified, proving the existence of excited nitrogen in the MW plasma. In order to study the Ga – N_2^* interactions in plasma, experiments in the carbon-free setup have been conducted. Altraform KVS 184/400 material with maximum vacuum operation temperature of 1800 °C served as thermal isolation felt. However, due to its high porosity, the reactor's atmosphere was contaminated with oxygen during the experiment at Tsource = 1200 °C. Therefore, only gallium oxide was deposited on the seed. Fig. 3 presents spectra of the growth atmosphere, recorded for the growth setup with graphite parts and the carbon-free growth setup. In case of the latter one only Ga lines at 287.42, 294.4, 403.3 and 417.2 nm and a NH band with the band head at 336 nm were observed. The absence of nitrogen bands in the OE spectra can be related to the fact that energy levels of excited Ga states are located far below the energy levels of excited nitrogen states. For instance, the excitation threshold of the 403.3 nm and 417.2 nm Ga lines equals 3.07 eV, while the $A^3\Sigma_u^+$ state energy of excited nitrogen molecule is 6.17 eV [2].
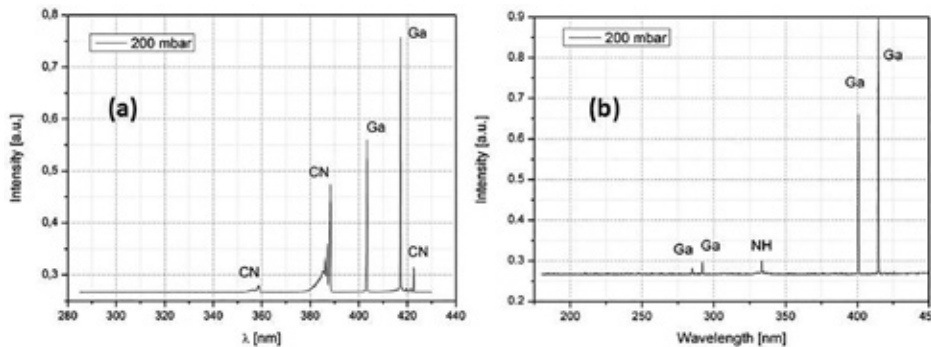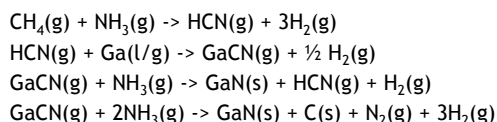

Fig. 2: Level of C doping for different GaN samples [1].

2) Pseudo-Halide Vapour Phase Epitaxy (PHVPE) of GaN:C layers

Cyano ions act as transport agent for Ga instead of chloride ions as in HVPE. The thermodynamic reactions postulated in former models could be confirmed by quantum chemical ab initio calculations [5]. To control the carbon doping in the grown layers, a carbon free setup was operated to establish

Fig. 3: OE spectra of the growth atmosphere (Tseed = 900 °C, Tsource = 1200 °C, pN2 = 200 mbar) in the setup a) with and b) without graphite parts [1].

the PHVPE process with controlled gaseous carbon supply (methane). To grow well defined C doped GaN semi-insulating layers and to clarify the role of C as deep acceptor at given impurity levels typical for the PHVPE process, is content of the QuartzGaN project, which has been approved by the DFG in 2013.

In the past it was shown, that with uncontrolled PHVPE thick GaN layers could be grown on ß-Ga$_2$O$_3$ (100) substrates [6]. In the last year we focused on establishing the process in a newly designed graphite-free reactor. Main efforts were put into stable production of HCN – transport agent for Ga. Moreover, in-situ exhaust gas analysis based on a Fourier Transform Infrared (FT-IR) Spectrometer was applied to quantify the reaction products. The reaction paths are as follows:

$CH_4(g) + NH_3(g) \rightarrow HCN(g) + 3H_2(g)$
$HCN(g) + Ga(l/g) \rightarrow GaCN(g) + \frac{1}{2} H_2(g)$
$GaCN(g) + NH_3(g) \rightarrow GaN(s) + HCN(g) + H_2(g)$
$GaCN(g) + 2NH_3(g) \rightarrow GaN(s) + C(s) + N_2(g) + 3H_2(g)$

From in-situ collected FT-IR spectrum of the exhaust gases presented in Fig. 4 it is plausible to quantify the HCN volume of approx. 0.6 % (+/- 0.06). At this cyanide percentage, the GaN growth rate does not exceed 5 µm/h. To achieve reasonable growth rates, it was necessary to increase the rate of HCN synthesis. As the HCN production is limited by the surface of Pt catalyst, the concept of the HCN production had to be changed. The metallic Pt meshes, where the surface is approx. 1 m^2/g, will be replaced by Pt deposited on 3.2 mm sized Al$_2$O$_3$ ceramic spheres, where the surface is 150-250 m^2/g. This should increase the production of HCN to a reasonable amount. With increased flow of Ga transport agent the growth rate of GaN crystals should increase proportionally.

In first experiments GaN was deposited on pure sapphire. After stable polycrystalline growth was achieved, the substrate was changed for AlN/Al$_2$O$_3$ or GaN/Al$_2$O$_3$ templates – depending on the process. Results of GaN growth on these substrates are presented in Fig. 5. Despite the very limited Ga transport up to 30 µm thick islands were grown with size up to 50 µm.

3) Low pressure, high density plasma based solution growth
In the last decade nitrides grown at low pressure have received great interest mainly with respect to processes that deposit directly from the gas phase. Both chemical- and physical vapor deposition are used at large scale in industry for dense amorphous layers and more recently also for crystalline layers at laboratory scale. Complementary our activity is attempting to use dense nitrogen plasma to dissolve nitrogen in a metallic solution and cause layer growth by oversaturation inside the solution. Hence our approach features a two stage process that is expected to be advantageous for fast thick layer growth, considering that growth occurs near thermal equilibrium even though the plasma itself is far away from equilibrium. In this case the energetic, dense plasma does not create layer damage that inhibits crystalline growth, because the growing layer is covered by the metallic solution. Furthermore, this technique is expected to be particularly suited for production of nitride films, since dissociated, soluble nitrogen gas has a very short lifetime in the gas phase and hence needs to be formed directly at the site of consumption. Unlike chemical reactions that produce dissociated nitrogen at the surface (e.g. by ammonia decomposition) the use of nitrogen plasma is independent of temperature and can be controlled to keep the surface free of a blocking crust.

At IKZ the process is developmend in an Inductively Coupled Plasma (ICP) reactor that has been constructed in the frame of a project funded by the Federal Ministry for Economic Affairs and Energy's (BMWi) Central Innovation Program for Small and Medium-sized Businesses
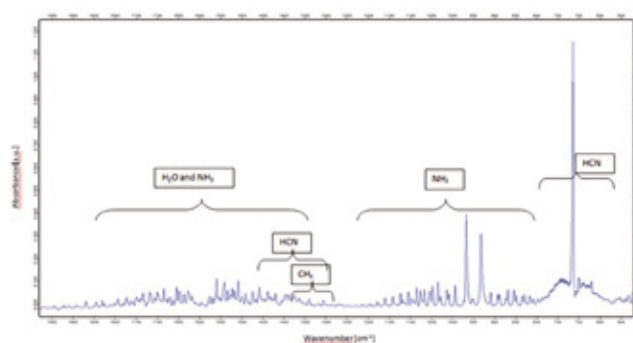

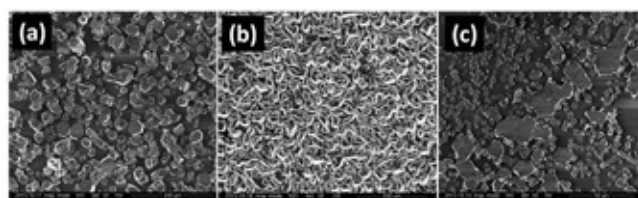*Fig. 4: In-situ FTIR spectrum of exhaust gas with bands for HCN, NH$_3$, CH$_4$ and H$_2$O.*

Fig. 5: Bird eye view of GaN islands grown on (a) Al$_2$O$_3$ and (b) AlN/Al$_2$O$_3$ (c) GaN/Al$_2$O$_3$ templates (SEM).
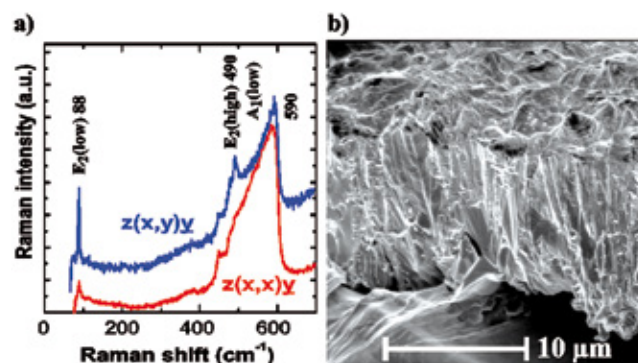

Fig. 6: a) Raman measurement of InN formed on the surface of In:N solution b) Bird eye view of this crust-like layer: From top to bottom the surface, the cleaved layer with columnar structure and solidified indium are visible (SEM image).

(ZIM). Thick indium nitride (InN) layers (Fig. 6) have been grown on a molten indium surface. A general problem in nitrides is the low solubility of nitrogen in gallium or indium. For GaN in Ga it is 3×10^{-5} mol fraction at 1150 °C [7] and plasma easily leads to super-saturation on the solvent surface or even N2-bubbles formation. Therefore, one of the major challenges in achieving controlled layer growth is to obtain a large temperature difference between the hotter solution surface and the seed at the bottom of the solution, where a lower temperature should lead to super-saturation with solved nitrogen. In this way, the nitrogen concentration gradient and temperature gradient over the melt height are increased and should enhance diffusive transport to the seed. Eventually, an increased growth rate as compared to solely chemical solution techniques is expected.

References

[1] R. Zwierz, Plasma Enhanced Growth of GaN Single Crystalline Layers from Vapour Phase, PhD thesis, Brandenburg University of Technology (BTU) Cottbus-Senftenberg

[2] R. Zwierz, S. Golka, K. Kachel, D. Siche, R. Fornari, P. Sennikov, A. Vodopyanov and A. V. Pipa, Cryst. Res. Technol., 48, 4 (2013) 186

[3] K. Jacobs, D. Siche, D. Klimm, H.-J. Rost, and D. Gogova, J. Crystal Growth, 312 (2010) 750

[4] Y. Mori, M. Imade, M. Maruyama, and M. Yoshimura, ECS J. Solid State Sci. Technol., 2 (2013) N3068

[5] O.B. Gadzhiev, P.G. Sennikov, A.I. Petrov, D. Gogova, D. Siche; Cryst. Growth Des. 13 (2013) 1445

[6] K. Kachel, M. Korytov, D. Gogova, Z. Galazka, M. Albrecht, R. Zwierz, D. Siche, S. Golka, A. Kwasniewski, M. Schmidbauer, R. Fornari; CrystEngComm, 14 (2012) 8536

[7] R.A. Logan, C.D. Thurmond; J. Electrochem. Soc. 119 (1972) 1727

Aluminium Nitride

Head: Dr. J. Wollweber

Team: Dr. A. Dittmar, Dr. C. Guguschev, C. Hartmann, S. Kollowa, F. Langhans

Einleitung

Elektronisch aktive AlGaN-Schichten mit hohem Al-Anteil werden als vielversprechendes Halbleitermaterial für UVC-Lichtemitter, für schnelle Hochleistungstransistoren und für Piezosensoren betrachtet. Im Gegensatz zu anderen Anwendungen kann das Potential von AlGaN-Schichten aber nur genutzt werden, wenn es gelingt, die Defektkonzentration unter 106 cm^{-2} zu halten. Die Abscheidung dieser Schichten auf Fremdsubstraten, wie SiC oder Saphir ist daher keine Option. Der einzig sinnvolle Weg, diese Fremdsubstrate zu ersetzen, ist die Nutzung von AlN als Quasi-Eigensubstrat. Leider kommt AlN aber weder in der Natur vor, noch lag es bisher als technisches Produkt vor.

Die Entwicklung einer sinnvollen Züchtungstechnologie, Sublimation-Rekondensation (PVT) ist hier die allgemein anerkannte Methode, stößt allerdings an die Grenzen des technisch Machbaren. Prozesstemperaturen über 2000 °C und extrem aggressive Gasspezies aus Al und Restverunreinigungen (O, C) begrenzen die Wahl der Tiegelmaterialien auf wenige Varianten. Schlüsselelemente wie Keime, hochreines Quellmaterial und geeignete Tiegelmaterialien sind weder kommerziell noch aus Laborfertigung erhältlich und müssen praktisch selbst entwickelt werden.

In den letzten 10 Jahren wurde daher im IKZ eine eigene Technologie für das homoepitaktische Wachstum von AlN-Volumenkristallen einschließlich der erforderlichen Infrastruktur entwickelt. Epitaxietaugliche AlN-Wafer (max. 10 x 10 mm^2, rocking curve FWHM ~ 20 arcsec, Abb. 1 aus dieser Technologie sind bereits an Partner im Verbundprojekt WideBase (gefördert durch das BMBF) für die Bauelemente-Entwicklung geliefert worden. Dabei haben erste Tests von optisch gepumpten Laserstrukturen, trotz offener technologischer Probleme bei der MOCVD-Schichtabscheidung, die Konkurrenzfähigkeit AlN-Substrate klar erkennen lassen, obwohl sich diese noch in der Entwicklung befinden [1].

Als ein Resultat dieser vorkommerziellen Entwicklungsphase steigt die Nachfrage nach industrierelevanten Wafergrößen (Ø > 1"), homogener Fremdstoffverteilung und gut definierten optischen, elektrischen und strukturellen Eigenschaften. Die Entwicklung dieser Parameter wird auch ein besseres Verständnis der facettenspezifischen Wachstumsprozesse auf mikroskopischer Ebene auch unter Fremdstoffeinfluss, die Kristallaufweitung, sowie optimierte Temperaturfelder umfassen.

Unsere Forschungsaktivitäten werden im Rahmen des Projektes "Advanced UV for Life" als Teil der BMBF Innovationsinitiative für die neuen Länder „Unternehmen Region" weitergeführt.

Introduction

Al-rich active AlGaN layers are considered as very promising semiconductor material for deep UV light emitters, fast high-performance transistors, and piezo sensors. In contrast to other applications the potential of AlGaN layers can only be realized if it is possible to keep the defect concentration below 106 cm^{-2}. Therefore, layer deposition on foreign substrates like SiC or sapphire is not an option. The only possible choice to replace them is AlN as a quasi-native substrate. Unfortunately, AlN does not occur in nature or as technical product so far.

The development of a suitable growth technology, sublimation-recondensation (PVT) is the commonly accepted method for that, takes it to the edge of engineering constraints. Process temperatures above 2000 °C and extreme aggressive gas species from Al and residual impurities (O, C) restrict the choice of crucible materials to just a few variants. Key elements like seeds, high-purity source material, and appropriate crucible materials are available neither on the commercial market nor from laboratory production and had to be developed through own efforts.
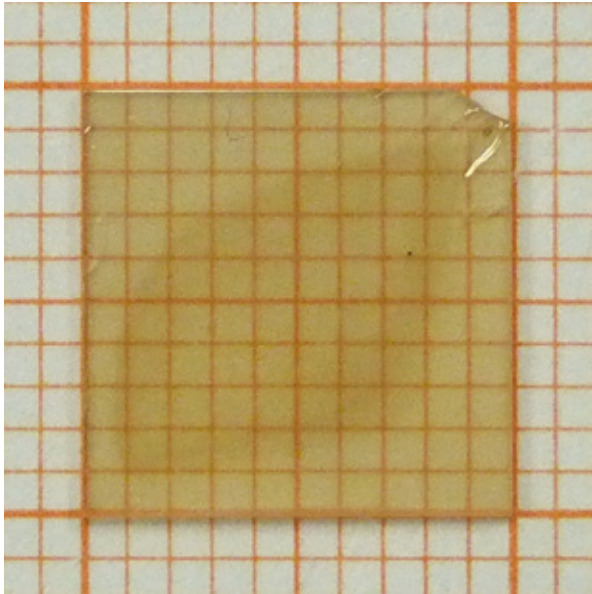
Abb. 1: AlN-Wafer (c-orientiert, 10 x 10 mm^2) präpariert aus einem homoepitaktisch gewachsenen Kristall, epitaxietaugliche Oberflächenbearbeitung auf Al-polarer Seite durch chemo-mechanische Politur für AlGaN-Schichtabscheidung.

Fig. 1: AlN wafer 10 x 10 mm^2, prepared from a homo-epitaxial grown crystal, N-polar (000-1) facet finished by CMP (chemo-mechanical planarization) for AlGaN layer deposition.

Over the last ten years, an IKZ in-house technology for homoepitaxial growth of AlN bulk crystals by sublimation was developed including the required infrastructure. Epi-ready AlN wafers (max. 10 x 10 mm^2, rocking curve FWHM ~ 20 arcsec (Fig. 1)) from this process have been delivered to partners in the Berlin WideBase framework (funded by BMBF) for device processing. Despite remaining technology issues in MOCVD layer deposition, first tests of optical pumped laser structures clearly indicate the competitiveness of AlN substrates even in their current state [1].

As a result of this pre-commercial stage, the demand for sizes of industrial relevance (Ø > 1"), homogeneous impurity incorporation, and well defined optical, electrical, and structural properties arises. Work in this direction implies a deeper understanding of facet specific growth processes on the micro-scale, including impurity-related effects and geometry enlargements, as well as well adapted temperature fields. Our research activities will be continued in the frame of project "Advanced UV for Life" funded as part of Federal Ministry BMBF Innovation Initiative "Entrepreneurial Regions".

Results

In the last few years, growth of AlN single crystals by spontaneous nucleation with high structural perfection has been developed at the IKZ [2]. On this basis, subsequent homo-epitaxial growth runs with smooth diameter enlargement have demonstrated to maintain the crystalline quality [3]. Nevertheless, the road towards the commercialisation of the growth technology still provides two key challenges to be overcome: (i) diameter enlargement to industrial relevant sizes of finally >= 2", and (ii) adjustable (or at least defined) homogeneous optical, electrical, and structural properties across the entire crystal volume.

The fundamental approach to solve for both issues is a reproducible growth under extreme growth conditions. In this context, a major advance has been achieved by the development of the TaC crucible preparation as a currently not yet commercialized product in the process chain with regard to properties like chemical inertness and tightness over several growth runs [4]. This progress is based in the first place on the use of a cold isostatic press (CIP) which allows a computer controlled processing with very smooth pressure reduction resulting in reproducible and precise crucible designs of up to 100 mm in diameter. Because of the large dimensions, parts of the crucible are exposed to higher temperature gradients resulting in higher local stresses during sintering. Stress calculations of TaC crucibles have helped us to reduce the stress load below 1.8 x 10^7 Nm^{-2} (von Mises stress, 600 mbar N$_2$, 2100 °C, COMSOL Multiphysics). The mean crucible lifetime is obviously increasing as a result of this approach.

Moreover, the durability also suffers from the differences in thermal expansion between TaC and growing AlN, resulting in a tendency to crack crucible parts with AlN in contact, and even the grown crystals. To avoid this effect, TaC material mixtures were prepared. During their preparation, care must be taken to ensure that the thermal expansion coefficient of the material mixture matches that of AlN as closely as possible (ZIM project, IKZ/Fine Ceramics Technology GmbH). The temperature dependence of the thermal expansion coefficients of the different mixed samples, crystalline AlN, and AlN source material were determined by in-situ XRD (in-house, up to 1400 °C) as well as by dilatometer measurements (Linseis Thermal Analysis GmbH, up to 1750 °C. A clear tendency to enhance the crucible lifetime resulted from applying these refractory mixtures.

The progress in understanding the processes and related reactor behaviour allows new constructive solutions. When growing in [000-1] direction, a reasonable diameter enlargement can be achieved, according to current knowledge, by a strongly convex temperature field around a seed which suppresses the {10-10} prismatic facets during the first millimetres of growth [3]. This approach conflicts with general principles of defect reduction during crystal growth. Therefore, a balance must be achieved between diameter enlargement and structural perfection. In the case of AlN the diameter increase is restricted to about 2 mm per growth run. A larger expansion results inevitably in a formation of small-angle grain boundaries. Performing subsequent growth with small diameter enlargement from one growth run to the other appear to be the most promising way to industrial relevant dimensions within the next years without making use of large foreign substrates like SiC and their negative implications.

In addition, the continuous diameter expansion is accompanied by concerns about the wafer homogeneity. In order to develop techniques to provide defined homogenous properties, one has to draw attention to the natural growth mode of the AlN crystals which is presented as a self-similar zonar structure reflecting facet specific growth (Fig. 2)[5].

The yellowish core zone is growing in the step flow mode on a N-polar (000-1) facet which expands as growth proceeds. At the same time a second growth zone forms in perpendicular directions to the yellowish region, resulting in six prismatic {10-10} facets of nearly colourless appearance. Using a (000-1) seed instead of spontaneous nucleation the same growth zones are formed with the sole difference that the yellowish growth zone is not only nucleating on a single point but on the complete seed surface.

The structural quality is very high in both zones (core zone: dislocation density DD < 10^3 cm^{-2}, edge region DD < 10^5 cm^{-2}). Typical crystals do not show any small-angle grain boundaries.

The concentrations of the main impurities C, O, and Si determine the optical and electrical properties in the different growth zones. Total impurity concentrations of at least ~5 x 10^{19} cm^{-3} can be incorporated without affecting the structural quality of the AlN crystals. According to the ratio of the impurity elements, the electrical properties can be shifted between semi-isolated and n-type conductivity: Carbon acts as a deep acceptor which promotes semi-insulating AlN (SI-AlN) but results in a strong optical absorption band at 265 nm hindering its efficient usage in opto-electronic deep UV devices. Oxygen forms DX centres related to a 1 eV charge state below the conduction band which prevents SI properties of AlN at elevated temperatures if oxygen is the dominating impurity. Furthermore, if [O] > 2[C], the charge state of the carbon defect can be changed. By this way the strong deep UV absorption can be suppressed.

Fig. 3 shows a c-plane wafer cut from the middle of a spontaneously nucleated crystal. SIMS measurements (secondary ion mass spectrometry) have revealed stronger oxygen incorporation within the yellowish core area grown on the (000-1) facet than in the outer edge area. The carbon concentration remains nearly the same in both zones. Interestingly, the high [O] / [C] ratio in the core area results in lowered deep UV absorption. A corresponding model explaining this effect is outlined in the report of the group Physical Characterization in this report.

While studying impurity behaviour, the question for intentionally doping of AlN is obvious. Silicon might be a good candidate for n-type doping of AlN as it forms shallow donor levels. However, ab-initio calculations predict an enhanced solubility of aluminium vacancies in n-type AlN which compensate the shallow donors and hamper n-type doping [6]. Nevertheless, n-type conductive AlN has already been demonstrated in silicon doped thin AlN films and in silicon doped AlGaN alloys with high Al content [7]. For this reason, the AlN group started investigations in intentionally doping during growth that aims on a technology allowing to grow AlN crystals with defined and adjustable electrical and optical properties in addition to its efforts in reducing background impurities in PVT growth.

For development of an appropriate doping technology, process characteristics of PVT growth, namely the high growth temperatures and aggressive gaseous species in PVT growth have to be taken into account. Especially insertion of a doping gas without premature decay and/or damaging the crucible material seems a challenge. One way to such a technology suitable at least for basic research in spite of all the disadvantages, that demands only minor modifications to existing growth setups, is adding dopant-containing high temperature stable compounds to the source. Such compounds have to have a melting/decomposition point close or even higher to that of AlN. At the same time, the partial pressure of the dopant over the solid compound must be sufficiently high under growth conditions.

WSi$_2$ (T_{melt}= 2160 °C) matches those prerequisites for Si doping. Thermodynamic equilibrium calculations show that the Si partial pressure over solid WSi$_2$ should be high enough for doping. To realize a smooth Si release, WSi$_2$ was sintered together with TaC as host and added to the source material for the growth runs. Embedding WSi$_2$ in the TaC sinter body provides a diffusion barrier enabling a rather constant supply of Si without risking Si condensation. Using this approach, a nearly constant Si incorporation of 1.7 – 2.0 x 10^{18} cm^{-3} was achieved in the
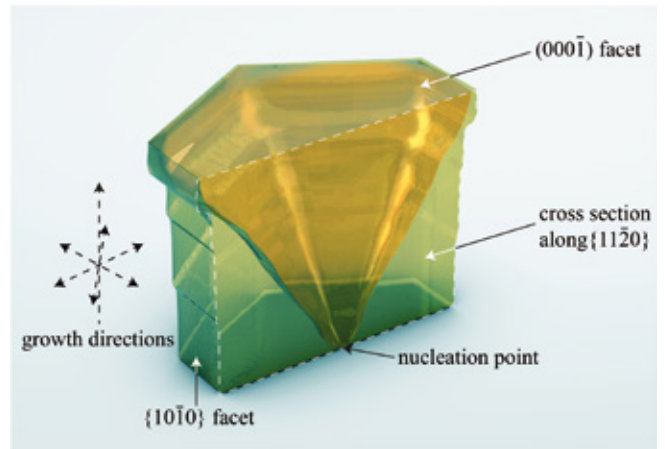

Fig. 2: 3D sketch of an isometric grown freestanding crystal with zonar structure; the yellowish volume part was grown on a N-polar (000-1) facet; the nearly colourless volume part was grown via prismatic {10-10} facets.
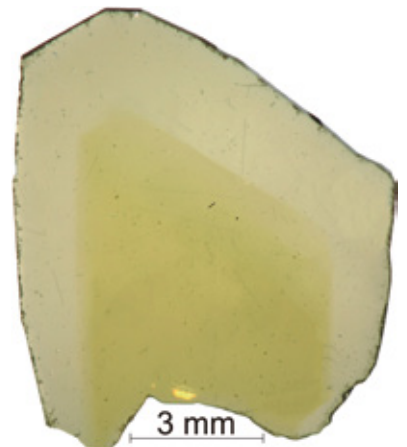

Fig. 3: Zonar structure in a freestanding grown AlN crystal, cut perpendicular to the c-axis; the yellowish part was grown on N-polar (000-1) facet; the more colorless part was grown via prismatic {10-10} facets; carbon content nearly independent of growth mode; the graphs in the lower row show the UV absorption as a function of growth mode and oxygen content at constant C level.
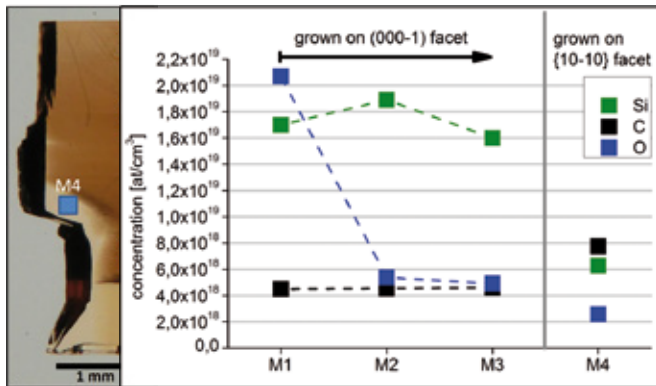
Fig. 4: Si incorporation in AlN crystal depending on growth time and growth mode, axial cut, measured by SIMS; growth direction is upwards.

whole crystal volume grown on the (000-1) facet, while the oxygen and carbon contamination remained at about 5×10^{18} cm^{-3} in all but the initial layer of growth (Fig.4). Preliminary electrical and optical characterization proved a n type conductivity in the range of 10^{-2} (Ωcm)$^{-1}$ at room temperature (undoped single crystals: 10^{-11}-10^{-13} (Ωcm)$^{-1}$ at 300 K [8]). This value corresponds to that from intentionally doped AlN layers [8].

In view of a further optimization of the doping technology, the minimization of residual impurities has to remain in focus. Thus, a complete package from technological design to specified AlN wafers will be offered in future.

References

[1] M. Martens, F. Mehnke, Chr. Kuhn, Chr. Reich, V. Kueller, A. Knauer, C. Netzel, C. Hartmann, J. Wollweber, J. Rass, T. Wernicke, M. Bickermann, M. Weyers, and M. Kneissl, IEEE Photonics Technology Letters **26** (2014), 342

[2] C. Hartmann, J. Wollweber, A. Dittmar, K. Irmscher, A. Kwasniewski, F. Langhans, T. Neugut, M. Bickermann, Jpn. J. Appl. Phys., 52 (2013) 08JA06

[3] C. Hartmann, A. Dittmar, J. Wollweber and M. Bickermann, Semicond. Sci. Technol. 29 (2014) 084002 (10pp)

[4] Patent application in preparation

[5] C. Hartmann, *Aluminiumnitrid-Volumenkristallzüchtung mittels physikalischen Gasphasentrans-port,* Dissertation, BTU Cottbus, 2013

[6] C. Stampfl, C.G. Van de Walle, Appl. Phys. Lett., 72 (1998) 459

[7] F. Mehnke, T. Wernicke, H. Pingel, Chr. Kuhn, Chr. Reich, V. Kueller, A. Knauer, M. Lapeyrade, M. Weyers, and M. Kneissl, Appl. Phys. Lett. 103 (2013), 212109

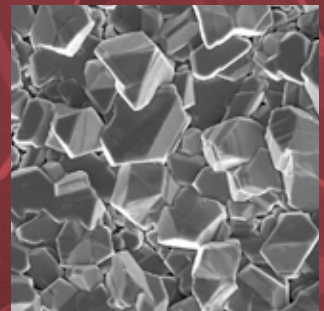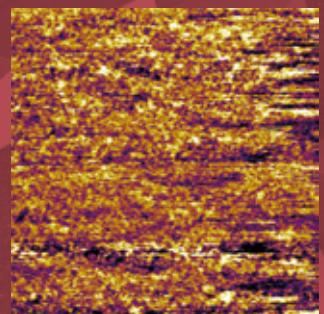[8] V.W.L., Chin at al., J. Appl. Phys. 75, 11 (1994), 7365

Semiconducting Oxide Layers
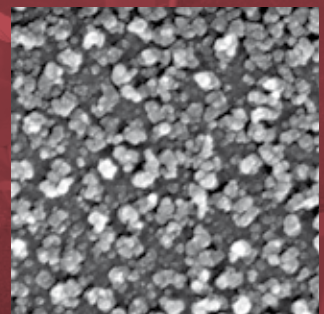
Si/Ge Nanocrystals

Ferroelectrical Oxide Layers

Layers & Nanostructures

Acting head of department: Dr. Günter Wagner

In der Abteilung "Schichten und Nanostrukturen" werden folgende Themen bearbeitet:
- *Grundlegende Untersuchung der Keimbildung und Wachstumsmechanismen*
- *Weiterentwicklung von Abscheidungstechnologien*
- *Herstellung und Charakterisierung von Schichten und Nanostrukturen für die Sensorik, Mikroelektronik, Photovoltaik, Speicher und thermoelektrische Anwendungen*

Eine Hauptaufgabe dieser Abteilung besteht darin, die physikalischen Eigenschaften verschiedener kristalliner Substanzen durch maßgeschneiderte Größe, Form, chemische Zusammensetzung und Verspannungszustand gezielt einzustellen, um neue Anwendungsgebiete zu erschließen.

Folgende Forschungsaktivitäten wurden 2013 in den drei Gruppen der Abteilung bearbeitet:
Epitaktisches Wachstum von transparenten halbleitenden Oxidschichten: Dies umfasst die Abscheidung von β-Ga_2O_3-Schichten auf einkristallinen Al_2O_3- und β-Ga_2O_3 Substraten und die Substitution von Ga durch In bei der Abscheidung von $Ga_{(2x-1)}InxO_3$-Schichten. Ein weiteres Ziel ist die Erzeugung und Einstellung einer n-Leitfähigkeit in den Schichten durch Dotierung mit Si und Sn.

Abscheidung von ferro-/piezoelektrischen bleifreien Oxidschichten: Hierzu zählen ferro-/piezoelektrische $Na_xK_{1-x}NbO_3$ Schichten und Übergitterstrukturen mit variabler Zusammensetzung (x = 0-1), $SrTiO_3$ Schichten, sowie leitfähiges $SrRuO_3$ und $La_{0.7}Sr_{0.3}MnO_3$ als Elektrodenschichten. Zudem erfolgt die Abscheidung auf gitterfehlangepassten Oxidsubstraten (Heteroepitaxie) zum gezielten Einbau von Gitterverspannungen und der Untersuchung ihres Einflusses auf die funktionellen Eigenschaften.

Si- und Ge-Nanodrähte; Abscheidung von polykristallinem Si auf Glas: In der Gruppe wird das VLS-Wachstum von Ge-Nanodrähten auf <111>Si-Substraten erforscht, sowie die Herstellung von polykristallinen Si-Saatschichten durch die Amorph-Liquid-Kristallin (ALC) Umwandlung mittels Zinn und anschließendem Auswachsen der Saatschichten mittels der Temperatur-Differenz-Methode (TDM) in einer Silicium-Zinn-Lösung zu geschlossenen Si-Schichten.

Die Abteilung verfügt über eine sehr moderne, hochwertige Ausstattung:
Molekularstrahlepitaxie, sowohl flüssigkeits- als auch gasbasierte MOCVD, Physikalische Gasphasenabscheidung, gepulste Laserabscheidung, Flüssigphasenepitaxie mit Schiebekassette und eine selbst entworfene Epitaxieapparatur für die Temperatur-Differenz-Methode.

The activity carried out within the department „Layers and Nanostructures" is focused on:
- fundamental investigation of nucleation and growth mechanisms
- development of deposition technologies
- growth and characterization of layers and nanostructures or sensors, microelectronics, photovoltaics, memories and thermoelectric applications.

By controlling chemical composition and strain of epitaxial layers as well as size, shape and position o nanostructures it is possible to tailor the physical characteristics and make them suitable for novel applications.

The department includes three groups, which performed the following research activities in 2013:
Epitaxy of transparent semiconducting oxides: This includes deposition of b-Ga_2O_3-layers on Al_2O_3 and b-Ga_2O_3-single crystalline substrates, substitution of Ga by In during epitaxy in order to grow $Ga_{2(1-x)}In_{2x}O_3$-layers, as well as realizing and tuning the n-type conductivity by doping with group IV elements (Si, Sn).

Deposition of ferro-/piezoelectric lead-free oxide layers: The research tasks focus on ferro-/piezoelectric $Na_xK_{1-x}NbO3$ layers and superlattice structures with variable composition (x = 0-1), deposition of $SrTiO_3$ layers and conductive $SrRuO_3$ and $La_{0.7}Sr_{0.3}MnO_3$ as electrode layers. Another topic is the deposition on lattice mismatched oxide substrates (heteroepitaxy) for targeted adjustment of lattice strain and investigation of the influence of the layers' functional properties.

Si and Ge nanowires; deposition of polycrystalline Si on glass: Mainly two topics are investigated here, namely heteroepitaxial VLS growth of Ge nanowires on <111> Si substrates and preparation of polycrystalline seed layers of silicon on glass by amorphous-liquid-crystalline (ALC) transition, using tin as a catalyst. This is followed by epitaxial growth of silicon on seed layers by temperature difference method (TDM) from tin-silicon solutions.

The department has an excellent infrastructure for the deposition and characterization of epilayers and nanostructures:
Molecular Beam Epitaxy,both liquid-delivery and conventional MOCVD, Physical Vapor Deposition, Pulsed Laser Deposition, sliding-boat Liquid Phase Epitaxy, and in-house designed Temperature Difference Method Epitaxy.

Semiconducting Oxide Layers

Head: Dr. Günter Wagner
Team: Dr. M. Baldini, Dr. D. Gogova, R. Grüneberg

Überblick

Das Interesse an Metalloxiden als Wide Bandgap-Halbleiter ist in den letzten Jahren aufgrund ihrer speziellen Eigenschaften gestiegen. Dazu zählt u.a. die Transparenz bis in den tiefen UV-Bereich, oder die hohe chemische und thermische Stabilität. Diese Eigenschaften ermöglichen potentielle, neue Anwendungen in der Optoelektronik, der transparenten Mikroelektronik, aber auch in der Photovoltaik, in der Leistungselektronik und Sensorik. Für diese Bandbreite von Anwendungen werden insbesondere einkristalline Oxidschichten mit hoher struktureller Qualität und hoher Ladungsträgerkonzentration in der Größenordnung von 10^{16}–10^{18} cm^{-3} benötigt, die besondere elektronische oder optoelektronische Eigenschaften aufweisen. Insbesondere Ga_2O_3 hat sich mit seiner direkten Bandlücke von 4,9 eV und damit verbunden der Transparenz bis in den tiefen UV-Bereich hinein als besonders interessanter Kandidat aus dieser Materialklasse erwiesen. die Durchbruchfeldstärke von 8 MV/cm gewährleistet geringe Verluste bei Anwendungen in der Leistungselektronik.

Unsere Forschungsarbeiten erfolgen im Rahmen des Projekts „Homo- und Heteroepitaxie transparenter halbleitender Oxidschichten im ternären System Ga_2O_3 – In_2O_3 – Al_2O_3 auf *ß*-Ga_2O_3 und In_2O_3 Substraten". Das Projekt wurde im Rahmen des Wettbewerbs der Leibniz-Gemeinschaft (früher SAW-Verfahren) zur Förderung ausgewählt. Im mittlerweile zweiten Projektjahr konzentrierten sich die Aktivitäten auf:

1. das Homoepitaktische Wachstum von ß-Ga_2O_3 Schichten
2. die Substitution von Ga-Atomen durch In-Atome im ß-Ga_2O_3 Gitter
3. den Einbau von Zinn zur Abstimmung der elektrischen Eigenschaften der abgeschiedenen Schichten

Overview

The study and development of transparent metal oxides as a new class of semiconductors is a rapidly expanding research field that could lead up to the realization of innovative devices and the understanding of new exciting physics. By growing single-crystal thin oxide films with high purity and a controlled carrier concentration level in the range of 10^{16}–10^{18} cm^{-3}, as for conventional semiconductors, they open up a new class of wide-band gap electronic materials, with applications in transparent microelectronics, short wavelength photonics and chemical/biological sensor devices. Ga_2O_3 has been widely studied in the last year, emerging as one of the most interesting example in this class of materials. Monoclinic ß-Ga_2O_3 is transparent up to the deep UV, thanks to its direct 4.9 eV bandgap (Eg), and has a very high break down field (8 MV/cm), which allows to minimize losses in high power electronics.

Our research is carried out in the frame of the project "Homo- and Heteroepitaxy of transparent semiconducting oxide layers of the Ga_2O_3 – In_2O_3 – Al_2O_3 ternary system on *B*-Ga_2O_3 and In_2O_3 substrates", funded in the frame of the Leibniz Competition (formerly SAW procedure). In the second year of the project, the activities were concentrated on three topics:

1. Homoepitaxial growth of ß-Ga_2O_3 films
2. Substitution of Ga-atoms by In atoms in the ß-Ga_2O_3 lattice
3. Incorporation of Sn to tune the electrical properties of the grown layers

Homoepitaxial growth of ß-Ga_2O_3 layers
Thin layers were deposited on one side polished 1x1 cm^2 ß-Ga_2O_3 substrates. For this purpose, high quality n-type single crystals grown by the Czochralski method were provided by IKZ group Oxides/Fluorides and processed subsequently by CrysTec GmbH, Berlin.

The epitaxial growth of ß-Ga_2O_3 was carried out in a commercial vertical MOVPE reactor (SMI inc., USA) at low pressure conditions. The structural properties of the ß-Ga_2O_3 layers were analysed in close co-operation with the

IKZ groups Physical Characterization and Electron Microscopy by means of high resolution X-ray diffraction and transmission electron microscopy. In addition, spectroscopic ellipsometry, atomic force microscopy and scanning electron microscopy investigations were carried out in order to determine the layer thickness and composition and to reveal the surface morphology of the epitaxial layers. Capacitance-voltage and conductivity measurements have been performed to characterize the electrical properties of the grown layers [1].

Fig. 1: SEM-image of ß-Ga$_2$O$_3$ crystals grown on a ß-Ga$_2$O$_3$ single crystalline substrate from TMGa and pure oxygen: T_g = 775 °C, O/Ga ratio = 1200 (a); T_g = 800°C, O/Ga ratio = 3200 (b).

In 2012, we reported on the successful deposition of ß-Ga$_2$O$_3$ on sapphire, using. TMGa and pure oxygen as precursors. To prevent dissociation of the Ga$_2$O$_3$-substrate surface an oxygen flux of 400 sccm was maintained in the reactor during the heating up to the growth temperature and also during cooling down. Nevertheless the deposition of ß-Ga$_2$O$_3$ on ß-Ga$_2$O$_3$ substrates employing the same set of growth parameters as used for sapphire revealed completely different growth results. Fig. 1 shows a SEM image of a layer surface after growing for 15 min at a temperature of 775°C and chamber pressure of 20 mbar, under Ga and oxygen fluxes of 5 and 400 sccm, respectively.

The deposition of ß-Ga$_2$O$_3$ was characterized by three-dimensional growth of ß-Ga$_2$O$_3$ grains up to two dimensional structures of nanometric size. ß-Ga$_2$O$_3$ deposited in form of long wires, up to 500 nm in length and up to 100 nm in diameter, preferentially (100)-oriented (Fig 1a). At a deposition temperature of 800°C and increased oxygen-to-gallium ratio of 3200 the grown Ga$_2$O$_3$ material looked like an agglomeration of nanocrystals (Fig 1b).

It has to be mentioned that all wires are growing epitaxially but the coherency of the layer is lost. All attempts to deposit closed homoepitaxial layers of ß-Ga$_2$O$_3$ on (100)-oriented ß-Ga$_2$O$_3$-substrates using oxygen and TMGa as precursors failed, although the growth parameters were varied in a wide range: substrate temperatures between 750 and 850°C, chamber pressure between 5 and 100 mbar, and oxygen-to-gallium ratios up to 9500 were used. In all cases only ß-Ga$_2$O$_3$ nano-crystals (either wires or agglomerates) were obtained. This suggests that pure oxygen is not suitable for growth of ß-Ga$_2$O$_3$ homoepitaxial layers. For this reason we turned the attention to another source of oxygen, namely water vapour.

ß-Ga$_2$O$_3$ deposition by using trimethylgallium and water as oxygen source

Trimethylgallium and ultra pure water were used as precursors and Ar as the carrier gas. The temperature of the water bubbler was fixed at 50°C and the pressure at 300 mbar. The chosen deposition temperature of 800°C represents a compromise between deposition efficiency and crystalline quality. With increasing deposition temperature a decrease of the growth rate was observed. This is due to formation and desorption of gallium suboxide, Ga$_2$O, which is formed more readily at higher temperatures. On the other hand, for the initial step of nucleation as well as for the subsequent layer growth a higher substrate temperature is desirable since it increases the species mobility on the growth interface and improves the growth kinetics.

Fig.2: SEM (a) and AFM (b) images of a ß-Ga$_2$O$_3$ homoepitaxial layer grown at 800°C and 20 mbar chamber pressure. Layer thickness of about 170 nm, RMS: 6.5 nm.

After a deposition time of 30 minutes a layer of about 170 nm was grown. A typical layer surface morphology as measured by SEM and AFM is shown in Fig. 2 (a) and (b) respectively. The surface of the grown layer presents a terrace-like morphology similar to the ß-Ga$_2$O$_3$ substrate but with strong tendency to step bunching.

The structural properties of the ß-Ga$_2$O$_3$ epitaxial layers were characterized by high resolution XRD diffraction pattern and high resolution transmission electron microscopy. As-grown layers show sharp XRD-peaks that were assigned to the monocline gallium oxide phase and odd reflections that could be assigned to plane deformation by extended defects. The high density of stacking faults and twins in the epitaxial ß-Ga$_2$O$_3$ layer that is found in high resolution TEM images induces strong vertical stacking disorder.

The presence of hydrogen has a positive effect on kinetic conditions of the substrate surface and hence may support the layer-by-layer growth. The influence of the oxygen precursor on the growth mode may be qualitatively discussed as follows. When pure O$_2$ is employed the formation energy of oxygen vacancies is substantially increased which in turn lowers their concentration. At the same time H$_2$O and CO$_2$ are present in comparable concentrations,
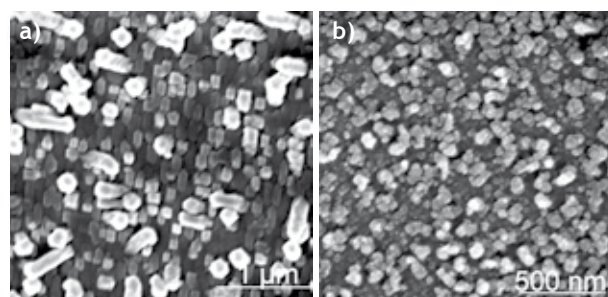
which can promote the formation of $Ga_2(CO_3)_3$ at the growth surface as described above. Such compounds act as a mask and whiskers grow out of the unmasked areas. On the other hand when H_2O is employed the oxygen partial pressure is considerable lower and oxygen vacancies are expected to form spontaneously. Since H_2O is present at much higher concentrations than CO_2 the adsorption is prevented and H_2O will spontaneously dissociate at oxygen vacancy sites, thus promoting growth. An additional mechanism can also take place: hydrogen may occupy oxygen vacancy sites by forming Ga-H species and reduce the surface state density. As a consequence, the chemical potential of the surface will be more homogeneous and diffusion of desorbed atoms on the surface will be enhanced. Therefore, the relatively high partial pressure of hydrogen deriving from water dissociation could have a positive effect on the kinetics at the substrate surface and hence support the layer-by-layer growth.
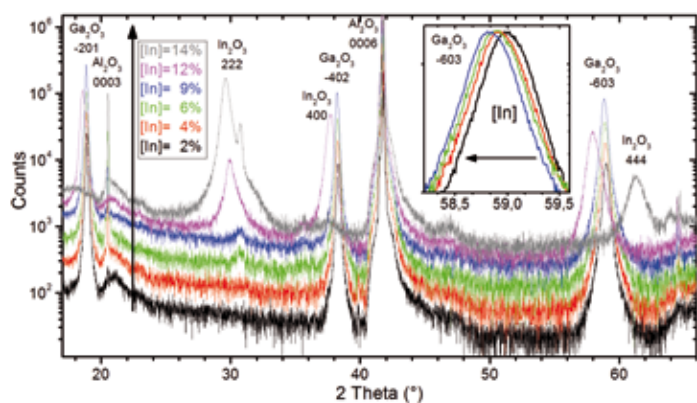

Fig. 3: XRD spectra of $(Ga_{1-x}In_x)_2O_3$ layers on Al_2O_3 grown with increasing In content from 2% (bottom) to 14% (top). Inset: detail of 603 β-Ga_2O_3 peaks, which show a shift towards lower angles with higher In amounts.

2. Growth of $(Ga_{1-x}In_x)_2O_3$ layers

Following the promising results obtained in the end of 2012, the growth of $(Ga_{1-x}In_x)_2O_3$ proceeded by using H_2O as oxygen source instead of pure O_2. The employment of the latter, in fact, caused the formation of the undesirable In_2O_3 phase, independent of the indium amount x [x=In/(In+Ga)] incorporated in the layer. Moreover, with H_2O it is possible to obtain layers with a smoother surface morphology, showing a 2-D-like growth feature.

By using the optimal growth parameters identified for pure Ga_2O_3 (p = 5 mbar, T = 800 °C, TMGa = 5 sccm, H_2O = 200-500 sccm), indium was not detectable as a component of the layers by energy-dispersive X-ray (EDX) spectroscopy, even at very high trimethylindium molar flow rates, up to 1×10^{-5} mol/min (the same of TMGa). The only visible effect of inserting such a high amount of In into the reactor was a drastic decrease of the growth rate. This behaviour shows that TMIn reacts directly with H_2O and then the resulting compounds either desorbs too fast from the layers to be correctly incorporated or are directly expelled through the exhaust system. By increasing the TMIn flow, more and more H_2O is consumed by In, leaving less oxygen to react with Ga which results in increasingly thin Ga_2O_3 layers. XRD spectra are identical to those of samples grown in the presence of O_2, except for the absence of In_2O_3-related peaks, confirming the growth of stoichiometric Ga_2O_3 and the epitaxial correlation of the (-201) Ga_2O_3 planes with the (0001) Al_2O_3 ones.

Since in presence of H_2O indium seems to form very volatile compounds, the reactor base pressure was increased, in order to minimize the desorption process. This expedient revealed to be successful: the amount of In in the layers increases almost linearly with the reactor pressure at constant TMIn flux. Moreover, by fixing the pressure at values comprised between 50 and 200 mbar, the In percentage is proportional to the amount of TMIn introduced into the reactor. On the other side, since the growth rate decreases with increasing both P and TMIn flux, a compromise must be achieved in order to grow layers with a definite amount of In in a reasonable lapse of time.

$(Ga_{1-x}In_x)_2O_3$ samples grown at "high" pressure maintain the typical Ga_2O_3 XRD pattern for a wide In concentration range (Fig. 3). With the above-mentioned experimental conditions, the solubility limit of In in $(Ga_{1-x}In_x)_2O_3$ is ~10% in atomic percent, corresponding to a partial In composition of x = 0.25. At higher values phase separation occurs due to the different crystallographic systems of Ga_2O_3 and In_2O_3, with the diffraction peaks relative to the latter that become sharper and sharper. By observing in detail the 2θ position of XRD peaks, a shift towards smaller angles in respect to the bulk values is clearly visible (inset of Fig. 3). Since the shift increases with In content, this phenomenon can be correlated to the increase of the lattice parameter of Ga_2O_3 due to the substitution of Ga^{3+} (r_{ion}=0.62 Å) with In^{3+} (r_{ion}=0.81 Å). The mixed $Ga_{2(1-x)}In_{2x}O_3$ phase is, therefore, effectively achieved.

A confirmation of this result comes from optical absorption measurements. The transparency of the layer, which remains between 80% and 90% from the absorption edge to the long-wavelength region, is a little lower in comparison to samples grown with O_2, but the most relevant feature of the spectra is the presence of a single absorption edge for samples with In content lower than 10%. In O_2-based growths, on the contrary, a double step feature always appeared at about 330 nm, corresponding to the 3.7 eV optical energy gap of In_2O_3, becoming more and more pronounced as the In content increases.

The structural properties of the $(Ga_{1-x}In_x)_2O_3$ samples were investigated by transmission electron microscopy (TEM). The layers showed the typical grain structure of Ga_2O_3 grown on Al_2O_3, due to the mismatch and the different crystal structure of the two materials. No In_2O_3 clusters were identified in samples with [In] < 10%, but the most interesting feature observed is a reduced amount of stacking fault in comparison to analogous Ga_2O_3 samples grown with the

same experimental parameters but without TMIn. In, therefore, seems to contribute to improve the crystal quality of the layers. A further evidence of the favorable effect of In on the growth of Ga_2O_3 is that in cathodoluminescence experiments the self-trapped exciton luminescence has been observed only in samples grown with In, while for pure gallium oxide layers no excitonic peaks were detectable. The effects of In on the structural properties and defect density in $(Ga_{1-x}In_x)_2O_3$ layers with [In] < 10% is a focus of the present investigations.

In December 2013 we have grown $(Ga_{1-x}In_x)_2O_3$ layers for the first time on Ga_2O_3 substrates and started to analyze the surface morphology by atomic force microscopy measurements and scan-

a) b)

Fig. 4 (a): SEM picture of a $(Ga_{1-x}In_x)_2O_3$ layer on Ga_2O_3 layer grown at 800 °C and 50 mbar with 200 sccm TMIn; (b) AFM picture of the same sample. The growth-steps are clearly visible.

ning electron microscopy. Figure 4 shows the morphology of a layer grown on a 1.5° off-oriented (100) Ga_2O_3 substrate at 800 °C, 50 mbar and with 5, 200 and 550 sccm of TMGa, TMIn and H_2O, respectively. In the SEM picture (fig. 4a) the presence of elongated terraces on the surface can be observed, around 2-5 μm wide, with irregular shape. By increasing the magnification (Fig. 4b), the terraces appear very flat (RMS = 200 pm) and it is possible to observe the presence of growth-steps on their surface. Such features are never been observed in samples without In, confirming that the latter enhances a step-flow growth mode. A more accurate characterization of these samples is currently in progress through TEM and HR-XRD analyses.
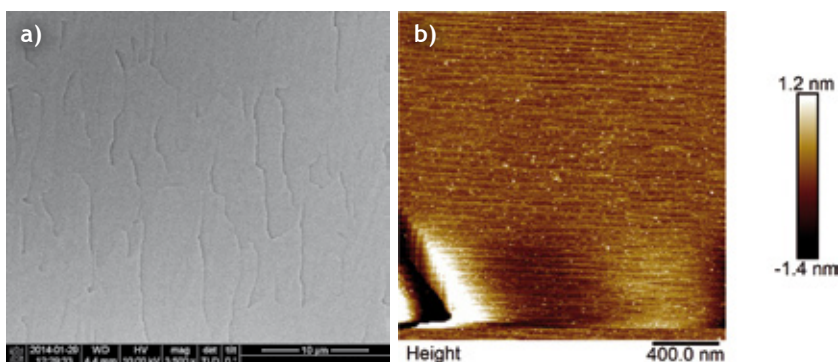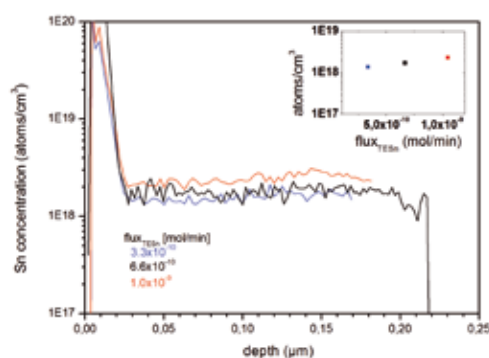

Fig.5: SIMS depth profile of three ß-Ga_2O_3 layers grown with different Sn-flux in the atmosphere. Inset graph shows the dependence of the Sn-concentration on the Sn-flux.

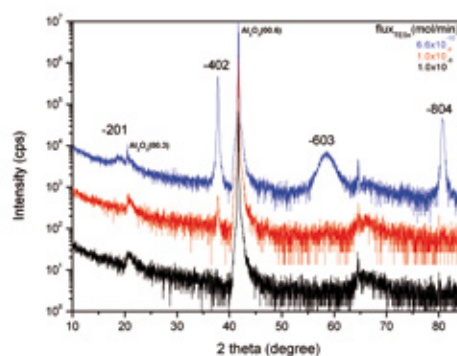*Fig.6: XRD spectra of three layers grown at equivalent growth parameters but with different Sn-flux, given in the legend.*

n-type doping of ß-Ga_2O_3 layers

In 2013 we have continued to perform doping experiments with Si, changing the Si concentration within the typical semiconducting range. To activate the Si donors some additional annealing procedures for 1 h and 30 min at a temperature ranging from 850 to 1050 °C in O_2- and N_2- atmosphere were performed. Some layers were annealed in forming gas (5% H_2 in Ar) at temperatures of 600 and 700 °C for 15 min. However, neither type of annealing has changed the resistivity of the samples, i.e. they remained semi-insulating.

Since the doping by Si donors was not effective to get semiconducting layers we have decided to use Sn, which is known as a successful donor in bulk crystal growth or in ß-Ga_2O_3 layers. As a tin source we have taken triethyltin (TESn). The reactor base pressure in this series of experiments was changed from 5 to 20 mbar and the tin flux was adjusted between $3x10^{-11}$ and $1x10^{-8}$ mol/min. At a deposition temperature of about 800 °C layers with thickness between 90 and 550 nm, at a growth rate from 2 up to 5 nm/min, have been grown with Sn concentration in the range from $5x10^{19}$ to $1x10^{18}$ cm^{-3}. Figure 5 shows the SIMS depth profile of three Ga_2O_3:Sn layers with a chemically incorporated Sn concentration between $1,3x10^{18}$ and $2,3x10^{18}$ cm^{-3}. Increasing the Sn-flux in the growth atmosphere by one order of magnitude the chemical Sn-concentration in the layers increased of about 40 %.

Fig. 6 illustrates three typical XRD spectra of layers grown at equivalent conditions on $Al_2O_3(0001)$ with different Sn doping. At a chemically Sn-concentration of $1x10^{18}$ cm^{-3} the characteristic XRD pattern of ß-Ga_2O_3 with

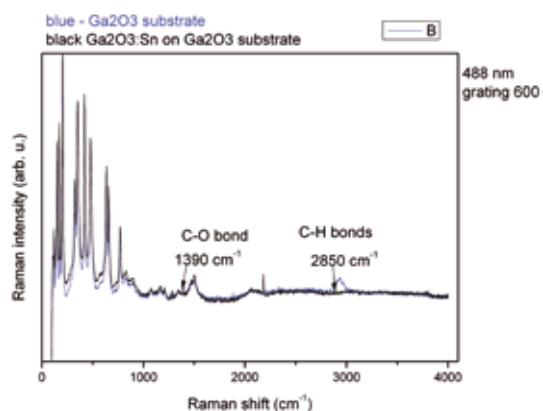*Fig.7: Raman spectra of ß-Ga₂O₃:Sn layer grown by homoepitaxy and of the pure ß-Ga₂O₃ substrate.*

the (-201), (-402), (-603) and (-804) Bragg reflections are visible, proving the epitaxial relationship between (-201) ß-Ga_2O_3 planes and the (0001) Al_2O_3 ones. At higher Sn-doping (3×10^{18} cm^{-3}) the (-201) and the (-603) Bragg peaks disappear (red curve). Further increase of doping might bring amorphization of the films (black curve).

Our experiments with MOVPE ß-Ga_2O_3 doped with Si and Sn in the same range, as-grown and exposed to annealing in O_2 or N_2, however, provided non-conductive material. At this stage we are inclined to believe that this may derive from formation of some complexes of structural defects with yet unidentified impurities that passivate the Si donors. Theoretical studies [2] have shown that the formation of Ga-vacancies at oxygen-rich conditions (like ours) may have even negative formation energy and carbon on oxygen site may behave as a double acceptor.

By Raman spectroscopy measurements we have observed carbon-compound related bands in the epitaxial layers (black curve in Fig. 7), such as CO_2 at 1390 cm^{-1} and C-$H_{i=1-3}$ groups at about 3000 cm^{-1} that do not exist in the spectrum of the substrate (blue curve). Similar bands were observed by FTIR for the thickest samples. The relative C concentration in the layers was determined by SIMS to be two magnitudes higher than in the Ga_2O_3 bulk crystal grown from the melt. It is possible that the C-concentration is equal or higher than the concentration of the intentionally introduced donors. It is known that C has ambipolar behavior [3] and can act as an acceptor on O-site. Thereby, there could be a compensation effect of the Si- and Sn-donors by C, which is a residual from the organic precursors.

Further high resolution TEM-, Raman- and SIMS investigations are in progress to shed more light on this concept. A new series of experiments with another Ga-precursor – triethyl-gallium – which is known from the MOVPE growth of III-nitrides to reduce the carbon concentration up to 50 times in comparison to TMGa, is planned.

References:

[1] G. Wagner, M. Baldini, D. Gogova, M. Schmidbauer, R. Schewski, M. Albrecht, Z. Galazka, D. Klimm, R. Fornari, physica status solidi (a) 211, 1 (2014) 27

[2] J.B. Varley, J.R. Weber, A. Janotti, C.G. Van de Walle, Appl. Phys. Lett. 97 (2010) 142106.

[3] C. H. Seager and A. F. Wright, J. Yu and W. Götz, J. Appl. Phys., Vol. 92, No. 11, (2002), 6553

Si/Ge Nanocrystals

Head: Dr. T. Boeck
Team: R. Bansen, J. Schmidtbauer, H.-P. Schramm, F. Schütte, Dr. T. Teubner
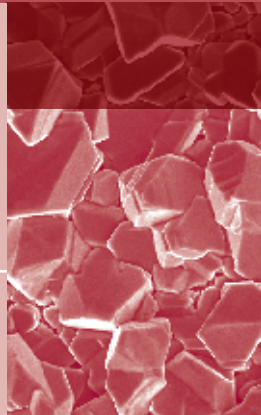
Überblick

Die Gruppe befasst sich mit zwei Forschungsthemen: (1) Abscheidung von polykristallinem Silizium auf Glas, (2) Vapour-Liquid-Solid-Wachstum (VLS) von Silizium und Germanium Nanodrähten.

Nur wenige Mikrometer Silizium sind relevant für die Umwandlung von Licht in elektrische Energie, daher konzentrieren sich die Forschungsarbeiten im Bereich der Photovoltaik auf die Entwicklung einer Technologie zur Abscheidung von dünnen Siliziumschichten auf kostengünstigen Substraten. Während dabei die Schichten eine möglichst hohe kristalline Qualität aufweisen müssen, würde der Einsatz von Glas als Substratmaterial die Kosten erheblich senken. Schließlich könnte die Schichtabscheidung direkt in den Herstellungsprozess der Solarmodule integriert werden.

Um polykristalline Si Schichten für die Photovoltaik bei niedrigen Temperaturen auf kostengünstigem Glas Substraten aufwachsen zu können, wird ein zweistufiger Prozess angewandt. Zunächst wird amorphes Si abgeschieden und bei ca. 300 °C mittels Metalltröpfchen kristallisiert. Bei dem von uns entwickelten und patentierten ALC Prozess (engl.: amorphous-liquid-crystalline), löst sich amorphes Si in den Metalltröpfchen und wird gleicher Temperatur in die stabilere kristalline Phase überführt. Dabei bewegen sich die Tröpfchen auf dem Substrat, wodurch eine Spur kristallinen Siliziums entsteht. In einem zweiten Prozessschritt wirken diese Si Keimkristalle als Vorlage für das Auswachsen der Schicht. Hierfür wird in einer von uns konzipierten Züchtungsanlage die Temperatur-Differenz-Methode (TDM) angewandt, in der Metalle als Lösungsmittel eingesetzt werden und ein konstanter Temperaturgradient thermodynamische Triebkraft für das Wachstum ist. Der Ersatz des Lösungsmittels Indium durch Zinn war ein Forschungsschwerpunkt im Berichtszeitraum, sowohl beim TDM Verfahren als auch bei dem ALC Prozess. TEM Untersuchungen lieferten wertvolle Aussagen zu Wachstumsvorgängen. Des Weiteren wurden Voruntersuchungen durchgeführt, um Oxide von Si Keimschichten vor der TDM Prozess mittels UV Laserstrahlung zu entfernen.

Ein zweites Thema der Gruppe ist das Wachstum von Nanodrähten, da diese Strukturen den Weg für neue Anwendungen und Bauelemente erschließen können. Wichtige Voraussetzung dafür ist jedoch die definierte Einstellung von Größe, Position und Kristallorientierung der Whisker. Ein Schwerpunkt bei dieser Thematik lag auf dem Wachstum von Germanium Nanodrähten auf Silizium-Substraten. Zusätzlich wurde untersucht, wie die Oberflächenrauigkeit von Germanium-Substraten das Wachstum von Germanium-Nanodrähten beeinflusst. Die Forschung an Nanodrähten, welche in der Substratebene wachsen, wurde abgeschlossen.

2014 startet das im Rahmen des 7. Rahmenprogramms geförderte EU-Projekt CHEETAH. Im Fokus des Projekts stehen zum einen die Forschungsaktivitäten auf dem Gebiet des Si-Wachstums auf kostengünstigen Substraten mittels TDM. Ein zweites Teilthema dieses Projektes ermöglicht es unserer Gruppe, ein neues Vorhaben in Angriff zu nehmen: In Zusammenarbeit mit dem Helmholtz-Zentrum Berlin (HZB), der Bundesanstalt für Materialforschung und Prüfung (BAM) und anderen Partnern gilt es, neue CIGS-basierte Mikro-Konzentrator-Solarzellen zu entwickeln. Das Projekt ist entstanden aus einer Initiative der European Energy Research Alliance (EERA), deren Mitglied das Institut ist, und unsere Gruppe wird in diesem Rahmen in den nächsten vier Jahren mit insgesamt 33 EU Partnern zusammenarbeiten.

Die Charakterisierung von Halbleiternanostrukturen für die Thermophotovoltaic ist Gegenstand eines gemeinsames BMBF-Projektes mit dem Paul-Drude-Institut für Festkörperelektronik (PDI) und der Abteilung für Physik der Halbleiter und Mikroelektronik der Yerevan State University (YSU), Armenien. Gefördert durch das Internationale Büro des BMBF wird unserer Gruppe die Fortführung der langjährigen Forschungskooperation mit unserem armenischen Partner auch für die Jahre 2013/14 ermöglicht.

In alle Arbeiten unserer Gruppe sind Nachwuchswissenschaftler integriert. Im Jahr 2013 hat Dr. Jan Schmidtbauer seine Dissertation „MBE Wachstum und Charakterisierung von Germanium Nanodrähten" an der Brandenburger Technische Universität Cottbus-Senftenberg mit Auszeichnung abgeschlossen. Darüber hinaus hat Franziska Schütte von der Beuth Hochschule für Angewandte Wissenschaften eine Auszeichnung von der Berlin-Brandenburg Sektion des Vereins Deutscher Ingenieure (VDI) für ihren Bachelor-Abschluss erhalten, nachdem sie ihre Bachelorarbeit zum Thema Ge-Nanodrähte in unsere Gruppe im Jahr zuvor abgeschlossen hatte. Sie unterstützt unsere Arbeit weiterhin als studentische Hilfskraft.

Overview

The team has focused on two research topics: (1) the deposition of polycrystalline silicon on glass, and (2) the vapor-liquid-solid growth of Si and Ge nanowires.

Since in photovoltaics only the first few micrometer of silicon are relevant for the conversion of light in electrical energy, research is focused on the development of a technology suitable for the deposition of thin silicon films on cheap substrates. While the crystalline quality of these films has to be as high as possible, glass as substrate material would lower the costs of production since the deposition steps could be integrated in the regular production process of photovoltaic cells. To achieve low temperature deposition of crystalline silicon on glass, as is desirable for photovoltaics, a two-step process is applied. In the first step, amorphous Si thin films are crystallized at temperatures around 300 °C by means of metal-induced crystallization. Contact of the liquid metallic solvent with amorphous Si hereby leads to an in-plane movement of the metal droplets, which is accompanied by precipitation of crystalline Si, a process we call amorphous-liquid-crystalline (ALC) transition and for which we have a patent pending. In the second step, the crystallized films serve as templates for further Si deposition by steady-state liquid phase epitaxy (SS-LPE), also known as the temperature difference method (TDM), using metals as solvent. In 2013, the research has focused on Si crystallization when applying the metallic solvent tin, both for TDM growth and for the ALC process, on the characterization of indium-grown samples by transmission electron microscopy (TEM), and on preliminary experiments for UV laser supported oxide removal from Si seed layers prior to TDM processing.

Our second focus is on the growth of nanowires, which are assumed to open the path to new applications and to new electronic devices. One prerequisite for their application is the control of size and position, but also the crystallographic orientation. In the field of nanowires, the main points have been the growth of germanium nanowires on Si substrates, and the investigation of the influence of surface roughness of Ge substrates on germanium nanowire growth. The research on in-plane nanowire growth was concluded.

An application for the CHEETAH project, that brings together the expertise of 33 institutions of the European Energy Research Alliance (EERA), was approved in 2013. Starting in 2014, it will promote the research activities in the field of Si growth by TDM and in addition, it opens up a new field of research for our group in cooperation with the Helmholtz-Zentrum Berlin (HZB) and the Federal Institute for Materials Research and Testing (BAM), namely CIGS-based micro-concentrator solar cells.

A joint project of the Si/Ge Nanocrystals group, the Paul-Drude-Institut für Festkörperelektronik (PDI), and the Department of Physics of Semiconductors and Microelectronics of the Yerevan State University (YSU), Armenia, under the auspices of the German Federal Ministry of Education and Research (BMBF) is under way. Key aspect is the characterization of semiconductor nanostructures for thermophotovoltaics.

Students and postgraduates have been involved in all topics of our research. In 2013, Dr. Jan Schmidtbauer completed his research activities and defended his PhD thesis "MBE growth and characterization of germanium nanowires" at Brandenburg Technische Universität Cottbus-Senftenberg with outstanding results. In addition, Frankziska Schütte from Beuth University of Applied Sciences received a graduate award from the Berlin-Brandenburg section of the Association of German Engineers (VDI) for her bachelor degree, after she had finished her bachelor thesis on the topic of Ge nanowires in our group the year before. She continues supporting our work as a student research assistant.
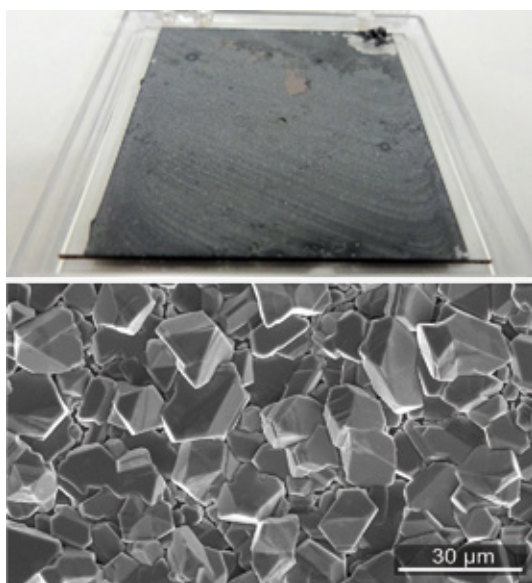
Fig. 1: Photograph of glass substrate covered with crystalline silicon on glass (left). Scanning electron microscopy (SEM) image of Si crystals, grown by TDM from Sn solution (right).

Results

Silicon on glass

While for using indium as solvent it was not possible to obtain samples fully covered by Si crystallites, turning to tin as solvent enabled us to increase the areal density of crystals in the previous year, and we succeeded now for the first time in obtaining full coverage, cf. figure 1.

During an internship of a student from Humboldt University, a systematic investigation of the ALC process with tin has been carried out. As can be seen in figure 2, the results are generally comparable to ALC growth achieved with indium as solvent. While the span of process parameters turned out to be more limited for Sn compared with In, the quality of the layers grown within the parameter range is high.

A more detailed characterization of the previously indium-grown samples by transmission electron microscopy (TEM), especially the investigation of samples with particularly small crystals, have led to a deeper understanding of the crystallites' growth mechanism, cf. figure 3. Growth starts from individual specimens of the larger seed crystals. The epitaxial relationship between the grown crystals and their starting seed has been proven by twin boundaries continuing from the seed into the crystal. In the adjacent areas, random grain boundaries indicate that no epitaxial growth took place there, i.e. they were laterally overgrown. Around the seeds of the grown crystals high defect densities have been found, which decrease with increasing distance.

To address the problem of surface oxidation of the seed layers during handling and heat-up prior to the TDM growth step, preliminary experiments with a nitrogen UV laser provided valuable information on proper wavelength and energy density parameters laser-assisted oxide removal. More results are expected after installation of a commercial UV laser and laser scanner system.

There is an ongoing cooperation with the HZB in the field of crystalline Si on glass, pertaining to electrical characterization, and to transparent conductive oxides (TCO) as contact layers. For the latter, samples with functional layers have been annealed in ultra pure hydrogen.

Germanium nanowires

While germanium nanowires are widely accepted to be promising nanostructures for future electronic and optoelectronic devices, another prospective field of application is their use for high performance anodes in lithium-ion batteries, which has attracted high interest in recent years [2].

Ge nanowires have been successfully grown by the vapor-liquid-solid (VLS) process in a MBE system. Gold droplets serve as metal solvent to define the place and diameter of the growing wires, while both Ge and Si wafers served as substrates. The work has focused on the heteroepitaxial growth on silicon substrates, which has been promoted by means of silicon oxide interlayers in order to enhance the germanium diffusion and suppress island growth between the droplets. Starting in 2012, activities have been intensified in this field in 2013. Eventually, the results of Ge nanowire research were summarized in the very successfully defended PhD thesis by Dr. Jan Schmidtbauer [1].

Future work will focus on the growth of SiGe nanowires, which are promising building blocks for efficient thermoelectric devices [3]. One key aspect is the growth of SiGe compound nanowires with Ge contents intentionally tuned between 30% and 40%. Starting with pure Si nanowires, the latter are supposed to serve as a basis for a stepwise increase of the Ge content. Preliminary experiments have been carried out in order to establish Si nanowire MBE growth on Si(111). Figure 4 shows SEM micrographs of such VLS-grown Si nanowires.

A main drawback of nanowire growth by conventional solid-source MBE is the strong influence of diffusive material transport on the substrate surface, which leads to a process-related limitation of the achievable length and aspect ratio. To target this issue, a gas-source MBE system, working with silane and germane as precursors, is going to be implemented. Planning and acquisition of the equipment is basically managed by the team and resulted in a fully instrumented process chamber. Main hardware components (vacuum system, gas supply) have been attached to the UHV cluster according to the drawing in figure 5.

Experiments in cooperation with the Crystal Machining group of Dr. U. Juda regarding the influence of substrate surface roughness on Ge nanowire growth led to insightful results: even minor surface irregularities left from chemical-mechanical polishing (CMP) on otherwise atomically flat substrates can have a paramount influence on nanowire growth, provided the scale of these irregularities matches the scale or the spacing of the used catalyst droplets. It is assumed that small protrusions on the surface serve as pinning points to the droplets. This behavior promotes the vertical growth of nanowires and avoids lateral movement of droplets or classical island formation [4].

A paper [5] summarizing the results on Ge in-plane nanowires concluded this field of research in 2013.
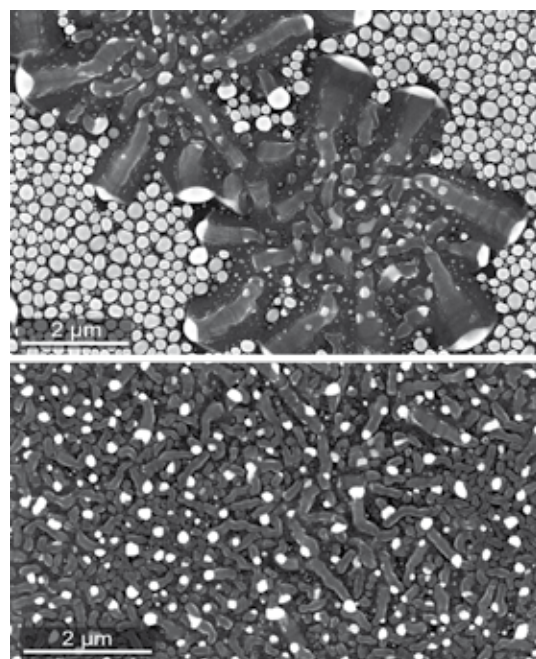
Fig. 2: SEM images of ALC process with Sn as solvent. Moving droplets form circular areas during growth (left). After completion of ALC transition, the substrate is covered with c-Si traces (right).
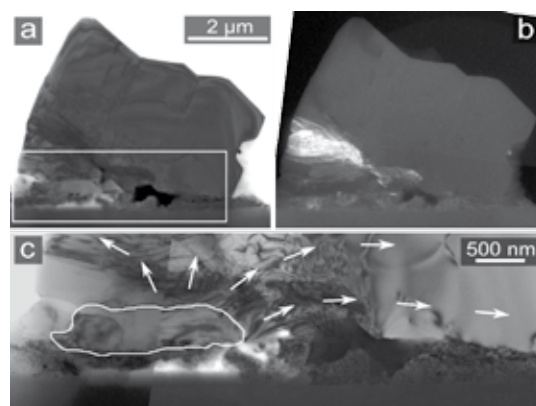
Fig. 3: Cross-sectional TEM micrographs of a Si crystal grown by TDM from In solution. (a) Bright field image of entire crystal, with In inclusion (dark spot). (b) Dark field image showing high defect density around seed crystal. (c) Enlargement of white box in (a), showing large seed crystal (marked in white) and assumed growth directions for lateral overgrowth (marked by arrows).
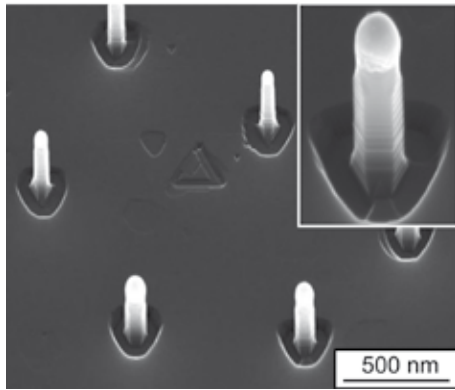
Fig. 4: SEM micrograph of Si nanowires grown on a Si(111) substrate. The sample is tilted by 30°. As can be seen in the inset, the nanowires have hexagonal cross sections and show pronounced nano-faceting on the {112} sidewalls.
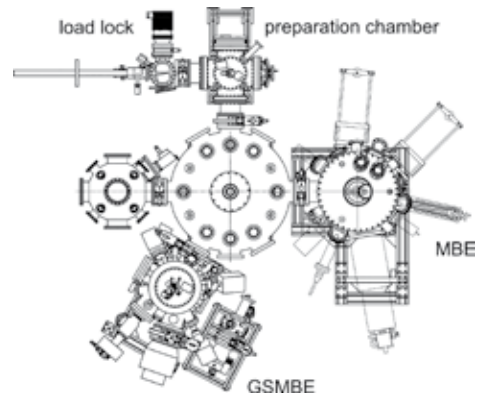
Fig. 5: Technical drawing of the UHV cluster system with MBE and gas-source MBE process chambers attached to the central handling unit.

References

[1] J. Schmidtbauer, MBE growth and characterization of germanium nanowires, TU Berlin, 2013

[2] A.M. Chockla, K.C. Klavetter,C.B. Mullins, B.A. Korgel, ACS Appl. Mater. Interfaces **4** (2012), 4658

[3] A.I. Boukai, Y. Bunimovich, J. Tahir-Kheli, J.-K. Yu, W. a Goddard, J.R. Heath, Nature, **451** (2008), 168

[4] R. Bansen, J. Schmidtbauer, U. Juda, T. Markurt, Th. Teubner, R. Heimburger, T. Boeck, Physica Status Solidi (RRL) – Rapid Research Letters, **7** (2013), 831

[5] R. Bansen, J. Schmidtbauer, R. Gurke, Th. Teubner, R. Heimburger, T. Boeck, CrystEngComm **15** (2013), 3478

Ferroelectrical Oxide Layers

Head: Dr. J. Schwarzkopf
Team: A. Duk, D. Braun, S. Markschies, J. Sellmann
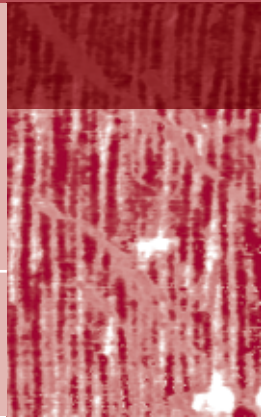
Überblick:

Die Abscheidung von dünnen Oxidschichten eröffnet einen weiten Einsatzbereich für potentielle Anwendungen. Dies ergibt sich sowohl aus der Vielzahl von möglichen chemischen Zusammensetzungen in den Schichten und deren Kombinationsmöglichkeiten mit verschiedenen Substratmaterialien, als auch aus der möglichen Kontrolle ihrer physikalischen, insbesondere ihre ferro- und piezoelektrischen, Eigenschaften. Entsprechend könnten sie als Basismaterial für zukünftige miniaturisierte Speicher- und Mikrowellenbauelemente oder Sensoren dienen. Dazu müssen jedoch zunächst die fundamentalen Mechanismen der Entstehung ferroelektrischer Domänen und die Kopplung zwischen Gitterverspannung und elektrischer Polarisation im Detail verstanden werden. Gleichzeitig ist es erforderlich, geeignete Depositionstechnologien für die Industrie in einer langfristigen Perspektive zu entwickeln.

Obgleich der Gebrauch von bleihaltigen Materialien nach EU Recht seit 2006 verboten ist, werden Verbindungen mit Blei-Zirkonium-Titanat (PZT) bis heute von diesem Verbot ausgenommen. Wegen ihrer ausgezeichneten piezo-/ferroelektrischen Eigenschaften und dem Mangel an verfügbaren Materialien mit geringerer Umweltbelastung wird PZT weiterhin in vielen Anwendungen wie in nichtflüchtigen Speichersystemen oder Sensoren, z.B. in der Automobilindustrie, eingesetzt. Als Alternative finden zunehmend Alkaliniobat-basierte Materialien wie $NaNbO_3$, $KNbO_3$ und ihre Festkörpermischungen Beachtung [1,2]. Sie weisen ähnlich exzellente piezo-/ferroelektrischen Eigenschaften auf Blei-Zirkonium-Titanat-basierte Materialien, sowie hohe Curie Temperaturen und komplexe Phasendiagramme. Obwohl deren Volumenkristalle in der Vergangenheit gut untersucht wurden, wurden die piezo-/ferroelektrischen Eigenschaften und Domänen in dünnen $(Na,K)NbO_3$ Schichten bisher wenig erforscht. Jedoch sind das Verständnis und die Kontrolle von Domänen wesentlich für ihre weitere Anwendung in elektrischen Bauelementen mit funktionalen Einheiten im Nanometerbereich. Eine Möglichkeit zur Kontrolle von Domänen und Polarisation ist durch den Einbau einer (anisotropen) Gitterverspannung durch das epitaktische Wachstum auf gitterfehlangepassten Substraten gegeben. Das kann in den Schichten Phasenübergänge ermöglichen, die für die entsprechenden Volumenkristalle nicht beobachtet werden, wie z.B. Rotationsphasen mit deutlich erhöhten dielektrischen Eigenschaften.

In Bezug auf die Realisierung von nicht-flüchtigen Speicheranwendungen hat das polare/nicht-polare Interface zwischen einer ferroelektrischen Komponente und $SrTiO_3$ in den letzten Jahren großen Interesse geweckt. Die Existenz eines zweidimensionalen Elektronengases (2DEG) wurde theoretisch für das $(Na,K)NbO_3/SrTiO_3$ Interface vorhergesagt [3], dessen Eigenschaften vermutlich durch das Switchen der ferroelektrischen Polarisation in den $(Na,K)NbO_3$ Schichten moduliert werden können [4].

Overview

Thin oxide films are opening a wide range of possible applications, due to the large availability of possible chemical compositions, of combinations with various substrates and the ability to control their physical, in particular ferro- or piezoelectric, properties. They may be assumed as basic material for future miniaturized memory and microwave devices or sensors. To develop their full potential, fundamental mechanisms of ferroelectric domain formation and coupling between strain and electrical polarization have to be understood in detail. Moreover, appropriate deposition technologies applicable for industry on a long-time perspective have to be developed.

Even though the use of lead containing materials is forbidden under EU law since 2006, compounds like lead-zirconate-titanate (PZT) are still excluded from this regulation. Due to its superior piezo-/ferroelectric properties and the lack of materials with comparably outstanding characteristics but less environmental impact, PZT is used in many applications like non-volatile memory systems or sensors, e.g. in the automotive industry. Alkaline niobate based materials, like $NaNbO_3$, $KNbO_3$ and their solid-solutions, have attracted much interest due to their excellent piezo-/ferroelectric properties similar to those of lead-zirconate-titanate based materials, their high Curie temperatures and complex phase diagrams [1,2]. Although bulk crystals have been well investigated in the past,

piezo-/ferroelectric properties and domains in $(Na,K)NbO_3$ thin films are rarely studied yet. However, understanding and controlling of domains is essential for their further application in nanometer sized electronic devices. One possibility of domain and polarization control is given by the incorporation of (anisotropic) lattice strain by epitaxial growth of thin films on lattice mismatched substrates. This can provide new phase transitions in these films which are not observed in corresponding bulk crystals, for instance rotational phases with significantly enhanced dielectric properties.

With regard to the realization of non-volatile memory applications polar/non-polar interfaces between a ferroelectric constituent and $SrTiO_3$ has gained enormous interest in recent years. The existence of a two-dimensional electron gas (2DEG) has been theoretically predicted for the $(Na,K)NbO_3/SrTiO_3$ interface [3], which properties are supposed to be modulated by ferroelectric polarization switching of the $(Na,K)NbO_3$ film [4].

Results

Strained $NaNbO_3$ and $(Na,K)NbO_3$ thin films have been epitaxially grown on different oxide substrates ($NdGaO_3$, $SrTiO_3$ as well as the rare-earth scandates $ReScO_3$ with Re = Dy, Tb, Gd, Nd) by liquid-delivery metal-organic chemical vapor deposition (MOCVD) and pulsed laser deposition (PLD). Structural and electrical properties of the films are significantly affected by the incorporation of anisotropic biaxial in-plane lattice strain and the variation of deposition conditions, especially the oxygen partial pressure.

Ferroelectric domain formation in anisotropically strained $NaNbO_3$ thin films
$NaNbO_3$ films grown on $NdGaO_3$ substrates exhibit anisotropic in-plane lattice strain. Piezoresponse force microscopy (PFM) measurements on coherently grown, compressively strained $NaNbO_3$ films on $NdGaO_3$ substrates exhibit large out-of-plane polarization components as well as an in-plane signal. These findings are in good agreement with the orthorhombic $Pmc2_1$ phase deduced from HRTEM images and corresponding simulations, where the polarization vector runs along the $<101>_c$ pseudocubic direction. However, no distinctive domain structure could be evaluated. This observation is attributed to the small domain size which cannot be resolved by PFM measurements. Increasing film thickness leads to the onset of plastic strain relaxation and thus to a reduction of the compressive lattice strain. This is accompanied by a phase transition to a monoclinic M_A phase, where the polarization vector can freely rotate in a $\{110\}_c$ plane and which is often observed for ferroelectric relaxors in PZT-based materials. Temperature and frequency dependent C-V measurements performed at FZ Jülich, AG Prof. R. Wördenweber, have confirmed ferroelectric relaxor behavior in these compressively strained $NaNbO_3$ films on $NdGaO_3$ [5,6]. This observation has been attributed to the lowering of crystal symmetry and related polarization instability [7]. These results show that with the application of anisotropic lattice strain the occurrence of low-symmetry phases can be controlled, which provides the unique possibility to grow lead-free oxide films with improved electromechanical properties and anisotropic ferroelectric properties.

When tensile lattice strain is provoked by the epitaxial growth on $DyScO_3$, $TbScO_3$ and $GdScO_3$ single crystalline substrates provided in-house by the group Oxides/Fluorides, the $NaNbO_3$ films behave rather like a normal ferroelectric. PFM measurements show that the application of these rare-earth scandate substrates yields well-ordered ferroelectric stripe domains of the type $a_1/a_2/a_1/a_2$. Arrangement and polarization directions of these domains are determined by the lattice mismatch to and the symmetry of the underlying substrate [8,9]. Influence of lattice mismatch and strain relaxation process in tensily strained $NaNbO_3$ films are described in detail in "Highlights" and is one of the topics reported by the group Physical Characterization.
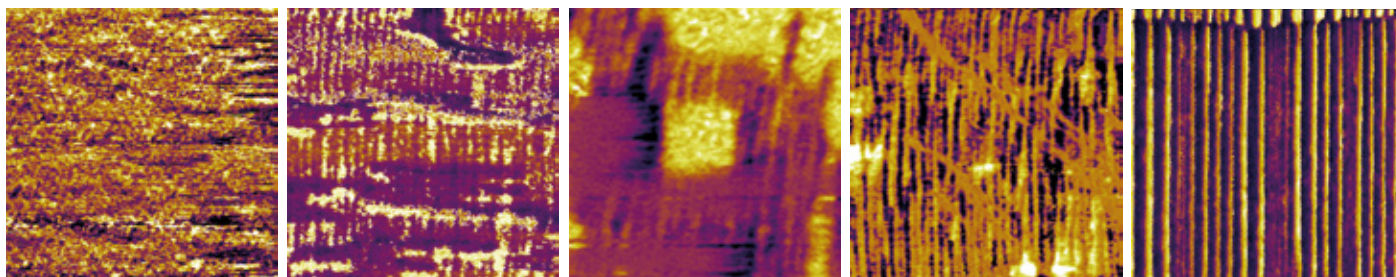
Fig. 1: PFM phase images (scan area: 1 µm x 1 µm) of $NaNbO_3$ PLD thin films on $DyScO_3$ substrates under different growth conditions: (a) 600 °C, 0.05 mbar, stoichiometric target, (b) 600 °C, 0.7 mbar, stoichiometric target, (c) 900 °C, 2 mbar, stoichiometric target, (d) 600 °C, 0.05 mbar, NaO_2 excess target. For comparison the PFM phase image of $NaNbO_3/DyScO_3$ grown by MOCVD is given in (e).
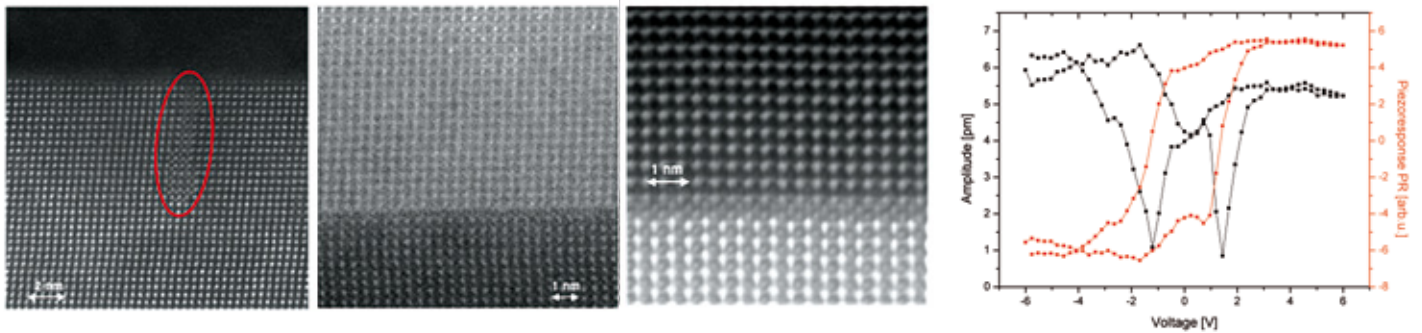
Fig. 2: HRTEM images of (a) a NaNbO$_3$ PLD film grown on DyScO$_3$ at 600 °C and 0.05 mbar from a stoichiometric target, (b) a NaNbO$_3$ PLD film grown on TbScO$_3$ at 900 °C and 2 mbar from a stoichiometric target, (c) NaNbO$_3$ MOCVD film grown on DyScO$_3$ at 700 °C and 20 mbar, (d) Local hysteresis curve of a NaNbO$_3$ PLD film grown on a Nb-doped SrTiO$_3$ substrate at 900 °C and 2 mbar from a stoichiometric target recorded by switching spectroscopy PFM.

Beside incorporated lattice strain ferroelectric domain formation is critically determined by the deposition conditions of the NaNbO$_3$ thin films, especially the oxygen partial pressure. In this regard – for a comparison – NaNbO$_3$ films were grown on DyScO$_3$ substrates by PLD, which is known to yield to oxygen and sodium deficiency in the films. For a systematic study on the one hand we varied the oxygen partial pressure during deposition process and on the other hand we used stoichiometric as well as Na$_2$O excess PLD targets. Substantial reduction of the sodium and oxygen deficiency was achieved by increasing the oxygen partial pressure from 0.05 mbar to 2 mbar and by Na$_2$O enrichment of the targets. It was found that Na$_2$O excess targets influence the final composition of NaNbO$_3$ PLD films and the ferroelectric domain formation more effectively than an increase of the oxygen partial pressure in the reactor chamber (see Fig. 1) [10]. HRTEM images of oxygen/sodium deficient films (grown at p(O$_2$) = 0.05 mbar and from a stoichiometric target) show precipitates presumably attributed to niobium-oxide (Fig. 2a). In contrast, nearly stoichiometric films grown at 2 mbar do not exhibit foreign phases and defects (Fig. 2b), comparable to MOCVD films (Fig. 2c). Optimized growth conditions have been resulted in well-opened ferroelectric hysteresis measurements (Fig. 2d).

Na$_{1-x}$K$_x$NbO$_3$ thin films grown by MOCVD and PLD
Additionally to the deposition and investigation of NaNbO$_3$ thin films we have started to extend our materials basis to solid solutions consisting of NaNbO$_3$ and KNbO$_3$. The influence of Na/K ratio and the incorporation of compressive and tensile lattice on the domain formation and ferroelectric hysteresis curves were of particular interest. First results on MOCVD films have shown that piezoelectric response and domain pattern substantially vary with incorporated lattice strain and K concentration. Ongoing HRTEM and HRXRD measurements are necessary for a detailed understanding of the domain formation.

Superlattices of (NaNbO$_3$)$_n$/(KNbO$_3$)$_m$ allows the deposition of fully strained films with a thickness exceeding the critical thickness of plastic relaxation. While growth of alternating layers by PLD with a KNbO$_3$ thickness of up to three monolayers result in single Na$_{1-x}$K$_x$NbO$_3$ solid solution films, (NaNbO$_3$)$_n$/(KNbO$_3$)$_m$ superlattices were obtained with individual layer thicknesses of seven or more monolayers. Incorporation of K in any case leads to improved piezoelectric coefficients of the films. We will continue to explicitly investigate the influence of potassium on ferro-/piezoelectric properties of such films.

Oxide interfaces
With regards to the predicted formation of a 2DEG at heteropolar oxide interfaces preliminary works have been performed. HRTEM images of NaNbO$_3$ thin films on different substrates revealed a cation intermixing layer between NaNbO$_3$ films on ReScO$_3$ (Re = Dy, Tb) substrates, independent on the deposition method. This observation is tentatively explained by a compensation effect of the charge imbalanced NaO – ScO$_2$ interface. In contrast no intermixing layer has been observed for NaNbO$_3$/SrTiO$_3$ and KNbO$_3$/ReScO$_3$ heterostructures. Further detailed structural and electrical investigations on the nanometer scale will be necessary for a better understanding of the interface formation and charge compensation mechanisms.

Characterization by PFM
Regarding the difference of "classical" ferroelectric and relaxor behavior exciting questions arise how switching processes proceed. For that purpose we have investigated compressively strained NaNbO$_3$ films on NdGaO$_3$ and K$_x$Na$_{1-x}$NbO$_3$ films on SrTiO$_3$ substrates. PFM phase images show irregularly arranged, nanometer sized domains with both large in-plane and out-of-plane piezoresponse. For in-
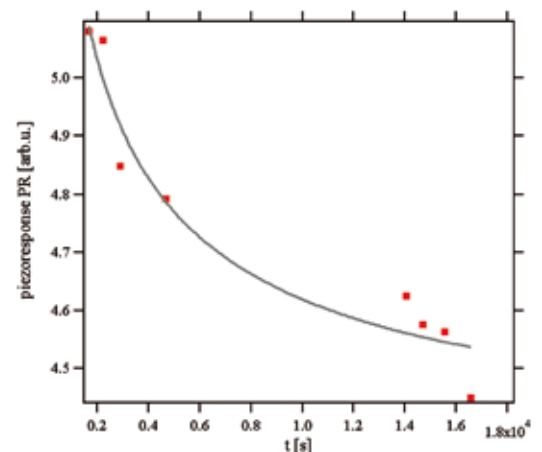
Fig. 3: Piezoelectric decay characteristic of a partially relaxed, compressively strained NaNbO$_3$ film on NdGaO$_3$ grown by MOCVD.

vestigation of the relaxation behavior in the films time-dependent decays of the piezoresponse (PR) were recorded on uniformly poled films. In both cases the decay of the PR signal as a function of time is well described by the Kohlrausch-Williams-Watts (KWW) relaxation function with $\beta \approx 0.7$ and $\beta \approx 0.4$ for $NaNbO_3/NdGaO_3$ (Fig. 3) and $K_xNa_{1-x}NbO_3/SrTiO_3$, respectively. The occurrence of $\beta < 1$ indicates the existence of different decay processes and is typical for relaxors.

For the case of $NaNbO_3/NdGaO_3$ we have also recorded the temperature dependency of the domain size. It was found that increasing the surrounding temperature leads to lateral growth of existing domains, which is well known from lead-based relaxors. Hence, together with the above describe relaxation characteristic we attribute these results to relaxor behavior.

References:

[1] Y. Saito, H. Takao, T. Tani, T. Nonoyama, K. Takatori, T. Homma, T. Nagaya, and M. Nakamura, Nature **432,** 84 (2004).

[2] H.D. Megaw, Ferroelectrics **7,** 87 (1974).

[3] M.K. Niranjan, Y. Wang, S.S. Jaswal, and E.Y. Tsymbal, Phys. Rev. Lett. **103,** 016804 (2009).

[4] J. Hoffman, X. Pan, J. W. Reiner, F. J. Walker, J. P. Han, C. H. Ahn, and T. P. Ma, Adv. Mater. **22,** 2957 (2010).

[5] R. Wördenweber, J. Schwarzkopf, E. Hollmann, A. Duk, B. Cai, and M. Schmidbauer, Appl. Phys. Lett. **103,** 132908 (2013).

[6] B. Cai, J. Schwarzkopf, E. Hollmann, M. Schmidbauer, M.O. Abdel-Hamed, and R. Wördenweber, J. Appl. Phys. 115, 224103 (2014).

[7] J. Schwarzkopf, D. Braun, M. Schmidbauer, A. Duk, and R. Wördenweber, J. Appl. Phys. 115, 204105 (2014).

[8] A. Duk, M. Schmidbauer, and J. Schwarzkopf, Appl. Phys. Lett. **102,** 091903 (2013).

[9] M. Schmidbauer, J. Sellmann, D. Braun, A. Kwasniewski, A. Duk, and J. Schwarzkopf, Phys. Status Solidi RRL, 1–5 (2014) / DOI 10.1002/pssr.201409012 (2014).

[10] J. Sellmann, J. Schwarzkopf, A. Kwasniewski, M. Schmidbauer, D. Braun, and A. Duk, submitted to Thin Solid Films (2014).

Physical Characterization

Electron Microscopy

Chemical & Thermodynamic Analysis

Crystal Machining

Simulation & Characterization

Head of the section: PD Dr. habil. Detlef Klimm

Like in the previous reporting periods, a big share of the activities was devoted on the support of the crystal growth groups. Besides, cooperations with external partners were running on specific tasks, especially by the Electron Microscopy Group. It should be underlined that the external funding acquired by this group (Federal Ministry of Education and Research, European Union, German Research Foundation, Industry) contributes significantly to the financing of the larger number of collaborators, and especially PhD students, that are working in this group. The groups of the section contributed to the work on nitrides, which will play a major role at IKZ in the forthcoming years: The Crystal Machining Group developed a technology for chemo-mechanical polishing (CMP) that allows now the preparation of epi-ready AlN wafers for partners, e.g. in the framework of "Advanced UV for Life". The Electron Microscopy Group presents in this Annual Report a new approach for the chemical analysis of (In,Ga)N quantum wells with atomic resolution, that is based on the separation of chemical and strain contributions to the contrast function. The Physical Characterization Group revealed a new point defect type that may be present in AlN bulk crystals: 3 neighboring carbon atoms can substitute for Al and N and impede optical properties in the ultraviolet spectral range. Details can be found in their contribution in this report. The Chemical & Thermal Analysis Group contributed by the analysis of starting and auxiliary materials, and by different thermodynamic calculations.

Other work was devoted to oxides, which means epitaxial ferroelectric layers as well as Transparent Conducting Oxides (TCO's) in the bulk or in layers. We hope that the "Forschergruppe" (together with Humboldt University) comes soon into life, to supply a sound framework for this quickly developing field with significant scientific and technological potential. Meanwhile, the growth of at least 4 corresponding bulk crystals was demonstrated at IKZ: ZnO, $\beta\text{-}Ga_2O_3$, In_2O_3, SnO_2. All of them have quite distinct physical and 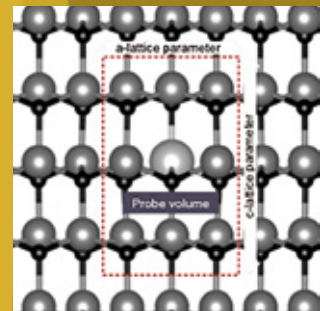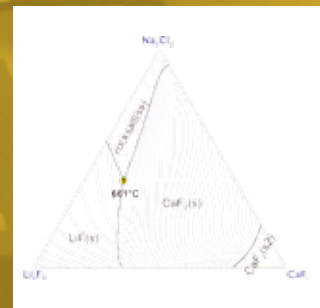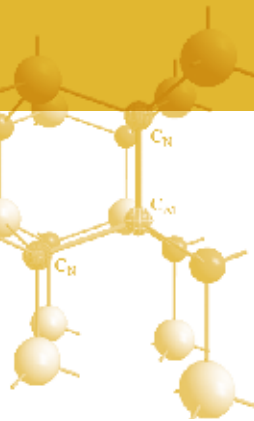chemical properties, which is an interesting challenge not only for growth and investigation, but also for their mechanical treatment, including cutting and polishing. Here a somewhat broader technical and personnel basis of the Crystal Machining Group would be desirable.

Wie schon in früheren Berichtszeiträumen diente die Arbeit der Sektion zum beträchtlichen Teil der Unterstützung der Züchtergruppen. Darüber hinaus wurde mit externen Partnern zu speziellen Themen kooperiert, die gilt in besonders hohem Maße für die Gruppe Elektronenmikroskopie. Es ist hervorzuheben dass erst die beträchtlichen von dieser Gruppe eingeworbenen Drittmittel (BMBF, EU, DFG, Industrie) den Aufbau einer solch großen und aktiven Gruppe mit vielen Doktoranden ermöglichten.

Alle Gruppen der Sektion trugen zur im IKZ betriebenen Forschung an Nitriden bei, die auch in den kommenden Jahren große Bedeutung besitzen wird: Die Gruppe „Kristallbearbeitung" entwickelte eine Technologie zur chemo-mechanischen Politur (CMP), welche die Herstellung von „epi-ready" Wafern für externe Partner ermöglicht, z.B. im Rahmen von „Advanced UV for Life". Die Elektronenmikroskopie-Gruppe stellt in diesem Report einen verbesserten Ansatz zur chemischen Analyse von (In,Ga)N Quantengräben mit atomarer Auflösung vor; hierbei wird der Beitrag von chemischer Zusammensetzung und mechanischer Verzerrung separiert. Die Gruppe „Physikalische Charakterisierung" entdeckte einen neuen Punktdefekttyp, der in AlN Bulk-Kristallen auftreten kann: 3 benachbarte Kohlenstoffatome substituieren dabei Al bzw. N, welches zu signifikanter Beeinträchtigung optischer Eigenschaften im UV-Bereich führt. Details werden in diesem Jahresbericht beschrieben. Die Gruppe „Chemische & Thermodynamische Analyse" begutachtete Ausgangsmaterialien und Hilfsstoffe; des weiteren erfolgten thermodynamische Berechnungen.

Des weiteren wurde zu Oxiden gearbeitet, und zwar sowohl zu ferroelektrischen Schichten als auch zu transparenten leitfähigen Oxiden (TCO) sowohl im Bulk als auch in Schichten. Wir hoffen, dass die gemeinsam mit der Humboldt-Universität initiierte Forschergruppe bald ihre Arbeit aufnehmen kann, womit ein formeller Rahmen für dieses sich schnell entwickelnde Arbeitsfeld mit hohem wissenschaftlichen und technischen Potential geschaffen wäre. Bisher wurden mindesten 4 entsprechende Substanzen als Volumenkristalle in IKZ gezüchtet: ZnO, $\beta\text{-}Ga_2O_3$, In_2O_3, SnO_2. Diese besitzen teilweise signifikant verschiedene physikalische und chemische Eigenschaften, welches eine interessante Herausforderung sowohl für Züchtung und Charakterisierung, aber auch für ihre mechanische Bearbeitung inklusive Schneiden und Polieren darstellt. Letzteres würde durch eine etwas breitere technische und personelle Basis der Gruppe „Kristallbearbeitung" erleichtert.

Physical Characterization

Head: Dr. K. Irmscher
Team: K. Banse, A. Kwasniewski, M. Naumann, M. Pietsch, Dr. M. Schmidbauer

Übersicht

Die Gruppe Physikalische Charakterisierung beschäftigt sich hauptsächlich mit der Untersuchung der im IKZ gezüchteten Volumenkristalle und epitaktischen Schichten mittels Röntgenbeugung, optischer Spektroskopie und Bildgebung, elektrischer Messungen sowie verwandter Techniken. Einerseits liefern die Ergebnisse dieser Messungen die erforderliche Rückinformation an die Kristallzüchter, um die Züchtungsprozesse zu optimieren. Andererseits können interessante physikalische Effekte, die von grundlegendem oder anwendungsspezifischem Interesse sind, nachgewiesen werden. Viele wichtige Resultate werden in den Einzelberichten der entsprechenden Züchtungsgruppen beschrieben. Hier konzentrieren wir uns auf zwei ausgewählte Themen unserer Arbeit: (i) Es wurden die ferroelektrischen Domänen in $NaNbO_3$ Dünnschichten mit Hilfe der Röntgenbeugung unter streifendem Einfall untersucht. Die Arbeit entstand durch enges Zusammenwirken von Martin Schmidbauer und Albert Kwasniewski aus der Gruppe Physikalische Charakterisierung mit der Gruppe Ferroelektrische Oxidschichten und profitierte in hohem Maße von der Verfügbarkeit geeigneter Oxidsubstratkristalle, die in der Gruppe Oxide/Fluoride gezüchtet werden. (ii) In AlN-Volumenkristallen wurde ein Tri-Kohlenstoffdefekt mit Hilfe der Spektroskopie lokaler Schwingungsmoden identifiziert. Dieser reichlich vorhandene Defekt dominiert die schädliche, unterhalb der Bandlücke auftretende Ultraviolettabsorption. Die Arbeit wurde durchgeführt von Klaus Irmscher und Mike Pietsch aus der Gruppe Physikalische Charakterisierung in Zusammenarbeit mit der Gruppe Aluminiumnitrid, die die AlN-Kristalle unter verschiedenen Wachstums- und Dotierungsbedingungen präparierten.

Overview

The group Physical Characterization is mainly concerned with investigations of bulk crystals and epitaxial layers grown at IKZ using x-ray diffraction, optical spectroscopy and imaging, electrical measurements, and related techniques. On one hand the results of these measurements provide necessary feedback to the crystal growers for optimizing the growth processes. On the other hand interesting physical effects in these crystals may be revealed being of basic as well as application specific interest. Many important results are communicated in the individual reports of the respective crystal growth groups. Here we focus on two selected topics of our work: (i) Ferroelectric domains in $NaNbO_3$ films were studied by using grazing-incidence x-ray diffraction. The work arose from a close collaboration of Martin Schmidbauer and Albert Kwasniewski of the group Physical Characterization with the group Ferroelectric Oxide Layers and has greatly benefited from the unique availability of appropriate oxide substrate crystals which are grown in the group Oxides/Fluorides. (ii) In AlN bulk crystals a tri-carbon defect was identified by using local vibrational mode spectroscopy. This highly abundant defect dominates the detrimental, below band gap ultraviolet absorption. The work was performed by Klaus Irmscher and Mike Pietsch of the group Physical Characterization in cooperation with the group Aluminum Nitride who prepared AlN crystals under various growth and doping conditions.

Results

Ferroelectric domains in $NaNbO_3$ films studied by grazing-incidence x-ray diffraction
Size and symmetry of ferroelectric domains have a large impact on the ferro/piezoelectric properties of thin films. They can be controlled by incorporation of lattice strains, which has been shown to result e.g. in a change of the film orientation, a shift of the Curie temperature, and an increase of the remnant polarization and piezoelectric coefficients [1,2]. By changing the substrate material the lattice mismatch between the thin film and the substrate can be intentionally tuned thus facilitating film growth under varying compressive or tensile stresses. In a previ-

ous paper [3] we have studied the ferroelectric domain structure of NaNbO$_3$ thin films deposited under tensile strain on orthorhombic (110) TbScO$_3$ substrates. In order to examine the influence of tensile strain in more detail we have extended our investigations to NaNbO$_3$ thin films grown with reduced tensile strain on (110) DyScO$_3$ (DSO) substrates, and corresponding results have been published in Ref. 4. All samples were grown by pulsed layer deposition (PLD) and metal organic chemical vapor deposition (MOCVD) in the group of Jutta Schwarzkopf (IKZ) – for a detailed description of the PLD and MOCVD growth parameters see Ref. 5 and 6, respectively.

For all samples the surface morphologies consist of a smooth stepped surface with corresponding rms roughness smaller than 0.5 nm strongly indicating that the thin films were deposited in step flow growth mode. X-ray reciprocal space maps show that coherent film growth is present up to a thickness of about 27 nm. Piezoresponse force micrographs (PFM) of these films exhibit a regular stripe domain pattern which is aligned along the [001] DSO substrate direction. The domain pattern is of the type a1/a2/a1/a2 with exclusive in-plane polarization (Fig. 1b, c). Ongoing plastic strain relaxation, which is observed for thicknesses larger than 27 nm, is accompanied by transformation of the stripe domain pattern into a 2D domain pattern where the electric polarization exhibits also an out-of-plane component (Fig. 1d, e, f). For film thicknesses below 6 nm, the PFM images do not reveal clear evidence of a domain pattern (see Fig. 1a).

The PFM and x-ray reciprocal space maps suggest a correlation between the symmetry of the ferroelectric domain pattern and plastic strain relaxation. In order to obtain additional information on the strain relaxation process we have performed grazing-incidence in-plane x-ray diffraction (GIXD) experiments at BESSY (KMC-2). These investigations reveal that, while the NaNbO$_3$ crystal lattice remains coherent at the domain walls, alternating in-plane monoclinic distortions ($\pm\beta$) occur for the NaNbO$_3$ pseudocubic unit cells of adjacent domains with respect to the [1-10] DSO direction. These alternating monoclinic distortions show up as satellite peaks (P1, P2) in the GIXD intensity pattern (see Fig. 2a). Our data suggest an interesting two-step strain relaxation process: With increasing film thickness the monoclinic distortion angle β increases monotonously and eventually approaches the value $\beta = 0.67°$ of bulk NaNbO$_3$ at film thicknesses larger than 27 nm (Fig. 2b). From the x-ray reciprocal space maps it is known that at about 27 nm thickness the NaNbO$_3$ thin film starts to plastically relax by the incorporation of misfit dislocations at the film/substrate interface. A similar two-step relaxation process was found for NaNbO$_3$ thin films grown on TbScO$_3$ substrates [3].

The GIXD diffraction patterns allow the evaluation of the transversal domain size D along the [1-10] DSO in-plane direction as a function of the film thickness (Fig. 2c). For large film thicknesses the relationship between domain
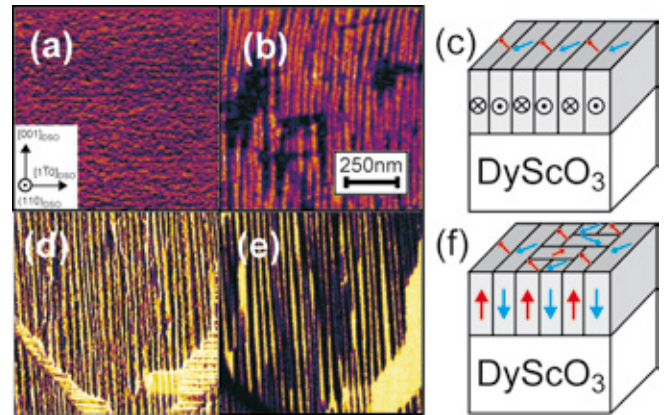

Fig. 1: Lateral (LPFM) and vertical (VPFM) piezoresponse force micrographs of NaNbO$_3$ films with thicknesses of (a) 1.5 nm (LPFM), (b) 6.0 nm (LPFM), and (d,e) 27.3 nm (LPFM, VPFM) with schemes of the ferroelectric domain structure (c,f).
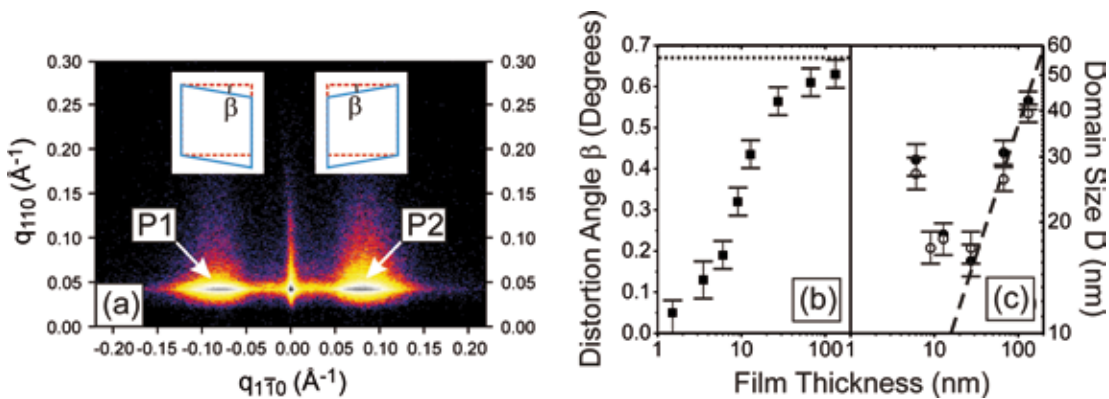

Fig. 2: (a) GIXD intensity distribution of a 27 nm NaNbO$_3$ film in the vicinity of the 008 DyScO$_3$ reciprocal lattice point. P1 and P2 mark two satellite peaks arising from adjacent NaNbO$_3$ domains. The insets illustrate the in-plane unit cells of NaNbO$_3$ domains (blue solid line) and DyScO$_3$ (red dashed line). (b) Monoclinic distortion angle β and (c) lateral domain size D deduced by PFM (open circles) and GIXD (full circles) as a function of film thickness. The horizontal dotted line represents the bulk NaNbO$_3$ monoclinic distortion angle β = 0.67°.

size and film thickness can be approximated by the well known square root dependence [7], illustrated by the dashed line in Fig. 2c. However, our data show a minimum domain size at about 20 nm film thickness which can be explained by elastic interactions among the domains and the substrate [7,8].

We would like to thank D. Többens and I. Zizak for assistance in the x-ray experiment at BESSY and S. Markschies for technical support during MOCVD growth. We are also grateful to R. Uecker and his group for providing us with high quality $DyScO_3$ substrates.

Defect identification in AlN bulk crystals: The tri-carbon defect and its relation to the detrimental ultraviolet absorption

AlN is the ideal substrate for the epitaxial growth of Al-rich $Al_xGa_{1-x}N$ films that enable deep ultraviolet (UV) emitters. Appropriate AlN bulk crystals can be grown by physical vapor transport (PVT). Besides high structural perfection, such substrate crystals should possess high UV transparency and, ideally, electrical conductivity. However, at the high growth temperatures (> 2000°C) it is very difficult to avoid the incorporation of impurities. In particular carbon, oxygen and silicon are known as major impurities in PVT grown AlN. If substitutionally incorporated, carbon and oxygen are believed to introduce deep levels and consequently lead to additional optical absorption or electrical compensation [9]. In particular, Collazo et al. suggested that isolated carbon on nitrogen site in its negatively charged state $(C_N)-$ causes the strong UV absorption band at 4.7 eV [10].
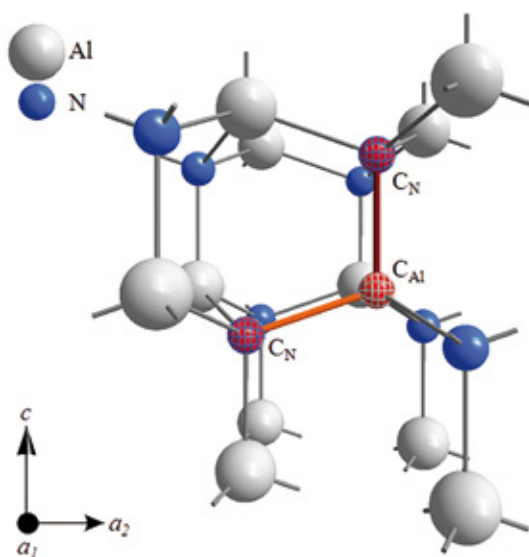
Recently, we could identify a tri-carbon defect in AlN by using local vibrational mode (LVM) spectroscopy combined with intentional ^{13}C isotope doping [11]. We proved that the defect consists of exactly three carbon atoms arranged on nearest-neighbor substitutional sites, replacing two nitrogen atoms and one aluminum atom, whereby one carbon-carbon bond is directed non-parallel and the other parallel to the crystal's c axis ($C_N – C_{Al}$ -c- C_N, see Fig. 3). This proof is essentially based on the following facts.

(i) The LVM at 1769 cm^{-1} observed in unintentionally doped crystals containing carbon of the natural isotopic composition (98.9% ^{12}C and 1.1% ^{13}C) splits into eight lines in a crystal enriched with the isotope ^{13}C as shown in Fig. 4. The relative frequency shifts and the intensity ratios of the eight lines can be well explained based on the model of a harmonic oscillator and on the binomial distribution of the isotopes ^{12}C and ^{13}C over three neighboring, but non-equivalent, lattice sites taking account of the local isotopic ratios.

(ii) The description of the defect in analogy to a bent tri-carbon molecule that is incorporated into the AlN crystal (thereby quenching rotational motion) gives a refined picture of the observed LVMs and their interpretation. The LVM at 1769 cm^{-1} originates from the antisymmetric stretching mode of the pure ^{12}C triatomic defect molecule. The other seven LVMs are the corresponding counterparts due to the isotope effect. From their frequency shifts a bonding angle of about 130° can be estimated that considerably exceeds the bonding angles in undistorted wurtzite AlN (around 109°). For the most probable defect configurations $C_N – C_{Al} – C_N$ (both bond directions are non-parallel to c) and $C_N – C_{Al}$ -c- C_N, the direction of the electric dipole moment of the antisymmetric stretching mode is parallel (or nearly parallel) to the connecting line between the two carbon atoms on nitrogen sites. Taking into account the three crystallographically equivalent realizations of each defect configuration within the AlN lattice the observed polarization dependence of the LVM absorption coefficient can only be explained by the configuration $C_N – C_{Al}$ -c- C_N. This has been surprising since one might have expected a similar formation probability for both configurations, which is obviously not the case.

Furthermore we suggest that the defect can exist in three different charge states, hence possesses two transition levels within the band gap, and that the singly negative charge state $(C_N – C_{Al}$ -c- $C_N)-$ essentially contributes to the UV absorption band at 4.7 eV (see Fig. 5(a)). These assumptions are based on the observation of a strong correlation between the signal intensity of the LVM at 1769 cm^{-1} and that of the absorption band at 4.7 eV. In particular, simultaneous quenching of both absorption signals takes place when the oxygen concentration considerably exceeds the carbon concentration (cf. Fig. 5). Additionally,

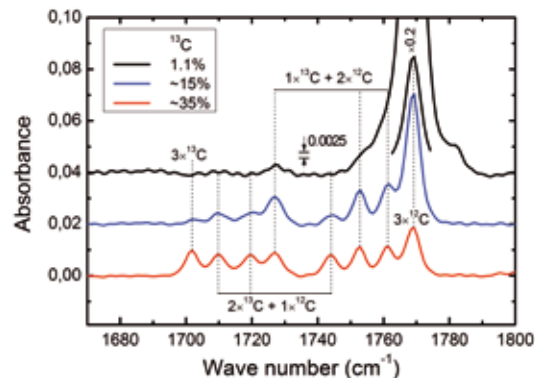Fig. 3: Model of the tri-carbon defect $C_N – C_{Al}$ -c- C_N in AlN.

Fig. 4: Absorbance spectra of an AlN crystal doped with ^{13}C measured at two regions of different ^{13}C enrichment (red line ~35% and blue line ~15%) in comparison to the spectrum of a sample containing the natural carbon composition (black line: 1.1% ^{13}C, 98.9% ^{12}C). The spectra are base line corrected and shifted by 0.02 and 0.04, respectively. The dotted lines group the LVMs according to the occupation of three lattice sites by two carbon isotopes.
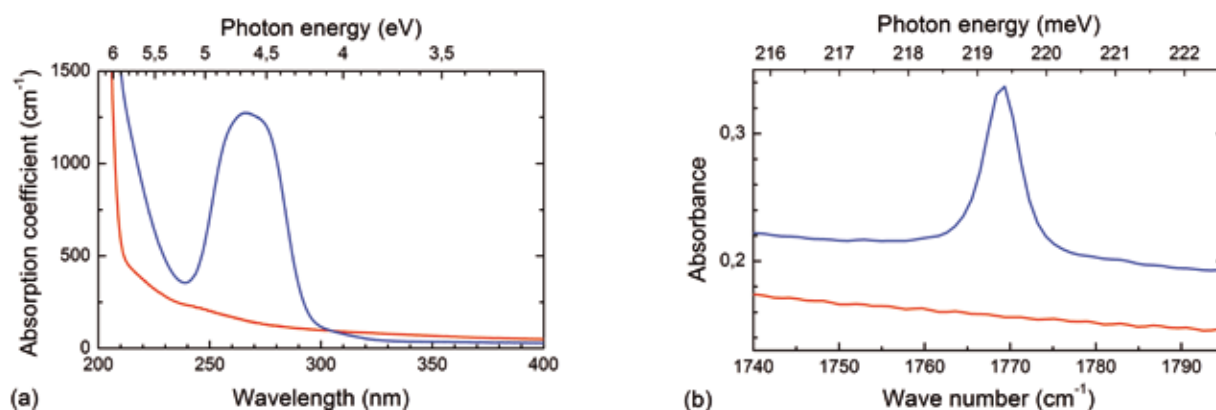
Fig. 5: Ultraviolet (a) and local vibrational mode (b) absorption spectra of a c-plane wafer cut from a PVT grown AlN crystal. For the UV absorption measurement the wafer was thinned down from 580 µm to 60 µm. Two different crystal regions are shown: One contains 5×10^{18} cm^{-3} carbon, 6×10^{18} cm^{-3} oxygen, and 3×10^{17} cm^{-3} silicon (blue curves), the other contains 4×10^{18} cm^{-3} carbon, 2×10^{19} cm^{-3} oxygen, and 8×10^{17} cm^{-3} silicon (red curves). Both signals, the LVM at 1769 cm^{-1} and the UV absorption band at 4.7 eV, disappear in the region where the oxygen concentration considerably exceeds the carbon concentration.

x-ray irradiation reduces the intensity of both signals, and storage of the sample at room temperature or annealing at slightly elevated temperatures (100 – 200°C) recover the original intensity. Our conclusion is that the appearance and disappearance of both signals depend on the position of the Fermi level and hence on the combined doping effect of all impurities and defects present in the crystal. The above mentioned signal quenching by high oxygen concentrations is accordingly due to raising the Fermi level nearer to the conduction band edge and stabilizing the tri-carbon defect in the doubly negative charge state that is inactive in UV and LVM absorption. This behavior offers the possibility to grow UV transparent AlN crystals by intentional oxygen (or appropriate donor impurity) doping if a sufficient suppression of the carbon incorporation will not be attained.

References

[1] K.J. Choi, M. Biegalski, Y.L. Li, A. Sharan, J. Schubert, R. Uecker, P. Reiche, Y. B. Chen, X. Q. Pan, V. Gopalan, L.-Q. Chen, D. G. Schlom, and C. B. Eom, Science 306, 1005 (2004); D.G. Schlom L.-Q. Chen, C.-B. Eom, K.M. Rabe, S.K. Streiffer, and J.-M. Triscone, Annu. Rev. Mater. Res. **37,** 589 (2007).

[2] H.M. Christen, J.H. Nam, H.S. Kim, A.J. Hatt, and N.A. Spaldin, Phys. Rev. B **83,** 144107 (2011).

[3] A. Duk, M. Schmidbauer, and J. Schwarzkopf, Appl. Phys. Lett. **102,** 091903 (2013).

[4] M. Schmidbauer, J. Sellmann, D. Braun, A. Kwasniewski, A. Duk, and J. Schwarzkopf, Physica Status Solidi RRL 1-5 (2014) / DOI 10.1002/pssr.201409012.

[5] J. Sellmann, J. Schwarzkopf, A. Kwasniewski, M. Schmidbauer, D. Braun, and A. Duk, submitted to Thin Solid Films (2014).

[6] J. Schwarzkopf, M. Schmidbauer, T. Remmele, A. Duk, A. Kwasniewski, S. Bin Anooz, A. Devi, and R. Fornari, J. Appl. Crystallogr. **45,** 1015 (2012).

[7] N.A. Pertsev and A.G. Zembilgotov, J. Appl. Phys. **78,** 6170 (1995).

[8] W. Pompe, X. Gong, Z. Suo, and J.S. Speck, J. Appl. Phys. **74,** 6012 (1993).

[9] D. W. Palmer, *Electronic Energy Levels in Group-III Nitrides.* In: P. Bhattacharya, R. Fornari, and H. Kamimura (eds.), *Comprehensive Semiconductor Science and Technology,* Vol. 4, pp. 390-447 (Elsevier, Amsterdam, 2011).

[10] R. Collazo, J. Xie, B. E. Gaddy, Z. Bryan, R. Kirste, M. Hoffmann, R. Dalmau, B. Moody, Y. Kumagai, T. Nagashima, Y. Kubota, T. Kinoshita, A. Koukitu, D. L. Irving, and Z. Sitar, Appl. Phys. Lett. **100,** 191914 (2012).

[11] K. Irmscher, C. Hartmann, C. Guguschev, M. Pietsch, J. Wollweber, and M. Bickermann, J. Appl. Phys. **114,** 123505 (2013).
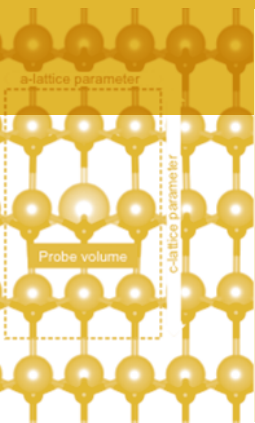
Electron Microscopy

Head: Dr. M. Albrecht
Team: K. Banse, M. Khazaee, Dr. M. Korytov, T. Markurt, S. Mohn, T. Remmele, R.Schewski, Dr. T. Schulz

Übersicht

Die Arbeitsgruppe Elektronenmikroskopie charakterisiert kristalline Materialen mit elektronenmikroskopischen Methoden sowohl im Rahmen des wissenschaftlichen Service als auch im Bereich der Grundlagenforschung. Thematischer Schwerpunkt ist der Zusammenhang zwischen physikalischen Eigenschaften und Struktur von Hableitern. Die Methoden reichen von der Rasterelektronenmikroskopie (energie- und wellenlängendispersive Röntgenspektroskopie, Elektronenrückstreubeugung (EBSD), Kathodolumineszenz) über die Ionenstrahlbearbeitung bis zur Transmissionselektronenmikroskopie (aberrationskorrigierte Transmissionselektronen-mikroskopie und Rastertransmissionselektronenmikroskopie mit atomarer Auflösung). Die Arbeitsgruppe arbeitet eng mit Gruppen des Kristallwachstums, der *ab-initio* Modellierung und der Simulation zusammen und trägt wesentlich zur Qualifizierung des wissenschaftlichen Nachwuchses bei. Innerhalb der Gruppe arbeiten drei Doktoranden und eine Doktorandin. Doktoranden und Doktorandinnen, Master- und Bachelorstudierende anderer Arbeitsgruppen des Institutes werden in elektronenmikroskopische Verfahren eingewiesen oder gemeinsam betreut. Neben der Standardcharakterisierung von Oberflächen und der chemischen Analyse von Phasen und Einschlüssen werden insbesondere grundlegende Arbeiten zu Wachstums- und Relaxationsprozessen sowie zu Kristalldefekten durchgeführt. Um bildgebende Verfahren zu verbessern und sie auf die spezifischen Probleme und die laufenden Arbeiten am Institut anzupassen werden eigenständige methodische Arbeiten durchgeführt. Die Gruppe arbeitet in nationalen und internationalen Forschungsprojekten und Forschungsverbünden.

Da einige der Ergebnisse der Elektronenmikroskopie in den Berichten der Arbeitsgruppen der Kristallzüchtung und als „Highlight" vertreten sind, sollen im Folgenden zwei ausgewählte Themen unserer derzeitigen Arbeit dargestellt werden, die mit externen Kooperationspartnern im Rahmen des EU-Projektes SINOPLE, des BMBF-Projektes GaNonSi und des im Rahmen des "World Materials Network" geförderten Projektes "Science of heteropolar interfaces" durchgeführt wurden: (i) eine avancierte Technik zur kompositionellen Analyse von Halbleiterlegierungen mit atomarer Auflösung (ii) ein quantitatives Modell für die kritische Dicke von Gruppe III Nitrid basierten Heterostrukturen und (iii) eine Analyse der Nukleation von AlN auf Saphir. Die Arbeiten unter (i) und (ii) wurden in Zusammenarbeit mit dem Max-Planck-Institut für Eisenforschung (MPIE) in Düsseldorf, OSRAM Optical Semiconductors in Regensburg und der polnischen Forma TopGaN durchgeführt, während (iii) aus einer Zusammenarbeit mit der North-Corolina State University und der Technischen Universität Berlin hervorgegangen ist.

Overview

The electron microscopy group performs scientific service and basic research in the field of characterization of crystalline material by means of electron microscopy. Main focus is the relation between physical properties and structure. The methods cover the whole field ranging from scanning electron microscopy, i.e. energy and wavelength dispersive spectroscopy, electron backscatter diffraction, cathodoluminescence through transmission electron microscopy, i.e. aberration corrected transmission electron microscopy and scanning transmission electron microscopy with atomic resolution. The team works in close collaboration with groups performing crystal growth and ab-initio modelling and simulation. The group contributes to the education of young scientists. Within the group 3 PhD students are working. PhD students, master and bachelor of other groups in the institute are introduced into electron microscopy techniques and are commonly supervised. Standard characterization of surfaces and composition, phase analysis and analysis of inclusions are performed as well as basic analyses of growth and relaxation mechanisms and of defects. Besides this, methodological work is done to improve electron optical imaging techniques and to adopt them to the specific problems at the institute. The group works in collaborative national and international research projects.

Since some of the results are described in the individual reports of the groups working in crystal growth the following chapter will highlight two selected topics of our current work, which have been performed with exter-

nal partners in the framework of the EU-project SINOPLE and the BMBF-project GaNonSi and the "world materials network" project Science of heteropolar interfaces: (i) an advanced technique for compositional analysis for semiconductor alloys at the unit cell scale the (ii) a quantitative model for the critical thickness for III-nitride heterostructures and (iii) nucleation of AlN on sapphire. The works (i) and (ii) were performed in close collaboration with the Max-Planck-Institut für Eisenforschung (MPIE) in Düsseldorf, OSRAM Optical Semicondcutors in Regensburg and the polish company TopGaN, while (iii) is a collaboration with North-Corolina State University and Technical University of Berlin.

Results

A novel approach for true compositional analysis of InGaN quantum wells by aberration corrected transmission electron microscopy

Compositional analysis of semiconductor heterostructures down to the atomic scale is a prerequisite for proper understanding of their physical properties. Transmission electron based methods are most powerful since they provide atomic resolution and high sensitivity. Essentially two approaches have been used in the past to quantify compositions at the atomic scale. The first is based on true chemical information, i.e. measuring electrons scattered into high angles with a high annular angular darkfield detector in a scanning transmission electron microscope. The second most common used is based on the analysis of lattice parameters in high resolution transmission electron images. For these analyses, it is assumed that the local in-plane lattice parameter (perpendicular to the projection and the growth direction) of a thin film perfectly adapts to the in-plane lattice parameter of the substrate. From the measured out-of-plane lattice parameter, one can then calculate the composition of the layer assuming a bi-, uniaxial or mixed strain, as deduced from, e.g., finite-element calculations. While this is a valid approach for considering mesoscopic probe volumes (with lateral extensions of several unit cells and/or comparatively thick samples in the range of several tenth of nm), it may fail once the probe volume is decreased, approaching the dimension of a single unit cell.

This is related to the fact that inherent local composition fluctuations necessarily induce strain fields in their proximity, whose extensions may be larger than the desired probe volume. This would hamper a correct quantification of the local alloy composition and raises the more general question of how to distinguish between the effects of strain and composition in lattice parameter maps. In a recent work, we have shown that retrieving chemical compositions of $In_xGa_{1-x}N$ at the near unit cell scale (i.e., considering a probe volume of $V = a \cdot c \cdot t$ with c as the out-of-plane lattice parameter (c-lattice parameter), a as the in-plane lattice parameter (a-lattice parameter), and t as the sample thickness) is possible if both, in- and out-of-plane lattice parameters are measured. Since the in-plane lattice parameter fluctuations can be very small (i.e., in the pm range), this approach becomes experimentally feasible only with recent progress in measuring precision [2]. Although it is of general applicability, we have studied this approach in detail for $In_xGa_{1-x}N$ quantum wells, which is today the fundament of blue/ white solid-state lighting. Many important and still debated questions dealing with e.g. the device efficiency or charge carrier localization can now be re-evaluated. The entire experimental procedure is as follows: First, we use optimized imaging conditions in an aberration corrected TEM so that the image pattern exactly corresponds to the positions of the metal (In, Ga) atoms. We then typically acquire 30 images using the same conditions and measure all c- and a-lattice parameters throughout the image series. The acquisition of 30 images instead of one considerably improves the measuring precision down to a standard deviation of only 1.5 pm per probe volume. We then combine the c- and a- lattice parameters

Fig. 1: Sketch of the probe volume and lattice parameters.

by a simple elastic continuum model which then allows calculating the local In content. In Fig. 1 the In content of the quantum well of an LED device is displayed using the above described approach. One can clearly make out the atomically flat interfaces at the lower/upper boundary, as well as the fact that the QW consists of two individual layers, one with a mean composition of about 6.5 % and the other with about 17 %. The local variation of the In composition are in good agreement with a randomly alloyed compound.
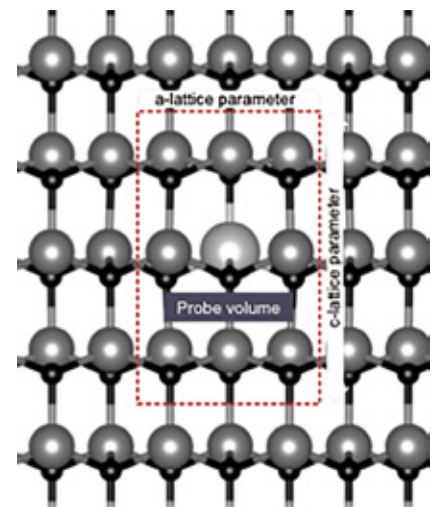
Critical thickness in AlGaN/GaN revisited

Mechanisms of strain relaxation by formation of misfit dislocations in III-Nitrides on c-plane substrates are still an open issue. In contrast to conventional semiconductors, III-Nitrides have a complex system of glide systems. Essentially three types of Burgers vectors (1/3<11-20>, 1/3,<11 23> and <0001>) and a variety of glide planes are present. However, easy glide systems ({0001}, {1-100} and {11-20}) exhibit zero shear stress in two-dimensionally grown, misfitting epitaxial layers on c-plane substrates, while glides systems that exhibit shear strain are sup-
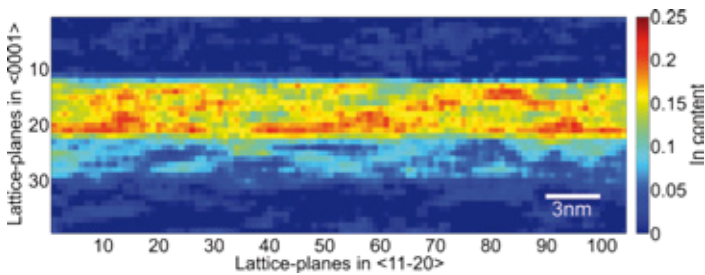
Fig. 2: Strain revised compositional analysis on the near atomic scale using the c- and a-lattice parameter map.

pressed by large Burgers vectors and high frictional forces. While this allows for extremely high critical thicknesses for dislocation formation in case of compressive strain (e.g. InGaN on GaN) [4] it leads to unwanted cracking in case of tensile strain (AlGaN on GaN). We have studied the strain relaxation mechanism at the interfaces of (0001)-oriented $Al_xGa_{1-x}N/GaN$ heterostructures. Based on our results we have developed a model which allows us to predict the critical thickness for the onset of plastic relaxation. $Al_xGa_{1-x}N/GaN$ heterostructures play nowadays an important role in many III-nitride based devices. An example is strain-engineering with thin $Al_xGa_{1-x}N$ interlayers in GaN (0001) films grown on silicon (111) substrates. Such $Al_xGa_{1-x}N$ interlayers are used to produce compressive strain in the epitaxial film and thus prevent cracking caused by tensile thermal strain arising during cool-down after the growth [3]. The microscopic relaxation mechanism at the interfaces of the $Al_xGa_{1-x}N$ interlayer itself as well as the dependency on growth parameter like the deposition temperature is, however, far from well understood. In a more general sense, theoretical considerations about the plastic relaxation of misfit strain in (0001)-oriented nitride films cannot explain experimental observations.

Our plan view and cross-sectional transmission electron microscopy (TEM) investigation has shown that plastic relaxation of the $Al_xGa_{1-x}N/GaN$ misfit strain is unexpectedly caused mainly by formation of a network of new a-type misfit dislocations at the heterointerface. TEM and atomic force microscopy revealed that beyond a certain layer thickness the surface morphology deviates from a perfect two-dimensional flat film. Depending on the growth conditions either cracking or a transition towards island growth occurs. In our experiment high/low deposition temperatures led to two-dimensional growth followed by cracking/island growth of the $Al_xGa_{1-x}N$ layer, respectively. In literature the same effect was reported by changing the III/V ratio [5]. On the one hand both surface modifications allow the system to relieve a part of the misfit strain by elastic relaxation during the initial stage of growth when mechanisms for plastic relaxation are still inoperable. On the other hand cracking as well as island growth of a strained layer will produce a shear stress on the basal plane and enable the $1/3<1120>|\{0001\}$ slip-system. It is important to note that the presence of island edges or cracks will not instantaneously lead to formation of new a-type misfit dislocations. In our case we have grown 8 nm (with island growth) and 11 nm (with cracks) thick $Al_{0.75}Ga_{0.25}N$ layer on a GaN buffer without observing misfit dislocations at the interface. Only if the thickness of the $Al_{0.75}Ga_{0.25}N$ layer was increased to 15 nm (with island growth) misfit dislocations were present. In literature 3.5-4 nm AlN (with island growth) on GaN without plastic relaxation was reported [6]. With the help of the finite element method we have calculated the spatial distribution of the shear stress for relevant geometries (see Fig. 3 (a) for the case of cracking and (b) for hexagonal islands). We have used these results to calculate the critical thickness for nucleation of a-type dislocation half-loops at cracks and island edges in order to estimate the onset of plastic relaxation in $Al_xGa_{1-x}N/GaN$ heterostructures (see Fig. 3(c)). Our predictions are in much better agreement with experimental results than critical thickness values based on standard equilibrium theory. Interestingly, the critical thickness for the onset of plastic relaxation predicted by our model is higher than the critical thickness for fracture based on the Griffith approach (see Fig. 3(c)) [7]. Thus our model is also in agreement with the above mentioned experimental finding that nucleation of new a-type dislocations does not happen instantaneously after cracking or island growth has occurred but some further increase of the layer thickness is required.
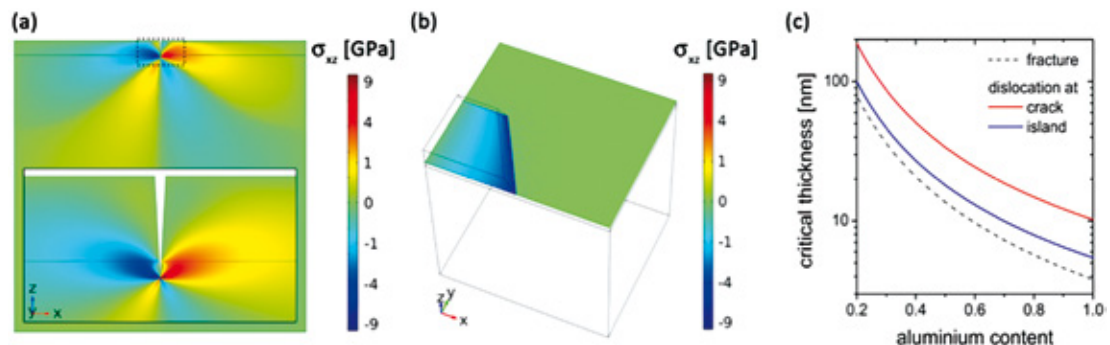

Fig. 3: Distribution of the shear stress on the (0001) plane for AlN/GaN heterostructures in the case of (a) cracking and (b) island growth. (c) Critical thickness for the nucleation of a-type misfit dislocations at cracks (solid red line) and island edges (solid blue line) and critical thickness for fracture (dashed line) of $Al_xGa_{1-x}N/GaN$ heterostructures.

Polarity control in III-Nitrides

Control of the polarity of III-Nitrides by an appropriate buffer is the key to obtain devices with high structural perfection and high efficiency on sapphire substrates. With the development of lateral polarity heterostructures that allow realizing novel device concepts for optoelectronic applications or nonlinear optical devices, polarity control gained renewed attention. Since the pioneering work by Amano et al. [8] deposition of a low temperature AlN buffer layer on a nitridated sapphire substrate is *the* well known concept to get metal polar epitaxial layers. Despite of a number of theoretical and experimental studies [9], little is known on the atomic structure of the interface between the III-nitride layer and the sapphire substrate and the atomic processes that govern the polarity.
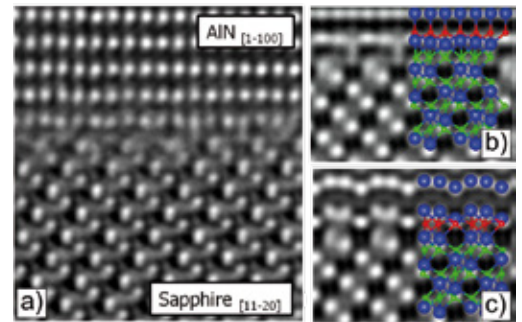

Fig. 4: (a) HR-TEM image of the interface between Sapphire and AlN. (b) The pattern of the interface is corresponding to the N-polar AlN interface of the simulated patterns. (c) Simulated contrast pattern of N-polar AlN on sapphire with a ball and stick model of the lattice. Blue: Aluminium, Red: Nitrogen, Green: Oxygen Simulated pattern of Al-polar AlN on Sapphire.

This is mainly due to the fact that transmission electron microscopes were not capable to reveal structure at an atomic level. However, aberration corrected transmission electron microscopes now open new possibilities to resolve even single oxygen atoms with high spatial resolution and sensitivity.

In the frame of the Materials World Network-project "Science of polar homo- and heterointerfaces" Leibniz Institute for Crystal Growth is collaborating with the North Carolina State University (NCSU) and the Technical University in Berlin (TUB). The NCSU is providing suitable MOCVD-grown samples for the investigation of the elementary processes that govern the key steps for the control of the polarity by aberration corrected transmission electron microscopy. The initial steps for the growth of device-quality smooth Ga-polar films are:

- Nitridation of sapphire surfaces and nucleation of AlN in an ammonia ambient at 950 °C
- Growth of a thin layer of AlN at low temperatures (LT) around 650 °C on top of the nitridated sapphire.
- Annealing of the buffer layer with Ammonia at 1050 °C.

The growth of the final GaN or AlN layers takes place at 1050 °C and keeps the polarity of the buffer layer. TEM samples were prepared in the two major projections, i.e. along <1-100> and <11-20> direction. With the achievable resolution we were able to resolve Al, O and N atomic positions for sufficiently thin samples.

During the nitridation in ammonia ambient, AlN is nucleated on the surface. It was shown by Vennegues et al. [10], that it is possible to grow several monolayers of a continuous AlN layer only by the nitridation of the substrate. For our samples we haven't found a closed monolayer but only small islands of AlN. GaN or AlN grown at high temperatures on top of nitridated sapphire surfaces leads to N-polar films. To get a better understanding of the nitridation process, the nucleation of AlN can be seen as growth of AlN under N-rich conditions, where the Al-atoms are provided by the sapphire surface.
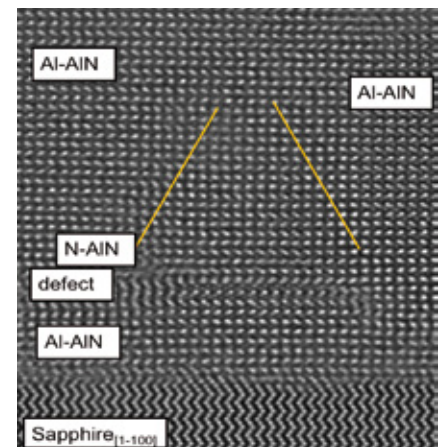

Fig. 5: HR-TEM picture of an AlN buffer layer grown at low temperatures on Sapphire. After 6 monolayers AlN buffer layer is Al-polar. After a defect the polarity is turned back to N-polar AlN. This area is lateral overgrown by Al-polar AlN, which is leaves a pyramidal shaped inversion domain boundary (marked by the yellow lines).

The energetics and the atomic structure of AlN films grown on sapphire have been theoretically investigated by DFT-calculations in the work of DiFelice et al. [11]. They were able to give predictions for the interface structure of Al- and N-polar films grown on sapphire. Contrast simulations based on their models are enabling the interpretation of the interface structure found by HR-TEM measurement. The comparison of the simulated and the measured patterns (see Figure 4) for the interface shows a good agreement with the N-polar model. With the growth of the low temperature AlN buffer layer and the following annealing step the polarity can be switched from N-polar to Al-polarity.

Figure 5 shows the <11-20>-projection of the interface of an LT-AlN buffer layer grown on sapphire. In this projection the polarity of the AlN-layer can be easily seen in the picture. Since the AlN-layer is grown on nitridated sapphire, the growth starts on N-polar material. After the first 6 monolayers the polarity of the layers already can be identified as Al-polar AlN. With increasing thickness of the AlN-buffer layer it can be seen, that the polarity of the film was switched back to N-polarity after some kind of defect. This area is then overgrown by Al-polar AlN, leaving inversion domain boundaries behind that are comparable to the pyramidal inversion domain boundaries in GaN:Mg.

References:

[1] T. Schulz, A. Duff, T. Remmele , M. Korytov, T. Markurt , M. Albrecht, L. Lymperakis , J. Neugebauer, C. Cheze, C. Skierbiszewski, J.Appl. Phys. **115,** 033113 (2014).

[2] T. Schulz, T. Remmele, T. Markurt, M. Korytov and M. Albrecht, J. Appl. Phys. **112,** 033106 (2012).

[3]   A. Dadgar, J. Bläsing, A. Diez, A. Alam, M. Heuken, and A. Krost, J. J. Appl. Phys. 39, L1183 (2000)

[4]   D. Holec, Y. Zhang, D. V. Sridhara Rao, M. J. Kappers, C. McAleese, and C. J. Humphreys, J. Appl. Phys. 104, 123514 (2008)

[5]   M. Gherasimova, G. Cui, Z. Ren, J. Su, X.-L. Wang, J. Han, K. Higashimine, and N. Otsuka, J. Appl. Phys. 95, 2921 (2004); S. Keller, G. Parish, P. T. Fini, S. Heikman, C.-H. Chen, N. Zhang, S. P. DenBaars, U. K. Mishra, and Y.-F. Wu, J. Appl. Phys. 86, 5850 (1999)

[6]   P. Vennegues, Z. Bougrioua, J.-M. Bethoux, M. Azize, and O. Tottereau, J. Appl. Phys. 97, 024912 (2005)

[7]   A.A. Griffith, Phil. Trans. Roy. Soc. A, 221, 163 (1921)

[8]   H. Amano et al. Jpn. J. Appl. Phys. 37, L1540 (1998).

[9]   M. Sumiya and S. Fuke, MRS INTERNET JOURNAL OF NITRIDE SEMICONDUCTOR RESEARCH, Vol. 9, No. 1. (2004).

[10] P. Vennegues et al., Appl. Phys. Lett. 75, 4115 (1999)

[11] R. Di Felice and J. Northrup, Appl. Phys. Lett. 73, 936 (1998)

Chemical & Thermodynamic Analysis

Head: Dr. D. Klimm
Team: Dr. R. Bertram, T. Neugut

Überblick

Die Arbeitsgruppe widmet ihre Tätigkeit überwiegend der wissenschaftlichen Unterstützung der Züchtergruppen des Instituts. In erster Linie erweist sich die Bestimmung von Phasendiagrammen durch Messungen und thermodynamische Rechnungen als wichtiges Instrument zur Züchtung von Kristallen definierter Zusammensetzung. Thermische und chemische Analysen erlauben die Kontrolle von Oxidationszuständen, die oft wesentlich die Anwendbarkeit von Kristallen bestimmen: zum Beispiel sind Ce^{3+}-dotierte Oxide wegen ihrer breitbandigen Emission im grünen Spektralbereich interessant, während das unter üblichen Züchtungsbedingungen vorherrschende Ce^{4+} keine Emission in diesem wichtigen Spektralbereich zeigt.

Zweitens kommt der Analyse von Ausgangsmaterialien zur Kristallzüchtung insbesondere für die Gruppe Oxide/Fluoride wachsende Bedeutung bei, um Qualität und Reproduzierbarkeit zu gewährleisten. Vor allem für optische Materialien und Oxid-Halbleiter bestimmen oft schon Verunreinigungsspuren die Verwendbarkeit. Es muss betont werden, dass der Kauf „hochreiner" Chemikalien (4N bis 5N entsprechend 99.99%-99.999%) oft keine hinreichende Voraussetzung für Erfolg ist, weil Reinheitsgehalte in der Regel „on metals basis" angegeben werden und der Anionen-Gehalt nicht berücksichtigt wird. Zwar ist diese Erkenntnis im Wesentlichen bekannt; wird aber doch gelegentlich übersehen. Schon vor einen Jahrzehnt publizierten wir Analysenergebnisse einer $CaCO_3$-Charge mit 99.999% nominaler Reinheit, die nicht weniger als 0,5% $Ca(OH)_2$ enthielt – was den relevanten Ca-Gehalt deutlich verschiebt und die Züchtung mehrkomponentiger Kristalle erschwert [1]. Solche Probleme nahmen in den letzten Jahren zu und erzwingen stärkere Anstrengungen in der Materialanalyse.

Im Jahre 2013 verteidigte Jan Philippen erfolgreich seine Doktorarbeit "Fiber crystal growth of cerium doped calcium scandate, strontium yttrium oxide, and tristrontium silicate", in welcher er einige Oxide mit sehr hohem Schmelzpunkt jenseits 2000°C untersuchte. Seine Arbeit wurde überwiegend im Rahmen der Oxid/Fluorid-Gruppe durchgeführt und im Bericht dieser Gruppe etwas eingehender vorgestellt. Es soll jedoch erwähnt werden, dass chemische Analyse (durch ICP-OES) und thermische Analyse (meist durch Philippen selbst mit der Hochtemperatur STA 429 durchgeführt, die bis 2400°C arbeiten kann) wesentlich zu den interessanten Ergebnissen der Doktorarbeit beitrugen. Insbesondere konnte Philippen zeigen dass das bei 2110°C schmelzende Ce^{3+}:$CaSc_2O_4$ aus der Schmelze ohne das sonst übliche Kodotieren mit Na^+ möglich ist, welches bei keramischen Phosphoren für weiße LEDs der Ladungskompensation dient (Abb. 1 rechts). Je nach Atmosphäre verdampft bei der Züchtung Ca oder CaO, was berücksichtigt werden muss. Bei der liquidus-Temperatur des $CaSc_2O_4$ und unter den zur Ce^{3+}-Stabilisierung nötigen reduzierenden Bedingungen beträgt die Fugazität von Ca etwa 1 mbar, was zu merklicher Verdampfung führt. Das in Abb. 1 links gezeigte pseudobinäre Phasendiagramm Sc_2O_3-CaO wurde abgeleitet. Toni Markurt, Doktorand in der Elektronenmikroskopie-Gruppe, zeigte dass Ce^{3+} erwartungsgemäß Ca^{2+} substituiert, was günstig für die Emission künftiger optischer Emitter sein dürfte. Christo Guguschev (Gruppe Oxide/Fluoride) gelang inzwischen die Züchtung eines Ce^{3+}:$CaSc_2O_4$-Volumenkristalls.

Obwohl des EU-Projekt ENSEMBLE bereits im April 2012 abgeschlossen wurde, währt die wissenschaftliche Zusammenarbeit mit den Partnern von ITME Warszawa (Polen) und CSIC Universidad de Zaragoza (Spanien) an. ENSEMBLE arbeitete zu selbstorganisierten Mikrostrukturen die sich in einigen eutektischen Systemen ausbilden. Die Partner aus Zaragoza fokussierten ihre Arbeiten auf Halogenide mit vielversprechenden Transmissionseigenschaften im Terahertz-Bereich. Bereits zwei Mal (2012 und 2013) arbeitete die spanische Doktorandin María F. Acosta einige Monate am IKZ. Bisher entstanden zwei gemeinsame Publikationen [4,5]. Im englischen Teil dieses Beitrages werden einige neue und teilweise bisher unveröffentlichte Ergebnisse zu diesem Thema vorgestellt.

Overview

A major share of the group's work is devoted to the scientific support of the crystal grower's groups of our institute. First, the determination of phase diagrams by measurements and thermodynamic calculations performed in our group has proved a useful tool for the growth of crystals with defined composition. The thermodynamic and chemical analysis provides control of oxidation states, which can significantly influence the applicability of the material: for instance, while Ce^{3+} doped oxides may be used in solid state optical emitters due to the broad green luminescence, wrong growth conditions may lead to oxidation to Ce^{4+} and the loss of optical emission in this favourable range.

Second, analysis of chemicals as starting material for crystal growth is increasingly gaining importance since it strongly influences the crystalline quality and reproducibility of the growth runs. Continuously, the analysis of starting materials especially for the Oxides/Fluorides group is a challenge. For some crystals such as optical materials and oxide semiconductors already trace impurities can have a major impact on applicability. It should be noted that the purchase of nominally "high purity" chemicals, which means typically 4N to 5N (99.99%-99.999%) is often insufficient, because all purity data are given "on metals basis", and deviations in the anion content are not taken into account. This problem is essentially known, but nevertheless forgotten occasionally. We published already a decade ago that a $CaCO_3$ batch with 99.999% nominal purity may contain as much as 0.5% $Ca(OH)_2$ – which shifts the relevant Ca assay considerably and impedes the growth of certain multicomponent crystals [1]. It turned out that similar problems became more frequent in recent years, which requires larger efforts in the analysis of materials prior to growth experiments..

In 2013 Jan Philippen finished successfully his PhD thesis "Fiber crystal growth of cerium doped calcium scandate, strontium yttrium oxide, and tristrontium silicate", in which he investigated several oxides with very high melting points beyond 2000°C. His work was performed mainly in the framework of the Oxides/Fluorides group and will not be reported here in detail; but it should be mentioned that chemical analysis (by ICP-OES) and thermal analysis (mainly with high-T STA 429 operating up to 2400°C, run by himself) contributed significantly to his interesting results [2,3]. Especially, Philippen could show that the growth of Ce^{3+}:$CaSc_2O_4$ single crystals is possible from the melt (fusion point 2110°C) without the typical codoping by Na^+ which is necessary so far in phosphors for white LEDs for charge compensation (Fig. 1 right). Evaporation of Ca or CaO, depending on atmosphere, has to be taken into account and can be kept on an acceptable low level under suitable growth atmosphere. It should be noted that close to the liquidus temperature of $CaSc_2O_4$ and under reducing conditions (which are beneficial for the stabilization of Ce^{3+} instead of the usually prevailing Ce^{4+}) the fugacity of Ca approaches 1 mbar, which results in considerable evaporation. The pseudo-binary phase diagram Sc_2O_3-CaO as shown in Fig. 1 left was revealed in this thesis. Toni Markurt, another PhD student from the Electron Microscopy group, could show that Ce^{3+} substitutes for Ca^{2+} in the crystal structure, which might be beneficial for future light emitting devices based on Ce^{3+}:$CaSc_2O_4$. Meanwhile, a bulk Ce^{3+}:$CaSc_2O_4$ crystal could be grown by Christo Guguschev in the Oxide/Fluoride group.

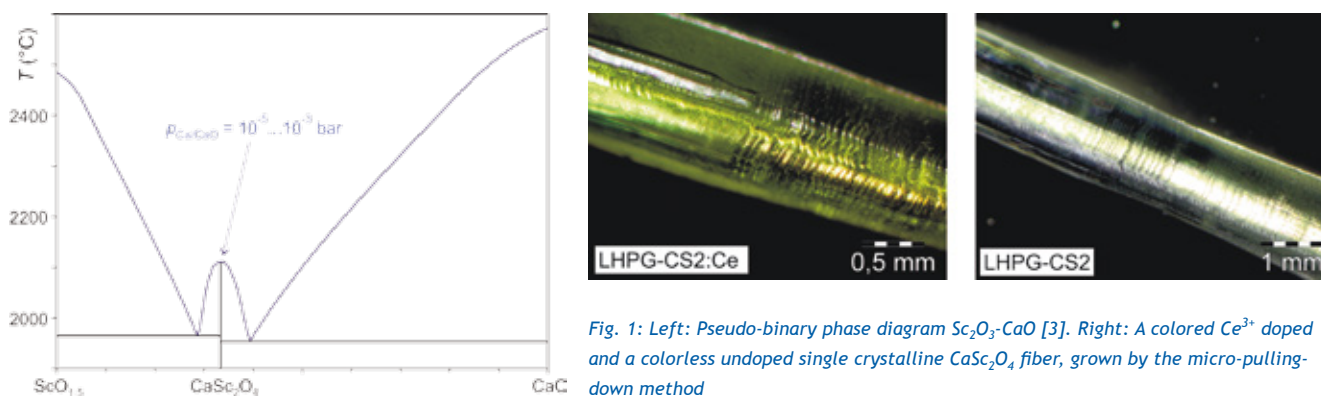*Fig. 1: Left: Pseudo-binary phase diagram Sc_2O_3-CaO [3]. Right: A colored Ce^{3+} doped and a colorless undoped single crystalline $CaSc_2O_4$ fiber, grown by the micro-pulling-down method*

Even if the European project ENSEMBLE is finished since April 2012, scientific collaboration with project partners from ITME Warszawa (Poland) and CSIC-Universidad de Zaragoza (Spain) is continued. ENSEMBLE was devoted to self-organized microstructures which are formed in several eutectic systems, and the partners in Zaragoza were focusing there on several halide systems with promising transmission properties for terahertz waves. Already twice (2012 and 2013) the Spanish PhD student María F. Acosta was working for several months at IKZ. So far, two common publications on eutectics between lithium fluoride and rare earth fluorides are published [4,5]. In this report, some new and partially not yet published results on this topic will be presented.

Results

For a given eutectic system, the concentration of each component is fixed as the eutectic point is invariant. Upon crystallization at the eutectic temperature T_{eut}, all components undergo transition from the liquid to their solid phases. The entropy change ΔS at T_{eut} determines via the Jackson parameter $a \approx \Delta S /R$ the morphology of each phase. Typically, the entropy change is small for metals or semiconductors. Then one has $a \leq 2$ which leads to rough interfaces. The entropy gain is considerably larger (often $\Delta S \approx 3R$) for ionic substances. The Jackson factor approach is valid also for the simultaneous crystallization of several phases in eutectic systems, where the entropy of the interphases S_I contributes to ΔS [6].

For some systems, including many halides, the eutectic solid consists of rods made up from the minor component which are embedded in a majority component matrix. The systems LiF–REF_3 are good examples which contain for RE = rare earth element from europium to luthetium an intermediate compound $LiREF_4$ with peritectic (Eu, Gd, Tb, Dy, Ho, Er, and also Y) or congruent (Tm, Yb, Lu) melting behavior. Between LiF and $LiREF_4$ eutectis are formed with a "volume filling factor" around $f \approx 40\%$ LiF in the $LiREF_4$ matrix.
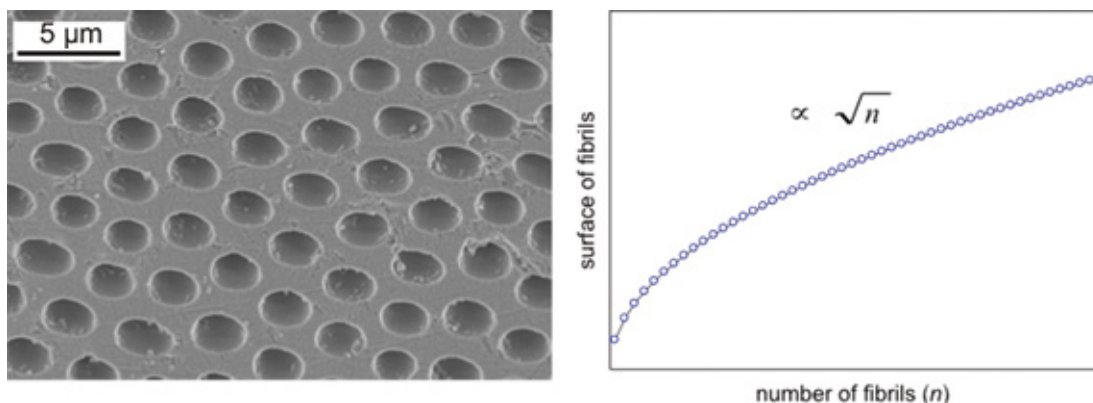

Fig. 2: Left: SEM micrograph of a soap-water etched surface of LiF-LiYF$_4$ eutectic. The persistent tetragonal LiYF$_4$ matrix grows almost single crystalline with mosaicity around 3° and growth direction close to the c-axis (reprinted from ref [5] with permission from Elsevier). Right: For a constant volume fraction of the components, the surface scales with the square-root of the number of fibrils [6].

The left panel in Fig. 1 shows an example where the LiF fibrils (which are soluble in water) are etched away, resulting in a sieve-like microstructure. For a given f, the surface of all fibrils, and hence the surface entropy, becomes larger with decreasing diameter. It can be shown [6] that f and with it S_I scales with the square-root of n, where n is the number of fibrils (Fig. 2 right). Consequently, large growth rates v with accordingly large rates of (solidification) entropy change enables the system to compensate for large surface entropy "production", with smaller particle sizes and spacing λ. The Jackson-Hunt theory gives a relationship $\lambda^2 v = $ const. [6], and indeed raising the crystallization rate for different LiF–$LiREF_4$ eutectics from 4 mm/h (Bridgman, performed in Zaragoza) to 300 mm/h (micro-pulling-down, performed at IKZ) allowed to reduce λ from >10 µm to <1 µm [4,5].

For further experiments CaF_2 was added to alkaline halide systems as third component. The melting point of CaF_2 is rather high (1418°C) compared with the alkaline halides, and Fig. 3 shows that the ternary eutectic composition contains this component with the smallest concentration (Na_2Cl_2:Li_2F_2:CaF_2 = 39.61:44.57:15.82, or NaCl:LiF:CaF_2 = 43.02:48.40:8.58). It will be shown in the following that Fig. 3 gives a too simplified description of the system, and problems arise mainly from the circumstance that two anions (Cl$^-$ and F$^-$) interact independently with the three cations.

It should be noted that the left rim system LiF-NaCl of the concentration triangle corresponds with published binary diagrams [7]. A substantially better representation is as "reciprocal salt pair", which is shown in Fig. 4. Here all ions of the pseudo-binary alkali halide system are treated independently, and four basic compounds can be formed where only LiF has fixed stoichiometry, and "rocksalt" as well as "NaF-[LiF]" are solid solutions. The left rim of Fig. 3 corresponds with the diagonal from bottom left to top right of Fig. 4.
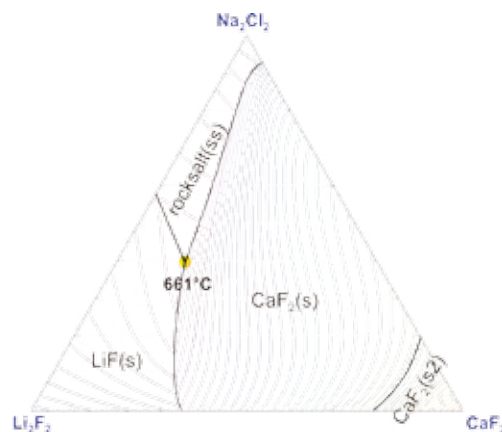

Fig. 3: Gibbs triangle NaCl-LiF-CaF$_2$, projection onto liquidus, 20 K isotherms, first components doubled to have identical anion numbers. "Rocksalt" crystallizes as solid solution, the other phases have fixed stoichiometry.
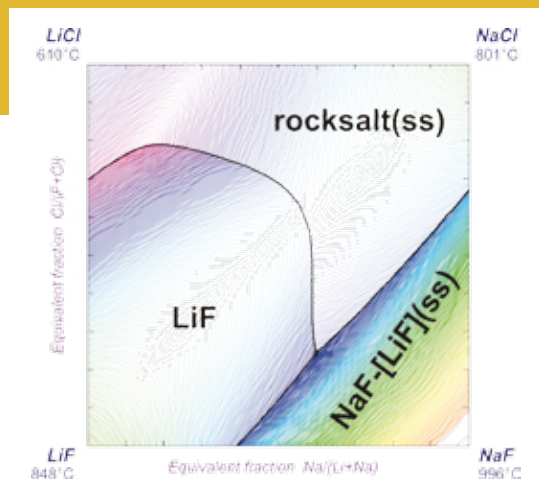
Fig. 4: Alternative representation for the left rim system of Fig. 3 as reciprocal salt pair (projection onto liquidus, 2 K isotherms). The connection LiF-NaCl crosses the eutectic valley starting from the left in a saddle point.
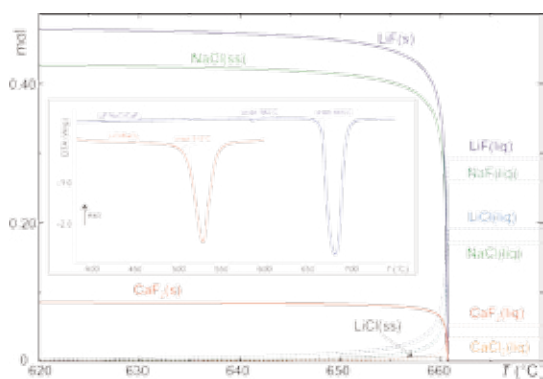

Fig. 5: Calculated phase equilibrium of a eutectic mixture LiF/NaCl/CaF₂ (see Fig. 3) around the eutectic temperature 661°C. Insert: Measured DTA heating curves for this eutectic mixture (blue, top) compared to a LiCl/BaCl₂ eutectic.
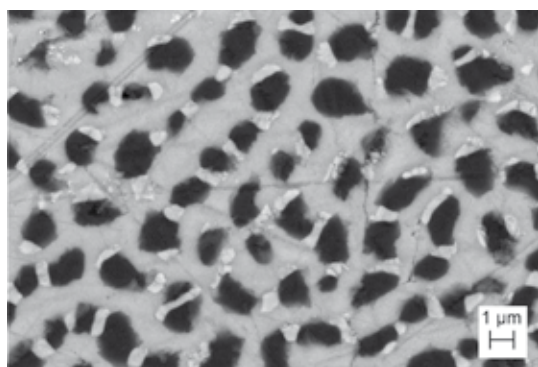

Fig. 6: SEM micrograph of a LiF/NaCl/CaF₂ eutectic fiber that was grown by micro-pulling-down with 30 mm/h. Matrix: NaCl, dark: LiF, bright: aF₂. NaF is not visible in the micrograph. Courtesy of M. F. Acosta, Zaragoza.

If one adds CaF_2 to the reciprocal pair as additional component, the graphical representation of the whole system becomes difficult, however the paper by Gladushchenko and Zakharchenko [8] gives some valuable insight by showing it as a trigonal pyramid with the three fluorides on the top, and the chlorides at the bottom corners. In our study, the composition was fixed to the eutectic point in Fig. 3, leaving the temperature as single degree of freedom. Consequently the behavior of the system is given by calculating the composition and/or quantity of different phases as function of T, which is done in Fig. 5

The liquid (for $T > T_f = 661°C$) consists practically of isolated cations and anions; the given concentrations should be regarded virtual. At T_f, transition to stoichiometric solid LiF and CaF_2, as well as the rocksalt solid solution (Na,Li)Cl(ss) is not immediately complete. Instead, some molten phase remains because several equilibrium species (e.g. LiCl with $T_f = 610°C$) have low melting points. Besides, the composition of the rocksalt phase changes with T, as demonstrated by the maximum of the dashed LiCl(ss) curve just below T_f. It should be noted that in the solidified fibres NaF can be identified although this substance does not belong to the initial components of the mixture. NaF, however, must be expected from the calculation in Fig. 5.

A DTA measurement of the eutectic mixture (blue curve in the insert of Fig. 5) reveals that the thermodynamic equilibrium calculations are realistic: as much as 83 K lower than the eutectic peak at 665°C a small endothermal event indicates the begin of melt formation. This event is reproducible and appears also in cooling curves in exothermal direction. In "normal" eutectic systems (see LiCl/$BaCl_2$ which is shown for comparison in the insert) any melting events below the eutectic temperature are ruled out. With the current experiments in the LiF/NaCl/CaF_2 system it could be shown that it is not simply ternary. Small amounts of liquid phase are present below the ternary "eutectic temperature", where the main body crystallizes, and segregation in the (Na,Li)Cl(ss) continues.

References

[1]   R. Bertram, D. Klimm, thermochimica acta 419 (2004) 189-193.

[2]   J. Philippen, C. Guguschev, R. Bertram, D. Klimm, J. Crystal Growth 363 (2013) 270-276.

[3]   D. Klimm, J. Philippen, T. Markurt, A. Kwasniewski, MRS Proceedings 2013 Fall, Symposium OO "Solid-State Chemistry of Inorganic Materials", Volume 1655 (2014)

[4]   D. Klimm, M. F. Acosta, I. A. dos Santos, I. M. Ranieri, S. Ganschow, R. I. Merino, MRS Online Proceedings Library, Volume 1508 (2013).

[5]   M. F. Acosta, S. Ganschow, D. Klimm, S. Serrano-Zabaleta, Á. Larrea, R. I. Merino, J. Europ. Ceram. Soc., 34 (2014) 2051-2059.

[6]   V. M. Orera, J. I.Peña, P. B. Oliete, R. I. Merino, A. Larrea, J. Crystal Growth 360 (2012) 99-104. See also Handbook of Crystal Growth, Vol. 2B, Elsevier 1994.

[7]   H. M. Haendler, P. S. Sennett, and C. M. Wheeler, Jr., J. Electrochem. Soc. 106 (1959) 264-268.

[8]   V. A. Gladushchenko, M. A. Zakharchenko, Zh. Neorg. Chim. 11 (1966) 916-919; engl. Translation in: Russ. J. Inorg. Chem. 11 (1966) 493-495.

Crystal Machining

Head: Dr. U. Juda
Team: M. Imming, V. Lange, T. Neugut, T. Wurche

Kristallbearbeitung

Zu den Hauptaufgaben der Themengruppe Kristallbearbeitung gehören

- die Probenpräparation für die Routinediagnostik der im Haus gezüchteten Kristalle,
- die Bereitstellung kristallographisch orientierter Keime und Substrate für die Kristallzüchtung,
- die Entwicklung von Präparationstechnologien für den Wafer-Herstellungsprozess (Trennen und Polieren) speziell für neue am Institut gezüchtete Materialien und
- Übernahme von Serviceaufgaben bzw. Sonderanfertigungen für Universitäten, für die Industrie und Forschungseinrichtungen.

Die die enge personelle und gerätetechnische Vernetzung mit der Themengruppe Physikalische Charakterisierung ermöglicht einen schnellen Zugriff auf Methoden der Oberflächencharakterisierung und erlaubt neben den täglichen Routineaufgaben auch die Betrachtung von wissenschaftliche Aspekte der Probenpräparation.

Die Bearbeitung von Halbleitermaterialien und Kristallen für optische Anwendungen, für die Charakterisierung oder die Herstellung von Substraten für die Epitaxie erfordert meist eine hohe Präzision und damit eine entsprechende Anlagentechnik. Unabhängig von Material oder Verwendungszweck durchläuft jede Probe bzw. jeder Wafer bis zur Fertigstellung verschiedene Arbeitsschritte. Diese beinhalten Formatieren und Trennen des Kristalls in Wafer und anschließende Oberflächenpräparation mittels verschiedener Schleif-, Läpp- und Polierprozesse. Die bei uns zur Verfügung stehenden Methoden umfassen:

- röntgenografisches Orientieren von Kristallen
- Trennschleifen von Kristallen und Wafern mit verschiedenen Verfahren – Diamantdraht-, Multidiamantdraht- und Diamant-Innentrennsägen (Abb. 1)
- Flachschleifen mit Diamantwerkzeugen
- Läppen und Polieren mit verschiedenen Abrasiven (Aluminiumoxid, Ceroxid, Siliciumcarbid, Borcarbid, Diamant unterschiedlichster Korngrößen) und Suspensionen
- mechanisches und chemo-mechanisches Polieren mit Präzisionspoliermaschinen (Abb. 2)
- Oberflächencharakterisierung mittels Lichtmikroskopie, Konfokalmikroskopie (CFM), Atomkraftmikroskopie (AFM), Rasterelektronenmikroskopie (REM) und diversen röntgenografischen Methoden,
- Bestimmung von geometrischen Oberflächenparametern wie Waferdicke, Durchbiegung, Ebenheit, Parallelität und Oberflächenrauigkeit mittels Weißlicht-Sensor kombiniert mit einem Konfokalmikroskop (Abb.3 und 4).

Die entsprechende anlagentechnische Ausstattung und fachliche Kompetenz aller Mitarbeiter macht es möglich, anspruchsvolle Service- und Forschungsaufgaben für die Industrie, für Hochschulen und außeruniversitäre Forschungseinrichtungen zu übernehmen, die von der Präparation spezieller Proben bis zur Entwicklung von Bearbeitungstechnologien inklusive der Erstellung zugehöriger Dokumentationen reichen. Daneben können auch Sonderanfertigungen mit speziellen Anforderungen an Geometrie und Oberflächenqualität kurzfristig und in hoher Qualität hergestellt werden.
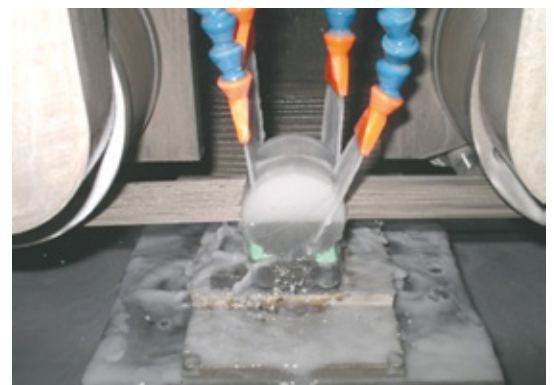
Fig. 1: Multi diamond wire saw for cutting crystal wafers (here sapphire)
Abb. 1: Multi-Diamantdrahtsäge zur Waferherstellung (hier Saphir)

Fig. 2: Polishing machine for chemo-mechanical polishing processes
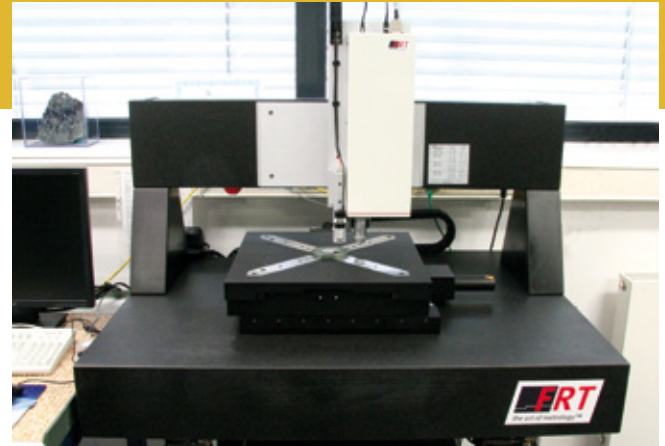*Abb. 2: Poliermaschine für chemo-mechanische Polierprozesse*

Fig. 3: MicroProf® – Measurement equipment for determination of standard surface parameters (consisting of a chromatic white light sensor and a confocal microscope)
Abb. 3: MicroProf® – Messgerät zur Bestimmung von Oberflächenparametern (bestehend aus Weißlichtsensor und Konfokalmikroskop)

Main tasks of the work of the crystal machining group are

- sample preparation for routine characterization of the in-house grown crystals,
- preparation of seed crystals and substrates with a very precise orientation for use in crystal growth,
- development of preparation processes for wafering (sawing and polishing) of crystalline materials mainly for new materials grown at the institute and
- Service for universities, industrial customers and research institutions.

The intensive cooperation with the characterization group by a personal- and device-related network enables us to check the surface quality and contributes to a more scientific approach to crystal machining.

The preparation of crystals for semiconductor and optical applications, for diagnostics or as substrates for epitaxial processes requires high-precision machining. Whatever the application or material, each sample or wafer undergoes several stages during manufacture, which include formatting, slicing the wafer from the crystal and preparing the surface using different grinding, lapping and polishing techniques. The methods used in our group include

- crystal orientation using x-ray techniques,
- crystal cutting and wafering by different methods – single and multi diamond wire (see fig. 1) and inner diameter diamond sawing,
- wafer grinding with diamond tools,
- wafer lapping and polishing with various abrasives (aluminum oxide, cerium oxide, silicon carbide, boron carbide, diamond) in different particle sizes and suspensions,
- mechanical and chemo-mechanical polishing with high precision polishing machines (see fig. 2),
- surface characterization by light microscopy, confocal microscopy (CFM), atomic force microscopy (AFM), scanning electron microscopy (REM) and x-ray techniques,
- determination of standard wafer geometry and surface parameters like thickness, bow, evenness, parallelism and roughness using a white light interferometer probe combined with a confocal microscope (see fig 3 and 4).

The available equipment and the experience and proficiency of all staff members enable us to supply custom-made samples and to accomplish ambitious service and research orders from industry, universities and other research institutions, ranging from the fabrication of machined samples to the development of technologies and related documentations. Special demands on geometry and surface quality of various samples could be fulfilled in short time and with high quality.

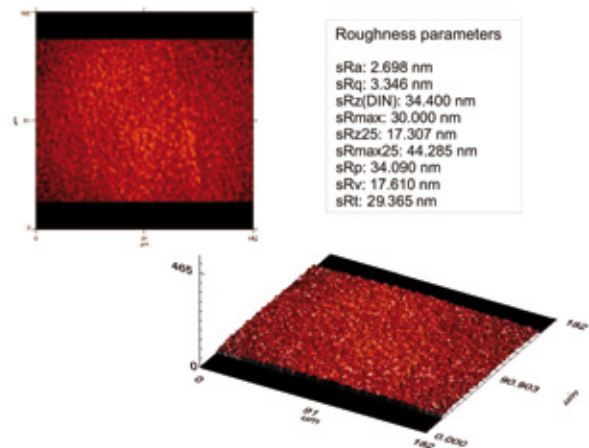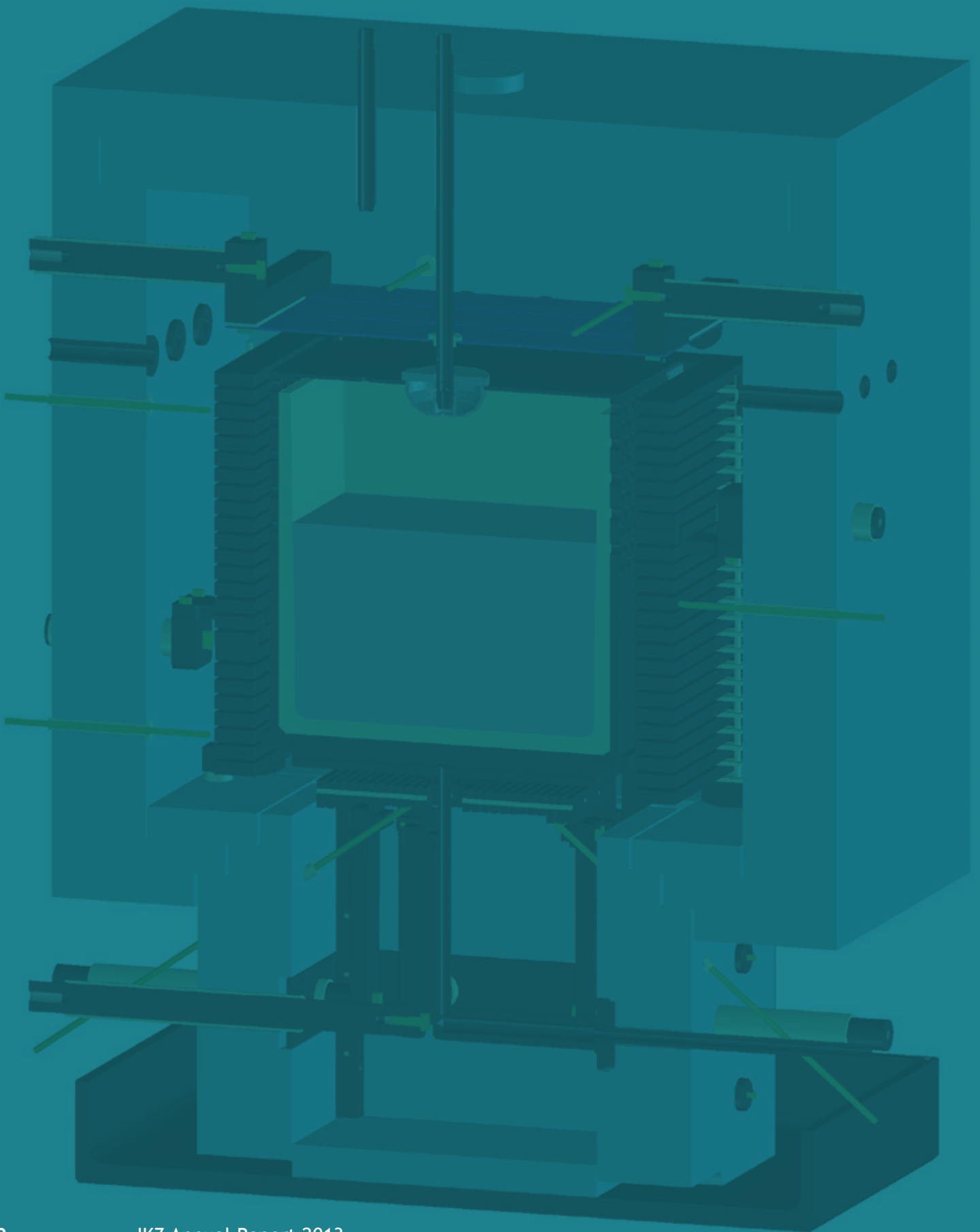
Fig. 4: Measurement of surface roughness parameters of a polished sample
Abb. 4: Messung von Oberflächenrauigkeits-Parametern einer polierten Probe

Cross-sectional Activities

Equipment maintenance and development at IKZ

Numerical Modelling

Numerical Modelling

Numerische Modellierung

The research objective of the numeric modeling is to develop models for solving the complex interaction of interface dynamics, heat and mass transport, as well as multiphase and multicomponent flow in various industry-related crystal growth processes. The progress of numerical models, particularly in Computational Fluid Dynamics (CFD) enables the study of complex multiphase/interfacial flow physics. Modeling provides a fundamental understanding of flow and crystal growth. It is an effective tool for feasibility studies of new growth processes. The key advantage and benefit of using numerical models is a quick and cost-effective alternative to a whole series of experimental tests. The first step of improving an established growth process or introducing a new one is the planning of the furnace construction or its dedicated change. At that point typically a joint effort of construction and numerical modelling is done to find a well-designed solution. Depending on the problem, numerical calculations might be axisymmetric ones or complex 3D computations. The first kind is easy to handle and fast in computation whereas the second one needs considerable time both for set-up and calculation. Once the construction is established numerical calculations of the process itself will be performed to find the relation between process parameters as e.g. cooling rate, temperature gradient, rotation rate and the growth process. The outcome of such computations gives a better understanding of the process as a basis for further improvements or can give directly parameters for a better processing. The successful interlocking of numerical modeling, construction and crystal growth is illustrated e.g. on the development of the new generation of a heater magnet module for the simultaneous crystallization of four VGF crystals under the influence of traveling magnetic field as shown in detail in the report of the GaAs group.

The above mentioned support by numerical modelling is also provided as a service to external partners, especially to industry. Here our service comprises feasibility studies based on modeling as well as equipment development in cooperation with engineers from our construction group. The KRIST*MAG*® concept may serve as an example here, where travelling magnetic fields (TMF) allow a selective influence on the melt convec-

Das Forschungsziel der numerischen Modellierung ist die Entwicklung von Modellen, um das komplexe Zusammenspiel von Grenzflächendynamik, Wärme- und Stofftransport, als auch Multiphasen- und Multikomponentenströmung in unterschiedlichen (Industrie-) relevanten Kristallzüchtungsprozessen zu verstehen. Der Fortschritt bei den numerischen Modellen, insbesondere bei der Computational Fluid Dynamics (CFD), ermöglicht das Studium komplexer Multiphasen-Strömungsphysik unter Einbeziehung von Grenzflächen. Die Modellierung bietet dabei den Zugang zu einem grundlegenden Verständnis von Strömung und Kristallwachstum und ist ein probates Mittel zur Einschätzung der Machbarkeit von neuen Züchtungsprozessen. Der Hauptvorteil beim Einsatz von numerischen Modellen ist die schnelle und preiswerte Alternative zur experimentellen Durchführung von Testserien. Dabei besteht der erste Schritt für die Verbesserung eines etablierten, bzw. der Einführung eines neuen Züchtungsprozesses in der Planung und ggf. gezielten Modifikation der Ofenkonstruktion. Hierzu arbeiten typischerweise Konstruktion und numerische Modellierung eng an der Entwicklung einer probaten Design-Lösung zusammen. Abhängig vom Problem werden axialsymmetrische oder komplexe 3D-Berechnungen durchgeführt. Der erste Typ ist einfach zu handhaben und schnell in der Berechnung, während der zweite erhebliche Zeit für die Erstellung als auch für die Durchführung der Berechnung erfordert. Ist die Konstruktion erstellt, erfolgen numerische Berechnungen zum Züchtungsprozess selbst, um die optimale Relation zwischen Züchtungsparametern wie z.B. Kühlrate, Temperaturgradient, Rotationsrate und dem Wachstumsprozess zu ermitteln. Auf diese Weise führt die Modellierung zu einem besseren Verständnis des Prozesses und davon abgeleitet zu einer verbesserten Prozessführung bzw. der Vorgabe geeigneter Prozessparameter. Das erfolgreiche Zusammenwirken von numerischer Modellierung, Konstruktion und Kristallzüchtung wird u.a. durch die Entwicklung einer neuen Generation eines Heizer-Magnet-Moduls für die gleichzeitige Kristallisation von vier VGF-Kristallen illustriert, wie sie im Detail im Folgenden im Bericht der Gruppe Galliumarsenid in dargelegt wird.

tion and thus enhancing crystal quality and/or allowing higher productivity. The key feature of this concept is a combined heater magnet module, simultaneously generating heat and a magnetic field. Development of this module has been significantly enhanced by combination of crystal growth with modeling and construction. Feasibility studies and adaptation to various crystal growth systems led to industrial application of the concept, as well as further research activities like described in the by the groups "Multicrystalline Silicon" and "Gallium Arsenide" in this report. More information may also been found in the annual reports of recent years. One example for the service of numerical modeling is the feasibility study for applying the KRIST*MAG*® concept in the liquid phase epitaxy of CdZnTe (see Fig. 1). An improvement of the growth conditions was predicted and the practice exhibits a significantly increased epilayer quality (J. Crystal Growth 318, 1034, 2011). For the realization the originally used furnace could be kept – only the control system had to be changed. Patents granted for

Die oben erwähnte Unterstützung durch Numerische Modellierung wird auch externen Partnern als Service angeboten, insbesondere aus der Industrie. Dieser Service umfasst beispielsweise die Erstellung von Machbarkeitsstudien, basierend auf numerischer Modellierung, sowie wie die Entwicklung von Bauteilen in Kooperation mit unserer Konstruktionsgruppe. Das KRIST*MAG*®-Konzept kann hier als Beispiel dienen: Wandermagnetfelder erlauben einen selektiven Einfluss auf die Schmelzkonvektion und verbessern so die Kristallqualität bzw. erlauben eine höhere Produktivität. Kern des Konzepts ist ein kombiniertes Heizer-Magnet-Modul, das gleichzeitig Wärme- und Magnetfeld erzeugt. Die Entwicklung dieses Moduls wurde durch die Zusammenarbeit von Konstruktion und Modellierung entscheidend vorangetrieben. Machbarkeitsstudien und die Anpassung an verschiedene Züchtungssysteme ermöglichten die industrielle Anwendung des Konzepts, sowie zu weiteren Forschungsaktivitäten, die in den Berichten der Gruppen "Multikristallines Silizium" und "Galliumarsenid" beschrieben werden bzw. in den Jahresberichten der vergangenen Jahre. Ein Beispiel für industrielle Anwendung ist die Flüssigphasenepitaxie von CdZnTe (siehe Abb. 1). Berechnungen zur Verbesserung der Wachstumsbedingungen führten in der Praxis zu einer deutlich verbesserten Qualität der abgeschiedenen Schichten (J. Crystal Growth 318, 1034, 2011). Die Übertragung des
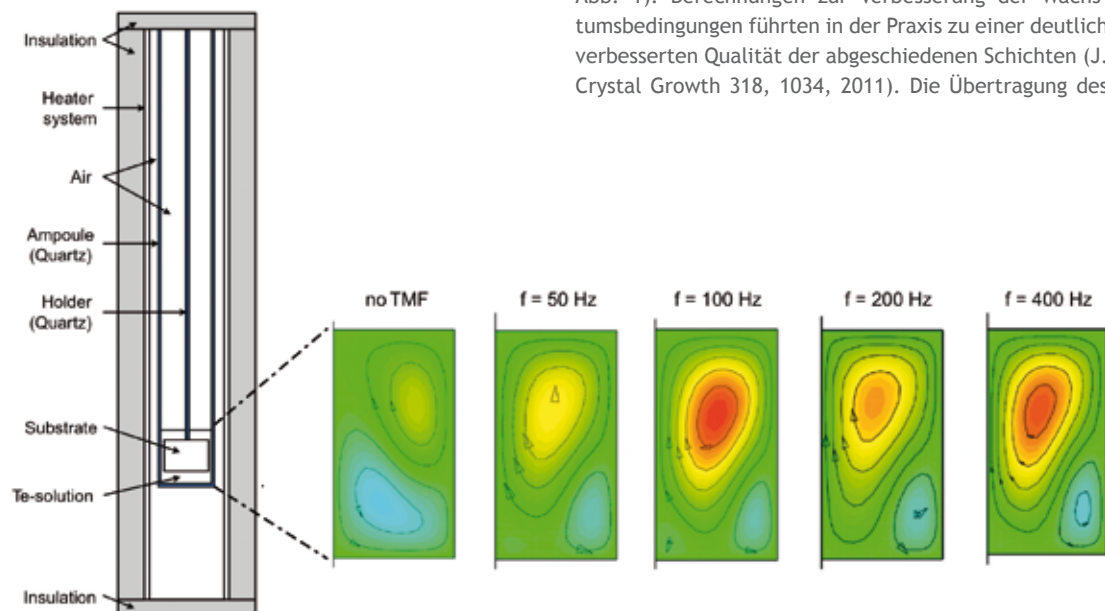
Fig. 1: Example of numerical simulations for a feasibility study of the KRISTMAG® concept: Liquid phase epitaxy of CdZnTe in an equipment using a commercial furnace (furnace not shown here). The parameters of the TMF for improving the growth have been found by a series of axisymmetric numerical calculations. The enhancement of flow (stream function is shown) with increasing frequency can be seen (please note that only half of the liquid is shown).
Abb. 1: Beispiel einer numerischen Simulation für eine Machbarkeitsstudie des KRISTMAG®-Konzepts: Flüssigphasenepitaxie von CdZnTe in eine Anlage mit einem kommerziellen Ofens (Ofen hier nicht abgebildet). Die Parameter für TMF zur Verbesserung des Wachstums wurden durch eine Serie von n axialsymmetrischen numerischen Berechnungen ermittelt. Das Anwachsen der Strömung (gezeigt ist die Stromfunktion) mit steigender Frequenz ist deutlich erkennbar (es ist nur die Hälfte der Flüssigkeit gezeigt).

the KRIST*MAG*® concept can be found in the appendix.

Another field for numerical modelling at IKZ is growth kinetics. The topics are motivated by the subjects and problems of bulk crystal and epitaxial growth at IKZ. One example is the detailed study of the grain evolution during the direct solidification of silicon by means of a phase field method adapted for the peculiarities of silicon. These investigations will be the basis for large scale simulations. The current state-of-the-art was also subject of a DFG supported workshop organized by IKZ and KIT Karlsruhe.

Numerical modeling is integrated in most of the research activities at IKZ, because it has proved a very powerful tool and may give valuable insight in growth processes. The main working tools for the support of construction and processing are ANSYS Emag, ANSYS CFX, and COMSOL multi physics. The latter is a general finite element solver and allows the input of any partial differential equation up to second order by its weak form. While these software tools are applicable on various aspects and may be helpful to get an insight in the underlying processes, their utilization requires considerable experience and know-how. At the time being, four researchers are using this kind of approach directly to support the crystal growers: Dr. Böttcher, Dr. Dropka, Dr. Menzel, and Dr. Miller. In addition, other researcher and technicians use specialized software on dedicated problems for supporting their work.

Selected references (see also patents listed in the appendix of this annual report):

- N. Dropka, Ch. Frank-Rotsch; **Accelerated VGF-crystal growth of GaAs under travelling magnetic fields;** Journal of Crystal Growth 367 (2013) 1 – 7
- N. Dropka, Ch. Frank-Rotsch, P. Rudolph; **Comparison of stirring efficiency of various non-steady magnetic fields during unidirectional solidification of large silicon melts;** Journal of Crystal Growth 365 (2013) 64 – 72
- Ch. Kudla, A.T. Blumenau, F.Büllesfeld; N. Dropka, Ch. Frank-Rotsch, F. Kiessling, O. Klein, P. Lange, W. Miller, U. Rehse, U. Sahr, M. Schellhorn, G. Weidemann, M. Ziem, G. Bethin, R. Fornari, M. Müller, J. Sprekels, V. Trautmann, P. Rudolph; **Crystallization of 640 kg mc-silicon ingots under traveling magnetic field by using a heater magnet module;** Journal of Crystal Growth 365 (2013) 54 – 58

Konzepts wurde dabei unter Beibehaltung des ursprünglichen Ofens realisiert – nur das Steuerungssystem musste gewechselt werden. Eine Übersicht der angemeldeten und erteilten Patente findet sich im Anhang.

Ein weiterer Anwendungsbereich der numerischen Modellierung ist die Wachstumskinetik. Probleme in der Volumenkristallzüchtung oder der Schichtabscheidung geben hier die Motivation für entsprechende Themen. Ein Beispiel ist das detaillierte Studium der Kornentwicklung bei der Silizium-Erstarrung mittels einer Phasenfeldmethode, die den Besonderheiten bei Silizium angepasst worden ist. Diese Untersuchungen dienen als Basis für Simulationen auf großer Skala. Der gegenwärtige Stand der Technik war auch Gegenstand eines durch die DFG geförderten Workshops, der gemeinsam von IKZ und KIT Karlsruhe organisiert wurde.

Numerische Modellierung ist in die meisten Forschungsaktivitäten am IKZ integriert, da es sich als sehr mächtiges Instrument erwiesen hat um wertvolle Einblicke in den Züchtungsprozess zu erhalten. Die Hauptarbeitsmittel zur Unterstützung von Konstruktion und Prozess sind ANSYS Emag, ANSYS CFX und COMSOL multi physics. COMSOL ist ein allgemeiner Finite-Element-Löser, der die Eingabe jeder partiellen Differentialgleichung bis zu zweiter Ordnung in ihrer schwachen Form erlaubt. Diese Softwarepakete sind auf unterschiedliche Fragestellungen anwendbar und können einen genaueren Einblick in die Prozesse bieten, erfordern aber einiger Erfahrung und Know-how. Zurzeit benutzen vier Forscher diese Herangehensweise, um die Kristallzüchter zu unterstützen: Dr. Böttcher, Dr. Dropka, Dr. Menzel und Dr. Miller. Darüber hinaus wird spezialisierte Software von weiteren Forschern und Technikern für ausgewählte Probleme benutzt, um ihre jeweilige Arbeit zu unterstützen.

Ausgewählte Publikationen (siehe auch Patente im Anhang dieses Jahresberichts):

- N. Dropka, Ch. Frank-Rotsch; **Accelerated VGF-crystal growth of GaAs under travelling magnetic fields;** Journal of Crystal Growth 367 (2013) 1 – 7
- N. Dropka, Ch. Frank-Rotsch, P. Rudolph; **Comparison of stirring efficiency of various non-steady magnetic fields during unidirectional solidification of large silicon melts;** Journal of Crystal Growth 365 (2013) 64 – 72
- Ch. Kudla, A.T. Blumenau, F.Büllesfeld; N. Dropka, Ch. Frank-Rotsch, F. Kiessling, O. Klein, P. Lange, W. Miller, U. Rehse, U. Sahr, M. Schellhorn, G. Weidemann, M. Ziem, G. Bethin, R. Fornari, M. Müller, J. Sprekels, V. Trautmann, P. Rudolph; **Crystallization of 640 kg mc-silicon ingots under traveling magnetic field by using a heater magnet module;** Journal of Crystal Growth 365 (2013) 54 – 58

Equipment maintenance and development at IKZ

Anlagentechnik und -entwicklung am IKZ

The technical production of crystals often requires sophisticated growth equipment providing specified conditions required for crystal growth. This includes, among others, processes under various ambient gas compositions at different pressures, mechanical movement or adjustment of thermal gradients.

The wide range of crystalline materials as well as the application and development of corresponding technologies for growth or deposition of these materials is correlated to a large number of different growth systems at IKZ. The tasks of the engineering group include de-velopment and construction of mechanical and electrical components and assemblies, repair and mainte-

Die technische Züchtung von Kristallen erfordert meist hoch entwickelte Kristallzüchtungsanlagen, die in der Lage sind, bestimmte Umgebungsbedingungen (z.B. Atmosphären aus verschiedenen Gasen zu unterschiedlichen Drücken, mechanische Bewegungen, thermische Gradienten) zu realisieren. Aufgrund der Vielfalt der unterschiedlichen Züchtungsmethoden und des breiten Spektrums der entwickelten kristallinen Materialien verfügt das Institut über einen großen Bestand an Anlagen für die Züchtung von Kristallen bzw. der Abscheidung kristalliner Schichten. Entsprechend sind die Arbeitsschwerpunkte der Gruppe Anlagentechnik sehr vielfältig. Sie umfassen die Entwicklung und Konstruktion mechanischer und elektronischer Baugruppen für Kristallzüchtungsanlagen, die Durchführung von Reparatur-, Wartungs- und Umbauarbeiten und Beratungsleistungen in allen technischen Fragen für die Themengruppen. Für die Durchführung der Arbeiten verfügt die Gruppe über ein modernes CAD-System für die effiziente Erstellung fertigungsgerechter Zeichnungen und die Erstellung von Modellen für die konstruktionsbegleitende FEM-Simulation in Bezug auf thermisches und mechanisches Verhalten der Baugruppen. Es erfolgt eine enge Zusammenarbeit mit der hauseigenen mechanischen und elektronischen Werkstatt.

Die Anlagenentwicklung und -modifikation und die im Institut vorhandenen Kompetenzen unserer Mitarbeiter spielen für die Entwicklung von Kristallzüchtungstechnologien häufig eine bedeutende Rolle und ermöglichen Forschungsansätze, die mit herkömmlichen Anlagen nicht zu realisieren wären. Für die Vielfalt der Anlagenkonstruktion sollen an dieser Stelle zwei Beispiele dienen: Abbildung 1 zeigt den Halbschnitt eines Modells der Konstruktion einer Verfahrensausrüstung für eine PV-Silicium-Erstarrungsanlage (VGF, Vertical Gradient Freeze) der Größe G2, bestehend aus 8 Heizern, welche ein Wandermagnetfeld erzeugen können, der Isolations- und Sicherheitseinrichtungen sowie einer aktiven Ingotkühlung. Mit Hilfe des Wandermagnetfeldes können die Phasengrenzfläche und die Strömung in der Schmelze zielgerichtet beeinflusst werden. Die in türkis dargestellte Isolation hat eine Kantenlänge von über einem Meter.
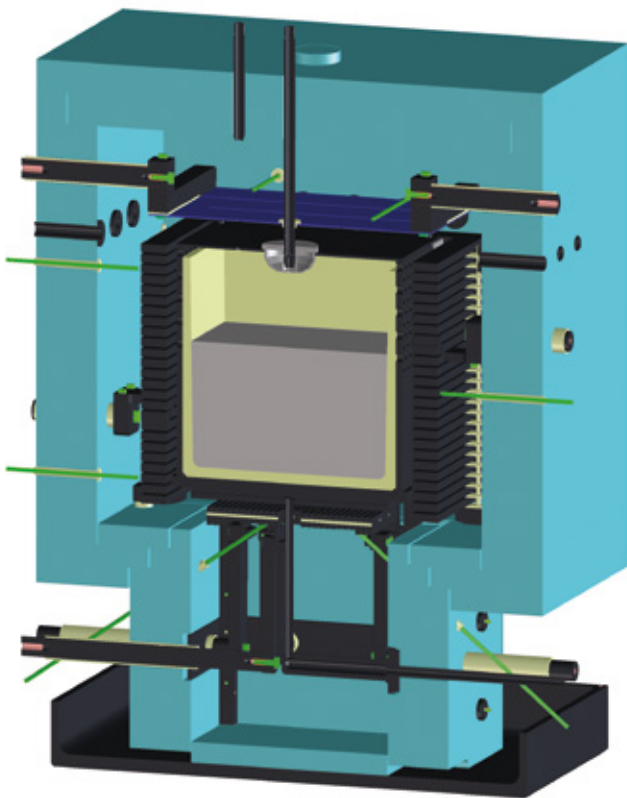

Fig. 1: Vertical Gradient Freeze system for growth of PV silicon
Abb. 1: PV-Silicium Erstarrungsanlage

nance as well as modification of crystal growth systems and consulting service in all technical questions. A modern CAD-system allows efficient manufacturing oriented design and construction, including models suitable for FEM simulations of the thermal and mechanical behavior of the systems. The work is performed in close cooperation with the institute's workshop and with high proficiency of our technicians and engineers.

Equipment development and modification plays an important role in many research projects at the institute and allows scientific approaches which could not be realized with commercial growth assemblies. Just two short examples may be given here: Fig. 1 shows a half cut of a model for process equipment in a size G2 VGF (Vertical gradient freeze) system for growth of PV silicon, including 8 heaters for the simultaneous generation of heat and magnetic fields, as well as insulation and safety equipment and a system for active cooling of the ingot. Applying a magnetic field allows a targeted influence of the melt flow and the phase boundary surface during the growth process. Edge length of the insulation (shown in blue) is larger than one meter.

In Fig. 2 the half cut of a model of a furnace for gallium nitride growth is shown, with a double walled inner construction completely made of quartz. The two part heater ensures a temperature regime for crystal growth between 800°C and 1100°C.
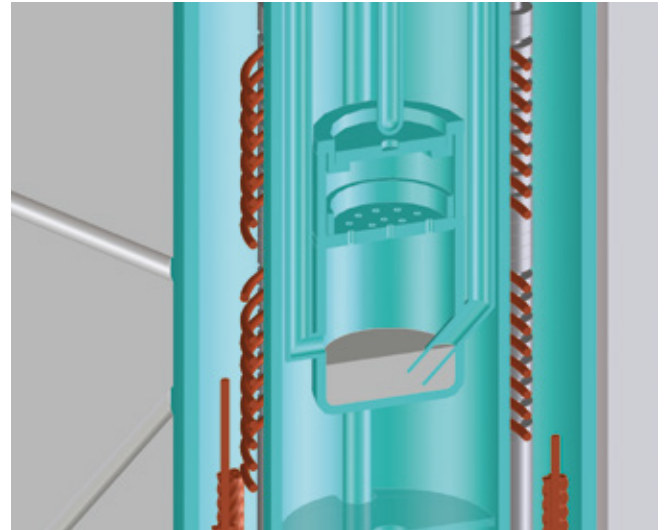
Fig. 2: Growth furnace with double walled inner construction made of quartz
Abb. 2: Züchtungsofen mit doppelwandigem Innenaufbau aus Quarz

Abbildung 2 zeigt einen Halbschnitt eines Modells eines Züchtungsofens für die Züchtung von Galliumnitrid, dessen innerer Aufbau doppelwandig und komplett aus Quarzglas ausgeführt ist. Der zweiteilige Heizer gewährleistet einen Züchtungstemperaturbereich zwischen 800°C und 1100°C.

Appendix

Publications

Talks and Posters

Patents

Teaching and Education

Membership in Committees

Guest Scientists at the IKZ

Colloquia at the IKZ

External Funding

Publications

Articles in international peer reviewed journals

Aroutiounian V. M., Gambaryan K. M., Harutyunyan V. G., Soukiassian P. G., Boeck T., Schmidtbauer J., Bansen R.; *The Ostwald Ripening at Nanoengineering of InAsSbP Spherical and Ellipsoidal Quantum Dots on InAs (100) Surface;* J. Contemp. Phys. **48** (2013) 37 – 42

Bagli E., Bandiera L., Guidi V., Mazzolari A., De Salvador D., Maggioni G., Berra A., Lietti D., Prest M., Vallazza E., Abrosimov N.V.; *Coherent effects of high-energy particles in a graded $Si_{1-x}Ge_x$ crystal;* Phys. Rev. Lett. **110** (2013) 175502_1 – 175502_6

Bansen R., Schmidtbauer J., Gurke R., Teubner Th., Heimburger R., Boeck T.; *Ge in-plane nanowires grown by MBE: influence of surface treatment;* CrystEngComm **15** (2013) 3478 – 3483

Bansen R., Schmidtbauer J., Juda U., Markurt T., Teubner T., Heimburger R., Boeck T.; *Influence of surface roughness on Ge nanowire growth by MBE;* Phys. Status Solidi RRL **7** (2013) 831 – 834

Bertram R.; *Chemische Analyse in der Kristallzüchtung;* GIT Labor Fachz. (2013) 45 – 47

Bertram R.; *Kalibrierung und Matrixeinfluss;* GIT Labor Fachz. (2013) 237 – 239

Chèze C., Siekacz M., Muziol G., Turski H., Grzanka S., Krysko M., Weyher J. L., Bockowski M., Hauswald C., Lahnemann J., Brandt O., Albrecht M., C. Skierbiszewski; *Investigation on the origin of luminescence quenching in N-polar (In,Ga)N multiple quantum wells;* J. Vac. Sci. Technol. B **31** (2013) 03C130-1 – 03C130-7

dos Santos I.A., Klimm D., Baldochi S.L., Ranieri I.M.; *Experimental evaluation and thermodynamic assessment of the LiF-LuF$_3$ phase diagram;* Thermochim. Acta **552** (2013) 137 – 141

Dropka N., Frank-Rotsch Ch.; *Accelerated VGF-crystal growth of GaAs under travelling magnetic fields;* J. Crystal Growth **367** (2013) 1 – 7

Dropka N., Frank-Rotsch Ch., Rudolph P.; *Comparison of stirring efficiency of various non-steady magnetic fields during unidirectional solidification of large silicon melts;* J. Crystal Growth **365** (2013) 64 – 72

Duk A., Schmidbauer M., Schwarzkopf J.; *Anisotropic one-dimensional domain pattern in NaNbO$_3$ epitaxial thin films grown on (110) TbScO$_3$;* Appl. Phys. Lett. **102** (2013) 091903-1 – 091903-4

Ezhevskii A.A., Popkov S.A., Soukhorukov A.V., Guseinov D.V., Gavva V.A., Gusev A.V., Abrosimov N.V., Riemann H.; Monoisotopic silicon ^{28}Si in spin resonance spectroscopy of electrons localized at donors; Semiconductors **47** (2013) 203- 208

Feneberg M., Romero M.F., Neuschl B., Thonke K., Röppischer M., Cobet C., Esser N., Bickermann M., Goldhahn R.; *Negative spin-exchange splitting in the exciton fine structure of AlN;* Appl. Phys. Lett. **102** (2013) 52112

Feneberg M., Romero M.F, Röppischer M., Cobet C., Esser N., Neuschl B., Thonke K., Bickermann M., Goldhahn R.; *Anisotropic Absorption and Emission of Bulk (1-100) AlN;* Phys. Rev. B **87** (2013) 235209

Gadzhiev O.B., Sennikov P.G., Petrov A.I., Gogova D., Siche D.; *Quantum chemical study of gas-phase reactions regarding GaN crystal growth in carbon based transport system;* Cryst. Growth Des. **13** (2013) 1445 – 1457

Galazka Z., Irmscher K., Pietsch M., Schulz T., Uecker R., Klimm D., Fornari R.; *Effect of heat treatment on properties of melt-grown bulk In$_2$O$_3$ single crystals;* CrystEngComm **15** (2013) 2220 – 2226

Galazka Z., Uecker R., Irmscher K., Schulz D., Klimm D., Albrecht M., Pietsch M., Ganschow S., Kwasniewski A., Fornari R.; *Melt growth, characterization and properties of bulk In$_2$O$_3$ single crystals;* J. Cryst. Growth **362** (2013) 349 – 352

Gogova D., Petrov P. P., Buegler M., Wagner M. R., Nenstiel C., Callsen G., Schmidbauer M., Kucharski R., Zajac M., Dwilinski R., Phillips M. R., Hoffmann A., Fornari R.; *Structural and optical investigation of non-polar (1-100) GaN grown by the ammonothermal method;* J. Appl. Physics **113** (2013) 203513-1 – 203513-6

Gusev A.V., Gavva V.A., Kozyrev E.A., Riemann H., Abrosimov N.V.; *Crucibles for Czochralski growth of isotopically enriched silicon single crystals;* Inorg. Mater. **49** (2013) 1167 – 1169

Hartmann C., Wollweber J., Dittmar A., Irmscher K., Kwasniewski A., Langhans F., Neugut T., Bickermann M.; *Preparation of Bulk AlN Seeds by Spontaneous Nucleation of Freestanding Crystals;* Jpn. J. Appl. Phys. **52** (2013) 08JA06-1 – 08JA06-6

Hempel M., Tomm J. W., La Mattina F., Ratschinski I., M. Schade, Shorubalko I., Stiefel M., Leipner H. S., Kießling F. M., Elsaesser T.; *Microscopic Origins of Catastrophic Optical Damage in Diode Lasers*; IEEE J. Sel. Top. Quant. Electron. **19** (2013) 1500508

Hens P., Müller J., Wagner G., Liljedahl R., Spiecker E., Syväjärvi M.; *Defect generation and annihilation in 3C-SiC-(001) homoepitaxial growth by sublimation;* Mater. Sci. Forum **740 -742** (2013) 283 – 286

Hübers H.-W., Pavlov S.G., Lynch S.A., Greenland Th., Litvinenko K.L., Murdin B., Redlich B., van der Meer A.F.G., Riemann H., Abrosimov N.V., Becker P., Pohl H.-J., Zhukavin R.Kh., Shastin V.N.; *Isotope effect on the lifetime of the $2p_0$ state in phosphorus-doped silicon;* Phys. Rev. B **88** (2013) 035201_1 – 035201_5

Irmscher K., Hartmann C., Guguschev C., Pietsch M., Wollweber J., Bickermann M.; *Identification of a tri-carbon defect and its relation to the ultraviolet absorption in aluminum nitride;* J. Appl. Physics **114** (2013) 123505-01 – 123505-11

Kaiser J., Szczerba W., Riesemeier H., Reinholz U., Radtke M., Albrecht M., Lua Y., Ballauff M.; *The Structure of AuPd Nanoalloys Anchored on Spherical Polyelectrolyte Brushes Determined by X-ray Absorption Spectroscopy;* Faraday Discuss. **162** (2013) 45 – 55

Kamba S., Goian V., Nuzhnyy D., Bovtun V., Kempa M., Prokleška J., Bernhagen M., Uecker R., Schlom D.G.; *Polar phonon anomalies in single-crystalline TbScO3 ;* Phase Transitions **86** (2013) 206 – 216

Karzel P., Ackermann M., Gröner L., Reimann C., Zschorsch M., Meyer S., Kiessling F., Riepe S., Hahn G.; *Dependence of phosphorous gettering and hydrogen passivation efficacy on grain boundary type in multicrystalline silicon;* J. Appl. Physics **114** (2013) 244902

Kobertz D., Guguschev C., Müller M.; *Investigations at high temperature in both equilibrium and kinetic state with Knudsen Effusion Mass Spectrometry (KEMS) and a skimmer integrated coupling system of Mass spectrometer and thermal analysis (STAMS);* The Open Thermodynamics Journal **7** (2013) 71 – 76

Kovalevsky K.A., Zhukavin R.Kh., Tsyplenkov V.V., Shastin V.N., Abrosimov N.V., Riemann H., Pavlov S.G., Hübers H.-W.; *Shallow-donor lasers in uniaxially stressed silicon;* Semiconductors **47** (2013) 235 – 241

Kudla Ch., Blumenau A.T., Büllesfeld F., Dropka N., Frank-Rotsch Ch., Kiessling F., Klein O., Lange P., Miller W., Rehse U.,Sahr U., Schellhorn M., Weidemann G., Ziem M., Bethin G., Fornari R., Müller M., Sprekels J., Trautmann V., Rudolph P.; *Crystallization of 640 kg mc-silicon ingots under traveling magnetic field by using a heater magnet module;* J. Crystal Growth **365** (2013) 54 – 58

Lee C.H., Orloff N.D., Birol T., Zhu Y., Goian V., Rocas E., Haislmaier R., Vlahos E., Mundy J.A., Kourkoutis L.F., Nie Y., Biegalski M.D., Zhang J., Bernhagen M., Benedek N.A., Kim Y., Btock J.D., Uecker R., Xi X.X., Gopalan V., Nuzhnyy D., Kamba S., Muller D.A., Takeuchi I., Booth J.C., Fennie C.J., Schlom D.G.; *Exploiting dimensionality and defect mitigation to create tunable microwave dielectriccs;* Nature **502** (2013) 532 – 536

Lee C. H., Skoromets V., Biegalski M. D., Lei S., Haislmaier R., Bernhagen M., Uecker R., Xi X., Gopalan V., Marti X., Kamba S., Kuzel P., Schlom D. G.; *Effect of stoichiometry on the dielectric properties and soft mode behavior of strained epitaxial $SrTiO_3$ thin films on $DyScO_3$ substrates ;* Appl. Phys. Lett. **102** (2013) 082905-1 – 082905-5

Markurt T., Lymperakis L., Neugebauer J., Drechsel P., Stauss P., Schulz T., Remmele T., Grillo V., Rotunno E., Albrecht M.; *Blocking growth by an electrically active subsurface layer – the effect of Si as an anti-surfactant in the growth of GaN;* Phys. Rev. Lett. **110** (2013) 036103-1 – 036103-5

Mazur Yu. I., Dorogan V. G., Benamara M., Ware M.E., Schmidbauer M., Tarasov G.G., Johnson S.R., Lu X., Yu S-Q., Tiedje T., Salamo G. J.; *Effects of spatial confinement and layer disorder in photoluminescence of GaAs$_{1-x}$Bi$_x$ / GaAs heterostructures;* J. Phys. D: Appl. Phys. **46** (2013) 065306

Mazur Yu.I., Dorogan V.G., Schmidbauer M., Tarasov G.G., Johnson S.R., Lu X., Ware M.E., Yu S.-Q., Tiedje T., Salamo G.J.; *Strong excitation intensity dependence of the photoluminescence line shape in GaAs$_{1-x}$Bi$_x$ single quantum well samples. ;* J. Appl. Phys. **113** (2013) 144308-1 – 144308-5

Murdin, B.N., Li, J., Pang, M.L., Bowyer, E.T., Litvinenko, K.L., Clowes, S.K., Engelkamp, H., Pidgeon, C.R., Galbraith,I., Abrosimov, N.V., Riemann, H., Pavlov S.G., Hübers H.-W., Murdin P.G.; *Si:P as a laboratory analogue for hydrogen on high magnetic field white dwarf stars;* Nature Commun. **4** (2013) 1469_1 – 1469_8

Philippen J., Guguschev C., Bertram R., Klimm D.; *Laser-heated pedestal growth of cerium doped calcium scandate crystal fibers;* J. Crystal Growth **363** (2013) 270 – 276

Prasai D., John W., Weixelbaum L., Krüger O., Wagner G., Sperfeld P., Nowy S., Friedrich D., Winter S., Weiss T.; *Highly reliable silicon carbide photodiodes for visible-blind ultraviolet detector applications*; J. Mater. Res. **28** (2013) 33 – 37

Rantzsch U., Haber T., Klimm D., Kloess G.; *The cooling rate of the El'gygytgyn impact glass*; Meteorit. Planet. Sci. **48** (2013) 1351 – 1358

Saeedi K., Simmons S., Salvail J.Z., Dluhy P., Riemann H., Abrosimov N.V., Becker P., Pohl H.-J., Morton J.J.L., Thewalt M.L.W.; *Room-temperature quantum bit storage exceeding 39 minutes using ionized donors in silicon-28*; Science **342** (2013) 830 – 833

Sawicka M., Chèze C., Turski H., Muziol G., Grzanka S., Hauswald C., Brandt O., Siekacz M., Kucharski R., Remmele T., Albrecht M., Krysko M., Sochacki T., Skierbiszewski C.; *Ultraviolet light-emitting diodes grown by plasma assisted molecular beam epitaxy on semipolar GaN (20$\bar{2}$1) substrates*; Appl. Phys. Lett.; **102** (2013) 111107-1 – 111107-4

Sawicka M., Chèze C., Turski H., Smalc-Koziorowska J., Krysko M., Kret S., Remmele T., Albrecht M., Cywinski G., Grzegory I., Skierbiszewski C.; *Growth mechanisms in semipolar (20$\bar{2}$1) and nonpolar m-plane (10$\bar{1}$0) AlGaN/ GaN structures grown by PAMBE under N-rich conditions*; J. Crystal Growth **377** (2013) 184 – 191

Sawicka M., Muziol G., Turski H., Grzanka S., Grzanka E., Smalc-Koziorowska J., Weyher J. L., Chèze C., Albrecht M., Kucharski R., Perlin P., Skierbiszewski C.; *Ultraviolet laser diodes grown on semipolar (20$\bar{2}$1) GaN substrates by plasma-assisted molecular beamepitaxy*; Appl. Phys. Lett. **102;** (2013) 251101_1 – 251101_5

Schmidt M., Heck S., Bosbach D., Ganschow S., Walther C., Stumpf T.; *Characterization of powellite-based solid solutions by site-selective time resolved laser fluorescence spectroscopy*; Dalton Trans. **42** (2013) 8387 – 8393

Terziyska P. T., Butcher K. S. A., Gogova D., Alexandrov D., Binsted P., Wu G.; *InN nanopillars grown from In-rich conditions by migration enhanced afterglow technique*; Mater. Lett. **106** (2013) 155 – 157

Uecker R., Klimm D., Bertram R., Bernhagen M., Schulze-Jonack I., Brützam M., Kwasniewski A., Gesing Th. M., Schlom D.G.; *Growth and Investigation of Nd$_{1-x}$Sm$_x$ScO$_3$ and Sm$_{1-x}$Gd$_x$ScO$_3$ Solid-Solution Single Crystals*; Acta Phys. Pol. A **124** (2013) 295 – 300

Winkler J., Neubert M., Rudolph J.; *A Review of the Automation of the Czochralski Crystal Growth Process*; Acta Phys. Pol. A **124** (2013) 181 – 192

Wolfowicz G., Tyryshkin A.M., George R.E., Riemann H., Abrosimov N.V., Becker P., Pohl H.-J., Thewalt M.L.W., Lyon S.A., Morton J.J.L.; *Atomic clock transitions in silicon-based spin qubits*; Nat. Nanotechnol. **8** (2013) 561 – 564

Wördenweber R., Schwarzkopf J., Hollmann E., Duk A., Cai B., Schmidbauer M.; *Impact of compressive in-plane strain on the ferroelectric properties of epitaxial NaNbO$_3$ films on (110) NdGaO$_3$*; Appl. Phys. Lett. **103** (2013) 132908-1 – 132908-4

Wu H., Gauger E.M., George R.E., Möttönen M., Riemann H., Abrosimov N.V., Becker P., Pohl H.-J., Itoh K.M., Thewalt M.L.W., Morton J.J.L.; *Geometric phase gates with adiabatic control in electron spin resonance*; Phys. Rev. A **87** (2013) 032326_1 – 032326_5

Zwierz R., Golka S., Kachel K., Siche D., Fornari R., Sennikov P., Vodopyanov A., Pipa A. V.; *Plasma enhanced growth of GaN single crystalline layers from Ga vapour*; Cryst. Res. Technol. **48** (2013) 186 – 192

Articles in conference proceedings

Klimm D., Acosta M.F., dos Santos I.A., Ranieri I.M., Ganschow S., Merino, R.I.; *Growth of Self Organized Eutectic Fibers from LiF – Rare Earth Fluoride Systems*; Materials Research Society Symposium Proceedings, **1508** (2013) 12-17, Cambridge

Richter S., Werner M., Schley M., Schaaff F., Riemann H., Rost H.-J., Zobel F., Kunert R., Dold P., Hagendorf C.; *Structural and chemical investigations of adapted Siemens feed rods for an optimized float zone process*; Energy Proceedia Proceedings of the 3rd International Conference on Crystalline Silicon Photovoltaics (Silicon-PV 2013) **38** (2013) 604 – 610

Tomm J. W., Hempel M., La Mattina F. , Kießling F. M., Elsaesser T.; *Analysis of bulk and facet failures in AlGaAs-based high-power diode lasers*; Proc. SPIE 8640, Novel In-Plane Semiconductor Lasers XII, 86401F (March 4, 2013); (2013)

Talks and Posters

Invited talks at national and international conferences

Abrosimov N.V.; *Highly enriched monoisotopic silicon crystal growth;* Third International Symposium on Nanotechnology, Energy and Space (NES-2013); Almaty, Kazakhstan; August 2013

Albrecht M., Duff A., Lymperakis L., Neugebauer J., Markurt T., Schulz T., Remmele T., Drechsel P., Stauss P.; *GaN on Silicon Substrates for Solid State Lighting: Strain Compensation, Dislocation Mechansims and Device Results;* 10th International Conference on Nitride Semiconductors; Washington, D.C., USA; August 2013

Albrecht M., Markurt T., Schulz, T., Remmele T., Duff A., Lymperakis L., Neugebauer J., Drechsel P., Stauss P; *Dislocation Mechanisms and Strain Relaxation in the Growth of GaN on Silicon Substrates for Solid State Lighting;* Annual World Congress on Advanced Materials; Suzhou, P.R. China; June 2013

Albrecht M., Schulz T., Remmele T., Markurt T., Korytov M., Duff, A., Lymperakis L., Neugebauer J.; *Indium fluctuations in the Age of Reason Atomic Resolution Transmission electron microscopy of III-Nitride Heterostructures;* European Materials Research Society, Spring Meeting; Strasbourg, France; May 2013

Fornari R.; *Growth from the melt of high-quality In_2O_3 and Ga_2O_3 single crystals;* DPG Frühjahrstagung der Sektion Kondensierte Materie; Regensburg, Germany; March 2013

Fornari R.; *High-quality In_2O_3 and b-Ga_2O_3 grown from the melt;* 19th American Conf. on Crystal Growth and Epitaxy (ACCGE-19); Keystone, Colorado, USA; July 2013

Fornari R.; *Il fotovoltaico in Europa;* IL Polo Fotovoltaico del Veneto; Padova, Italy; April 2013

Frank-Rotsch Ch., Dropka N., Juda U., Glacki A., Root O.; *Enhanced VGF-growth of GaAs using a heater magnet module;* 19th American Conf. on Crystal Growth and Epitaxy (ACCGE-19); Keystone, Colorado, USA, July 2013

Frank-Rotsch, Ch., Dropka N., Juda U., Glacki A., Root O.; *Vertical gradient freeze growth of GaAs using a heater magnet module (HMM);* 17th Int. Conf. on Crystal Growth and Epitaxy (ICCGE-17); Warschau, Poland, August 2013

Galazka Z., Uecker R., Irmscher K., Klimm D., Pietsch M., Albrecht M., Schulz D., Ganschow S., Kwasniewski A., Schewski R., Bertram R., Bickermann M., Fornari R.; *Growth and properties of bulk single crystals of selected transparent semiconducting oxides (TSOs): b-Ga_2O_3, In_2O_3 and SnO_2;* 17th Int. Conf. on Crystal Growth and Epitaxy (ICCGE-17); Warschau, Poland; August 2013

Ganschow S.; *Growth of $LiNbO_3$ single crystals from the melt and high-temperature solution;* International Workshop on Stoichiometric Lithium Niobate; Goslar, Germany; September 2013

Gogova D., Siche D., Kachel K., Korytov M., Galazka Z., Albrecht M., Zwierz R., Rost H.J., Fornari R.; *A new approach for free-standing GaN: growth of hexagonal GaN on monoclinic -Ga2O3 and its selfseparation;* Int. Workshop on Bulk Nitride Semiconductor (IWBNS-VIII); Seeon, Germany; October 2013

Miller W., Popescu A., Czupalla M., Albrecht, M.; *Facet Formation during Solidification of Silicon;* 7th Int. Workshop on Crystalline Silicon Solar Cells (CSSC-7); Kasuga, Fukuoka, Japan; October 2013

Zwierz R., Siche D.; Golka S., Kachel K., Fornari, R.; *Nitrogen plasma at higher pressure for GaN vapour growth;* Int. Workshop on Bulk Nitride Semiconductor (IWBNS-VIII); Seeon, Germany; October 2013

Invited seminars at national and international institutions

Albrecht M., Markurt T., Schulz T., Remmele T., Duff A., Lymperakis L., Neugebauer J.; *Dislocation Mechanisms and Strain Relaxation in the Growth of GaN on Silicon Substrates for Solid State Lighting;* Suzhou Institute of Nano-Tech and Nano-Bionics, Chinese Academy of Sciences, Suzhou, P.R. China; June 2013

Albrecht M., Schulz T., Remmele T., Markurt T., Korytov M., Duff A.,. Lymperakis L, Neugebauer J.; *Alloy fluctuations in III-Nitrides revisited by aberration corrected transmission electron microscopy;* Institute for high Pressure Physics, Polish Acadmy of Sciences, Warsaw, Poland; February 2013

Albrecht M., Schulz T., Remmele T., Markurt T., Korytov M., Duff A., Lymperakis L., Neugebauer J.; *Aberration corrected transmission electron microscopy of III-Nitride heterostructures;* V. Bakul Institute of Superhard Materials NAS of Ukraine (ISM), Kiew, Ukraine; February 2013

Albrecht M.; *Atomic structure of alloys, interfaces and defects in semiconductors studied by aberration-corrected transmsission electron microscopy*; Materials Science and Engineering Seminar, North Craolina State University, Raleigh, North Carolina, USA; June 2013

Albrecht M.; *Dislocation Processes in III-Nitrides*; Freiberger Compound Materials GmbH, Freiberg, Germany; January 2013

Galazka Z.; *Melt-grown bulk In_2O_3 single crystals*; Institute of Laser-Physics, Universität Hamburg, Germany; January 2013

Galazka Z.; *Bulk single crystals of transparent semiconducting / conducting oxides (TSOs/TCOs)*; Winter School "Characterization of micro- and nano-materials", Brandenburgische Technische Universität Cottbus-Senftenberg, Germany; February 2013

Galazka Z.; *Growth, characterization and properties of bulk single crystals of transparent semiconducting oxides (TSOs): beta-Ga_2O_3, In_2O_3 and SnO_2*; Seminar for students, University of Notre Dame, South Bend, USA; June 2013

Irmscher K.; *Optical and electrical properties of transparent semiconducting oxides*; Winter School "Characterization of micro- and nano-materials", Brandenburgische Technische Universität Cottbus-Senftenberg, Germany; February 2013

Klimm D.; *In_2O_3 und andere halbleitende Oxide: Thermodynamik und Kristallzüchtung*; Clemens-Winkler-Kolloquium; TU Bergakademie Freiberg (Sa.), Germany; Oktober 2013

Markurt T.; *Pinning of basal stacking faults by AlGaN interlayer in semi-polar GaN*; Kolloqium AG Kneissl, Technische Unviversität Berlin, Germany; July 2013

Mohn S.; *Polarity control in III-Nitrides for polar homo- and heterointerfaces: TEM studies*; Institute of High Pressure Physics, Polish Academy of Sciences, Warsaw, Poland; October 2013

Schwarzkopf J., Duk A., Schmidbauer M., Sellmann J., Gnanapragasam S., Fornari R.; *Strain engineering of lead-free, ferroelectric oxide films*; Materialwissenschaftliches Kolloquium, Materialwissenschaften TU Darmstadt, Germany; January 2013

Uecker R.; *Introduction to crystal growth from melt and the historical development of the Czochralski method*; Czochralski Seminar, Department of Chemistry, Adam Mickiewicz University; Poznan, Poland; October 2013

Wagner G., Baldini M., Gogova D., Schewski R., Albrecht M., Schmidbauer M., Irmscher K., Klimm D., Grüneberg R., Kwasniewski A.; *Homo- and Heteroepitaxy of transparent semiconducting oxide layers of the Ga_2O_3 – In_2O_3 – Al_2O_3 ternary system on b-Ga_2O_3 substrates*; Leipzig, Germany; November 2013

Oral contributions at national and international conferences

Bansen R., Heimburger R., Teubner T., Boeck T.; *Solution Growth of Crystalline Si on Glass*; 23. International Photovoltaic Science and Engineering Conference (PVSEC-23); Taipei, Taiwan; November 2013

Bickermann M., Hartmann C., Dittmar A., Langhans F., Kollowa S., Neugut T., Wollweber J.; *Current topics in sublimation growth of bulk aluminum nitride (AlN)*; 19th American Conf. on Crystal Growth and Epitaxy (ACCGE-19); Keystone, Colorado, USA; July 2013

Bickermann M.; *AlN substrates for optoelectronic devices*; 2nd 'Berlin WideBaSe' Conference on Technology and Applications of Nitride Semiconductors; Berlin, Germany; September 2013

Dropka N., Frank-Rotsch Ch., Rudolph P.; *Simultaneous magnetic stirring and interface shaping during directional solidification of large silicon ingots*; International Conference on Heating by Electromagnetic Sources (HES-13); Padua, Italy; Mai 2013

Dropka N., Frank-Rotsch Ch.; *Enhanced VGF-crystal growth of GaAs under travelling magnetic fields*; The International Symposium on Electromagnetic Flow Control in Metallurgy, Crystal Growth and Electrochemistry; Dresden, Germany; March 2013

Dropka N., Frank-Rotsch Ch.; *Numerical comparison of scale-up and numbering-up concepts for VGF-GaAs growth under TMF*; 19th American Conf. on Crystal Growth and Epitaxy (ACCGE-19); Keystone, Colorado, USA; July 2013

Ervik, T., Stokkan, G., Buonassisi, T., Mjøs, Ø., Lohne, O.; *Dislocation formation in quasi-monocrystalline silicon for solar cell*; DGKK-Arbeitskreis Herstellung und Charakterisierung von massiven Halbleitern; Erlangen, Germany; October 2013

Frank-Rotsch Ch, Dropka N., Juda U., Glacki A.; *Optimierung des GaAs-VGF-Züchtungsprozesses unter Nutzung eines Heizer-Magnet-Moduls*; DKT 2013 – DGKK Jahrestagung; Erlangen, Germany; March 2013

Frank-Rotsch Ch., Dropka N., Glacki A., Juda U.; *Effiziente VGF-GaAs-Züchtung unter TMF-Einfluss*; DGKK-Arbeitskreis Herstellung und Charakterisierung von massiven Halbleitern; Erlangen, Germany; October 2013

Galazka Z., Uecker R., Irmscher K., Klimm D., Pietsch M., Albrecht M., Schulz D., Ganschow S., Schewski R., Kwasniewski A., Bertram R., Bickermann M., Fornari, R.; *Growth, characterization and properties of bulk single crystals of transparent semiconducting oxides (TSOs): b-Ga$_2$O$_3$, In$_2$O$_3$ and SnO$_2$*; 55th Electronic Materials Conference; South Bend, USA; June 2013

Glacki A., Frank-Rotsch Ch., Juda U., Naumann M.; *Influence of a traveling magnetic field on micro- and macrosegregation during VGF growth of 4''-GaAs*; DKT 2013 – DGKK Jahrestagung; Erlangen, Germany; March 2013

Hartmann C., Wollweber J., Dittmar A., Kollowa S., Neugut T., Langhans F., Irmscher K., Bickermann M.; *Sublimation growth of bulk AlN crystal;* 2nd Polish-German Workshop on Nitride-Semiconductors; Warschau, Poland; April 2013

Hartmann C., Wollweber J., Dittmar A., Langhans F., Kollowa S., Neugut T., A. Kwasniewski A., Naumann M., Irmscher K., Bickermann M.; *Influence of seed orientation on structural and optical properties of homoepitaxial grown bulk AlN single crystals*; 10th International Conference on Nitride Semiconductors; Washington, D.C., USA; August 2013

Hartmann C., Wollweber J., Dittmar A., Langhans F., Kollowa S., Neugut T., Bickermann M.; *Technological considerations for seeded AlN bulk growth*; Int. Workshop on Bulk Nitride Semiconductor (IWBNS-VIII); Seeon, Germany; October 2013

Hwang W.S., Verma A., Protasenko V., Rouvimov S., Xing H.G., Seabaugh A., Haensch W., Van de Walle C., Galazka Z, Albrecht M., Fornari R., Jena D.; *Nanomembrane b-Ga$_2$O$_3$ High-Voltage Field Effect Transistors*; Device Research Conference; South Bend, USA; June 2013

Klimm D.; *Hochtemperatur-Thermodynamik*; Workshop Hochtemperaturwerkstoffe für die Kristallzüchtung; Workshop Hochtemperaturwerkstoffe für die Kristallzüchtung der DGKK, Miltenberg, Germany; November 2013

Linke D., Dropka N., Kiessling F. M., König M., Krause J., Lange R.-P., Sontag D.; *Characterization of a 75 kg mc-Si ingot grown in a* KRISTMAG® *-type G2-sized DS furnace*; 2nd Silicon Materials Workshop; Rom, Italy; October 2013

Linke D., Dropka N., Kiessling F.M., König M., Krause J., Lange R.-P., Sontag D.; *Characterization of a 75 kg mc-Si ingot grown in a* KRISTMAG®*-type G2-sized DS furnace*; DGKK-Arbeitskreis Herstellung und Charakterisierung von massiven Halbleitern; Erlangen, Germany; October 2013

Markurt T., Lymperakis L., Neugebauer J., Schulz T., Remmele T., Drechsel P., Stauss P., Albrecht, M.; *Unveiling the anti-surfactant effect of Si in GaN (0001) epitaxy*; 10th International Conference on Nitride Semiconductors; Washington, D.C., USA; August 2013

Markurt T., Lymperakis L., Neugebauer J., Schulz T., Remmele T., Rotunno E., Grillo V., Drechsel P., Stauss P., Albrecht, M.; *Unveiling the anti-surfactant effect of Si in GaN (0001) epitaxy*;18th Microscopy of Semiconducting Materials (MSM XVIII); Oxford, UK; April 2013

Miller W., Frank-Rotsch Ch., Czupalla M., Neubert M., Rudolph P.; *Czochralski Growth of Quadratic Silicon Crystals by Means of TMF: Simulations and Experiments;* The International Symposium on Electromagnetic Flow Control in Metallurgy, Crystal Growth and Electrochemistry; Dresden, Germany; March 2013

Miller W., Popescu A.; *Solidification of multicrystalline silicon – phase field studies of micro-structures*; 17th Int. Conf. on Crystal Growth and Epitaxy (ICCGE-17); Warschau, Polen; August 2013

Miller W., Popescu A.; *Study of grain growth by phase field methods*; DKT 2013 – DGKK Jahrestagung; Erlangen, Germany; March 2013

Miller W., Popescu A.; *Growth kinetics and equilibrium shapes during grain evolution of direct solidification of Si*; 14. Kinetikseminarder DGKK; Berlin, Germany; November 2013

Mohn S., Irmscher K., Kirste R., Rajan J., Hoffmann M., Collazo R., Sitar Z., Albrecht M.; *The Inversion Domain Boundary Luminescence in Heteropolar GaN Induced by a Strain and Doping Discontinuity*; 10th International Conference on Nitride Semiconductors; Washington, D.C., USA; August 2013

Petrov P., Miller W.; *Simulations of quantum dots formation by a fast kinetic Monte Carlo method*; DKT 2013 – DGKK Jahrestagung; Erlangen, Germany; March 2013

Petrov P., Miller W.; *Fast kinetic Monte Carlo simulations of quantum dots*; DPG Spring Meeting of the Condensed Matter Division; Regensburg, Germany; March 2013

Philippen J., Guguschev C., Klimm D.; *Growth and Characterization of Ce³⁺ doped CaSc₂O₄ single crystal fibers*; 21. Jahrestagung der Deutschen Gesellschaft für Kristallographie; Freiberg, Germany; March 2013

Richter S., Werner M., Schley M., Schaaff F., Riemann H.-J, Rost H.-J, Zobel F., Kunert R, Dold P., Hagendorf C.; *Structural and Chemical Investigations of Adapted Siemens Feed Rods for an Optimized Float Zone Process*; SiliconPV 2013; Hameln,Germany; March 2013

Rost H.-J, Riemann H.,.Kunert R, Dold P., Zobel F., Becker F.; *Czochralski based Float-Zone (CFZ) silicon - a low cost and high efficient alternative for commercial solar cell production*; 7th Int. Workshop on Crystalline Silicon Solar Cells (CSSC7); Kasuga, Fukuoka, Japan; October 2013

Schmidbauer M., Duk A., Kwasniewski A., Schwarzkopf J.; *Anisotropic one-dimensional Domain Pattern in NaNbO₃ Epitaxial Thin Films Grown on (110) TbScO₃*; European Materials Research Society, Spring Meeting; Strasbourg, France; May 2013

Schmidbauer M., Duk A., Schwarzkopf J.; *Anisotropic one-dimensional Domain Pattern in NaNbO₃ Epitaxial Thin Films Grown on (110) TbScO₃*; 21. Jahrestagung der Deutschen Gesellschaft für Kristallographie; Freiberg, Germany; March 2013

Schwarzkopf J., Duk A., Schmidbauer M.; *Anisotropic domain formation in NaNbO₃ thin films under tensile lattice strain*; MAMA Trend: Trends, challenges and emergent new phenomena in multi-functional materials; Sorrento, Italy; May 2013

Sellmann J., Schwarzkopf J., Duk A., Braun D., Gnanapragasam S., Kwasniewski A., Schmidbauer M., Markurt T., Müller P., Albrecht M.; *Growth of epitaxially strained, ferroelectric NaNbO₃ thin films by Pulsed Laser Deposition*; 14. Kinetikseminar der DGKK; Berlin, Germany; November 2013

Sellmann J., Schwarzkopf J., Duk A., Kwasniewski A., Schmidbauer M., Gnanapragasam S., Markurt R., Fornari R.; *Investigation of growth conditions on structural and ferroelectric properties of strained NaNbO₃ thin films grown by PLD*; DPG Spring Meeting of the Condensed Matter Division; Regensburg, Germany; March 2013

Wagner G., Baldini M., Gogova D., Schmidbauer M., Albrecht M., Klimm D., Schewski R.; *Influence of the different oxygen precursors on layer growth and the properties of Ga₂O₃ layers by using MOVPE*; 14. Kinetikseminar der DGKK; Berlin, Germany; November 2013

Wagner G., Baldini M., Gogova D., Schmidbauer M., Schewski R., Albrecht M., Klimm D.; *Homoepitaxial growth of b-Ga₂O₃ by metal-organic vapor-phase epitaxy*; MRS Fall Meeting & Exhibit; Boston, USA; December 2013

Weinstein O. Virozub A., Miller W., Brandon S.; *Modeling anisotropic shape evolution in Czochralski growth of oxide single crystals*; 17th Int. Conf. on Crystal Growth and Epitaxy (ICCGE-17); Warschau, Poland; August 2013

Wuenscher M., Riemann H.,Rost H.-J., Menzel R., Haufe S.; *Guided gas flow as an effective mean to overcome crystal diameter limitations in FZ growth of large silicon crystals*;17th Int. Conf. on Crystal Growth and Epitaxy (ICCGE-17); Warschau, Poland; August 2016

Zwierz R.; *Plasma enhanced vapour growth of GaN single crystalline layers*; DKT 2013 – DGKK Jahrestagung; Erlangen, Germany; March 2013

Poster presentations at national and international conferences

Baldini M., Gogova D., Irmscher K., Schmidbauer M., Wagner G., Fornari R.; *Heteroepitaxy of (Ga₁₋ₓInₓ)₂O₃ layers by MOVPE with different oxygen sources*; Italian Crystal Growth 2013; Parma, Italy; November 2013

Bansen R., Heimburger R., Schütte F., Teubner T., Boeck T.; *UV laser supported oxide removal from Si seed layers for thin-film solar cells*; DPG Spring Meeting of the Condensed Matter Division; Regensburg, Germany; March 2013

Bertram, R.; *Analyse von Hauptelementen mit ETV-ICP OES – Realität oder Utopie?*; 17. Tagung Festkörperanalytik; Chemnitz, Germany; July 2013

Dropka N., Linke D., Lange P., Rehse U.; *Numerical study of innovative gas management concept in a* KRIST*MAG*® *– type G2 DS-furnace*; 2nd Silicon Materials Workshop; Rom, Italy; October 2013

Gericke E., Weidemann S., Fischer S., Bansen R., Boeck T., Emmerling F., Rademann K.; *Selective Growth of Trigonal and Hexagonal Shaped Silver Micro-Nano-Platelets at the Water-Oil Interface*; 15. JCF Frühjahrssymposium 2013; Berlin, Germany; March 2013

Glacki A., Frank-Rotsch Ch., Naumann M., Juda U.; *Improvement of VGF growth of 4'' GaAs single crystals with traveling magnetic fields*; World Materials Summit/Forum for Next Generation Researchers; Strasbourg, France; October 2013

Gogova D., Wagner G., Baldini M., Schmidbauer M., Irmscher K., Schewski R., Galazka Z., Albrecht M., Fornari R.; *Structural properties of Si-doped b-Ga$_2$O$_3$ layers grown by MOVPE*; 17th Int. Conference on Crystal Growth and Epitaxy (ICCGE-17); Warschau, Poland; August 2013

Hartmann C., Wollweber J., Dittmar A., Kollowa S., Irmscher K., Kwasniewski A., Neugut T., Bickermann M.; *Growth of AlN bulk crystals with low defect density*; European Materials Research Society, Spring Meeting; Strasbourg, France; May 2013

Klimm D., Philippen J.; Ce^{3+}:CaSc$_2$O$_4$ *Crystal Fibers for Green Light Emission: Growth Issues and Characterization*; 2013 MRS Fall Meeting & Exhibit; Boston, USA; December 2013

Machulik S., Nazarzadehmoafi M., Siebert A., Janowitz C., Galazka Z., Manzke R.; *Metal contacts on* the b-Ga$_2$O$_3$ *single crystal (100) surface*; 5th Joint BER II and BESSY II User Meeting; Berlin, Germany; December 2013

Markurt T., Ravash R., Dadgar A., Krost A., Albrecht M.; *Pinning of stacking faults by AlGaN interlayer in semipolar GaN films*; 10th International Conference on Nitride Semiconductors; Washington, D.C., USA; August 2013

Markurt T., Schulz T., Remmele T., Drechsel P., Stauss P., Fritze S., Krost A., Albrecht M.; *Growth and relaxation mechanisms of AlGaN interlayers for thermal strain compensation in GaN (0001) on silicon (111) substrates*; 10th International Conference on Nitride Semiconductors; Washington, D.C., USA; August 2013

Michalak P.P., Uecker R., Galazka Z., Munnik F., Renno A.D., Merchel S., Bernhagen M.; *Synthesis of multi trace element doped* Fe$_{0.6}$ Mn$_{0.4}$ Ta$_2$O$_6$ *tantalite reference crystals by Czochralski method*; 17th Int. Conference on Crystal Growth and Epitaxy (ICCGE-17); Warschau, Poland; August 2013

Mohn S., Kirste R., Hoffmann M., Collazo R., Sitar Z., Albrecht M.; *Polarity Control of III-Nitrides on Sapphire Studied by Aberration Corrected Transmission Electron Microscopy*; 10th International Conference on Nitride Semiconductors; Washington, D.C., USA; August 2013

Nazarzadehmoafi M., Machulik S., Neske F., Janowitz C., Galazka Z., Manzke R.; *Near-ohmic contact by Ag on* In$_2$O$_3$ *(111) single crystals*; 5th Joint BER II and BESSY II User Meeting; Berlin, Germany; December 2013

Rost H.-J., Riemann H., Menzel R.; *Float-Zone silicon – a reasonable alternative for commercial photovoltaic applications?*; DKT 2013 – DGKK Jahrestagung; Erlangen, Germany; March 2013

Schewski R., Albrecht M., Irmscher K., Galazka Z., Remmele T., Korytov M., Schulz T., Markurt T., Meuret S., Kociak M., Naumann M., Pietsch M., Fornari R.; *Coloration of Indium Oxide Crystals Caused by Light Extinction at Indium Nanoparticles*; 18th Microscopy of Semiconducting Materials (MSM XVIII); Oxford, UK; April 2013

Schmidbauer M., Schwarzkopf J., Kwasniewski A., Sellmann J., Braun D.; *Investigation of Piezoelectric Domain Patterns in NaNbO$_3$ Thin Films by Grazing Incidence X-Ray Diffraction*; 5th Joint BER II and BESSY II User Meeting; Berlin, Germany; December 2013

Schwarzkopf J., Duk A., Wördenweber R., Schmidbauer M., Braun D., Bin Anooz S.; *Domain Structure of Anisotropically Strained NaNbO$_3$ Thin Films Grown by MOCVD*; 20th Workshop on Oxide Electronics; Singapore, Republic of Singapore; September 2013

Sellmann J., Schwarzkopf J., Duk A., Braun D., Gnanapragasam S., Kwasniewski A., Schmidbauer M., Markurt T., Fornari R.; *Epitaxial PLD-Growth of strained Ferroelectric K$_x$Na$_{1-x}$NbO$_3$ thin films*; European Materials Research Socitey, Spring Meeting; Strasbourg, France; May 2013

Woll M., Burianek M., Klimm D., Gorfman S., Mühlberg M.; *Growth and characterization of (Bi$_{0.5}$Na$_{0.5}$)$_{1-x}$ Ba$_x$TiO$_3$ single crystals*; 21. Jahrestagung der Deutschen Gesellschaft für Kristallographie; Freiberg, Germany; March 2013

Wollweber J., Hartmann C., Dittmar A., Kollowa S., Langhans F., Neugut T., Bickermann M.; *Wachstum von AlN-Volumenkristallen mit geringer Defektdichte*; DKT 2013 – DGKK Jahrestagung; Erlangen, Germany; March 2013

Wollweber J., Hartmann C., Neugut T., Dittmar A., Kollowa S., Langhans F., Bickermann M.; *Influence of different AlN surface preparation methods on the quality of AlN bulk crystals*; 17th Int. Conference on Crystal Growth and Epitaxy (ICCGE-17); Warschau, Poland; August 2013

Zwierz R., Golka S., Kachel K., Siche D., Fornari R.; *Vapour phase growth of single crystalline GaN layers in hot microwave plasma*; 17th Int. Conference on Crystal Growth and Epitaxy (ICCGE-17); Warschau, Poland; August 2013

Zwierz R., Golka S., Kachel K., Siche D.; *Plasma enhanced vapour growth of GaN single crystalline layers*; 10th International Conference on Nitride Semiconductors; Washington, D.C., USA; August 2013

Patents

Granted

H. Riemann, H.-J. Rost
Vorrichtung zum tiegelfreien Zonenschmelzen von Halbleitermaterialstäben
DE 196 10 650.8

S. Ganschow, R. Bertram, D. Klimm, P. Reiche, R. Uecker
Verfahren und Anordnung zur Herstellung von ZnO-Einkristallen
DE 10 2004 003 596.2

Ch. Frank-Rotsch, P. Rudolph, R.-P. Lange, O. Klein, B. Nacke
Vorrichtung und Verfahren zur Herstellung von Kristallen aus elektrisch leitenden Schmelzen
DE 10 2007 028 548.7
08784553.3 (DK, ES, FR, NO)
KRIST*MAG*®

R.-P. Lange, M. Ziem, D. Jockel, P. Rudolph, F. Kießling, Ch. Frank-Rotsch, M. Czupalla, B. Nacke, H. Kasjanow
Vorrichtung zur Herstellung von Kristallen aus elektrisch leitenden Schmelzen
DE 10 2007 028 547.9
08784554.1 (DK, ES, FR, NO)
KRIST*MAG*®

Ch. Frank-Rotsch, P. Rudolph, R.-P. Lange, D. Jockel
Vorrichtung und Verfahren zur Herstellung von Kristallen aus elektrisch leitenden Schmelzen
DE 10 2007 046 409.8
KRIST*MAG*®

P. Rudolph, M. Ziem, R.-P. Lange
Vorrichtung zum Züchten von Einkristallen aus elektrisch leitfähigen Schmelzen
DE 10 2007 020 239.5
KRIST*MAG*®

R. Fornari, S. Ganschow, D. Klimm, M. Neubert, Schulz
Verfahren und Vorrichtung zur Herstellung von Zinkoxid-Einkristallen aus einer Schmelze
DE 10 2007 006 731.5

P. Rudolph, M. Ziem, R.-P. Lange, D. Jockel
Vorrichtung zur Herstellung von Kristallen aus elektrisch leitenden Schmelzen
DE 10 2008 035 439.2

U. Rehse, P. Rudolph, W. Miller, N. Dropka, F. Büllesfeld, U. Sahr
Verfahren zum Erstarren einer Nichtmetall-Schmelze
DE 10 2008 059 521.7
09 749 132.8 (DK, ES, IT, NO, R, GB)

R. Fornari
Vorrichtung und Verfahren zur Züchtung von III-Nitrid-Volumenkristallen
08 161 254.1 (DE, PL, FR, GB, SE)

P. Rudolph, R.-P. Lange, M. Ziem
Vorrichtung zur Herstellung von Sililziumblöcken
DE 10 2009 045 680.5

N. Dropka, U. Rehse, P. Rudolph
Verfahren und Anordnung zur Herstellung von Kristallblöcken von hoher Reinheit und dazugehörige Kristallisationsanlage
DE 10 2010 028 173.5

H. Riemann, N. Abrosimov, J. Fischer, M. Renner
Verfahren und Vorrichtung zur Herstellung von Einkristallen aus Halbleitermaterial
EP 2 504 470 (NO, ES, NL, FR, DK, GB, BE, IT)

P. Lange, M. Ziem, N. Dropka, Ch. Frank-Rotsch
Verfahren und Vorrichtung zur gerichteten Kristallisation von Kristallen aus elektrisch leitenden Schmelzen
DE 10 2012 204 313.6

N. Dropka, Ch. Frank-Rotsch, P. Rudolph, R.-P. Lange, U. Rehse
Kristallisationsanlage und Kristallisationsverfahren zur Herstellung eines Blocks aus einem Material, dessen Schmelze elektrisch leitend ist
DE 10 2010 041 061.6

Pending

U. Rehse, P. Rudolph, W. Miller, N. Dropka, F. Büllesfeld, U. Sahr
Method for the solidification of a non-metal melt
WO002012060802A3 (CN, US, TW)

O. Klein, F. Kießling, M. Czupalla, P. Rudolph, R.-P. Lange, B. Lux, W. Miller, M. Ziem, F. Kirscht
Verfahren und Vorrichtung zur Züchtung von Kristallen aus elektrisch leitenden Schmelzen, die in der Diamant- oder Zinkblendestruktur kristallisieren
DE 10 2009 027 436.7

R. Fornari, F. Kießling, P. Rudolph, V. Trautmann
Kristallisationsanlage und Kristallisationsverfahren
DE 10 2009 046 845.5

H. Riemann, N. Abrosimov, J. Fischer, M. Renner
Verfahren und Vorrichtung zur Herstellung von Einkristallen aus Halbleitermaterial
DE 10 2010 052 522.7
10801372.3 (EP), 13/511,751 (US), 2012-540285 (JP)

T. Boeck, R. Fornari, R. Heimburger, G. Schadow, J. Schmidtbauer, H.-P. Schramm, T. Teubner
Kristallisationsverfahren zur Erzeugung kristalliner Halbleiterschichten
DE 10 2010 044 014.0

F. Kießling, Ch. Frank-Rotsch, N. Dropka, P. Rudolph
Verfahren zur gerichteten Kristallisation von Ingots
DE 10 2011 076 860.2

Z. Galazka, R. Uecker, R. Fornari
Method and apparatus for growing indium oxide (In2O3) single crystals and indium oxide (In2O3) single crystal
PCT/EP2012/057447

M. Wünscher, N. Werner
Modellprädikative Regelung des Zonenschmelzverfahrens
DE 10 2012 108 009.7
PCT/EP2013/067893

M .Wünscher, H. Riemann
Vorrichtung für das tiegelfreie Zonenziehen von Kristallstäben
DE 10 2012 022 958.8
PCT/DE2013/000627

P. Lange, P. Krause, N. Dropka, Ch. Frank-Rotsch
Kristallisationsanlage und Kristallisationsverfahren zur Kristallisation aus elektrisch leitenden Schmelzen sowie über das Verfahren erhältliche Ingots
DE 10 2013 211 769.8
PCT/EP2014/059684

D. Linke
Vorrichtung zum Züchten von Ingots
DE 10 2013 220 130.3

Registered Trademark

KRIST*MAG*®

Teaching and Education

Prof. Dr. Matthias Bickermann
Kristallzüchtung I: Grundlagen und Methoden; Technische Universität Berlin, Institut für Chemie, SS 2013
Kristallzüchtung II: Methoden und Anwendungen; Technische Universität Berlin, Institut für Chemie, WS 2013/14

Prof. Dr. Roberto Fornari
Grundlagen und Methoden der modernen Kristallzüchtung; Humboldt-Universität zu Berlin, Institut für Physik, SS 2013

PD Dr. habil. Detlef Klimm
Festkörperchemie; Humboldt-Universität für Berlin, Institut für Chemie, SS 2013

PD Dr. habil. Martin Schmidbauer
Röntgenstreuung: Grundlagen und Anwendungen in der Materialwissenschaft ; Humboldt-Universität zu Berlin, Institut für Physik, SS 2013, WS 2013/14

apl. Prof. Dr. Dietmar Siche
Growth of single crystalline materials and selected applications; Brandenburgische Technische Universität Cottbus, Lehrstuhl für Kristallzüchtung, SS 2013

Doctoral theses (ongoing)

Roman Bansen
Herstellung und Charakterisierung von polykristallinem Silicium auf Glas

Dorothee Braun
Ferro- und -piezoelektrische Charakterisierungen von bleifreien Perowskitschichten

Alexander Glacki
Züchtung von GaAs aus der Schmelze unter Anwendung von Magnetfeldern

Krzysztof Kachel
GaN-Kristallzüchtung aus der Gasphase ohne chemischen Ga-Transport

Dirk Kok
Einfluss der Züchtungsbedingungen auf die Realstruktur von $SrTiO_3$

Sandro Kollowa
Dotierung und Kompensation bei der Sublimationszüchtung von AlN-Volumenkristallen

Frank Langhans
Untersuchung zur Wachstumskinetik und Oberflächenmorphologie bei der Sublimationszüchtung von AlN-Volumenkristallen

Toni Markurt
Elektronenmikroskopische Charakterisierung von InGaN basierten Quantenstrukturen

Stefan Mohn
Elektronenmikroskopische Charakterisierung von heteropolaren Nitrid- Nitrid- und Nitrid-Oxidgrenzflächen

Tom Neugut
Entwicklung eines Verfahrens für die Epitaxie-taugliche Oberflächenpräparation

Robert Schewski
Wachstum und Relaxation von Gruppe III Sesquioxiden

Jan Sellmann
Einfluss von epitaktischen Strain auf die funktionellen Eigenschaften von dünnen Perowskit-Schichten

Radoslaw Zwierz
Plasma-supported vapour phase growth of single-crystalline gallium nitride (GaN)

Doctoral theses (completed)

Nebojsa Crnogorac
Numerische Analyse der hydrodynamsichen Stabilität in der Schmelze bei der Czochralski-Züchtung oxidischer Kristalle

Andreas Duk
Abscheidung von alkalihaltigen Oxidschichten mittels Liquid-delivery MOCVD

Carsten Hartmann
Aluminiumnitrid-Volumenkristallzüchtung mittels physikalischen Gastransports

Jan Philippen
Fiber crystal growth of cerium doped calcium scandate, strontium yttrium oxide, and tristrontium silicate

Jan Schmidtbauer
MBE Growth and Characterization of Germanium Nanowires

Nico Werner
Analyse und Regelung von verschiedenen Varianten

Diploma, Master and Bachelor theses (completed)

Fabian Meurer
Theoretische Untersuchungen zur Beobachtbarkeit des Czochralski- und LEC-Verfahrens mit Hilfe eines nicht-linearen Kaman-Filters

Franziska Schütte
Wachstum und Charakterisierung von Si/Ge Nanostrukturen

Hrvoljub Vukmann
Automatisierung des Ankeimens bei der Floating Zone (FZ) Kristallzüchtung

Ulrike Lüders
Beeinflussung der Gasatmosphäre zur Reduzierung des Kohlenstoffgehalts in gerichtet erstarrtem mc-Si

Sandra Haufe
Untersuchungen zur Temperaturabhänigkeit der elektrischen Durchschlagsfestigkeit von Schutzgasen der FZ Silizium Kristallzüchtung

Sascha Kiske
Abscheidung kristalliner SnO_2-Schichten auf Al_2O_3-Substraten durch Reaktion in einer Lösung

Franz Kamutzki
Untersuchungen zum Einfluss der Schmelzzusammensetzung auf das Kristallisationsverhalten und die Kristallperfektion von $BaMgF_4$

Matthias Boos
Untersuchung und Optimierung der Prozessparameter beim Mikrowellensintern vom AlN-Presslingen unter Einfluss von Ammoniak

Membership in Committees

Committees

Rainer Bertram
- DIN – Deutsches Institut für Normung e.V. -NA 062 – Normenausschuss Materialprüfung (NMP), member

Prof. Matthias Bickermann
- Berlin WideBase, member of the steering committee

Prof. Roberto Fornari
- European Materials Research Society E-MRS, member of the executive committee
- International Organization of Crystal Growth (IOCG), president
- International University Menendez Pelayo, Master Programme on Crystallography and Crystallization, Spain, faculty member
- Vorstand des Forschungsverbunds Berlin e.V.

Dr. Christiane Frank-Rotsch
- DGKK-Vorstand, secretary
- European Network of Crystal Growth (ENCG), member of the council
- International Organization for Crystal Growth (IOCG), member of the council

Dr. Detlef Klimm
- International Union of Crystallography, Commission on Crystal Growth and Characterization of Materials, member

Dr. Wolfram Miller
- DGKK-Arbeitskreis Kinetik, chairman
- DGKK-Arbeitskreis Angewandte Simulation in der Kristallzüchtung, member of organization team
- European Network of Crystal Growth (ENCG), member of the executive committee

Editorial committees

Prof. Roberto Fornari
- Journal of Crystal Growth, Elsevier Science, associate editor
- Journal of Optoelectronics and Advanced Materials (Romania), associate editor
- Crystal Research and Technology, Wiley Interscience, editorial board member

Dr. Wolfram Miller
- DGKK-Mitteilungsblatt, editor
- Special issue of Journal of Crystal Growth (IC-CGE.17), guest editor

Dr. Uwe Rehse
- DGKK-Mitteilungsblatt, editor

apl. Prof. Dietmar Siche
- Crystal Research and Technology, advisory board member

Conference committees

Prof. Matthias Bickermann
- International Workshop on Bulk Nitride Semiconductors (IWBNS), member of the advisory committee

Guest Scientists at IKZ

01.01. 2013 – 31.12. 2013

Maria Fernanda Acosta Garcia
02.04. – 31.05.2013
Instituto de Ciencia de Materiales de Aragón, Zaragoza,
Spain

Dr. Michele Baldini
01.09. 2012 – 28.02.2013
IMEM-CNR, Parma, Italy

Joana Fernandes
05.08. – 27.09.2013
New University of Lisabon, Portugal

Dr. Sonia Gnanapragasam
01.06.2012 – 31.05.2013

Jorge Andrés Guerra Torres
04.11.2013 – 02.02.2014
Pontificia Universidad Católica del Perú, Peru

Prof. Dr. Anatolii Gusev
13.04. – 20.04.2013
Russian Academy of Science, Russia

Lindsay Hussey
04.11. – 15.11.2013
North Carolina State University, Dept. of Materials Science & Engineering, USA

MSc. Marta Sawicka
15.04. – 01.07.2013
TopGaN LTD., Warsaw, Poland

Prof. Dr. Petr G. Sennikov
02.01. – 09.01.2013
01.07. -31.08.2013
RAS – Institute of Applied Physics, Russia

Christopher Shelton
26.06. – 01.07.2013
North Carolina State University, Dept. of Materials Science & Engineering, USA

Dr. Czeslaw Skierbiszewski
15.04. – 14.06.2013
04.07. – 13.07.2013
Institute for High Pressure Physics, Academy of Sciences, Warsaw, Poland

Dr. Alexander Vodopyanov
01.06.2013 – 15.06.2013
Institute of Applied Physics of the Russian Academy of Science, Russia

Kolloquia at IKZ

Prof. Dr. Odile Stephan and Dr. Mathieu Kociak
Laboratoire des Physiques des Solides, Université Paris Sud, France
„Advances in spatially resolved spectroscopy in an electron microscope: new possibilities, new applications", January 2013

Dr. Marc Georg Willinger
Abteilung Anorganische Chemie, Fritz-Haber-Institut, Max-Planck-Gesellschaft Berlin
"Analysis of the near edge fine structure in electron energy loss spectrometry", March 2013

Prof. Dr. Wolf-Gero Schmidt
Department Physik, Fakultät für Naturwissenschaften, Universität Paderborn
„Materialwissenschaften aus ab-initio-Rechnungen: Von chiraler Erkennung bis zur Peierlskondensation", March 2013

Dipl.-Min. Frank Langhans
IKZ
„Surface morphology of AIN bulk crystals", March 2013

MSc.-Phys. Roman Bansen
IKZ
„Challenges in the Growth of Crystalline Si on Glass from a Tin Melt", April 2013

Prof. Dr. Bernd Rech
Institut für Silizium-Photovoltaik, Helmholtz-Zentrum Berlin (HZB)
„Three dimensional design of crystalline silicon based thin-film solar cells and challenges", April 2013

Prof. Dr. Bernd Szyszka
Technische Universität Berlin (TU Berlin) / PVcomB & Fhl für Schicht- und Oberflächentechnik Films (IST)
„Research on technology fort hin film devices at TU Berlin", May 2013

Prof. Dr.-Ing. Holger Fritze
Technische Universität Clausthal
„High-temperature Resonant Sensors", June 2013

Dipl.-Phys. Stefan Mohn
IKZ
„Interface analysis for polarity based electronics", June 2013

Prof. Dr. Matthias Wuttig
I. Physikalisches Institut der RWTH Aachen, Lehrstuhl für Physik neuer Materialien
"Phase Change Materials: From Optical Data Storage to Novel Electronic Memories", June 2013

Msc. Marta Sawicka
Institute of High Pressure Physics, Polish Academy of Sciences, Poland
"World first semipolar laser diodes grown by plasma-assisted molecular beam epitaxy", June 2013

Dr. Philippe Vennègués
Joint Service for Science, Centre of Research on Heteroepitaxy and its Applications, University Valbonne, France
"Defect reduction methods for III-Nitrides heteroepitaxial films grown along semi-polar orientations", June 2013

Dr. Takao Abe
Isobe R&D Center, Shin-Etsu Handotai, Japan
"Observation of vacancies on growth interface and interstitials inside crystals by detaching growing crystals from silicon melt", August 2013

Dr. Carsten Hartmann
IKZ
„Aluminiumnitrid-Volumenkristallzüchtung mittels physikalischen Gasphasentransports", September 2013

Dr. Klaus Irmscher
IKZ
„Identifizierung eines Tri-Kohlenstoff-Komplexes und sein Einfluss auf die Ultraviolett-Absorption in AlN", September 2013

Dr. Wolfram Miller
IKZ
"Facet Formation during Solidification of Silicon", October 2013

Dr. Rudolf Lauck
Max-Planck-Institut für Festkörperforschung, Stuttgart
„Ein Physiker allein im Chemielabor: Hinter den Kulissen der Züchtung von meist isotopischen Kristallen", October 2013

Prof. Dr. Manfred Mühlberg
Universität Köln, Institut für Kristallographie
„Growth and characterization of selected ferroelectrics with perovskite and tungsten bronze structure types", October 2013

Dr. Eva Monroy
CEA Grenoble – INAC/SP2M/NPSC, France
"Plasma-Assisted MBE of Al(Ga)N/GaN nanostructures: Application to infrared optoelectronics", November 2013

Prof. Dr. Saskia Fischer
Humboldt-Universität zu Berlin, Institut für Physik, Neue Materialen
"Investigation of transport properties in nanomaterials and ultra-thin layers", December 2013

Dipl.-Phys. Robert Schewski
IKZ
„TEM investigation of MOCVD grown ß-Ga_2O_3 layers", December 2013

External Funding

Joint Initiative for Research and Innovation

Effizienter Züchtungsprozess für GaAs im kombinierten Heizer-Magnet-Modul; 2011-2014

Homo- and heteroepitaxy of transparent semiconducting oxide layers of the Ga_2O_3-In_2O_3-Al_2O_3 ternary system on beta-Ga_2O_3 and In_2O_3-Substrates; 2012-2015

Growth of high perfection bulk SrTiO3 single crystals; 2013-2016

International programs

Phase diagram studies and crystal growth in rare earth fluoride systems (PROBAL); DAAD; 2011-2013

Surface engineered InGaN heterostructures on N-polar and nonpolar Substrates for green light emitters (SINOPLE); 2009-2013; Industry-Academia Partnerships and Pathways (EU RP7)

Development of scientific fundamentals for the method of production of high-purity isotopicallly enriched crystals of silicon and germanium by plasma-enchanced chemical vapor deposition (PECVD) from their fluorides; DAAD, 2013

Programs of Federal Ministry of Education and Research (BMBF) and Federal Ministry of Economics and Technology (BMWi)

FloatZone-Technologie für Hocheffizienz-Zellen aus einkristallinem Silizium (FZSil); Exzellenzcluster Solarvalley Mitteldeutschland; 2009-2013

Wachstumskern WideBase: Sublimationszüchtung von AlN-Einkristallen; BMBF, 2010-2013

SolarWinS: Einfluss nichtdotierender Verunreinigungen auf die elektrische Aktivität von Kristalldefekten; BMBF, 2011-2014

Entwicklung, Umsetzung und Professionalisierung eines Verwertungskonzepts am Leibniz-Institut für Kristallzüchtung; BMBF, 2011-2014

Alternative Wärmequellen zur Herstellung von Kapillaroptiken für röntgenanalytische Verfahren mit Ortsauflösung im Nanometerbereich (AlWaQ); AiF (Zentrales Innovationsprogramm Mittelstand ZIM); 2012-2013

Entwicklung hochtemperaturstabiler Tiegelkomponenten für die einkristalline Züchtung nitridischer Halbleiter (N-Keramik); BMWi (Zentrales Innovationsprogramm Mittelstand ZIM); 2012-2014

Investigation and surface characterization of InAsS-bP-, Si- and Ge-nanostructures for mid-infrared and thermoelectric applications; International Bureau of BMBF, 2013-2014

Erforschung des human- und ökotoxikologisch relevanten Löslichkeits- und Reaktionsverhalens von GaAs sowie verwandter Arsenide und Phosphide im Verbundprojekt TEMPO: Toxikologische, physikalisch-chemische und gesellschaftliche Erforschung innovativer Materialien und Prozesse der Optoelektronik; BMBF, 2013-2016

Induktiv gekoppelter Niederdruck-Plasmareaktor zur Nitrid-Einkristallzüchtung; BMWi (zentrales Innovationsprogramm Mittelstand ZIM); BMBF, 2013-2015

DFG

Multiskalenmodellierung zum Verständnis der Facettierung und des orientierungsabhängigen Wachstums von Aluminiumnitrid-Volumenkristallen aus der Gasphase; 2011-2013

Lösungsmittelgenerierte Phasenumwandlung zur Erzeugung kristalliner Si-Schichten; 2011-2014

Science of polar homo- and heterointerfaces; 2012-2015

Funding by partners from industry and other institutions

Growth and characterization of new oxide single crystals; CrysTec GmbH, Berlin, DE; 2005-2013

Growth and characterization of new oxide crystals for piezoelectric sensors; Kistler Instrumente AG, Winterthur, CH; 2005-2014

Polysilicon Analysis; REC Silicon Inc. (US), 2010-2013 Asymmetrisch geschnittene Siliziumkristalle für Blaze-Gitter; Helmholtz-Zentrum Berlin für Materialien und Energie, DE; 2011-2014

KILOGRAMM-2; Physikalisch-Technische Bundesanstalt, Braunschweig, DE; 2011-2015

Entwicklung einer 200mm GaN auf Silizium-Wafer-Technologie für die Herstellung von Leuchtdioden und Leistungselektronikbauelementen; Azzurro Semiconductors AG, DE; 2012-2014

Growth and characterization of silicon crystals; Elkem Solar A/S, NO; 2012-2013

Züchtungsexperimente zur Validierung der GFZ-Modellierung; Siltronic AG, Burghausen, DE; 2012-2014

Germanium-Kristalle für das GERDA-Experiment; Max-Planck-Institut für Physik, München; 2013-2016

Leibniz-Gemeinschaft

Leibniz-Institut für Kristallzüchtung
Max-Born-Str. 2
12489 Berlin
Germany

Phone   +49 (0)30 6392 3001
Fax   +49 (0)30 6392 3003
Email   cryst@ikz-berlin.de

www.ikz-berlin.de